

# Sheffield Hallam University

*Multi-Informative and Specific Detection of Blood in Fingermarks via MALDI-MS Based Strategies*

DEININGER, Lisa

Available from the Sheffield Hallam University Research Archive (SHURA) at:

<http://shura.shu.ac.uk/22431/>

## A Sheffield Hallam University thesis

This thesis is protected by copyright which belongs to the author.

The content must not be changed in any way or sold commercially in any format or medium without the formal permission of the author.

When referring to this work, full bibliographic details including the author, title, awarding institution and date of the thesis must be given.

Please visit <http://shura.shu.ac.uk/22431/> and <http://shura.shu.ac.uk/information.html> for further details about copyright and re-use permissions.

# **Multi-Informative and Specific Detection of Blood in Fingermarks via MALDI-MS Based Strategies**

Lisa Deininger

A thesis submitted in partial fulfilment of the requirements of Sheffield Hallam University for the degree of Doctor of Philosophy in collaboration with the Home Office CAST division.

December 2017

## Abstract

Currently employed enhancement and detection techniques for blood are not confirmatory due to targeting generic compound classes like proteins. As such, they are not sufficiently specific and are prone to false positives. The aim of this work was to confidently determine whether a crime scene sample is in fact blood and more specifically human blood. To achieve this, an in-solution bottom up proteomic approach was developed, targeting blood-specific proteins and employing MALDI-MS. The work was developed further to devise a protocol for proteomic *in situ* analysis of bloodied fingermarks with MALDI-MS imaging, enabling the mapping of blood peptides to fingermark ridges and thus establishing a strong link between the suspect and the event of bloodshed.

Putative peptide identifications were made for signals originating from a number of different blood-specific proteins, including not only the most abundant blood proteins like haemoglobin, but also several other proteins (e.g. complement C3 and hemopexin).

To further validate the method, a blind study was conducted analysing unknown samples ranging from different species' blood and human biofluids to other substances known to produce false positives with conventional techniques. Employing MALDI-MS, it was possible to confidently identify human blood samples of up to 34 years in age. This is potentially a huge step forward in the forensic analysis of suspected blood samples and shows potential for re-analysis of cold case samples or samples of disputed origin. It was found in this study that further optimisation of the data analysis approach is required for provenance determination of animal blood samples.

Traditionally, establishing the order of deposition of fingermarks associated with blood is difficult and subjective. Infinite focus microscopy was investigated for its potential to facilitate quantitative differentiation between the different deposition scenarios. However, results were highly dependent on the surface of deposition and thus the technique was shown to be unsuitable due to the wide range of surfaces potentially encountered in a forensic investigation.

## **Contributions made by other researchers**

The following data in this thesis was generated in collaborative research efforts.

The immobilised hydrophobin digests described in chapter 2 were prepared by Ekta Patel and Paola Cicatiello. Ekta Patel also carried out the data analysis of MS/MS spectra and the majority of the write up for publication. In-solution digests were prepared by the PhD candidate. Further data acquisition and analysis was carried out jointly.

Sample preparation and data acquisition in chapter 3 was carried out with the assistance of Ekta Patel.

VSC photography, sample extraction and the majority of in-solution digests in chapter 4 were performed by Judith Schramm under guidance and supervision by the PhD candidate, who was responsible for data acquisition. Judith Schramm also exported the acquired spectra from MassLynx into .txt files for analysis by the PhD candidate, was partially responsible for the generation of animal peptide libraries and compiled the table of protein concentrations in blood (Appendix 1, S 1.1). The FASTA database mentioned in chapter 4 was compiled by project student Gabriella Masuzzo.

Contact angle measurements in chapter 5 were performed by Abdusalam Essa.

## Acknowledgements

I would like to thank all my supervisors for their support, the many things they taught me and the multitude of opportunities they have granted me. Special thanks to Malcolm and Chris for stepping in when Simona was on maternity leave and for always having an open ear.

Thank you to Ekta Patel, Matt Kitchen and Daniel Kinsman for all the training and instrumental support they kindly offered.

Thank you to Dan English for always being up for a chat, laughing with me and chasing up many delayed orders.

*Danke* to Karin Glöckle for all the administrative support, kind words and occasionally making sure I still speak German. 😊

Thank you to Kevin Blake for all the invaluable IT support and many nice conversations. Thanks to everybody who offered a refreshing chat in the hallway, kitchen or lab and lent me an open ear at times, especially Talcs, Florian and Akram.

Thank you to those who supported me, listened to me and offered advice, kind words or a hug when I was struggling, particularly Aimee, Nicola, Jodi, Jill and Ekta.

Thank you to my all friends, near and far, old and new, who have been understanding and kept in touch, even if I was busy (or in a different country...) and didn't have time to see them as often as I would have liked to. Thanks for all the good memories and pints we shared!

A huge thank you to my friend Amanda Harvey for sticking with me, always being there and listening to me, keeping me sane when I was on the verge of losing it, cheering me up and letting me cuddle her cats when I was in need of "kitten therapy". Thank you for your amusingly brutal honesty, lots of delicious food, lunch breaks filled with laughter and a plethora of many other amazing memories. I don't know what I would've done without you, you made the BMRC a better place for me.

Special thanks also to "Lisa No. 2" Lisa Decotret for being another amazing Canadian buddy to share funny lunch breaks or have super slow BBQs with.

Finally, thank you to my family for their continual support, always making sure I feel missed and welcome at home and laughing with me at tales of life in Britain, while never letting me forget where my home is. A massive thank you to our late cat Ria for always welcoming me as if I'd never been away and regarding me with special love and attention when I was home, letting me forget everything else whilst listening to her soothing purr – I wish I could've spent more time with you and will always love and miss you, you were very special.

A huge thank you in particular also to my parents for always believing in me, supporting me in my decisions (Even if they meant that their only child's first time moving out was moving to a different country!) and pursuit of my dreams, even in tough times. Thank you for always letting me come home, loving me, welcoming me with open arms (and pretzels :D) and always being there for me, even when you physically couldn't be by my side. I couldn't have done it without you. I love you!

## List of abbreviations

A1AT	Alpha-1-antitrypsin
AB1	Acid black 1
ABTS	2,2'-Azino-di-[3-ethylbenzthiazolinesulfonate(6)] diammonium salt
ACE-V	Analysis, comparison, evaluation and verification
ACN	Acetonitrile
ACPO	Association of chief police officers
AFE	Automatic feature extraction
AFIS	Automated fingerprint identification system
AHSP	Alpha-haemoglobin-stabilizing protein
ALS	Alternative light source
AmBic	Ammonium bicarbonate
ApoA1	Apolipoprotein A-1
ATR FT-IR	Attenuated total reflectance fourier-transform-infrared spectroscopy
AV17	Acid violet 17
AY7	Acid yellow 7
BET	Blood enhancement technique
C3	Complement C3
CHCA	A-cyano-4-hydroxycinnaminic acid
DAB	3,3'-di-aminobenzidine
DESI_MS	Desorption electrospray ionisation-mass spectrometry
DFO	1,8-diazafluoren-9-one
DNA	Deoxyribonucleic acid
EPB3	Erythrocyte protein band 3
EPB4.2	Erythrocyte protein band 4.2
FTICR	Fourier-transform ion cyclotron resonance-mass spectrometry
FTIR	Fourier-transform infrared microscope
FWHM	Full width half maximum
GC-FID	Gas chromatography-flame ionisation detection
GC-MS	Gas chromatography-mass spectrometry
Hb $\alpha$	Haemoglobin alpha
Hb $\beta$	Haemoglobin beta
HDMS	High definition mass spectrometry
HPLC-MALDI-MS	High performance liquid chromatography-matrix-assisted laser desorption/ionisation mass spectrometry

HR	Hungarian red
IFM	Infinite focus microscope
IMS	Ion mobility mass spectrometry
KM	Kastle-Meyer test
LAET-MS	Laser activated electron tunneling-mass spectrometry
LCV	Leuco crystal violet
LMG	Leuco malachite green
MALDI-MS	Matrix-assisted laser desorption/ionisation-mass spectrometry
MALDI-MSI	Matrix-assisted laser desorption/ionisation-mass spectrometry imaging
miRNA	Micro RNA
mRNA	Messenger RNA
MS	Mass spectrometry
Nd:YAG	Neodymium-doped yttrium aluminum garnet (laser)
Nd:YVO <sub>4</sub>	Neodymium-doped yttrium orthovanadate (laser)
NIR	Near-infrared raman
PCA	Principle component analysis
S/N	Signal-to-noise ratio
SERS	Surface enhanced raman scattering
SWGFAST	The scientific working group on friction ridge analysis, study and technology
TFA	Trifluoroacetic acid
TMB	Tetramethylbenzidine
XRF	X-ray fluorescence
α-2-M	Alpha-2-macroglobulin

### List of proteins investigated in this study

A1AT (Alpha-1-antitrypsin)

AHSP (Alpha-haemoglobin-stabilizing protein)

α-2-M (Alpha-2-macroglobulin)

ApoA1 (Apolipoprotein A1)

Complement C3

Ceruloplasmin

c-reactive protein

EPB3 (Erythrocyte membrane protein band 3)  
EPB4.2 (Erythrocyte membrane protein band 4.2)  
Glycophorin A  
Haptoglobin  
Hba  
Hbβ  
Hemopexin  
Myoglobin  
Prothrombin  
Serotransferrin

# Contents

<b>Abstract .....</b>	<b>2</b>
Contributions made by other researchers.....	3
Acknowledgements.....	4
<b>1 Introduction .....</b>	<b>12</b>
1.1 Background: the evidential value of fingerprints and blood.....	13
1.1.1 Fingerprints – their use historically and now .....	13
1.1.2 Blood evidence.....	21
1.2 Currently used blood enhancement techniques (BET) and their shortcomings .....	25
1.2.1 Fluorescence-based tests and alternative light sources.....	27
1.2.2 Other chemical enhancement techniques .....	29
1.2.3 Microcrystalline tests .....	35
1.2.4 RNA analysis for body fluid identification .....	36
1.2.5 Spectroscopic techniques .....	37
1.2.6 Provenance determination of blood.....	40
1.3 Introduction to MALDI-mass spectrometry.....	42
1.3.1 Ionisation theory in MALDI .....	43
1.3.2 Mass analysers .....	45
1.3.3 MALDI-MS imaging .....	47
1.4 The principles of proteomics .....	48
1.5 Infinite focus microscopy.....	51
1.6 Aims and objectives.....	53
1.7 References .....	56
<b>2 A proteomic approach for the rapid, multi-informative and reliable identification of blood .....</b>	<b>82</b>

2.1	Introduction .....	83
2.2	Experimental.....	86
2.2.1	Materials.....	86
2.2.2	Instrumentation and data acquisition.....	86
2.3	Methods.....	86
2.3.1	Initial method development and optimisation of digest protocol .....	86
2.3.2	Preparation and enzymatic digestion of blood samples .....	88
2.3.3	Blood provenance determination.....	89
2.3.4	Analysis of a 9-year-old bloodstain.....	90
2.3.5	Data analysis.....	90
2.4	Results and discussion .....	91
2.4.1	Initial method development and optimisation of the in-solution digest approach .....	91
2.4.2	In-solution and hydrophobin digests.....	96
2.5	Conclusions .....	114
2.6	References .....	115
<b>3</b>	<b>Proteomics goes forensic: detection and mapping of blood signatures in fingermarks .....</b>	<b>118</b>
3.1	Introduction.....	119
3.1.1	Blood enhancement techniques currently employed.....	119
3.1.2	Blood visualisation analytical techniques .....	120
3.1.3	Application of MALDI-MS based techniques for the reliable visualisation and identification of blood .....	122
3.1.4	Scope and results of the study presented .....	123
3.2	Materials and methods.....	124
3.2.1	<i>In situ</i> tryptic digestion of blood fingermarks for MALDI-MS Imaging (MALDI-MSI) .....	124

3.2.2	Matrix deposition .....	125
3.2.3	Instrumentation and data acquisition.....	125
3.2.4	Data analysis.....	126
3.3	Results and discussion .....	127
3.3.1	Optimisation of trypsin concentration: MALDI-MSI of enzymatic digestion spots deposited on blood marks.....	127
3.3.2	Optimisation of trypsin deposition for mapping blood signatures on the ridges of blood marks .....	130
3.3.3	Key findings.....	136
3.4	Concluding remarks .....	137
3.5	References .....	139
<b>4</b>	<b>Blind study and other applications – a tale of forensic method validation .....</b>	<b>145</b>
4.1	Introduction .....	146
4.2	Methods and materials.....	149
4.2.1	Lifting of non-enhanced and AB1-enhanced bloodied marks .....	149
4.2.2	Preparation of blind samples.....	150
4.3	Results and Discussion.....	152
4.3.1	Lifting of bloodied fingermarks .....	152
4.3.2	Lifting of AB1-enhanced marks .....	153
4.3.3	Analysis of blind samples with MALDI-MS profiling.....	157
4.3.4	Analysis of blind sample fingermarks with MALDI-MSI .....	174
4.3.5	MALDI-MS analysis of a 34-year old ninhydrin-enhanced sample ...	175
4.4	Conclusion .....	178
4.5	References .....	180
<b>5</b>	<b>Investigation of infinite focus microscopy for the determination of the association of blood with fingermarks .....</b>	<b>182</b>

5.1	Introduction .....	183
5.2	Methods .....	188
5.2.1	Determination of error of measurement.....	188
5.2.2	Sample preparation .....	188
5.2.3	Data acquisition.....	190
5.2.4	Statistical analysis .....	190
5.2.5	Contact angle measurements .....	190
5.3	Results and discussion .....	191
5.4	Conclusions .....	209
5.5	References .....	210
<b>6</b>	<b>Conclusions and future work .....</b>	<b>213</b>
	<b>Publications and dissemination .....</b>	<b>221</b>
	<b>Appendix 1.....</b>	<b>222</b>
	<b>Appendix 4.....</b>	<b>226</b>

# Chapter 1

## **Introduction**

## 1.1 Background: the evidential value of fingermarks and blood

### 1.1.1 Fingermarks – their use historically and now

Fingermarks are unique patterns left behind on a surface when an individual's fingertip makes contact. These marks can be latent (invisible), patent (visible to the naked eye) or plastic (a negative impression in a malleable substance such as wax) and provide a wealth of information about the donor. It should be noted that in the UK, it is preferred to use the term *fingermark* for a latent crime scene impression and *fingerprint* for a known or willingly deposited or inked impression [1], whereas in other countries all impressions are simply referred to as *fingerprints* with the term *latent prints* used to make the distinction [2,3]. As the work reported in this thesis will cover and reference examples from both inside and outside the UK, the terms *fingermark* and *fingerprint* shall be used interchangeably and supplemented with added descriptions as necessary.

In forensics, fingerprints are mostly used for identification purposes where marks found at a crime scene are compared to fingermark databases or a suspect's print. The exact date of when the friction ridge patterns on each person's fingers started to be considered unique and became widely used for forensic identification is perhaps debateable and location-dependent. However their identifying capabilities were exploited as early as 1750 B.C., when Babylonians used fingerprints to sign their identities on clay tablets [4]. Similarly, they were considered proof of identity, used to sign and seal documents and even informed criminal investigations in 300 B.C. China, and encompassed in a law in 702 A.D. Japan that required illiterate individuals to sign documents written for them with their fingerprints [5]. J.G. Barnes compiled many other interesting historical facts surrounding fingerprints in chapter 1 of the *Fingerprint Source Book* [5] and presents a timeline, according to which fingermarks were only recognised as unique in Europe in 1788. Alongside a wealth of information about the early research into understanding and characterising fingermark patterns and the development of classification systems, it is reported that the first homicide case to be solved by fingerprint evidence was the Rojas murder case in 1892 Argentina, which interestingly centred on a blood fingerprint. The first use of fingerprints in UK courts is reported to have taken place in 1902, where an

Inspector from Scotland Yard testified to an individualisation made in a burglary case [5].

Nowadays, fingerprints can be used for verification or identification purposes. In verification, a 1:1 match is obtained, comparing the given fingerprint against a chosen fingerprint in a database, for example to open a biometrical lock [6]. This kind of verification is widely used not only in high security areas, but even in mobile phone technology, where fingerprint sensors have become common means to allow access to a locked phone.

For identification purposes, a given print is compared to all prints in a database (1:N match) using an automated fingerprint identification system (AFIS) in order to identify an unknown person. Aside from forensic use for identifying suspects, this kind of fingerprint recognition is also used in passports for example by the US in order to verify the identity of people entering the country and flagging potential false or duplicate credentials [6]. Additionally, fingerprints can be used to link crime scenes, even when an identification has not yet been made, by searching against an unsolved print database. This link can allow for the offender's actions to be anticipated and thereby might aid in their identification and arrest [7].

Regardless of the nature of a fingermark, three levels of information are commonly associated with the pattern and used for identification or verification purposes. Level 1 describes the general ridge flow and pattern configuration, namely arches, whorls and loops (Figure 1.1) as described by Sir Francis Galton in his 1892 book "Finger Prints" [8]. Several more complex classification systems have been developed, both for single prints and a full set of 10 prints, for example dividing into internal and external loops, describing tented and left- or right-inclined arches and even including ridge count values [9]. The presence of Level 1 information is commonly known, but due to its general nature it does not allow for identification by itself. It is, however, useful for primary classification, as for example individuals with all arched patterns can be excluded if a suspect print presents with whorls, and

similarly further investigation can be undertaken into potential matches if a suspect does have whorled fingerprints.

Level 2 information (Figure 1.1) is comprised of more characteristic formations such as ridge endings, bifurcations and islands, also known as *minutiae*, embedded in the general pattern. This level of information requires more attention to be observed and can be used as individualising characteristics of a mark.

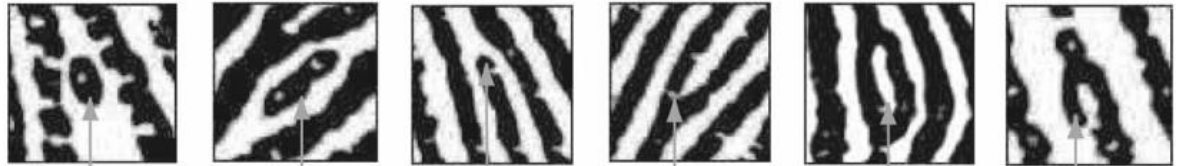
Level 3 detail (Figure 1.1) includes even finer features such as pores, scars, creases and dimensional attributes like the width, shape or contour of a ridge. Despite this very specific level of information, automated fingerprint identification systems do not actually exploit it, but only rely on level 1 and 2 detail obtained at an inadequate resolution for capturing level 3 detail [10]. For this reason, several studies have been undertaken looking into the added advantage of employing level 3 information [10–12] obtained with higher resolution sensors, which have become widely available. However, to date this level of information is only of limited use due to the lack of database entries, as most databases still only store lower resolution data [10]. Examples of each level of detail can be viewed in Figure 1.1, reproduced adhering to the IEEE copyright clearance for use of figures and tables in dissertations.

## LEVEL 1 FEATURES



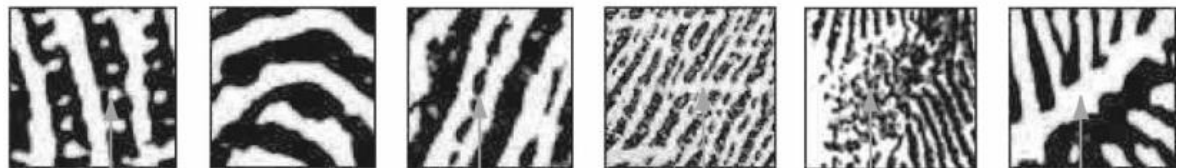
ARCH    TENTED ARCH    LEFT LOOP    RIGHT LOOP    DOUBLE LOOP    WHORL

## LEVEL 2 FEATURES



LINE-UNIT    LINE-FRAGMENT    ENDING    BIFURCATION    EYE    HOOK

## LEVEL 3 FEATURES



PORES    LINE SHAPE    INCIPIENT RIDGES    CREASES    WARTS    SCARS

**Figure 1.1** Visual examples of the three levels of information of fingerprints. Reproduced from Jain, Chen and Demirkus (2007) [10], ©2007 IEEE, as per the IEEE copyright clearance.

In England and Wales, a 16-point standard was implemented in 1953, meaning that any fingerprints matched with less than 16 *minutiae* could be challenged in court [1]. Evett and Williams investigated and challenged this standard in 1996, concluding that “There is no statistical justification for 16 points.” and that fingerprint identification is not an exact science [1]. Despite their findings and concerns, the system was in effect until 2001 [13], when it was changed after Scottish detective Shirley McKie had been wrongly accused of having left her prints at a murder scene [14]. It had already been under review by the Association of Chief Police Officers (ACPO) since 1996 [13] and the McKie case was perhaps only the final stimulus for the implementation of the recommendations made by Evett and Williams. A non-numerical system has since been implemented, similar to what Evett and Williams

described to be in place in the US and Canada at the time of their study, after they had visited bureaus in Europe and North America [1]. It should also be mentioned that although there is no need for a specific number of matching characteristics, identifications have to be made adhering to ACPO and Home Office guidelines, e.g. having been checked by three independent examiners, and that the discontinuation of the numerical standard did not appear to result in a larger number of erroneous conclusions (as reported 2005) [13], as was feared by some.

To supplement this non-numerical system and because recent years have seen a level of doubt regarding the uniqueness of fingerprints, several statistical models have also been developed and reviewed [15] to provide a probabilistic framework based on strong scientific principles as opposed to arbitrary numerical standards.

Although the name automated fingerprint identification system (AFIS) suggests the automation of fingerprint matching, latent print experts are usually still required to prepare prints, e.g. by identifying *minutiae* in the so-called mark-up, to be matched by the software and review the list of potential candidates generated in order to reach identification. Therefore both the crime scene mark and the ten-print marks in the database must be encoded with the identified *minutiae*. Whilst this is automated for the ten-prints, the quality of crime scene marks is usually inferior and the automatic feature extraction (AFE) marketed by some AFIS vendors varies in efficiency. For this reason, a latent print examiner or AFIS technician usually identifies and encodes the *minutiae* of latent prints manually [3]. However, several studies have noted discrepancies in the analysis made, mark-up and conclusions drawn between different experts [1,16]. This is especially true when it comes to challenging samples such as unclear or distorted marks, where the initial step might be to determine if a mark has value for identification or if any time analysing it would be wasted. This conclusion appears to be strongly linked with *minutiae* count [17]. However, it was also found that different examiners marked different *minutiae*, even when the overall number of *minutiae* marked was similar. Some examiners might mark more *minutiae* in unclear areas, thus assigning a higher value to a mark than others, who assigned fewer *minutiae* and therefore deemed the analysis inconclusive [18]. Furthermore, it

was found that examiners often revised their original mark-ups when comparing prints, raising concerns about comparison bias. However, the study also stated that the mere occurrence of such revisions was not usually indicative of erroneous conclusions and often reflected a change of value assignment from “value for exclusion only” to “value for individualisation” [2]. Nonetheless, findings like these underline the fact that fingerprint comparison is not an exact science but experience-based and standardisation at least in documentation of the Analysis, Comparison, Evaluation and Verification process might be advisable, as recommendations made by the Scientific Working Group on Friction Ridge Analysis, Study and Technology’s (SWGFAST) are unspecified and unenforced [2].

Several techniques are now available to enhance the visualisation of these three levels of information, with particular focus on the first two. However, these techniques only provide information regarding the physical conformation of a mark, enabling the match to a suspect. They completely neglect the retrieval of chemical information, which could provide additional intelligence on the individual that deposited their fingermarks. In recent years several analytical techniques have been exploited to generate a wealth of chemical information from fingerprints that, understandably, cannot be captured with a photograph of a crime scene mark.

Fingermarks, in fact, are a sweaty deposit consisting of endogenous and exogenous substances, mostly gland secretions such as lipids, fatty acids, amino acids, triacylglycerols, cholesterol, electrolytes and water [19], but also peptides and proteins such as skin keratins [19–21]. The chemical composition of latent fingermarks has been reviewed [21] and analysed with a number of techniques, which have been discussed in a 2016 review by Wei *et al.* [22] and 2017 by Francese *et al.* [23]. Some of those techniques, such as GC-MS and GC-FID, are destructive to ridge detail [24], while others, such as MALDI-MS [25], LAET-MS [26] and DESI [27,28], have imaging capabilities and therefore not only maintain ridge detail, but also map the distribution of the analytes investigated. Indeed, techniques have been reported that can image fingermarks down to pore level details [29,30]. In addition

to those unlabelled approaches, several protocols have been developed using nanoparticles, antibody-labels or antibody-functionalised nanoparticles for a targeted approach [31–34].

The exact chemical composition of each mark is affected by a number of factors such as donor characteristics, surface of deposition, environmental conditions to which the mark, fingers and surface were exposed and the enhancement techniques used to visualise the marks [21,35]. Often, these factors combine and affect the composition of the mark in an unpredictable way. This means that for example the level of fatty acids in a mark will be increased if the donor touched sebum-rich areas such as their face just prior to deposition [24]. It is known that cold and wet or previously washed hands leave poorer fingerprints [36], perhaps because the sweat glands secrete less in colder temperatures as the pores close and a lot of the natural secretions are washed away by wetting the hands, respectively.

In general, it is known that some people are better fingermark donors/secretors than others [30]. Such individual donor characteristics have also been exploited to determine the donor's sex from a fingermark, e.g. by statistical analysis of fingermark peptides and small proteins [37] or detection of different levels of sex hormones [26], potentially allowing investigators to narrow the pool of suspects. Although not relating to chemical information, other studies have been undertaken regarding sex determination through fingerprints, where the current consensus appears to be that fingerprints left by females have a higher ridge density than those of males [38].

In addition to characterising the general composition of fingermarks, several studies have been shown to successfully separate overlapping fingermarks. This is based on using individual donors' chemical constituents to give clear images of the individual prints [26,33,39]. Separating overlapping marks is very challenging to achieve with current computer algorithms. The use of chemical information to achieve this therefore provides a real advantage to fingerprint examiners in such cases, as they can successfully separate fingermarks and thereby provide more reliable evidence. The possible defence that a suspect's mark was not present, but

merely identified in error due to complex overlapping patterns can thus be refuted with this technique. Investigations have also been undertaken with regards to the age of a fingerprint to determine the time since deposition [40–43]. It should, however, be noted that the analytical techniques mentioned here have been considered in research projects, but are far from being exploited in crime laboratories.

In addition to endogenous chemicals and biochemicals, fingerprints can contain a wealth of information about the donor's lifestyle including diet and smoking habits [24,44], and possibly consumption of drugs of abuse via the detection of metabolites excreted [34,45–47].

As per Locard's principle, every contact leaves a trace. In the case of fingerprints, this means that, in addition to endogenous and excreted compounds, a range of external contaminants can be detected in them. These give an indication of what the donor has touched and may thereby help reconstructing events surrounding a crime. Exogenous contaminants can range from cosmetics or personal hygiene products [21,24,42], which might allow circumstantial evidence to be gathered regarding the perpetrator's identity, to compounds that link the donor to a crime. Contaminants reported include condom lubricants [48,49], gunshot residues, explosives [50,51], drugs [34,45,47,52,53] and biofluids such as blood [54–57].

Especially at the scenes of violent crimes, blood is a commonly encountered contaminant of fingerprints. The retrieval of information from both types of evidence, especially linking the two, can further inform and better direct investigations. Several drawbacks pertaining to the current analysis of blood and blood marks will be discussed in section 1.2. For these reasons, the study of blood forms the basis of the work presented in this PhD thesis, the aims of which are covered in section 1.6.

Due to the association of blood and fingerprints, the order of deposition can also be of interest in an investigation. This can be crucial when investigating the hypothesis or defence that a suspect touched a contaminated surface rather than having the

contaminant present on their fingers. This was reported by Bradshaw *et al.* (2011) pertaining to condom lubricants [48], but is also significant when it comes to questioned documents. As such, it has been shown that it can be determined if a fingerprint was deposited before or after a document was written or printed [58], therefore indicating whether the donor could have had knowledge of the document's contents. Following the same theoretical principle, fingermarks can have been left before, during or after an event of bloodshed and knowledge of the order of deposition can provide crucial information to an investigation. This is covered in more detail in section 1.1.2.

In conclusion, the evidential value of a fingermark reaches much further than its ridge detail and, employing novel analytical techniques, a wealth of additional chemical and structural information can be gathered to support the investigation by providing information about a donor's lifestyle or a link to the crime.

### **1.1.2 Blood evidence**

Blood is the most frequently encountered body fluid at the scene of a violent crime and can provide valuable intelligence in the forensic investigation of serious offences. However, various other biofluids might also be present and it can be of great importance to ascertain whether a trace found really contains blood or not.

With the robust and reliable detection of blood presence in spatter patterns, stains and fingermarks, such patterns can be interpreted to deliver information allowing the reconstruction of the sequence of events at a crime scene. Several books have been written on blood spatter pattern analysis [59,60] and papers are published on particular cases or scenarios of interest [61,62]. However, it can be difficult to determine the presence of blood with certainty, especially when it is suspected to be present in minute, invisible amounts or mixed with other biofluids and non-biofluid substances. This is due to the fact that currently used techniques for the detection of blood are not confirmatory, which is explained in more detail in chapter 1.2. Additionally, it can be challenging to ascertain if the suspected blood is of human origin or not. Furthermore, the presence of animal blood can further link a suspect

to the crime. An example of this was reported in a US murder case where no human blood was found on the suspects, but previously unidentified red stains on one suspect's sleeve were found to be the victim's dog's blood, placing the suspect at the crime scene [63]. Even in cases where no humans were harmed, animal blood has been able to incriminate suspects, for example when burglars silenced barking dogs by slitting their throats and contaminated their clothes with the dogs' blood [64]. In another curious case, a suspect's DNA was obtained from blood inside a leech, which was found at the scene of an armed robbery. A DNA match eventually linked the previously unidentified perpetrator to the crime when he was charged with unrelated drug offences 8 years later [65].

There are a number of additional scenarios from wildlife and veterinary forensics (including animal cruelty cases) where animal blood and establishing its provenance can be and has been of great importance [66,67], as well as animals being responsible for injuries or deaths. Most of these cases refer to DNA obtained from blood, which allows specific animals to be identified. However different DNA markers are required for each species. This means that identifying the candidate species beforehand reduces the number of DNA tests necessary, as the correct primers can be chosen directly instead of trialling several different species' primers. Furthermore, there might be a legitimate reason for the presence of DNA traces e.g. originating from saliva, whereas the presence of blood is usually regarded with much more suspicion. An animal cruelty case has been reported where llama blood was found on a teenager's clothing and identified as such through DNA testing [66]. While DNA analysis confirmed which specific llama was affected, it can perhaps be argued the presence of blood was incriminating in itself without this individualising information. It can be considered rather important to determine if the DNA profile was indeed obtained from llama blood or perhaps llama saliva, with which the suspect might have become contaminated when petting the animal.

Advances are being made with regards to determining blood provenance [54,68,69], which can inform the investigation further and be of great importance. Provenance determination can for example shed light on whether blood spatter on a car that is

suspected to have been involved in a “hit and run” incident or accident is in fact of human origin or might be the result of a road kill accident involving an animal. Establishing provenance can also corroborate or invalidate a suspect’s statement that blood found is not human but for example originated from an injured pet or meal preparation of a bloody steak. An example where such testing would have been useful is the Susan May case, where blood marks were found at the scene that were matched to Susan May’s prints. She, however, claimed the marks did not originate from her murdering her aunt but from preparing a steak for her [70].

Further information that is considered highly important to recover is the age (time since deposition) of blood (in a stain or fingermark), as this intelligence could provide information about the timeframe of the crime and thereby confirm or disprove a suspect’s alibi or statement in court. For this reason, several studies have attempted to date bloodstains [71–82] employing for example bioaffinity assays, reflectance spectroscopy or hyperspectral imaging for measuring changing ratios of biomolecules such as RNA or haemoglobin degradation products. However, again, these techniques are being researched rather than ready to be implemented and use in court would currently be unprecedented.

In addition to stains and spatter pattern analysis, blood has also been investigated in correlation to fingermarks [54,56,57] with regards to the association and order of deposition. In real casework, this can provide strong evidence that the fingermark donor was present at a crime scene during or in close time proximity to the event of bloodshed, as evidenced by the Rojas murder case [5] mentioned in 1.1.1. It can, however, also raise questions regarding the order of events, e.g. if a suspect claims to have arrived after the event of bloodshed; therefore the possibility of secondary transfer from dried blood stains has also been investigated [83]. However, it can be difficult to determine the order of deposition considering the following scenarios: a) bloodied mark, left by a bloodied finger; b) mark in blood or c) coincidental association, which originates from a clean fingertip on a clean surface and subsequent contamination with blood for example as a result of blood spatter. Especially scenario C is very difficult to identify, as the marks can visually appear

like genuine blood marks (therefore also called “faux blood marks”) [84]. To date no quantitative techniques have been developed to distinguish between them and the distinction is solely based on an examiner’s expertise, making it prone to errors.

Once the presence and provenance of blood has been demonstrated, it is, in theory, possible to obtain a plethora of additional information from it. Considering various blood diseases and protein variants like haemoglobinopathies, it might be possible to determine if the injured is suffering from a particular disease such as sickle cell disease [85], diabetes [86–88] or even myocardial infarction [89]. It can be hypothesized that this can narrow down the search by indicating that the injured will have to be taking a certain medication to treat the condition. Thereby it could also prove useful in unidentified missing person cases, where the identification of a disease via blood markers might indicate time constraints in locating the missing person in order for them to receive the necessary medication to treat life-threatening conditions. This could be particularly useful in combination with information on time since deposition to get an understanding of how long someone has been missing. In turn, determining that blood found at a scene belonged to e.g. a diabetic might provide clues to the whereabouts of a known missing diabetic even when DNA is not available for comparison. Medical conditions like diabetes are often included in missing person alerts [90].

In general, blood proteins are differentially expressed, meaning that some are much more abundant than others. As such, Anderson and Anderson report normal serum albumin concentrations of 35-50 mg/mL at the high abundance end, whereas Interleukin 6 is listed as a low abundance example with a normal range of 0-5 pg/mL serum [89]. Nonetheless, taking into account whole blood, haemoglobin is much more abundant with mean values ranging between 127-155 mg/mL, levels in females usually being slightly lower than in males [91], supporting observations that there are gender-specific differences in the blood proteome [92]. A table of a group of (blood) proteins and their normal ranges in blood can be found in Appendix 1. It should be noted that this includes blood-specific and non-specific proteins. Extensive research has been conducted pertaining to the characterisation of the

human plasma, serum and blood proteome, leading to the plasma proteome database (PPD, [www. plasmaproteomedatabase.org/](http://www.plasmaproteomedatabase.org/)) containing information on 10,546 serum/plasma proteins, including some mass spectrometric data [93].

In addition to gender differences and a normal range of variation in healthy subjects, protein expression levels change during life [92], potentially allowing the establishment of a likely age range for the injured. It is reported that plasma protein levels increase throughout infancy and that adult levels are reached by the age of 10, although a further increase can be observed with the onset of menopause [94]. Another study has investigated age-related differences in the plasma proteome from neonates to adults [92], and although this has mainly been in a clinical context, the potential to exploit this knowledge for forensic purposes should be evident, even though the potential for abnormal concentrations due to disease has to be taken into account.

Combining the information resulting from these individual areas of investigation therefore enables much more comprehensive intelligence that can narrow down both the number of possible crime scenarios and the range of suspects.

## **1.2 Currently used blood enhancement techniques (BET) and their shortcomings**

At a crime scene, potential blood stains or blood marks may be readily visible as a red stain or present in minute trace amounts that cannot be observed with the naked eye and therefore require enhancement to enable their detection. Either way, a red stain cannot automatically be assumed to be blood but requires presumptive tests to be performed in order to indicate its presence. To hold up in court, further tests are then required to confirm the presumptive identification. This sub-chapter covers techniques for the enhancement and detection of blood both in stains and fingermarks grouped by their target compounds or working mechanisms alongside methodologies for provenance determination. A variety of procedures has been developed in parallel, each providing its own advantages and disadvantages. A

chronological review of blood enhancement techniques (BETs) and their history is available in “Advances in Fingerprint Technology”, Chapter 9.1 [95].

The Home Office fingermark visualisation manual [36] describes a range of fingermark enhancement techniques (FET) as well as evaluating those that are suitable for the enhancement of blood-contaminated marks. It recommends workflows based on the evidence encountered and intelligence required, taking into account practical considerations such as the deposition surface or exhibits that have been subjected to the elements. In general, techniques are grouped into different categories. Category A describes techniques that are routinely used and considered safe. Categories B-F provide information about techniques that may offer potential for enhancement, may be used with caution or are not recommended for use, including a brief explanation why it is not a category A process. Unless use is not recommended, those techniques are considered for use in specific circumstances, e.g. where category A processes are not suitable or do not provide sufficient results. Furthermore, processes are assigned maturity levels, where high maturity means the process has been developed after years of scientific research with supportive operational data, and low maturity refers to limited scientific data and no operational data. Nonetheless, it is important to note that none of the BETs described are considered sufficiently confirmatory.

Three classes of chemically reactive BETs are commonly distinguished, in order of increasing specificity: (i) amino-reactive compounds, (ii) protein dyes and (iii) haem-reactive compounds [57]. It should be noted that amino-reactive and protein dyes are often grouped together or not further distinguished. This is due to fact that proteins are made of amino acids and both techniques are based on the reaction with the amine- or other functional groups found on proteins and amino acids [36,96]. In addition, several chemiluminescent and microcrystalline tests are known as well as spectroscopic techniques. The latter are the subject of current research and most have therefore not found their way into routine employment yet. Currently UK police forces recommend the use of acid dyes (also called protein dyes) as the most advanced and well-suited method for the enhancement of blood

and blood fingerprints [36]. It should be noted, however, that several different dyes and solvent formulations are available and whilst some are recommended category A processes, others fall into categories B-F, for example because an equivalent category A process produces better results [36]. Nonetheless, large scale screening, e.g. with alternative light sources, might be required prior to the more targeted enhancement with acid dyes.

### **1.2.1 Fluorescence-based tests and alternative light sources**

Several techniques are available for screening large areas of a crime scene for the presumptive presence of blood. These usually employ either alternative light sources (ALS), thereby being classed as optical methods, or fluorescent reagents that enable optical or spectroscopic methods to be applied due to the underlying chemical reaction that causes fluorescence to be observable under certain light conditions.

Luminol (5-amino-2,3-dihydro-1,4-phthalazinedione) is a reagent that exists in numerous formulations, usually containing either hydrogen peroxide or sodium perborate [97] in order to produce chemiluminescence aided by the peroxidising activity of haem [36,98,99]. While the reagent is highly sensitive to small traces of blood down to the nanogram level or 1:300,000 [36,99,100] or 1:1,000,000 [101], dark conditions are required in order to observe its fluorescence. Due to the ability of other compounds to catalyse peroxidation, a variety of false positives has been reported, ranging from vegetables to bleach, metals and terracotta tiles [97,100,102]. Experts claim, however, that it is possible for experienced investigators to distinguish blood from a false positive, e.g. based on small differences in the obtained spectral shift, i.e. the mean position of the peak [97,103]. Luminol is considered safer, is more sensitive and has been demonstrated to give a lower rate of false negatives than to other tests and reagents [100,104]. However, Virkler and Lednev [105] claim that Luminol and the UV wavelength employed to visualise it can damage DNA. Several other studies [98,103,106–108] have demonstrated that luminol is non-destructive to blood and surroundings and compatible with additionally carried out presumptive, confirmatory or serological tests for species determination and DNA analysis. These can be essential in criminal investigations. Luminol does not react with other body

fluids [103] and can be applied several times [100], although this does risk diffusion of the stain [101]. Whilst diffusion does not significantly affect the recovery of evidential stains, it would severely affect the integrity of the ridge pattern of blood fingermarks. As the lack of a fixative leads to diffusion and destruction of ridge detail [36], the Home Office discourages the use of luminol for fingermark enhancement and lists it as a category E process.

Another fluorescent reagent suitable for large-scale crime scene use is fluorescein, which is oxidised into fluorescein by a haem-catalysed reaction, similar to that of luminol. Unlike luminol, fluorescein only emits fluorescence when exposed to an ALS at a wavelength of 425-485 nm, and it is considered non-destructive to DNA [105,106]. The sensitivity of Hemascein®, a commercially produced fluorescein kit, on fabrics and linoleum is superior to luminol, but poor results were obtained on plywood [109].

Although not based on a chemical reaction, ALSs such as Polilight® can be used to screen a crime scene for the presence of blood. This is, however, less sensitive than the use of luminol and therefore provides little benefit on light-coloured backgrounds, where detectable bloodstains are generally visible to the naked eye in most cases. Polilight® also provides poor results on highly absorbent fabrics such as fleece, but has a considerable advantage over luminol in that it can visualise bloodstains that have been painted over. This is because it is based on blood's strong absorption at 415 nm, whereas some paints can exhibit fluorescence near-identical to that of luminol. Additionally, Polilight® can indicate the presence of other body fluids based on their fluorescence at certain wavelengths, although their identification is not possible [101]. Complementing this technique, digital enhancement and background correction algorithms of images have been successfully tested to improve visibility and detection rate of untreated bloodstains photographed under ALS illumination [110].

Seidl *et al.* investigated a portable forensic laser head and a mercury-arc lamp for the screening and detection of body fluids, but came to the conclusion that the laser

cannot detect blood at all. The mercury-arc lamp demonstrated poor sensitivity by detecting only dilutions down to 1:100 and an inability to differentiate body fluid stains from each other due to marginal differences in fluorescence [111].

## **1.2.2 Other chemical enhancement techniques**

Despite luminol's high sensitivity and ability to screen large areas for blood, several other techniques are still being used for the detection and presumptive or confirmatory identification of blood at a crime scene. Generally, these tests can be grouped into the following categories: haem-reactive or peroxidase-based reagents, amino-reactive reagents and protein dyes, immunogenic tests and microcrystalline tests, each exhibiting their own advantages and disadvantages.

### **1.2.2.1 Haem-reactive tests**

Haem-reactive tests are based on a haem-catalysed peroxidation-reaction that usually results in a colour change indicating the presence of haem and thereby blood. The general underlying mechanism of the haem-peroxidase activity as well as the structure of haem can be seen in Figure 1.2. However, due to the nature of the reaction, peroxidation can be facilitated by a number of other compounds, therefore resulting in false positives. Several haem-reactive tests are known and have been investigated with regards to their sensitivity, toxicity and error rates.

A popular (and reportedly the first) haem-reactive test which was used from 1904 onwards was using benzidine. Initially thought to be blood-specific, it was later found to be peroxidase-based, as all haem-reactive tests are. Due to its high sensitivity and drastic colour change from colourless to dark blue, benzidine was widely used until its adverse health effects were noted [112]. After the benzidine test was banned in the USA in 1974 due to its high toxicity and carcinogenicity [104,113], several structurally related compounds were investigated in attempts to identify a suitable replacement. Tetramethylbenzidine (TMB) was demonstrated to have the same sensitivity and specificity but lower toxicity and solubility. Despite producing false positives with e.g. horseradish and beet leaves that are commonly observed with

haem-based tests, Garner *et al.* claimed TMB was reliable “in the hand of experienced serologists” in 1976 [113]. The UK Home Office, however, discourages the use of TMB due to reduced sensitivity in comparison to e.g. acid black 1 and concerns about TMB’s possible carcinogenicity and mutagenicity [112]. Despite its ban in the US, benzidine was further investigated and termed “not sufficiently reliable” by a Spanish group in 1995 [114]. Similarly, 2,2’-azino-di-[3-ethylbenzthiazolinesulfonate(6)] diammonium salt (ABTS) is considered a safer, non-carcinogenic alternative to 3,3’-di-aminobenzidine (DAB), with its bright green colour being another advantage providing superior contrast on dark surfaces compared to DAB’s dark brown colour. Although both reagents are peroxidase-based, DAB can be used subsequently to ABTS [115]; however it has been shown to have little use for the enhancement of blood fingermarks. This is partially due to the solution’s instability and the dark brown product colour being very similar in appearance to dried blood [96].

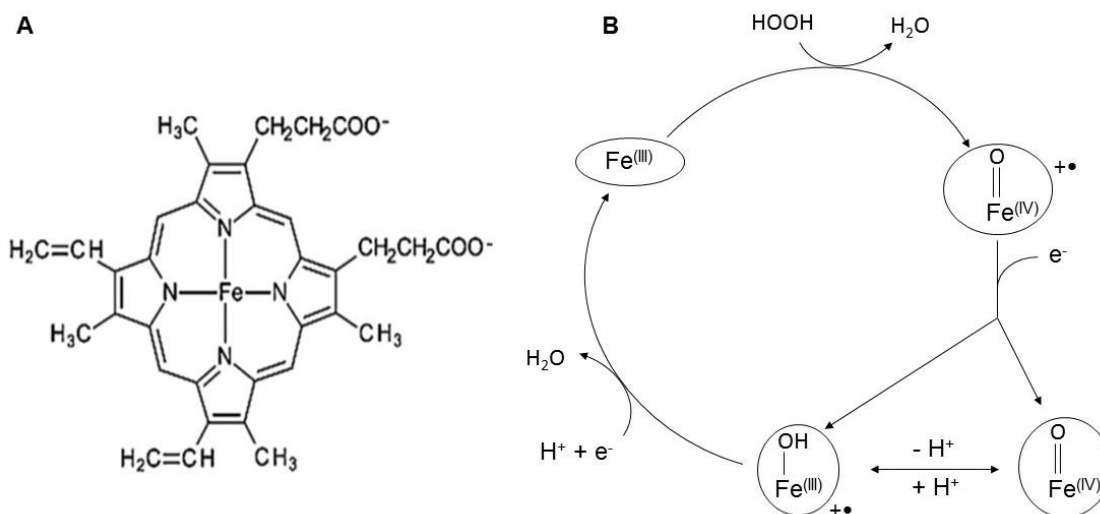


**Figure 1.2** A: Structure of haem. B: The catalytic redox cycle underlying haem-reactive compounds. Electrons ( $e^-$ ) are supplied by haem-reactive dyes and oxidised to form coloured compounds and water. (Re-drawn from [116].)

In 1991, Cox compared phenolphthalein, orthotolidine (o-tolidine), leuco malachite green (LMG) and TMB in terms of sensitivity and specificity and concluded that, while o-tolidine and TMB were most sensitive, LMG and phenolphthalein were most specific out of the four peroxidising reagents [117]. As LMG was found to be the least

sensitive, the use of phenolphthalein was recommended. Furthermore, the use of o-tolidine has since also been discontinued due to toxicity [104]. These authors also compared the Polilight® with haem-reactive tests Kastle-Meyer (KM; reactive ingredient phenolphthalein), LMG, luminol and Hemastix®, a haemoglobin chemical reagent test strip, and demonstrated that the least sensitive Polilight® is 50,000 times less sensitive than luminol and 10 times less sensitive than LMG. Hemastix®, KM and LMG exhibited reduced sensitivity when applied to swabs or filter paper, i.e. not directly to the stain [104] such as in Vandewoestyne *et al.*'s visualisation assay [118].

Variability in sensitivity of KM and LMG has been described alongside potential carcinogenicity. Studies carried out on haemoglobin solutions rather than blood showed that all techniques were still able to detect haemoglobin after 7 weeks of ageing [104].

Although the working agent in Hemastix® is TMB, it is more sensitive and specific than TMB alone, but still gives false positives [119]. It also gives false negatives in the case of highly degraded samples when EDTA is added to increase specificity, as this chelates haem. However, it was shown to remain efficient on archaeological samples, although low temperatures can pose problems [119]. When investigated for blood footwear impressions on fabric, Bluestar® Luminol was the only haem-reactive reagent to enhance all prints and provide clear detail on denim and leather, where LMG, leuco crystal violet (LCV) and fluorescein demonstrated poor results. Additionally, LMG and LCV provide poor enhancement on dark surfaces and it was shown that none of the reagents detected blood after laundering of the substrate fabric [120] although it was not clear whether this may have been due to efficient removal of the blood in the washing process.

Other researchers, however, have demonstrated the ability of KM, LMG, Hemastix®, TMB and Polilight® to detect bloodstains on fabric both after hand and machine washing. Hemastix® and KM were found to be the most, and LMG the least

sensitive, although results depended on the detergent used and the fabric's ability to retain blood [101,121–123].

In addition to the compounds commonly observed to cause false positives in haem-reactive tests [54,97,99–102,112,124–126], one study reports similar appearance of stains and reaction with phenolphthalein of legume root nodules due to their expression of leghemoglobin, which is structurally and functionally similar to haemoglobin. Moreover, the study demonstrated that if clothing presenting such a stain is submitted for DNA analysis, results show the wearer's DNA profile, thus potentially misleading investigators to believe the stain is composed of the wearer's blood [127]. Similarly, several tests were evaluated for their ability to distinguish blood from blow fly artefacts produced from flies feeding on blood, but proved to be unreliable [128].

#### **1.2.2.2 Amino-reactive reagents**

While some literature is available concerning haem-reactive tests for the enhancement of fingerprints [96,115,129,130], there seems to be no literature regarding the detection of bloodstains by amino acid-reagents or protein dyes. These appear to be predominantly used on blood fingermarks or other non-stain pattern shapes such as footwear impressions. Protein-reactive reagents react with the amine group or other functional groups within all proteins [96] to produce colour. To allow visualisation on various substrates, a range of formulations is available to choose from resulting in light, dark or even fluorescent colours; examples include fuchsin acid (acid violet 19, hungarian red), acid black 1 (ab1), acid yellow 7 (ay7), acid violet 17 (av17), ninhydrin, coomassie blue (acid blue 83) and crowle's double stain (acid blue 83 and acid red 71) [131]. An example illustrating the interaction between AB1 and a protein can be seen in Figure 1.3.

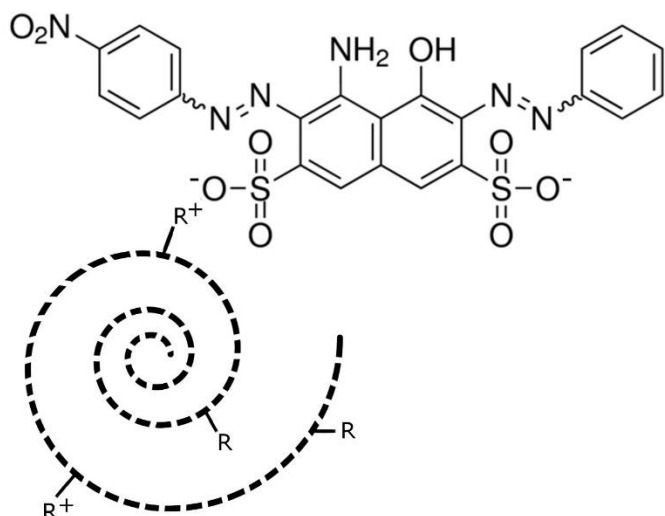


**Figure 1.3** Schematic interaction between acid black 1 (top) and a possible protein (bottom) with R and R<sup>+</sup> as possible protein side groups. (Chemical structure obtained from sigmaaldrich.com, CAS 1064-48-8; re-drawn from [57].)

An evident drawback for these reagents is the fact that their target substances are not exclusive to blood and can therefore elicit a vast range of false positives. Marchant and Tague compared ABTS and fluorescein with the protein dyes AB1 and Coomassie Blue for the enhancement of blood fingermarks on various surfaces, the success of which was dependent on the surface. Visual images of only 6-50% of fingermarks that tested positive for blood were usable for obtaining ridge detail, fluorescein demonstrating the poorest performance followed by aqueous AB1 (H<sub>2</sub>O-AB1) [130], which is known to diffuse ridge detail [132]. AB1 in a methanol-based formulation (MeOH-AB1) provided the best results and performed equally well on porous and non-porous surfaces, followed by ABTS which worked slightly better on porous surfaces than MeOH-AB1. It was, however, inferior on non-porous substrates [130], although ABTS had been reported to show little potential for use on blood fingermarks previously [96]. An issue that has been reported is that MeOH-AB1 may be more damaging to evidence and substrates than the water-based formulation by for example causing background discolouration [130,132,133]. In order to overcome problems associated with both AB1 solvent systems, an alternative ethanol/water-formulation was developed and is currently one of the protein dyes recommended by UK police forces for the enhancement of blood fingermarks, despite exhibiting slightly more background staining [36,132]. Other recommended dyes are the

fluorescent acid yellow 7 (AY7) for non-porous surfaces and acid violet 17 (AV17), both of which are especially useful on dark surfaces [120,134]. Further amino-reactive reagents have also been evaluated by both Pereira and Sears *et al.*, who list 1,8-diazafluoren-9-one (DFO) and ninhydrin (2,2-dihydroxy-1,3-indanedione) as alternatives for porous surfaces [96,133] including light-coloured fabrics [135]. These, however, also enhance latent, non-blood prints, whereas AB1, AV17 and AY7 only enhance blood [120,134] and have been demonstrated to remain effective for the recovery from fire scenes exposed to up to 200°C and soot removal, where e.g. LCV was ineffective even for lower temperatures [136].

In their review of enhancement techniques for blood fingermarks Bossers *et al.* claim haem-reactive compounds provide less background staining and are more specific to blood than protein dyes, some of which also enhance latent fingermarks. They also state that titanium dioxide (TiO<sub>2</sub>) has an affinity for proteins and amino acids, while cadmium telluride (CdTe) quantum dots have an affinity for haemoglobin [57]. This affinity has since been exploited for a specific blood lifting tape called ZarPro™, which is a paper-like strip impregnated with TiO<sub>2</sub> that is misted with an activator solution of 50% methanol and binds blood proteins upon contact with the stain or fingermark, allowing for a proteinaceous impression to be lifted off the surface. Although the strips are white and as such already provide good contrast for patent marks, they are also inherently fluorescent, allowing easy visualisation of faint, poorly visible marks [137].

Similar principles have been proposed for potential biosensing mechanisms that have been discussed for body fluid identification e.g. by inducing different coloured fluorescence based on the type of body fluid [138]. Although the proposing article suggested the usefulness of simultaneous biosensor use, the group originally published individual studies for various fluids. The biosensor for blood employed in their studies uses fluorescent semiconductor quantum dots conjugated with antibodies against the human glycophorin A, an erythrocyte membrane protein [139].

While the Home Office provides extensive recommendations regarding operational

workflows, deposition surfaces and suitable enhancement techniques for blood fingermarks in their fingerprint source book [140] and the fingerprint visualisation manual [36], studies have also been undertaken elsewhere regarding the recovery of blood fingermarks from fruit and vegetables, and here protein dyes have been deemed the most successful [141]. Several studies have also evaluated the effect of haem-reactive tests and protein-dyes on the success and sensitivity of DNA recovery and analysis, for example demonstrating a reduction in yield by a factor between 2 and 12 [129], especially if the process requires a de-staining step. No short-term effect on DNA amplification has been observed unless considering the discontinued benzidine [108] or LMG [142], which merely requires neutralisation before DNA analysis [143]. Long-term exposure, on the other hand, has been shown to affect DNA integrity and increase degradation [108,129,144], resulting in the recommendation to perform DNA analysis within a maximum of 30 days after enhancement, at which point e.g. Luminol starts degrading DNA. After 120 days, all treated samples showed DNA degradation, while non-treated samples did not [108]. Another study reported that H<sub>2</sub>O-AB1 and LCV negatively affect mRNA profiling [145].

### **1.2.3 Microcrystalline tests**

Microcrystalline tests are tests in which crystals are formed between haemoglobin and the reagent to indicate the presence of blood. The popular microcrystalline Takayama and Teichmann tests are commonly considered confirmatory. However, they require blood to be scraped off a surface and treated in a laboratory, making them unsuitable for onsite use and the analysis of blood fingermarks without destruction of ridge detail [95]. Additionally, it means that they cannot be used speculatively, as suspected blood must be visible and easily observed in order to be scraped off. However, fingerprinting powder does not affect the crystal-formation of microcrystalline tests and thus does not hinder blood identification [146] if carried out after visualisation with powders and photography of ridges.

Both tests are based on the reagent forming crystals with haemoglobin, which can be observed under a microscope [105,112,124,147–150]. In the case of the Teichmann test, these crystals are hematin, whereas hemochromogen is formed in

the Takayama test. Interestingly, these tests were developed as early as 1853 and 1912, respectively [131].

#### **1.2.4 RNA analysis for body fluid identification**

For forensic purposes, the analysis of nucleic acids such as deoxyribonucleic acid (DNA) is commonly used for identification of a subject or determination of familial relations. To do this, the number of repeats of various genes is compared between samples in what is often simply referred to as a “DNA test”. While undoubtedly useful, these analyses do not provide insight into the nature of the source, as they do not discriminate whether a sample originates from for example skin or blood cells. Therefore, they do not inherently allow the detection of blood, which can be of great importance to an investigation and suggest an entirely different dynamic of a crime.

However, another type of nucleic acid, ribonucleic acid (RNA) has been investigated to bridge the gap and allow blood detection through nucleic acid analysis. Mostly this is employing messenger RNA (mRNA), the expression of which varies between cell types [151]. Although it is usually expected to degrade rapidly [152], its stability in forensic stains has been demonstrated for samples of up to 16 years in age [153–155]. Due to its differential expression, several studies have evaluated mRNA markers for blood, however while they are most abundant in blood, they may not be entirely absent in other body fluids and tissues [151,156–158]. For example blood mRNA markers have been found in vaginal fluid at comparable expression levels [159] and some markers cannot be identified due to physiological variation in expression [151]. Multiplex assays, which can simultaneously detect multiple target analytes, have also been developed for body fluid identification, with some assays even cutting the need for fluorescently labelled primers to reduce time and cost. However, the majority of these multiplex assays only use two markers per body fluid [151,156–158]. In combination with the non-exclusive expression of those mRNA markers, this can be seen as a drawback potentially leading to misclassification of samples. Furthermore, those RNA multiplex systems have shown cross-reactivity with mRNA markers of domestic animals [160], compromising the confident identification of human blood. Further to mRNA, small, non-coding micro-RNAs have

also been employed for the identification of blood [161–164], being sensitive enough to detect as little as 50 pg of RNA [162].

Regardless of potential drawbacks, advances that have recently been made in the field of analysis may make it possible to combine the analysis of DNA with RNA analysis. Techniques are now available for the simultaneous co-extraction of DNA and RNA from one sample, which is useful if both are required [154,165]. It should be noted, though, that this combined extraction technique offers lower sensitivity for DNA than conventional extraction methods used for one target molecule.

### **1.2.5 Spectroscopic techniques**

Besides the chemical tests, there has been a growing interest in the development of spectroscopic techniques for the identification of blood and its discrimination from other body fluids. In particular, the development of hand-held devices potentially enables such analyses to be performed at the crime scene [166,167]. Statistical analysis of the peaks in Raman spectra, for example, is reported to allow the discrimination of body fluids even in mixtures with component contributions of a few percent [105,168–174], as well as differentiating between human and animal blood [175] and non-blood substances [148]. The ability to detect blood dilutions of 1:250 places the technique's sensitivity in line with that of KM, LGM and ALS, but below that of luminol [167,176]. Furthermore it allows the use of reconstituted samples, e.g. from fabric extracts, which also solves the problem of strongly luminescent substrates such as fabrics interfering with analysis [167,176].

Conflicting opinions exist on the identity of the two main components producing the peaks, with some researchers stating they originate from haemoglobin and haem aggregation products [177], indicating spectra are exclusively attributable to haemoglobin and its denaturation products, while others claim it is haemoglobin and fibrin [167,171]. As samples become heterogeneous in constituent distribution once dried, spectra at different points vary from each other and spectra of multiple points are required to satisfactorily represent a sample [172]. While some studies report that species determination is not possible based on Raman spectra due to the large haemoglobin sequence homology [148,149], others report it is possible with the aid

of principal component analysis (PCA) [68,175,178]. Although the detection of blood in heavily contaminated samples is still possible [179], in tape lifted blood mark samples, tapes may produce interference due to their large background fluorescence [148].

Surface enhanced raman scattering (SERS), a subset of Raman spectroscopy, has also been used for the analysis of plasma. It should be noted that it is therefore also looking at other biomolecules such as proteins, lipoproteins, carbohydrates and small organic molecules, instead of only haemoglobin and possibly fibrin, as has been reported for Raman. For this reason, it is demonstrating independence from haemoglobin signals, which form the exclusive basis of near-infrared Raman (NIR) spectra [180]. A SERS-substrate has been developed that increases the poor sensitivity of Raman by 2 orders of magnitude to 1:100,000 dilutions and allows swabbing of the substrate over the blood sample, thus providing another method for overcoming the luminescence of fabrics [176].

Spectrophotometric techniques used for the analysis of blood include UV-VIS microspectrophotometry, attenuated total reflectance Fourier-transform-infrared spectroscopy (ATR FT-IR), reflectance spectroscopy and NIR, all of which are able to differentiate body fluids but not blood species origin [124,148,149,181,182].

Hyperspectral imaging, which combines photography or optical imaging with spectroscopic analysis [183,184], has been used to distinguish blood from non-blood substances. However, it is unsuitable for black substrates and a reference spectrum is required from the substrate, which can be difficult in a crime scene-context as it cannot be taken for granted that the reference is blood-free. On red substrates, the sensitivity is reduced from 512-fold dilutions to 32-fold dilutions and it works best on light-coloured substrates [185]. Additionally, the instrument's imaging field and sample enclosure may be unsuitable for large samples containing blood marks that can be removed from the crime scene [183], such as baseball bats.

A study has been published on proton-nuclear magnetic resonance ( $^1\text{H-NMR}$ )

spectroscopy, which successfully demonstrated the identification of blood in body fluid mixtures via PCA. However, serum was studied rather than whole blood, extracts of crime scene stains were not mentioned and the differentiating features were not exclusive to a particular body fluid but merely chosen due to them exhibiting intense signals in all spectra of that body fluid [186]. This means that they could be present in other substances. Similarly, work on a self-calibrating X-ray fluorescence (XRF) system seemed to identify blood mainly based on the iron signal in its environmental signature and large preservative peaks were observed due to the blood being sourced from a blood bank [187], although this could be beneficial in identifying staged crimes, where blood from a blood bank may have been used.

#### **1.2.5.1 Mass Spectrometry**

Mass spectrometry (MS) has been used as a specific and confirmatory technique for the detection and identification of blood on its own or simultaneously with other body fluids and substances. MS has the advantage that no presumptive knowledge about sample identity is necessary [54,188] and matrix-assisted laser desorption/ionisation mass spectrometry (MALDI-MS) imaging of latent fingermarks has successfully been added to the Home Office fingermark visualisation manual as a category C process [36]. According to Espinoza *et al.*, who analysed blood samples from different animal species for their intact haemoglobin signals using electrospray ionisation mass spectrometry (ESI-MS), each species typically presents 2-5 haemoglobin variants [69]. This can perhaps affect the ability of other techniques to detect haemoglobin, for example if the variation results in an altered spectral shift or absorption band or an altered or sterically hindered antibody binding site used for provenance determination. Additionally, knowledge of the sequence variations is required in order to identify proteins or their tryptic peptides detected as haemoglobin or other blood-specific signals, without this knowledge they might be mistaken for other signals. Yang *et al.* employed high performance liquid chromatography-matrix-assisted laser desorption/ionisation-mass spectrometry (HPLC-MALDI-MS) for protein and peptide analysis of overnight digests of blood that underwent multiple lengthy sample preparation steps. However, they only analysed haemoglobin alpha and beta as well as band 3 anion transport protein (also known as erythrocyte

membrane protein band 3) [188]. Additionally, this group has analysed the proteome of menstrual blood and compared it to venous blood and vaginal fluid, the other two components of menstrual blood. In doing so, they identified 385 proteins (36% of the total proteome identified in the experiment) that did not originate from venous blood or vaginal fluid and can therefore be considered unique to menstrual blood [189].

### **1.2.6 Provenance determination of blood**

In addition to the problems previously described with false positives, the currently used blood enhancement techniques are not specific to human blood and the ability of spectroscopic techniques to identify the species origin of a blood sample is not proven. Because blood provenance can be of paramount importance in a criminal investigation [63,64,66,67,70], immunogenic tests such as crossover-electrophoresis, radioimmunoassay, Ouchterlony double diffusion and enzyme-linked immunosorbent assays (ELISAs) have been in use since the 1970s in an attempt to provide such additional intelligence [190–193]. The success of these tests depends on the target protein, as for example immunoglobulin G (IgG) was only detectable for up to 8 weeks after bloodshed, whereas albumin was still detectable after 15 months of ageing [193]. However, IgG is also expressed in body fluids other than blood, albeit at lower levels [194]. Similarly, many immunogenic tests cross-react with primate blood [192,195] due to the large sequence homology between human and primate proteins.

Although some tests have to be carried out in a laboratory, a variety of strip tests (usable in the field), such as Hexagon OBTI (Gesellschaft für Biochemica und Diagnostic mbH, Wiesbaden, Germany) or HemaTrace® (Abacus Diagnostics, West Hills CA, USA) are available. The majority are haemoglobin based and hence not only exhibit cross-reaction with primate blood, but with blood from other species, e.g. ferret blood [196]. The exception to this is the Rapid Stain Identification™-Blood (RSID™-Blood) strip test (Independent Forensics, Lombard IL, USA), which claims specificity for human blood via two antibodies against glycophorin A, a red blood cell membrane specific protein. This has been shown not to exhibit false positives with ferret, skunk or primate blood samples [126]. The test is also said to remain efficient

for samples of up to 10 years of age, albeit with lower sensitivity than haemoglobin-based tests [197].

Passi *et al.* also state that luminol has very little effect on the subsequent use of the Ouchterlony double diffusion test, in which 84.6% of luminol-treated samples could still be correctly typed for species determination using antibody-based techniques. This number reduces to 76.9% with bleach treatment, which may occur in an attempt to clean the crime scene [98]. While no success rate is given for untreated samples, it may be arguable whether a confidence interval of about 85% is sufficient or not for confirmatory species determination in a criminal investigation.

Another laboratory-based test has been developed to locate human-specific blood *in situ*, e.g. on fibres, by staining minute amounts of blood (as little as individual blood cells) with fluorescently labelled antibodies (anti-glycophorin A [HIR2], anti-CD45 [transmembrane protein tyrosine phosphatase], anti-MPO [hemoprotein in azurophilic granules within neutrophils] and anti-human histone H1). These can then be visualised with a fluorescence microscope. No cross-reaction was observed with ferret blood, but surprisingly primates were not tested [198].

Raman spectroscopy has recently emerged as a new technique for provenance determination, however this is only possible if advanced data analysis protocols such as PCA are applied. The features of Raman spectra correspond to vibrational modes of haemoglobin and it is suspected that the differences leading to separate PCA classes are due to interspecies differences in haemoglobin [68,175,178]. No references to the testing of primate blood were found, but it may be hypothesised that differentiation would be impossible due to the large sequence homology with human haemoglobin. As the technique also relies largely on slight differences in signal intensities, it remains questionable whether the correct classification of a mixed species sample would be possible. As it has been reported that 2-5 haemoglobin variants are commonly observed in each species [69], which has the potential to complicate haemoglobin-based species identification.

### 1.3 Introduction to MALDI-mass spectrometry

Mass spectrometry is an analytical technique that can be used to gain insight into a sample's chemical composition by measuring the molecular masses of components contained within it. Briefly, a mass spectrometer is composed of an ion source, in which compounds are ionised to produce gas-phase ions, followed by a mass analyser or selector, which separates ions based on their mass-to-charge ratio ( $m/z$ ), and a detector, which detects the ions produced and separated in the previous components and generates a spectrum displaying the ion signals detected.

Several different ionisation methods are available ranging from soft ionisation techniques (e.g. MALDI, ESI), which result in little to no fragmentation of molecular species, to high energy deposition ionisation techniques (e.g. electron ionisation), which produce fragment ions. Depending on the target analyte and conditions required, a variety of instruments and hyphenated instruments, which combine several techniques in sequence, are therefore available to choose from.

The soft ionisation technique MALDI was selected for this project for its high sensitivity (down to a few femtomoles of material [199]) and because its lack of fragmentation is advantageous for the analysis of proteins, peptides and other complex biomolecules. Additionally, its imaging capabilities allow the mapping of an analyte's spatial distribution in a sample, which is desirable for the biochemical analysis of fingerprints. The technique is also tolerant of low quantities of salts [200], which can be present in fingerprints and sweat.

The invention of MALDI-MS is the subject of some controversy. Whilst it was Koichi Tanaka who received part of the Nobel prize for Chemistry in 2002 for his development of a laser desorption ionisation technique [201], Karas *et al.* are credited with the idea of employing an organic matrix [202], which results in better ionisation efficiency and therefore is the approach widely used. In order for the sample to be ionised, it is mixed with a chemical called a matrix, typically a small, non-volatile and UV-absorbing weak organic acid containing a chromophore [53], and allowed to co-crystallise.

A laser, commonly nitrogen (N<sub>2</sub>) or neodymium-doped yttrium aluminium garnet (Nd:YAG), is fired at the matrix-sample co-crystals. The emitted laser energy, e.g. 355 nm in the case of the Nd:YAG or 337 nm in the N<sub>2</sub> laser in UV-MALDI [202], is absorbed by the matrix, leading to desorption and ionisation of the co-crystals. The matrix, which should have a strong absorbance at the laser's wavelength, absorbs most of the laser energy, thereby minimising analyte fragmentation. Several matrices are available, the choice of which is dependent on the target mass range, analyte type and instrument polarity. For this study,  $\alpha$ -cyano-4-hydroxycinnamic acid (CHCA) was chosen, which, like 2,5-dihydroxybenzoic acid (DHB), is commonly used for low molecular weight peptides and lipids, whereas sinapinic acid (3,5-dimethoxy-4-hydroxycinnamic acid, SA) is often used for proteins [203]. It should be noted that crystallisation is often inhomogeneous and the resulting "sweet spots" result in fluctuating ion signal intensities. As the matrix also ionises, it can produce strong background signals ("matrix peaks/clusters"), especially in the low mass range, or it may cause ion suppression of target analytes. One strategy to overcome the phenomenon of matrix cluster ions in peptide analysis is the addition of aniline to the matrix solution in order to suppress matrix peaks in the relevant mass range, as it enhances solubilisation of the matrix and aids crystallisation [204–208].

Due to its ability to detect a wide range of molecules, including drugs and biomolecules such as lipids and proteins, without the need for labelling with probes or antibodies, MALDI-MS has been previously applied to a variety of samples of biomedical and biochemical interest as well as forensic samples such as dyes [209] or blood for blood group genotyping [210].

### **1.3.1 Ionisation theory in MALDI**

The theory of desorption in MALDI has been reviewed by Dreisewerd in 2003, who describes one possible mechanism to be that analytes enter the gas phase through localised sublimation caused by the fast heating of co-crystals via vibrational excitation of matrix molecules during laser irradiation [211]. Similarly, multiple complex ionisation theories have been devised, although a consensus has been

reached that ionisation is achieved through a two-step process consisting of primary ionisation and secondary ion-molecule interactions [200]. However, the exact nature of these two steps is still discussed.

Two models discussed for primary ionisation in MALDI are the cluster model, devised by the Karas group, and the photoexcitation/pooling model. Both have been described in detail in Knochenmuss' review of ion formation mechanisms in UV-MALDI, alongside other less widely discussed models [200]. In the cluster model, the matrix is viewed as a desorption vehicle carrying pre-formed ions that are subjected to neutralisation in the ion plume (Figure 1.4). In the photoexcitation/pooling model it is theorised that neighbouring matrix molecules are separately photoexcited but distribute the energy to create pools of a higher excitation state, thereby reaching sufficient levels of energy to achieve ionisation (Figure 1.5) [200,212]. The secondary reactions are then described as collisions between matrix and analyte or analyte and analyte molecules in the ion plume, resulting in either proton transfer, electron transfer or cationisation, depending on the analyte and matrix chemistry and selected instrument polarity [200,213]. The theory widely accepted for positive mode MALDI is that of proton transfer from photo-ionised matrix molecules to analytes.

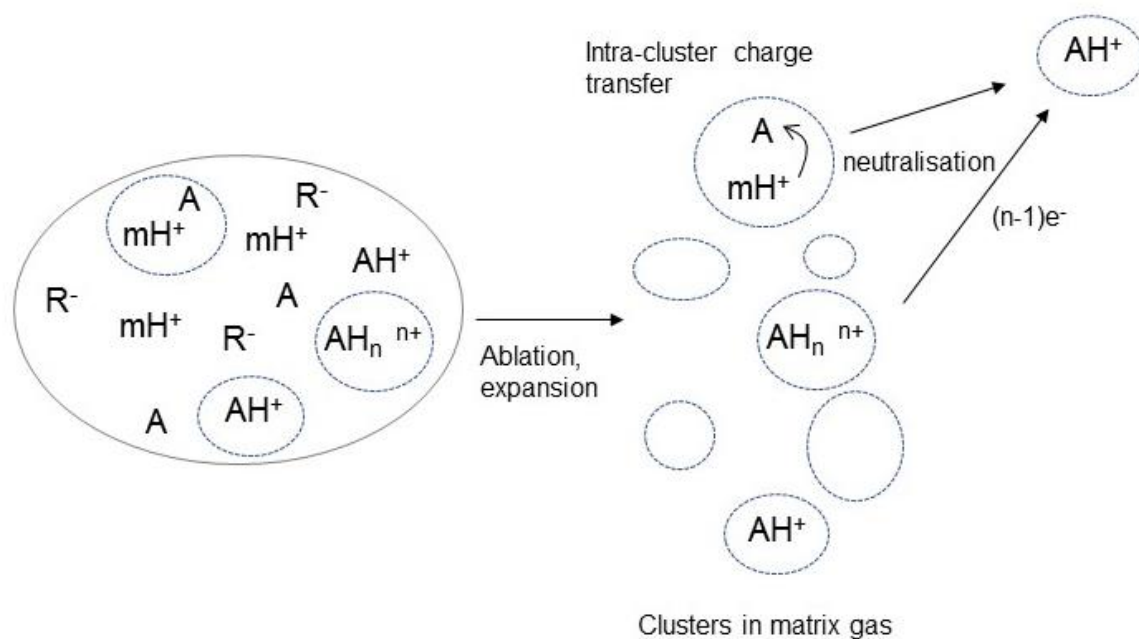


**Figure 1.4** Simplified schematic of the major process proposed in the cluster ionisation model.  $m$  = matrix,  $A$  = analyte,  $R^-$  = generic counter ion. (Re-drawn from [200]).

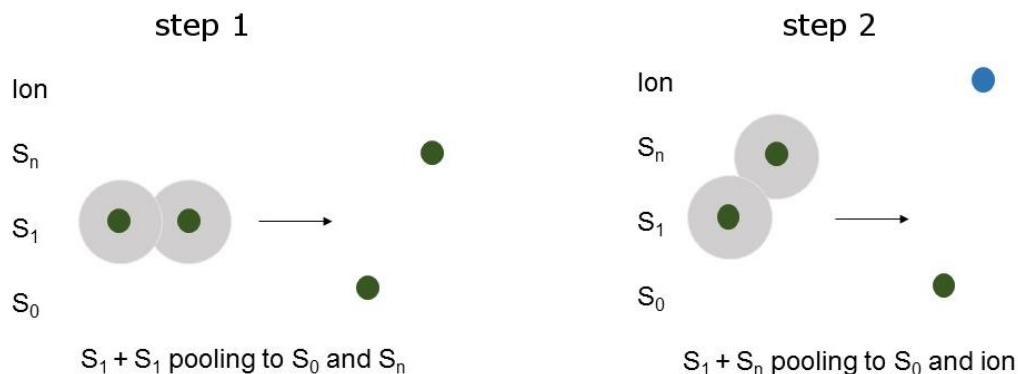


**Figure 1.5** Simplified schematic of the major process proposed in the photoexcitation/pooling ionisation model. Green = molecules, Grey = wavefunction overlap leading to redistribution of excitation energy to different excitations states, Blue = ion. (Re-drawn from [200]).

### 1.3.2 Mass analysers

Following the generation of ions, they must be separated according to their  $m/z$ , which can be achieved by different physical principles. Schematics of different types of mass analysers are available by Pól *et al.* [214], although it should be noted that they are often combined in sequence to enhance versatility, e.g. in the popular Q-

TOF, which combines time-of-flight (TOF) and quadrupole mass analysers. Only the analysers used in or relevant to this study shall be briefly described here and have been visualised in Figure 1.6.

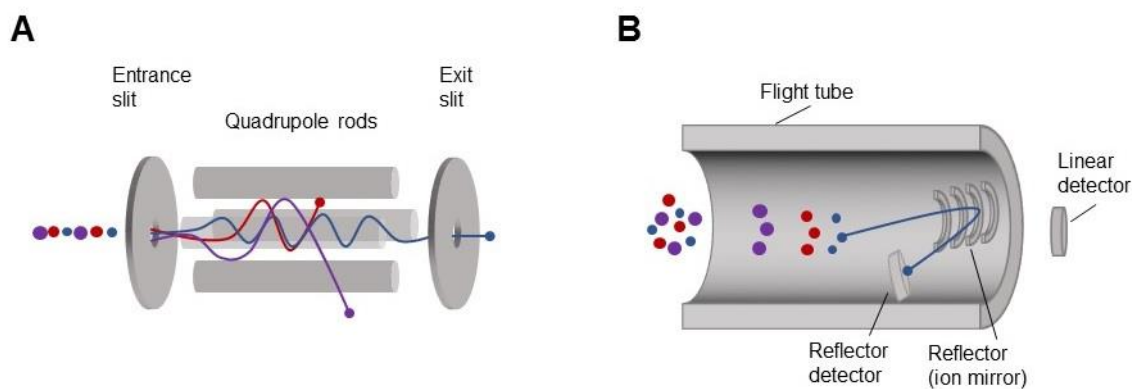


**Figure 1.6** Schematic diagram of A) Quadrupole and B) Time-of-Flight mass analysers.

The quadrupole, which was developed by Paul and Steinwedel in 1953 [215], employs an oscillating electrical field to separate ions based on the stability of their trajectories and is composed of four parallel, ideally hyperbolic rods. Opposing rods are connected and radiofrequency potentials are applied, whereas the opposite pair is subjected to a direct current potential. Ions are directed along the axis of the array and repelled by the changing potentials, resulting in complex flight paths, which can be stable or unstable. However, only ions with stable trajectories reach the detector, which means that knowing the calculations behind the trajectory path the conditions of the potentials applied can be varied to affect which ions have stable or unstable trajectories, hence allowing only selected ions of reach the detector (selected ion monitoring) [216]. Quadrupoles have a low resolution of 2000 full width half maximum (FWHM; the resolving power required to observe separated peaks) at  $m/z$  1000 and a limited mass range of up to 4000 Da with 100 ppm accuracy [216].

Time-of-flight (TOF) mass spectrometers, on the other hand, can have a mass resolution of 40,000 FWHM [217] and have been used to analyse ions in the megadalton range (1,900,000 Da) [218], although this cannot be considered a routine in mass spectrometry. Nonetheless, combined ToF instruments such as a MALDI-FTICR-IMS have been reported to operate with up to 75,000 FWHM [219].

In TOF instruments, ions are accelerated by an electrical field and then separated based on their velocity in a field-free region, the so-called drift tube, between the ion source and the detector. Because ions all receive the same kinetic energy, smaller ions travel faster than larger ones and therefore reach the detector first, i.e. have a short time-of-flight, allowing separation based on their  $m/z$  [216,220]. In reflectron mode, ions are deflected after exiting the field-free region and sent back through the drift tube to compensate for kinetic energy dispersion of ions with the same  $m/z$  [199,216].

The instrument used to acquire positive mode MALDI data in this study was the Synapt G2™ High Definition Mass Spectrometer (HDMS) system by Waters Corporation (Manchester, UK) equipped with a 1 kHz Nd:YAG laser, which combines a quadrupole with reflectron TOF and the possibility for ion mobility-MS, although this was not used in this case and shall therefore not be discussed further. In sensitivity mode, which was used for this study, the instrument offers a mass resolution of 10,000 FWHM, whereas it can achieve 20,000 FWHM in resolution and 40,000 FWHM in high resolution mode [217].

### **1.3.3 MALDI-MS imaging**

Mass spectrometry imaging (MSI) is possible with several techniques such as SIMS [221], DESI [27] and MALDI [25] and allows for the mapping of the spatial distribution of an analyte.

The first reported use of MALDI for imaging was made in 1994 [222]. However, it did not gain widespread attention until the seminal paper by Caprioli *et al.* in 1997, who mapped peptides and proteins in tissue sections and blots thereof [223]. Due to its wide mass range, MALDI-MSI finds wide applicability ranging from use in biomedicine, biotechnology and pharmaceuticals, for example in drug mapping and tumour diagnosis [224], to microbiology and various forensic problems such as the analysis of ink, drugs of abuse [225,226], condom lubricants [48,49] and fingerprints [25,53].

In principle, MALDI-MSI is similar to MALDI-MS profiling, where a spectrum is obtained without information on one spot or localised sample only. However, the laser can be automated to raster the section to be imaged. Full spectra of all ion signals are thereby collected at each x/y-coordinate (Figure 1.7A) and the intensity of each  $m/z$  can be extracted by specific imaging software to visualise its distribution across the entire sample (Figure 1.7B), i.e. which x/y-coordinate contains the  $m/z$  in question with which intensity. The quality of these distribution maps is, however, dependent on the laser spot size of each raster and the distance between laser shots as well as the sample preparation, which greatly affects the image quality. While in profiling applications the matrix is pre-mixed with or spotted onto the sample, it must be evenly and thinly applied onto a sample that is to be imaged in order to ensure that it is sufficiently covered with matrix to allow ionisation, but also prevent delocalisation of analytes caused by excess humidity. This is particularly challenging for the application of enzymes such as trypsin when peptide analysis is required, as trypsin requires moisture to be effective, or when tissues need to be sectioned, resulting in sample preparation being crucial for successful MSI analysis [203].

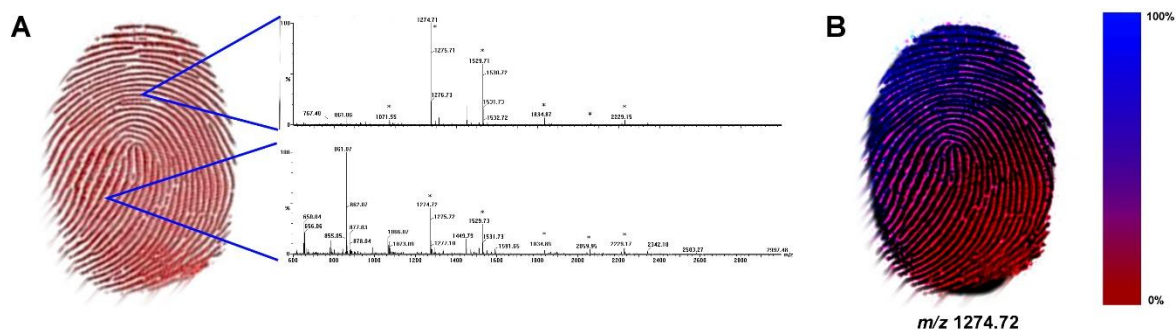


**Figure 1.7** Concept of MALDI-MS imaging, demonstrated on a fictional example. A: Localised spectra of individual coordinates within the sample. B: Intensity and distribution map of a selected  $m/z$  throughout the image.

## 1.4 The principles of proteomics

Proteomics is a large field concerning the study and characterisation of proteins, long chains of amino acids with various important biological functions, and peptides, their smaller building blocks or fragments. Broadly, proteomics can be divided into structural proteomics, expression proteomics and functional or interaction

proteomics. Often these fields overlap in order to investigate structure and quantity as well as physiological role, localisation, interactions, dynamics and varieties within a biological system. These biological systems can be entire species, single organs or particular pathways of interest. A range of techniques is available for these tasks depending on the desired outcome, employing for example immunoassays, gel electrophoresis, western blotting, affinity chromatography, x-ray crystallography, mass spectrometry or even comparatively simple dipsticks.

The human plasma proteome project for example set out to characterise the entire human plasma proteome, measuring protein concentrations using immunoassays and providing annotations via analysis of MS data [89,227,228]. The understanding of a healthy proteome and biological variation caused by physiological differences (e.g. age or gender) is imperative to the investigation for diagnostic purposes for instance in clinical proteomics. Without this basis, markers of disease like those found in samples from patients with kidney damage or cancer would not be identifiable as such [229]. Similarly, proteomics has been used for therapeutic purposes like monitoring changes in the proteome following drug treatment [206] as well as drug discovery and development through targeting protein pathways known to be involved in disease [230]. To identify these pathways, proteomics is employed for the investigation of the underlying mechanism of a disease and understanding protein interactions, like in the study of prion proteins, such as the one responsible for bovine spongiform encephalopathy [231], or  $\alpha$ -synuclein associated with Parkinson's disease [232]. With pertinence to this thesis, proteomics is also increasingly finding relevance in forensic sciences. Applications have for instance been reported analysing the human hair shaft proteome [233] and organ-specific protein expression patterns, aiming to identify the tissues a projectile traversed [234] to aid the identification of the lethal bullet in a case with multiple shots fired. Furthermore, studies have been undertaken investigating the proteome of several body fluids to allow their confident identification in forensic samples [188].

Although conventional analysis methods such as gel electrophoresis or western blots remain useful, the advent of MS facilitated the more reliable, reproducible and exact analysis of proteins and has therefore been widely accepted in the field. The possibility to not only characterise or identify proteins by their mass and, in the case of ion mobility-MS, their collisional cross section or structural properties, but also sequence them certainly makes MS-based approaches a popular choice in proteomics. However, it also means proteomic databases like UniProtKB are of paramount importance to allow researchers to form hypotheses, draw from existing knowledge and recognise connections to their data.

Regardless of the analysis platform chosen, two terms are commonly encountered in proteomics. Whilst the so-called "top-down" proteomics is concerned with detecting or sequencing intact proteins, "bottom-up" approaches analyse characteristic peptides generated from a protein by enzymatically cleaving it, a process called proteolysis or digestion. One such proteolytic enzyme that is frequently used in bottom-up proteomics is trypsin, which specifically cleaves at the C-terminal sites of the amino acids lysine and arginine, except when followed by proline [235]. This knowledge allows for *in silico* (theoretical) digests to be performed on known protein sequences (obtained from databases like UniProtKB) to predict the peptides produced by proteolysis. Especially the mass spectrometric analysis of such digests then allows the reliable measurement and identification of peptides and the proteins they originate from, respectively, with a given tolerance.

For trypsin to be effective, it has to be present in a substrate:trypsin ratio of approximately 50:1 [236] – if too much trypsin is present it starts autolysing, resulting in large trypsin signals in the mass spectrum, and if too little trypsin is present it cannot effectively lyse the excess of protein, resulting in a lack of peptide signals. Digests can be performed in-solution, adding trypsin solution to e.g. tissue homogenates, sample extracts or liquid samples, or *in situ*, where the sample is covered with thin layers of the protease in order to maintain the spatial distribution of analytes. This technique is frequently used for MALDI-MSI of digested tissue sections, in which case it is also referred to as an "on-tissue" digest [237]. Commonly,

20 µg/mL trypsin solutions are used for in-solution and on-tissue digests [20,206,208], but various other trypsin concentrations have been reported in the literature alongside differing substrate:trypsin ratios for a range of samples [189,238–244].

## **1.5 Infinite focus microscopy**

Infinite focus microscopy (IFM), also called focus variation microscopy (FVM), is a relatively new microscopy technique that allows for the computational generation of 3D images of a sample and thereby the characterisation of its surface. This can be considered a great advantage over conventional 2D microscopy, which doesn't allow for the observation or measurement of height features and can only be focused on one plane of the sample at a time.

Unlike confocal microscopy, which is regularly used for biological samples and is based on transmitted light, IFM works on reflected light and can therefore be used routinely in quality control and analysis of wear in material engineering and production processes, e.g. measuring metal parts and corrosion [245,246] as well as paper smoothness [247]. This is aided by the large, robust sample stage suitable for items of up to 20 kg [246]. In addition to quality control, IFM has been used for the comparison of toolmarks in a forensic context [248,249] as well as the analysis of archaeological and anthropological samples [250–256] and biological samples that are not amenable to confocal microscopy due to their opacity, such as teeth and bones [257–259].

Unlike conventional microscopy, IFM allows variation of the focus, meaning that it can automatically acquire focussed images at various focal planes with a vertical resolution of down to 10 nm [246,250]. This is achieved through the following principle: light hitting the specimen is reflected with equal strength into each direction if the topography is uneven, i.e. shows diffuse reflective properties, whereas it is mainly scattered into one direction in case of specular reflections, i.e. perpendicular, smooth samples. This reflected light is collected in the optics, which only have a small depth of field, by a light sensitive sensor behind a beam splitting mirror. Figure 1.8 shows a schematic of the IFM's optics. As the small depth of field means only

small portions of the image are in focus, data have to be captured continuously whilst vertically moving the optics along the optical axis. This permits full depth of field, i.e. sharp focus at each position, and allows complete analysis of the sample surface [260]. This focus variation is then processed by the software using specific algorithms [246,257], and by stacking of images acquired at each focal plane a final image is produced with a large depth of field based on the coordinate points that are best focussed. This stack thereby allows for the representation of the topology of a sample.

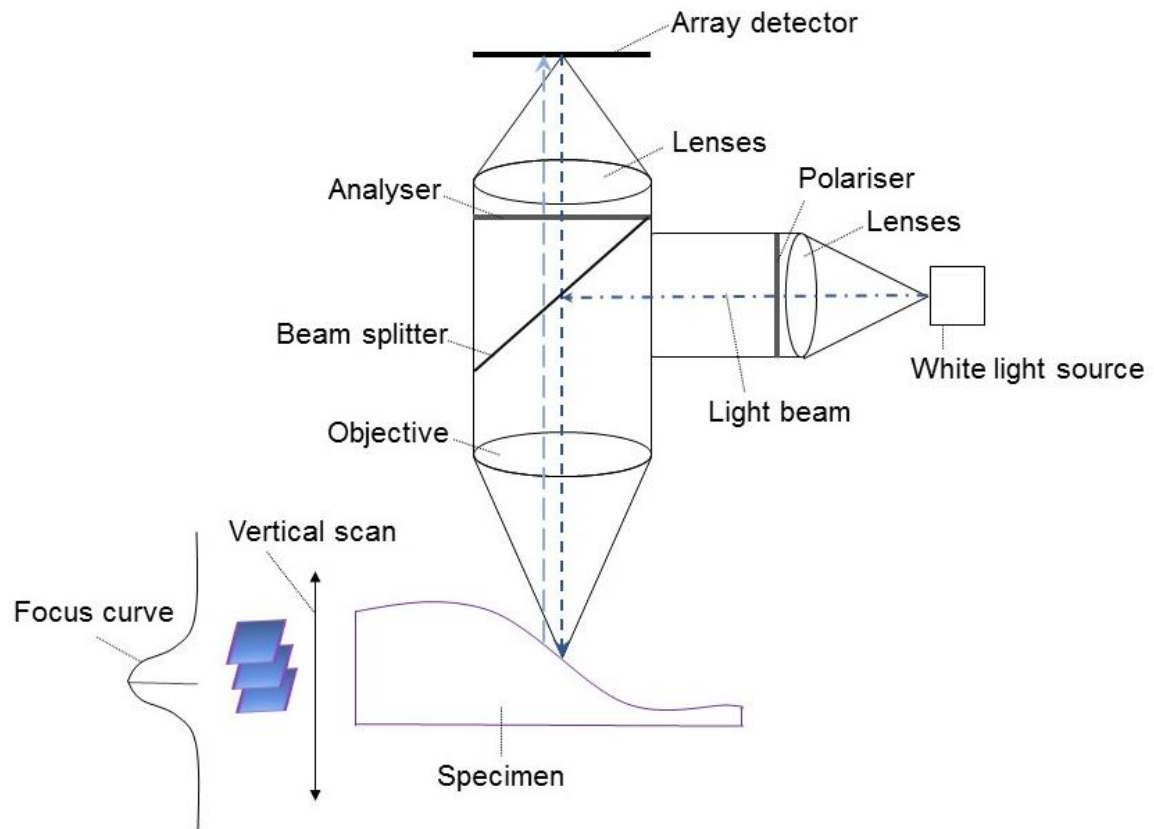


**Figure 1.8** Schematic of an infinite focus microscope. (Re-drawn from [261].)

The lateral resolution that can be achieved is currently 400 nm [246,250] and complex geometric samples with slopes of up to 85° can be analysed as well as highly reflective or rough surfaces [246,247]. To further characterise the samples, several analytical tools are available within the software, allowing various measurements to be performed on the sample, ranging from profiles, heights and volumes to statistical surface parameters [260]. Particularly the step height function

has been investigated in this work with regards to its suitability for the analysis of blood fingermarks.

## 1.6 Aims and objectives

Currently used tests and enhancement techniques for blood lack specificity, especially for species provenance, and the ability to provide a strong link between blood and a fingermark. This is due to their non-specific targets and mechanisms of action, leading to a range of false positives and, in some cases, false negatives, in addition to often being destructive to ridge detail.

Previous studies conducted at Sheffield Hallam University employed MALDI-MS for the analysis of intact haemoglobin, myoglobin and haem [54] in order to detect the presence of blood and its species origin. While this facilitated species differentiation between human, bovine and equine blood, it was realised that differentiation between other species would not be possible using intact protein analysis. This is due to the large sequence homology between some species, resulting in *m/z*s with little or no difference to one another. This can pose problems in their differentiation depending on the instrument's mass resolving power, especially in mixtures or samples contaminated with other protein sources. The UK Home Office further expressed special interest in the differentiation of human and chimpanzee blood, which share identical haemoglobin sequences, preventing their discrimination based on intact haemoglobin detection. Curiously, however, *in silico* digests of human and chimpanzee haemoglobin  $\beta$  present 17 proteotypic peptides for human and 11 for chimpanzee with the differences lying solely in post-translational modifications.

For these reasons, the study presented here aimed to develop a multi-informative, specific detection technique for blood in stains and fingermarks using MALDI-MS profiling and imaging in conjunction with bottom-up proteomics.

This approach is based on the theory that signals originating from blood-specific proteins are only detectable if the sample contains blood. It appeared sensible that the detection of a higher number of blood-specific proteins will increase confidence

and specificity of MS-based analysis compared to the detection of a single protein, haemoglobin.

Furthermore, the hypothesis was postulated that the use of a bottom-up approach will increase confidence and reliability of the analysis because a higher number of identified small, characteristic peptides provides a higher degree of confidence than a small number of intact proteins with large sequence homologies between species. In addition, this approach is thought to circumvent possible mass resolution problems resulting from high-homology protein sequences in top-down proteomics.

More-so, it was hypothesised that bottom-up proteomics will facilitate the identification of species-specific differences in the protein sequence or post-translational modifications, therefore allowing for reliable provenance determination.

To prove the hypothesis, it was envisioned to develop and optimise an in-solution digestion protocol for blood on known blood samples, targeting a number of blood-specific proteins. Analysis of aged samples was proposed to investigate the method's applicability to old and cold case samples and take into account possible sample degradation with age. This was to be followed by validation on unknown samples including human and non-human blood samples, biofluids and non-biofluid samples to thoroughly test the robustness of the methodology and identifications made. It was also intended to test the protocol in conjunction with commonly used enhancement techniques in order to evaluate possible interferences and be able to provide recommendations on which crime scene techniques to avoid when subsequent mass-spectrometric analysis is desired

Pertaining to blood and fingerprints, the development on an *in situ* proteolysis protocol was proposed in order to maintain ridge detail, catering to the same hypothesis as the in-solution digests. The aim was to thereby facilitate mapping of the identified blood peptides on the fingermark ridge detail via MALDI-MSI, thus providing a link between the event of bloodshed and the fingermark deposition as well as allowing species determination.

Nonetheless, there are three possible scenarios pertaining to the order of deposition of blood marks: a) bloodied mark, b) mark in blood and c) coincidental association (faux mark). To date, differentiation between the three is complicated, subjective and experience-based, rather than based on a numerical approach. However, knowledge of the order of deposition can be of paramount importance to an investigation. If a suspect claims to have arrived at the scene after a violent crime, their defence can be refuted if it can be proven that their marks are covered by blood as in a type C mark. Similarly, the presence of a suspect's marks in blood (B) will invalidate the defence that they left the scene before the event of bloodshed. Distinguishing between a type A bloodied mark and a type C coincidentally associated mark is of great importance to determine if it is possible that a suspect is innocent and had merely been at the scene prior to the crime, or if the marks have truly been left by their bloodied fingers. In theory, development of the MALDI-MSI approach outlined above will allow the differentiation of scenario A from B and C by mapping the blood peptides exclusively to ridge detail (scenario A) or the entire surface (B and C). However, the technique will not allow for the distinction of a mark in blood (B) from coincidental association (C).

In order to provide quantifiable data to solve this problem, an additional objective was investigating the suitability of IFM for determining the order of deposition of blood fingermarks. It was hypothesised that the three different deposition scenarios would present characteristically different ridge heights measurable with IFM. The study therefore aimed to investigate deposition surfaces and lifting tapes that are also suitable for obtaining IFM images, as well as potential ridge height changes over time. These have the potential to complicate analysis due to the fact the exact age of a crime scene mark is unlikely to be known and can therefore not be taken into account accurately. Furthermore, it is reasonable to assume that ridge heights will also be affected by different volumes of blood and the structure and porosity of the deposition surface.

For these reasons, several experiments had to be devised to determine if IFM or the statistical analysis of IFM data is suitable to solve the problem at hand. As current analysis is extremely difficult and reliant on the examiner's expertise, successful

proof of this hypothesis would then facilitate more quantifiable, reliable means of analysis for these samples.

The ultimate aim of study was therefore to develop a rapid MALDI-MS method that, in the near future, will be able to provide ridge detail, chemical information and confirmation regarding the presence and provenance of blood in fingermarks or stains in one single analysis, providing a link between a suspect's presence at a crime scene and the event of bloodshed. Additionally, it was aimed to differentiate the three possible associations of a fingermark with blood by employing the non-contact method IFM, ideally prior to MALDI-MSI analysis of the same sample to generate complementary datasets with maximum evidential value.

## 1.7 References

- [1] I. Evett, R. Williams, A Review of the Sixteen Points Fingerprint Standard in England and Wales, *J. Forensic Identif.* 46 (1996) 49–73.
- [2] B.T. Ulery, R.A. Hicklin, M.A. Roberts, J. Buscaglia, Changes in latent fingerprint examiners' markup between analysis and comparison, *Forensic Sci. Int.* 247 (2015) 54–61.
- [3] G. Langenburg, C. Hall, Q. Rosemarie, Utilizing AFIS searching tools to reduce errors in fingerprint casework, *Forensic Sci. Int.* 257 (2015) 123–133.
- [4] Fingerprints - Forensic Science & Forensic Medicine, (2016). <http://forensic-medicine.info/fingerprints.html>.
- [5] J.G. Barnes, The fingerprint sourcebook, in: A. McRoberts (Ed.), *Fingerpr. Sourceb.*, Nation Institute of Justice, U.S. Department of Justice, 2011: pp. 7–24.
- [6] A.K. Jain, J. Feng, K. Nandakumar, Fingerprint Matching, *Computer* (Long Beach. Calif). 43 (2010) 36–44.
- [7] I. Hefetz, Y. Liptz, S. Vaturi, D. Attias, Use of AFIS for linking scenes of crime, *Forensic Sci. Int.* 262 (2016) e25–e27.
- [8] F. Galton Sir, *Finger Prints*, MACMILLAN AND CO., London, 1892.
- [9] L.A. Hutchins, Systems of friction ridge classification, in: A. McRoberts (Ed.), *Fingerpr. Source B.*, Nation Institute of Justice, U.S. Department of Justice,

- 2011: pp. 1–26. <https://www.ncjrs.gov/pdffiles1/nij/225325.pdf>.
- [10] A.K. Jain, Y. Chen, M. Demirkus, Pores and ridges: High-resolution fingerprint matching using level 3 features, *IEEE Trans. Pattern Anal. Mach. Intell.* 29 (2007) 15–27.
- [11] Prince, M. Kaur, A. Mittal, Fingerprint matching system using Level 3 features, 2 (2010) 2258–2262.
- [12] R.M. Tayebi, S. Mazaheri, B.S. Bigham, A New Fingerprint Matching Approach Using Level 2 and Level 3 Features, in: *Proc. Fourth Int. C\* Conf. Comput. Sci. Softw. Eng.*, 2011: pp. 73–81.
- [13] M.J. Leadbetter, Fingerprint evidence in England and Wales - the revised standard, *Med. Sci. Law.* 45 (2005).
- [14] Court fingerprint system scrapped, *BBC News Scotl.* (n.d.). <http://news.bbc.co.uk/1/hi/scotland/5310246.stm> (accessed August 15, 2017).
- [15] J. Abraham, C. Champod, C. Lennard, C. Roux, Modern statistical models for forensic fingerprint examinations: a critical review., *Forensic Sci. Int.* 232 (2013) 131–50.
- [16] V. Mustonen, K. Hakkarainen, J. Tuunainen, P. Pohjola, Discrepancies in expert decision-making in forensic fingerprint examination, *Forensic Sci. Int.* 254 (2015) 215–226.
- [17] B.T. Ulery, R.A. Hicklin, G.I. Kiebusinski, M.A. Roberts, J.A. Buscaglia, Understanding the sufficiency of information for latent fingerprint value determinations, *Forensic Sci. Int.* 230 (2013) 99–106.
- [18] B.T. Ulery, R.A. Hicklin, M.A. Roberts, J.A. Buscaglia, Interexaminer variation of minutia markup on latent fingerprints, *Forensic Sci. Int.* 264 (2016) 89–99.
- [19] R. Ramotowski, Composition of Latent Print Residue, in: B.A.J. Fisher (Ed.), *Adv. Fingerpr. Technol.*, 2nd ed., CRC Press, London, 2001.
- [20] E. Patel, M.R. Clench, A. West, P.S. Marshall, N. Marshall, S. Francese, Alternative Surfactants for Improved Efficiency of In Situ Tryptic Proteolysis of Fingermarks, *J. Am. Soc. Mass Spectrom.* 26 (2015) 862–872.
- [21] A. Girod, R. Ramotowski, C. Weyermann, Composition of fingermark

- residue: a qualitative and quantitative review., *Forensic Sci. Int.* 223 (2012) 10–24.
- [22] Q. Wei, M. Zhang, B. Ogorevc, X. Zhang, Recent advances in the chemical imaging of human fingermarks (a review), *Analyst.* (2016) 6172–6189.
- [23] S. Francese, R. Bradshaw, N. Denison, An update on MALDI mass spectrometry based technology for the analysis of fingermarks – stepping into operational deployment, *Analyst.* 142 (2017) 2518–2546.
- [24] R.S. Croxton, M.G. Baron, D. Butler, T. Kent, V.G. Sears, Variation in amino acid and lipid composition of latent fingerprints., *Forensic Sci. Int.* 199 (2010) 93–102.
- [25] R. Wolstenholme, R. Bradshaw, M.R. Clench, S. Francese, Study of latent fingermarks by matrix-assisted laser desorption/ionisation mass spectrometry imaging of endogenous lipids, *Rapid Commun. Mass Spectrom.* 23 (2009) 3031–3039.
- [26] X. Tang, L. Huang, W. Zhang, H. Zhong, Chemical Imaging of Latent Fingerprints by Mass Spectrometry Based on Laser Activated Electron Tunneling, *Anal. Chem.* 87 (2015) 150213130830005.
- [27] D.R. Ifa, N.E. Manicke, A. Dill, R.G. Cooks, Latent Fingerprint Chemical Imaging by Mass Spectrometry, 321 (2008) 2008.
- [28] M. Morelato, A. Beavis, P. Kirkbride, C. Roux, Forensic applications of desorption electrospray ionisation mass spectrometry (DESI-MS), *Forensic Sci. Int.* 226 (2013) 10–21.
- [29] C. Elsner, B. Abel, Ultrafast high-resolution mass spectrometric finger pore imaging in latent finger prints., *Sci. Rep.* 4 (2014) 6905.
- [30] L.S. Ferguson, S. Creasey, R. Wolstenholme, M.R. Clench, S. Francese, Efficiency of the dry-wet method for the MALDI-MSI analysis of latent fingermarks., *J. Mass Spectrom.* 48 (2013) 677–84.
- [31] N. Lauzon, M. Dufresne, V. Chauhan, P. Chaurand, Development of Laser Desorption Imaging Mass Spectrometry Methods to Investigate the Molecular Composition of Latent Fingermarks, *J. Am. Soc. Mass Spectrom.* 26 (2015) 878–886.
- [32] A. Van Dam, M.C.G. Aalders, K. van de Braak, H.J.J. Hardy, T.G. Van

- Leeuwen, S.A.G. Lambrechts, Simultaneous labeling of multiple components in a single fingermark, *Forensic Sci. Int.* 232 (2013) 173–179.
- [33] H. Tang, W. Lu, C. Che, K. Ng, Gold nanoparticles and imaging mass spectrometry: double imaging of latent fingerprints., *Anal. Chem.* 82 (2010) 1589–93.
- [34] R. Leggett, E.E. Lee-Smith, S.M. Jickells, D.A. Russell, “Intelligent” fingerprinting: Simultaneous identification of drug metabolites and individuals by using antibody-functionalized nanoparticles, *Angew. Chemie - Int. Ed.* 46 (2007) 4100–4103.
- [35] A. Bécue, N. Egli, C. Champod, P.A. Margot, Fingermarks and Other Impressions Left by the Human Body, 16th Int. Forensic Sci. Symp. Interpol--Lyon 5 Th-8 Th Oct. 2010 Rev. Pap. 609 (2010).
- [36] H.L. Bandey, S.M. Bleay, V.J. Bowman, R.P. Downham, V.G. Sears, *Fingermark Visualisation Manual*, 1st ed., Centre for Applied Science and Technology (St. Albans), 2014.
- [37] L.S. Ferguson, F. Wulfert, R. Wolstenholme, J.M. Fonville, M.R. Clench, V.A. Carolan, S. Francese, Direct detection of peptides and small proteins in fingermarks and determination of sex by MALDI mass spectrometry profiling, *Analyst.* 137 (2012) 4686.
- [38] H. Oktem, A. Kurkcuoglu, I.C. Pelin, A.C. Yazici, G. Aktaş, F. Altunay, Sex differences in fingerprint ridge density in a Turkish young adult population: A sample of Baskent University, *J. Forensic Leg. Med.* 32 (2015) 34–38.
- [39] R. Bradshaw, W. Rao, R. Wolstenholme, M.R. Clench, S. Bleay, S. Francese, Separation of overlapping fingermarks by Matrix Assisted Laser Desorption Ionisation Mass Spectrometry Imaging, *Forensic Sci. Int.* 222 (2012) 318–326.
- [40] A. Girod, L. Xiao, B. Reedy, C. Roux, C. Weyermann, Fingermark initial composition and aging using Fourier transform infrared microscopy (FTIR), *Forensic Sci. Int.* 254 (2015) 185–196.
- [41] A. Girod, R. Ramotowski, S. Lambrechts, P. Misriellal, M. Aalders, C. Weyermann, Fingermark age determinations: Legal considerations, review of the literature and practical propositions, *Forensic Sci. Int.* 262 (2016) 212–

- [42] N.E. Archer, Y. Charles, J.A. Elliott, S. Jickells, Changes in the lipid composition of latent fingerprint residue with time after deposition on a surface., *Forensic Sci. Int.* 154 (2005) 224–39.
- [43] S. Muramoto, E. Sisco, Strategies for Potential Age Dating of Fingerprints through the Diffusion of Sebum Molecules on a Nonporous Surface Analyzed Using Time-of-Flight Secondary Ion Mass Spectrometry, *Anal. Chem.* 87 (2015) 8035–8038.
- [44] M. Benton, M.J. Chua, F. Gu, F. Rowell, J. Ma, Environmental nicotine contamination in latent fingermarks from smoker contacts and passive smoking, *Forensic Sci. Int.* 200 (2010) 28–34.
- [45] P. Hazarika, S.M. Jickells, K. Wolff, D.A. Russell, Imaging of latent fingerprints through the detection of drugs and metabolites, *Angew. Chemie - Int. Ed.* 47 (2008) 10167–10170.
- [46] P. Hazarika, S.M. Jickells, K. Wolff, D.A. Russell, Multiplexed detection of metabolites of narcotic drugs from a single latent fingermark, *Anal. Chem.* 82 (2010) 9150–9154.
- [47] G. Groeneveld, M. de Puit, S. Bleay, R. Bradshaw, S. Francese, Detection and mapping of illicit drugs and their metabolites in fingermarks by MALDI MS and compatibility with forensic techniques, *Sci. Rep.* 5 (2015).
- [48] R. Bradshaw, R. Wolstenholme, R.D. Blackledge, M.R. Clench, L.S. Ferguson, S. Francese, A novel matrix-assisted laser desorption/ionisation mass spectrometry imaging based methodology for the identification of sexual assault suspects., *Rapid Commun. Mass Spectrom.* 25 (2011) 415–22.
- [49] R. Bradshaw, R. Wolstenholme, L.S. Ferguson, C. Sammon, K. Mader, E. Claude, R.D. Blackledge, M.R. Clench, S. Francese, Spectroscopic imaging based approach for condom identification in condom contaminated fingermarks., *Analyst.* 138 (2013) 2546–57.
- [50] D.J. Phares, J.K. Holt, G.T. Smedley, R.C. Flagan, Method for characterization of adhesion properties of trace explosives in fingerprints and fingerprint simulations., *J. Forensic Sci.* 45 (2000) 774–784.

- [51] K. Kaplan-Sandquist, M. a. LeBeau, M.L. Miller, Chemical analysis of pharmaceuticals and explosives in fingermarks using matrix-assisted laser desorption ionization/time-of-flight mass spectrometry, *Forensic Sci. Int.* 235 (2014) 68–77.
- [52] P.H.R. Ng, S. Walker, M. Tahtouh, B. Reedy, Detection of illicit substances in fingerprints by infrared spectral imaging, *Anal. Bioanal. Chem.* 394 (2009) 2039–2048.
- [53] S. Francese, R. Bradshaw, L.S. Ferguson, R. Wolstenholme, M.R. Clench, S. Bleay, Beyond the ridge pattern: multi-informative analysis of latent fingermarks by MALDI mass spectrometry., *Analyst.* 138 (2013) 4215–28.
- [54] R. Bradshaw, S. Bleay, M.R. Clench, S. Francese, Direct detection of blood in fingermarks by MALDI MS profiling and Imaging, *Sci. Justice.* 54 (2014) 110–117.
- [55] L. Deininger, E. Patel, M.R. Clench, V. Sears, C. Sammon, S. Francese, Proteomics goes forensic: detection and mapping of blood signatures in fingermarks, *Proteomics.* 16 (2016) 1707–1717.
- [56] C. Au, H. Jackson-Smith, I. Quinones, B.J. Jones, B. Daniel, Wet powder suspensions as an additional technique for the enhancement of bloodied marks, *Forensic Sci. Int.* 204 (2011) 13–18.
- [57] L.C.A.M. Bossers, C. Roux, M. Bell, A.M. McDonagh, Methods for the enhancement of fingermarks in blood, *Forensic Sci. Int.* 210 (2011) 1–11.
- [58] M.J. Bailey, B.N. Jones, S. Hinder, J. Watts, S. Bleay, R.P. Webb, Depth profiling of fingerprint and ink signals by SIMS and MeV SIMS, *Nucl. Instruments Methods Phys. Res. Sect. B Beam Interact. with Mater. Atoms.* 268 (2010) 1929–1932.
- [59] T. Bevel, R.M. Gardner, *Bloodstain pattern analysis : with an introduction to crime scene reconstruction*, 2nd ed. ., Boca Raton, Fla. ; London : CRC, Boca Raton, Fla. ; London, 2001.
- [60] A.Y. Wonder, M.G. Yezzo, *Bloodstain Patterns Identification, Interpretation and Application*, Burlington : Elsevier Science, Burlington, 2014.
- [61] S.N. Kunz, H. Brandtner, H. Meyer, Unusual blood spatter patterns on the firearm and hand: A backspatter analysis to reconstruct the position and

- orientation of a firearm, *Forensic Sci. Int.* 228 (2013) e54–e57.
- [62] Y. Cho, F. Springer, F. a. Tulleners, W.D. Ristenpart, Quantitative bloodstain analysis: Differentiation of contact transfer patterns versus spatter patterns on fabric via microscopic inspection, *Forensic Sci. Int.* 249 (2015) 233–240.
- [63] F. Files, *Forensic Files - Historic Cases: Chief Evidence 2 (Season 7, Episode 17)*, (2002). <https://www.youtube.com/watch?v=q8jL8S2yle8>.
- [64] B. Wictum, T. Wood, Solving Human Crimes with Animal DNA, *Evid. Technol. Mag.* (n.d.).  
[http://www.evidencemagazine.com/index.php?option=com\\_content&task=view&id=1620](http://www.evidencemagazine.com/index.php?option=com_content&task=view&id=1620) (accessed September 7, 2017).
- [65] Z. Dawtrey, Robber caught by leech jailed for two years, *Sydney Morning Her.* (2009). <http://www.smh.com.au/national/robber-caught-by-leech-jailed-for-two-years-20091023-hd08.html> (accessed September 7, 2017).
- [66] B. Wictum, *Veterinary Forensics: A Voice for Animal Victims*, *Hum. Soc. Vet. Med. Assoc.* (2014).  
[http://www.hsvma.org/veterinary\\_forensics\\_voice\\_for\\_animal\\_victims#.WbE21sbkXIU](http://www.hsvma.org/veterinary_forensics_voice_for_animal_victims#.WbE21sbkXIU) (accessed September 7, 2017).
- [67] J. Reinitz, Man arrested for killing cat, *Courier.* (2016).  
[http://wfcourier.com/news/local/crime-and-courts/man-arrested-for-killing-cat/article\\_b6ea302d-de35-5907-a8a7-9f0ce8b0021e.html](http://wfcourier.com/news/local/crime-and-courts/man-arrested-for-killing-cat/article_b6ea302d-de35-5907-a8a7-9f0ce8b0021e.html).
- [68] G. McLaughlin, K.C. Doty, I.K. Lednev, Discrimination of human and animal blood traces via Raman spectroscopy, *Forensic Sci. Int.* 238 (2014) 91–95.
- [69] E.O. Espinoza, N.C. Lindley, K.M. Gordon, J.A. Ekhoﬀ, M.A. Kirms, Electrospray Ionization Mass Spectrometric Analysis of Blood for Differentiation of Species, *Anal. Biochem.* 268 (1999) 252–261.
- [70] K. Singh, D. Kyle, E. Weiss, Criminal Cases Review Commission, CCRC REPORT - STATEMENT OF REASONS for the case of Susan Hilda May, 1999. <http://susanmay.co.uk/ccrc.htm>.
- [71] K. Guo, N. Zhegalova, S. Achilefu, M.Y. Berezin, Bloodstain age analysis: toward solid state fluorescent lifetime measurements, in: A. Mahadevan-Jansen, T. Vo-Dinh, W.S. Grundfest (Eds.), *Prog. Biomed. Opt. Imaging - Proc. SPIE*, 2013: p. 857214.

- [72] K. Guo, S. Achilefu, M.Y. Berezin, Dating bloodstains with fluorescence lifetime measurements, *Chem. - A Eur. J.* 18 (2012) 1303–1305.
- [73] S. Strasser, A. Zink, G. Kada, P. Hinterdorfer, O. Peschel, W.M. Heckl, A.G. Nerlich, S. Thalhammer, Age determination of blood spots in forensic medicine by force spectroscopy, *Forensic Sci. Int.* 170 (2007) 8–14.
- [74] G. Edelman, T.G. van Leeuwen, M.C.G. Aalders, Hyperspectral imaging for the age estimation of blood stains at the crime scene, *Forensic Sci. Int.* 223 (2012) 72–77.
- [75] S. Arany, S. Ohtani, Age estimation of bloodstains: A preliminary report based on aspartic acid racemization rate, *Forensic Sci. Int.* 212 (2011) e36–e39.
- [76] S.E. Anderson, G.R. Hobbs, C.P. Bishop, Multivariate Analysis for Estimating the Age of a Bloodstain, *J. Forensic Sci.* 56 (2011) 186–193.
- [77] R.H. Bremmer, K.G. De Bruin, M.J.C. Van Gemert, T.G. Van Leeuwen, M.C.G. Aalders, Forensic quest for age determination of bloodstains, *Forensic Sci. Int.* 216 (2012) 1–11.
- [78] S.S. Kind, D. Patterson, G.W. Owen, Estimation of the age of dried blood stains by a spectrophotometric method., *Forensic Sci.* 1 (1972) 27–54.
- [79] E.K. Hanson, J. Ballantyne, A blue spectral shift of the hemoglobin soret band correlates with the age (time since deposition) of dried bloodstains, *PLoS One.* 5 (2010) 1–11.
- [80] Y. Fujita, K. Tsuchiya, S. Abe, Y. Takiguchi, S.I. Kubo, H. Sakurai, Estimation of the age of human bloodstains by electron paramagnetic resonance spectroscopy: Long-term controlled experiment on the effects of environmental factors, *Forensic Sci. Int.* 152 (2005) 39–43.
- [81] J. Agudelo, C. Huynh, J. Halánek, Forensic determination of blood sample age using a bioaffinity-based assay, *Analyst.* 140 (2015) 1411–1415.
- [82] H. Inoue, F. Takabe, M. Iwasa, Y. Maeno, Y. Seko, A new marker for estimation of bloodstain age by high performance liquid chromatography, *Forensic Sci. Int.* 57 (1992) 17–27.
- [83] B. Geller, Y. Volinits, H. Wax, Can dry bloodstains provide a source for a blood-contaminated fingerprint?, *J. Forensic Identif.* 67 (2017).

- [84] N. Praska, G. Langenburg, Reactions of latent prints exposed to blood., *Forensic Sci. Int.* 224 (2013) 51–8.
- [85] E. Khoriaty, R. Halaby, M. Berro, A. Sweid, H.A. Abbas, A. Inati, Incidence of sickle cell disease and other hemoglobin variants in 10,095 Lebanese neonates, *PLoS One.* 9 (2014).
- [86] P. Chen, R.T.H. Ong, W.T. Tay, X. Sim, M. Ali, H. Xu, C. Suo, J. Liu, K.S. Chia, E. Vithana, T.L. Young, T. Aung, W.Y. Lim, C.C. Khor, C.Y. Cheng, T.Y. Wong, Y.Y. Teo, E.S. Tai, A study assessing the association of glycosylated hemoglobin a1C (HbA1C) associated variants with HbA1C, chronic kidney disease and diabetic retinopathy in populations of asian ancestry, *PLoS One.* 8 (2013) 1–11.
- [87] J.K. Hertel, S. Johansson, H. Ræder, C.G. Platou, K. Midthjell, K. Hveem, A. Molven, P.R. Njølstad, Evaluation of four novel genetic variants affecting hemoglobin A1c levels in a population-based type 2 diabetes cohort (the HUNT2 study), *BMC Med. Genet.* 12 (2011) 20.
- [88] L.G. Chandrasena, H. Peiris, S. Williams, S.H. Siribaddana, Hemoglobin variants in patients with type 2 diabetes mellitus., *Southeast Asian J. Trop. Med. Public Health.* 41 (2010) 1247–51.  
<http://www.ncbi.nlm.nih.gov/pubmed/21073046>.
- [89] N.L. Anderson, N.G. Anderson, The human plasma proteome: history, character, and diagnostic prospects., *Mol. Cell. Proteomics.* 1 (2002) 845–867.
- [90] NUTLEY POLICE DEPARTMENT, Missing Person Alert: 59 Yr. Old with Diabetes Missing since June 15, Tap into Bloom. (n.d).  
<https://www.tapinto.net/towns/bloomfield/articles/missing-person-alert-59-yr-old-with-diabetes-mi-1> (accessed November 30, 2017).
- [91] E. Beutler, J. Waalen, The definition of anemia : what is the lower limit of normal of the blood hemoglobin concentration ? The definition of anemia : what is the lower limit of normal of the blood hemoglobin concentration ?, *Blood.* 107 (2006) 1747–1750.
- [92] V. Ignjatovic, C. Lai, R. Summerhayes, U. Mathesius, S. Tawfilis, M.A. Perugini, P. Monagle, Age-related differences in plasma proteins: How

- plasma proteins change from neonates to adults, *PLoS One*. 6 (2011).
- [93] V. Nanjappa, J.K. Thomas, A. Marimuthu, B. Muthusamy, A. Radhakrishnan, R. Sharma, A. Ahmad Khan, L. Balakrishnan, N.A. Sahasrabudde, S. Kumar, B.N. Jhaveri, K.V. Sheth, R. Kumar Khatana, P.G. Shaw, S.M. Srikanth, P.P. Mathur, S. Shankar, D. Nagaraja, R. Christopher, S. Mathivanan, R. Raju, R. Sirdeshmukh, A. Chatterjee, R.J. Simpson, H.C. Harsha, A. Pandey, T.S.K. Prasad, Plasma Proteome Database as a resource for proteomics research: 2014 update., *Nucleic Acids Res.* 42 (2014) D959-65.
- [94] C.A. Burtis, E.R. Ashwood, D.E. Bruns, B.G. Sawyer, *Fundamentals of Clinical Chemistry :6th Ed, 6th ed.*, Saunders Elsevier, St. Louis, 2008. <http://www.ccmhmtschoo.org/uploads/docs/tietz-fundamentals-of-clinical-chemistry.pdf>.
- [95] H.C. Lee, R.E. Gaensslen, *Advances in Fingerprint Technology*, 2001. <http://www.ncjrs.gov/App/Publications/abstract.aspx?ID=132296>.
- [96] V.G. Sears, C.P.G. Butcher, L.A. Fitzgerald, Enhancement of Fingerprints in Blood Part 3 : Reactive Techniques , Acid Yellow 7 , and Process Sequences, *J. Forensic Identif.* (2005).
- [97] T.I. Quickenden, J.I. Creamer, A study of common interferences with the forensic luminol test for blood., *Luminescence.* 16 (2001) 295–8.
- [98] N. Passi, R.K. Garg, M. Yadav, R.S. Singh, M. a. Kharoshah, Effect of luminol and bleaching agent on the serological and DNA analysis from bloodstain, *Egypt. J. Forensic Sci.* 2 (2012) 54–61.
- [99] T.I. Quickenden, P.D. Cooper, Increasing the specificity of the forensic luminol test for blood., *Luminescence.* 16 (2001) 251–253.
- [100] A. Castelló, M. Alvarez, F. Verdú, Accuracy, reliability, and safety of luminol in bloodstain investigation, *J. Can. Soc. Forensic Sci.* 35 (2002) 113–121.
- [101] N. Vandenberg, R.A.H. Van Oorschot, The use of Polilights in the detection of seminal fluid, saliva, and bloodstains and comparison with conventional chemical-based screening tests, *J. Forensic Sci.* 51 (2006) 361–370.
- [102] J.H. An, K.J. Shin, W.I. Yang, H.Y. Lee, Body fluid identification in forensics, *BMB Rep.* 45 (2012) 545–553.

- [103] L.T. Lytle, D.G. Hedgecock, Chemiluminescence in the visualization of forensic bloodstains., *J. Forensic Sci.* 23 (1978) 550–562.
- [104] J.L. Webb, J.I. Creamer, T.I. Quickenden, A comparison of the presumptive luminol test for blood with four non-chemiluminescent forensic techniques, *Luminescence.* 21 (2006) 214–220.
- [105] K. Virkler, I.K. Lednev, Analysis of body fluids for forensic purposes: from laboratory testing to non-destructive rapid confirmatory identification at a crime scene., *Forensic Sci. Int.* 188 (2009) 1–17.
- [106] A. Barbaro, P. Cormaci, A. Teatino, A. Barbaro, Validation of forensic DNA analysis from bloodstains treated by presumptive test reagents, *Int. Congr. Ser.* 1261 (2004) 631–633.
- [107] D.L. Laux, Effects of luminol on the subsequent analysis of bloodstains, in: *J. Forensic Sci.*, 1991: pp. 1512–1520.  
<http://www.scopus.com/inward/record.url?eid=2-s2.0-0025949277&partnerID=tZOtx3y1>.
- [108] J.P. de Almeida, N. Glesse, C. Bonorino, Effect of presumptive tests reagents on human blood confirmatory tests and DNA analysis using real time polymerase chain reaction., *Forensic Sci. Int.* 206 (2011) 58–61.
- [109] S.J. Seashols, H.D. Cross, D.L. Shrader, A. Rief, A Comparison of Chemical Enhancements for the Detection of Latent Blood, *J. Forensic Sci.* 58 (2013) 130–133.
- [110] W.C. Lee, A.F.L. Abdullah, B.E. Khoo, Forensic bloodstain imaging: a digital method for stain enhancement and background reduction, *Aust. J. Forensic Sci.* (2014) 1–9.
- [111] S. Seidl, R. Hausmann, P. Betz, Comparison of laser and mercury-arc lamp for the detection of body fluids on different substrates, *Int. J. Legal Med.* 122 (2008) 241–244.
- [112] S.M. Bleay, V.G. Sears, H.L. Bandey, A.P. Gibson, V.J. Bowman, R. Downham, L. Fitzgerald, T. Ciuksza, J. Ramadani, C. Selway, Chapter 5 : Alternative finger mark development techniques, in: *Fingerpr. Source B.*, 2012.
- [113] D.D. Garner, K.M. Cano, R.S. Peimer, T.E. Yeshion, An evaluation of

- tetramethylbenzidine as a presumptive test for blood., *J. Forensic Sci.* 21 (1976) 816–821.
- [114] F. a V Pascual, M.S.G. Grifo, Investigation of bloodstains: False negative results of the benzidine test, *Forensic Sci. Int.* 71 (1995) 85–86.
- [115] J. Caldwell, W. Henderson, N. Kim, ABTS : A Safe Alternative to DAB for the Enhancement of Blood Fingerprints, *J. Forensic Sci.* 45 (2000) 785–794.
- [116] M. Wirstam, M.R.A. Blomberg, P.E.M. Siegbahn, Reaction mechanism of compound I formation in heme peroxidases: A density functional theory study, *J. Am. Chem. Soc.* 121 (1999) 10178–10185.
- [117] M. Cox, A study of the sensitivity and specificity of four presumptive tests for blood., *J. Forensic Sci.* 36 (1991) 1503–1511.
- [118] M. Vandewoestyne, T. Lepez, D. Van Hoofstat, D. Deforce, Evaluation of a Visualization Assay for Blood on Forensic Evidence, *J. Forensic Sci.* 60 (2015) n/a-n/a.
- [119] C.D. Matheson, M.A. Veall, Presumptive blood test using Hemastix with EDTA in archaeology, *J. Archaeol. Sci.* 41 (2014) 230–241.
- [120] K.J. Farrugia, K.A. Savage, H. Bandey, T. Ciuksza, N. Nic Daéid, Chemical enhancement of footwear impressions in blood on fabric - Part 2: Peroxidase reagents, *Sci. Justice.* 51 (2011) 110–121.
- [121] S. Mushtaq, N. Rasool, S. Firiyal, Detection of dry bloodstains on different fabrics after washing with commercially available detergents, *Aust. J. Forensic Sci.* (2015) 1–8.
- [122] M. Cox, Effect of fabric washing on the presumptive identification of bloodstains, *J. Forensic Sci.* 35 (1990) 1335.
- [123] M. Vennemann, G. Scott, L. Curran, F. Bittner, S.S. Tobe, Sensitivity and specificity of presumptive tests for blood, saliva and semen, *Forensic Sci. Med. Pathol.* 10 (2014) 69–75.
- [124] S.L. Morgan, M.L. Myrick, Rapid Visualization of Biological Fluids at Crime Scenes using Optical Spectroscopy (Grant Report), 2011.
- [125] F. Barni, S.W. Lewis, A. Berti, G.M. Miskelly, G. Lago, Forensic application of the luminol reaction as a presumptive test for latent blood detection, *Talanta.* 72 (2007) 896–913.

- [126] B.A. Schweers, J. Old, P.W. Boonlayangoor, K.A. Reich, Developmental validation of a novel lateral flow strip test for rapid identification of human blood (Rapid Stain Identification™-Blood), *Forensic Sci. Int. Genet.* 2 (2008) 243–247.
- [127] D. Petersen, F. Kovacs, Phenolphthalein False-Positive Reactions from Legume Root Nodules, *J. Forensic Sci.* 59 (2014) 481–484.
- [128] A. Durdle, R.J. Mitchell, R.A.H. van Oorschot, The Use of Forensic Tests to Distinguish Blowfly Artifacts from Human Blood, Semen, and Saliva, *J. Forensic Sci.* 60 (2015) 468–470.
- [129] C.J. Frégeau, O. Germain, R.M. Fourney, Fingerprint enhancement revisited and the effects of blood enhancement chemicals on subsequent profiler Plus fluorescent short tandem repeat DNA analysis of fresh and aged bloody fingerprints., *J. Forensic Sci.* 45 (2000) 354–380.
- [130] B. Marchant, C. Tague, Developing Fingerprints in Blood : A Comparison of Several Chemical Techniques, *J. Forensic Identif.* 57 (2007) 76–93.
- [131] H.C. Lee, R.E. Gaensslen, *ADVANCES IN FINGERPRINT*, 3rd ed., CRC Press, London, 2013.
- [132] V.G. Sears, T.M. Prizeman, Enhancement of Fingerprints in Blood - Part 1: The Optimisation of Amido Black, *J. Forensic Identif.* 50 (2000) 470–480.
- [133] P. Pereira, The Use of Various Chemical Blood Reagents to Develop Blood Fingerprint or Footwear Impressions, *J. Forensic Identif.* 64 (2014) 43–70.
- [134] V.G. Sears, C.P.G. Butcher, T.M. Prizeman, Enhancement of fingerprints in blood--part 2 : Protein dyes, *J. Forensic Identif.* 51 (2001) 28–38.
- [135] K.J. Farrugia, H. Bandey, K. Savage, N. NicDaéid, Chemical enhancement of footwear impressions in blood on fabric - Part 3: Amino acid staining, *Sci. Justice.* 53 (2013) 8–13.
- [136] J. Moore, S. Bleay, J. Deans, N. NicDaeid, Recovery of fingerprint from arson scenes: Part 2 - Fingerprints in Blood, *J. Forensic Identif.* 58 (2008) 54–82.
- [137] M. Kemme, *EVALUATION OF ZAR-PRO LIFTING STRIP FIDELITY IN COMPARISON TO OTHER BLOOD FINGERPRINT ENHANCEMENT METHODS*, 2014.

- [138] N. Frascione, J. Gooch, B. Daniel, Enabling fluorescent biosensors for the forensic identification of body fluids., *Analyst*. 138 (2013) 7279–88.
- [139] N. Frascione, V. Pinto, B. Daniel, Development of a biosensor for human blood: New routes to body fluid identification, *Anal. Bioanal. Chem.* 404 (2012) 23–28.
- [140] S.M. Bleay, V.G. Sears, H.L. Bandey, A.P. Gibson, V.J. Bowman, R. Downham, L. Fitzgerald, T. Ciuksza, J. Ramadani, C. Selway, S. Barber, *Fingerprint Source Book*, 1st ed., Home Office, Centre for Applied Science and Technology (St. Albans), 2012.
- [141] L. Rae, D. Gentles, K. Farrugia, An investigation into the enhancement of fingermarks in blood on fruit and vegetables, *Sci. Justice*. 53 (2013) 321–327.
- [142] S.S. Tobe, N. Watson, N.N. Daéid, Evaluation of six presumptive tests for blood, their specificity, sensitivity, and effect on high molecular-weight DNA, *J. Forensic Sci.* 52 (2007) 102–109.
- [143] K. Tsukada, Y. Harayama, M. Shimizu, Y. Kurasawa, K. Kasahara, Influence of presumptive reagents on DNA typing, *Forensic Sci. Int. Genet. Suppl. Ser.* 3 (2011) e375–e376.
- [144] N.S. Alenazy, A.M. Refaat, S.R. Babu, Comparison of the effects of two presumptive test reagents on the ability to obtain STR profiles from minute bloodstains, *Egypt. J. Forensic Sci.* (2015).
- [145] a. Fox, M. Gittos, S. a. Harbison, R. Fleming, R. Wivell, Exploring the recovery and detection of messenger RNA and DNA from enhanced fingermarks in blood, *Sci. Justice*. 54 (2014) 192–198.
- [146] G.G. Shutler, A study on the inter-relationship between fingerprint developing techniques and bloodstain identification and typing methods, *J. Can. Soc. Forensic Sci.* 13 (1980) 1–8.  
<http://www.scopus.com/inward/record.url?eid=2-s2.0-0018840619&partnerID=tZOtx3y1>.
- [147] S.M. Bleay, V.G. Sears, H.L. Bandey, A.P. Gibson, V.J. Bowman, R. Downham, L. Fitzgerald, T. Ciuksza, J. Ramadani, C. Selway, S. Barber, Chapter 3 : Finger mark development techniques within scope of ISO 17025,

- in: Fingerpr. Source B., Home Office, 2013: pp. 1–66.
- [148] K. De Wael, L. Lepot, F. Gason, B. Gilbert, In search of blood - Detection of minute particles using spectroscopic methods, *Forensic Sci. Int.* 180 (2008) 37–42.
- [149] F. Zapata, M.Á. Fernández de la Ossa, C. García-Ruiz, Emerging spectrometric techniques for the forensic analysis of body fluids, *TrAC Trends Anal. Chem.* 64 (2015) 53–63.
- [150] S.M. Bleay, V.G. Sears, H.L. Bandey, A.P. Gibson, V.J. Bowman, R. Downham, L. Fitzgerald, T. Ciuksza, J. Ramadani, C. Selway, S. Barber, Chapter 6 : Specialist imaging techniques, in: *Fingerpr. Source B., Home Office*, 2012: pp. 484–503.
- [151] A.D. Roeder, C. Haas, mRNA profiling using a minimum of five mRNA markers per body fluid and a novel scoring method for body fluid identification, *Int. J. Legal Med.* 127 (2013) 707–721.
- [152] C. Haas, E. Hanson, W. Bär, R. Banemann, a. M. Bento, A. Berti, E. Borges, C. Bouakaze, A. Carracedo, M. Carvalho, A. Choma, M. Dötsch, M. Durianciková, P. Hoff-Olsen, C. Hohoff, P. Johansen, P. a. Lindenbergh, B. Loddenkötter, B. Ludes, O. Maroñas, N. Morling, H. Niederstätter, W. Parson, G. Patel, C. Popielarz, E. Salata, P.M. Schneider, T. Sijen, B. Sviezená, L. Zatkalíková, J. Ballantyne, mRNA profiling for the identification of blood - Results of a collaborative EDNAP exercise, *Forensic Sci. Int. Genet.* 5 (2011) 21–26.
- [153] C. Haas, B. Klessner, C. Maake, W. Bär, A. Kratzer, mRNA profiling for body fluid identification by reverse transcription endpoint PCR and realtime PCR, *Forensic Sci. Int. Genet.* 3 (2009) 80–88.
- [154] T. Conti, E. Buel, *Forensic stain identification by RT-PCR analysis (Report)*, 2009.
- [155] D. Zubakov, M. Kokshoorn, A. Kloosterman, M. Kayser, New markers for old stains: Stable mRNA markers for blood and saliva identification from up to 16-year-old stains, *Int. J. Legal Med.* 123 (2009) 71–74.
- [156] E.K. Hanson, J. Ballantyne, Rapid and inexpensive body fluid identification by RNA profiling-based multiplex High Resolution Melt (HRM) analysis,

F1000Research. (2013) 1–22.

- [157] J. Juusola, J. Ballantyne, Multiplex mRNA profiling for the identification of body fluids, *Forensic Sci. Int.* 152 (2005) 1–12.
- [158] A. Lindenbergh, M. De Pagter, G. Ramdayal, M. Visser, D. Zubakov, M. Kayser, T. Sijen, A multiplex (m)RNA-profiling system for the forensic identification of body fluids and contact traces, *Forensic Sci. Int. Genet.* 6 (2012) 565–577.
- [159] D. Zubakov, E. Hanekamp, M. Kokshoorn, W. Van IJcken, M. Kayser, Stable RNA markers for identification of blood and saliva stains revealed from whole genome expression analysis of time-wise degraded samples, *Int. J. Legal Med.* 122 (2008) 135–142.
- [160] C. Haas, E. Hanson, A. Kratzer, W. Bär, J. Ballantyne, Selection of highly specific and sensitive mRNA biomarkers for the identification of blood, *Forensic Sci. Int. Genet.* 5 (2011) 449–458.
- [161] C. Courts, B. Madea, Specific micro-RNA signatures for the detection of saliva and blood in forensic body-fluid identification, *J. Forensic Sci.* 56 (2011) 1464–1470.
- [162] E. Hanson, H. Lubenow, J. Ballantyne, Identification of forensically relevant body fluids using a panel of differentially expressed microRNAs, *Forensic Sci. Int. Genet. Suppl. Ser. 2* (2009) 503–504.
- [163] D. Zubakov, A.W.M. Boersma, Y. Choi, P.F. Van Kuijk, E. a C. Wiemer, M. Kayser, MicroRNA markers for forensic body fluid identification obtained from microarray screening and quantitative RT-PCR confirmation, *Int. J. Legal Med.* 124 (2010) 217–226.
- [164] S.S. Silva, C. Lopes, A.L. Teixeira, M.J. Carneiro De Sousa, R. Medeiros, Forensic miRNA: Potential biomarker for body fluids?, *Forensic Sci. Int. Genet.* 14 (2015) 1–10.
- [165] M. Bauer, D. Patzelt, A method for simultaneous RNA and DNA isolation from dried blood and semen stains, *Forensic Sci. Int.* 136 (2003) 76–78.
- [166] F. Yan, T. Vo-Dinh, Surface-enhanced Raman scattering detection of chemical and biological agents using a portable Raman integrated tunable sensor, *Sensors Actuators, B Chem.* 121 (2007) 61–66.

- [167] S. Boyd, M.F. Bertino, S.J. Seashols, Raman spectroscopy of blood samples for forensic applications, *Forensic Sci. Int.* 208 (2011) 124–128.
- [168] K. Virkler, I.K. Lednev, Raman spectroscopy offers great potential for the nondestructive confirmatory identification of body fluids, *Forensic Sci. Int.* 181 (2008) 1–5.
- [169] K. Virkler, I.K. Lednev, Forensic body fluid identification: the Raman spectroscopic signature of saliva., *Analyst.* 135 (2010) 512–517.
- [170] K. Virkler, I.K. Lednev, Raman spectroscopic signature of semen and its potential application to forensic body fluid identification, *Forensic Sci. Int.* 193 (2009) 56–62.
- [171] K. Virkler, I.K. Lednev, Raman spectroscopic signature of blood and its potential application to forensic body fluid identification, *Anal. Bioanal. Chem.* 396 (2010) 525–534.
- [172] V. Sikirzhytski, K. Virkler, I.K. Lednev, Discriminant analysis of Raman spectra for body fluid identification for forensic purposes, *Sensors.* 10 (2010) 2869–2884.
- [173] V. Sikirzhytski, A. Sikirzhytskaya, I.K. Lednev, Multidimensional Raman spectroscopic signature of sweat and its potential application to forensic body fluid identification, *Anal. Chim. Acta.* 718 (2012) 78–83.
- [174] V. Sikirzhytski, A. Sikirzhytskaya, I.K. Lednev, Multidimensional Raman spectroscopic signatures as a tool for forensic identification of body fluid traces: A review, *Appl. Spectrosc.* 65 (2011) 1223–1232.
- [175] K. Virkler, I.K. Lednev, Blood species identification for forensic purposes using Raman spectroscopy combined with advanced statistical analysis, *Anal. Chem.* 81 (2009) 7773–7777.
- [176] S. Boyd, M.F. Bertino, D. Ye, L.S. White, S.J. Seashols, Highly Sensitive Detection of Blood by Surface Enhanced Raman Scattering, *J. Forensic Sci.* 58 (2013) 753–756.
- [177] P. Lemler, W.R. Premasiri, A. DelMonaco, L.D. Ziegler, NIR Raman spectra of whole human blood: Effects of laser-induced and in vitro hemoglobin denaturation, *Anal. Bioanal. Chem.* 406 (2014) 193–200.
- [178] G. McLaughlin, K.C. Doty, I.K. Lednev, Raman Spectroscopy of Blood for

- Species Identification, *Anal. Biochem.* 86 (2014) 11628–11633.
- [179] A. Sikirzhyskaya, V. Sikirzhyski, G. Mclaughlin, I.K. Lednev, Forensic identification of blood in the presence of contaminations using raman microspectroscopy coupled with advanced statistics: Effect of sand, dust, and soil, *J. Forensic Sci.* 58 (2013) 1141–1148.
- [180] W.R. Premasiri, J.C. Lee, L.D. Ziegler, Surface-Enhanced Raman Scattering of Whole Human Blood, Blood Plasma, and Red Blood Cells: Cellular Processes and Bioanalytical Sensing, *J. Phys. Chem.* 116 (2012) 9376–9386.
- [181] C.-M. Orphanou, The detection and discrimination of human body fluids using ATR FT-IR spectroscopy, *Forensic Sci. Int.* 252 (2015) e10–e16.
- [182] R.H. Bremmer, G. Edelman, T.D. Vegter, T. Bijvoets, M.C.G. Aalders, Remote spectroscopic identification of bloodstains, *J. Forensic Sci.* 56 (2011) 1471–1475.
- [183] ChemImage, Hyperspectral Imaging Provides Detection and High Contrast Imaging of Biological Stains (White Paper), (2015).  
[www.chemimage.com/docs/white-papers/biological-stains-white-paper.pdf](http://www.chemimage.com/docs/white-papers/biological-stains-white-paper.pdf)  
(accessed July 19, 2015).
- [184] G.J. Edelman, E. Gaston, T.G. van Leeuwen, P.J. Cullen, M.C.G. Aalders, Hyperspectral imaging for non-contact analysis of forensic traces, *Forensic Sci. Int.* 223 (2012) 28–39.
- [185] B. Li, P. Beveridge, W.T. O'Hare, M. Islam, The application of visible wavelength reflectance hyperspectral imaging for the detection and identification of blood stains, *Sci. Justice.* 54 (2014) 432–8.
- [186] P. Scano, E. Locci, A. Noto, G. Navarra, F. Murgia, M. Lussu, L. Barberini, L. Atzori, F. De Giorgio, M.F. Rosa, E. D'Aloja, <sup>1</sup>H NMR metabolite fingerprinting as a new tool for body fluid identification in forensic science, *Magn. Reson. Chem.* 51 (2013) 454–462.
- [187] J.I. Trombka, J. Schweitzer, C. Selavka, M. Dale, N. Gahn, S. Floyd, J. Marie, M. Hobson, J. Zeosky, K. Martin, T. McClannahan, P. Solomon, E. Gottschang, Crime scene investigations using portable, non-destructive space exploration technology, *Forensic Sci. Int.* 129 (2002) 1–9.

- [188] H. Yang, B. Zhou, H. Deng, M. Prinz, D. Siegel, Body fluid identification by mass spectrometry, *Int. J. Legal Med.* 127 (2013) 1065–1077.
- [189] H. Yang, B. Zhou, M. Prinz, D. Siegel, Proteomic analysis of menstrual blood., *Mol. Cell. Proteomics.* 11 (2012) 1024–35.
- [190] M. Dorrill, P.H. Whitehead, The species identification of very old human blood-stains., *Forensic Sci. Int.* 13 (1979) 111–116.
- [191] R.W. Butt, Identification of human blood stains by radioimmunoassay., *J. Forensic Sci. Soc.* 23 (1983) 291–296.
- [192] Y. Yamamoto, A. Tsutsumi, H. Ishizu, Species identification of blood and bloodstains by enzyme-linked immunosorbent assay (ELISA) using anti-human immunoglobulin kappa light chain monoclonal antibody, *Forensic Sci. Int.* 40 (1989) 85–95.
- [193] C. Cattaneo, K. Gelsthorpe, P. Phillips, R.J.J. Sokol, Detection of human proteins in buried blood using ELISA and monoclonal antibodies: towards the reliable species identification of blood stains on buried material., *Forensic Sci. Int.* 57 (1992) 139–146.
- [194] I.P. Hurley, R. Cook, C.W. Laughton, N.A. Pickles, H.E. Ireland, J.H.H. Williams, Detection of human blood by immunoassay for applications in forensic analysis, *Forensic Sci. Int.* 190 (2009) 91–97.
- [195] M.N. Hochmeister, B. Budowle, R. Sparkes, O. Rudin, C. Gehrig, M. Thali, L. Schmidt, a Cordier, R. Dirnhofer, Validation studies of an immunochromatographic 1-step test for the forensic identification of human blood., *J. Forensic Sci.* 44 (1999) 597–602.
- [196] S. Johnston, J. Newman, R. Frappier, Validation study of the Abacus Diagnostics ABACard(R) HemaTrace(R) membrane test for the forensic identification of human blood, *J. Can. Soc. Forensic Sci.* 36 (2003) 173–183.
- [197] S. Turrina, G. Filippini, R. Atzei, E. Zaglia, D. De Leo, Validation studies of rapid stain identification-blood (RSID-blood) kit in forensic caseworks, *Forensic Sci. Int. Genet. Suppl. Ser.* 1 (2008) 74–75.
- [198] R. Thorogate, J.C.S. Moreira, S. Jickells, M.M.P. Miele, B. Daniel, A novel fluorescence-based method in forensic science for the detection of blood in situ, *Forensic Sci. Int. Genet.* 2 (2008) 363–371.

- [199] K.L. Busch, *Mass Spectrometry*, (2003) 145–158.
- [200] R. Knochenmuss, Ion formation mechanisms in UV-MALDI, *Analyst*. 131 (2006) 966.
- [201] L. Spinney, Nobel Prize controversy, *Sci.* (2002). <https://www.the-scientist.com/?articles.view/articleNo/21791/title/Nobel-Prize-controversy/> (accessed December 1, 2017).
- [202] M. Karas, D. Bachmann, F. Hillenkamp, Influence of the Wavelength in High-Irradiance Ultraviolet Laser Desorption Mass Spectrometry of Organic Molecules, *Anal. Chem.* 57 (1985) 2935–2939.
- [203] R.J.A. Goodwin, Sample preparation for mass spectrometry imaging: Small mistakes can lead to big consequences, *J. Proteomics*. 75 (2012) 4893–4911.
- [204] R. Lemaire, J.C. Tabet, P. Ducoroy, J.B. Hendra, M. Salzet, I. Fournier, Solid ionic matrixes for direct tissue analysis and MALDI imaging, *Anal. Chem.* 78 (2006) 809–819.
- [205] C.D. Calvano, S. Carulli, F. Palmisano, Aniline/*o*-cyano-4-hydroxycinnamic acid is a highly versatile ionic liquid for matrix-assisted laser desorption/ionization mass spectrometry, *Rapid Commun. Mass Spectrom.* 23 (2009) 1659–1668.
- [206] L.M. Cole, M.-C. Djidja, J. Bluff, E. Claude, V. a Carolan, M. Paley, G.M. Tozer, M.R. Clench, Investigation of protein induction in tumour vascular targeted strategies by MALDI MSI., *Methods*. 54 (2011) 442–53.
- [207] P.J. Hart, S. Francese, E. Claude, M.N. Woodroffe, M.R. Clench, MALDI-MS imaging of lipids in ex vivo human skin, *Anal. Bioanal. Chem.* 401 (2011) 115–125.
- [208] J. Franck, K. Arafah, a Barnes, M. Wisztorski, M. Salzet, I. Fournier, Improving tissue preparation for matrix-assisted laser desorption ionization mass spectrometry imaging. Part 1: Using microspotting, *Anal. Chem.* 81 (2009) 8193–8202.
- [209] K.S. Lovejoy, A.J. Lou, L.E. Davis, T.C. Sanchez, S. Iyer, C.A. Corley, J.S. Wilkes, R.K. Feller, D.T. Fox, A.T. Koppisch, R.E. Del Sesto, Single-pot extraction-analysis of dyed wool fibers with ionic liquids, *Anal. Chem.* 84

(2012) 9169–9175.

- [210] C. Gassner, S. Meyer, B.M. Frey, C. Vollmert, Matrix-assisted laser desorption/ionisation, time-of-flight mass spectrometry-based blood group genotyping-the alternative approach, *Transfus. Med. Rev.* 27 (2013) 2–9.
- [211] K. Dreisewerd, *The desorption process in MALDI*, 2003.
- [212] M. Karas, R. Krüger, Ion formation in MALDI: The cluster ionization mechanism, *Chem. Rev.* 103 (2003) 427–439.
- [213] R. Knochenmuss, R. Zenobi, MALDI ionization: The role of in-plume processes, *Chem. Rev.* 103 (2003) 441–452.
- [214] J. Pól, M. Strohal, V. Havlíček, M. Volný, Molecular mass spectrometry imaging in biomedical and life science research, *Histochem. Cell Biol.* 134 (2010) 423–443.
- [215] R.E. March, J.F.J. Todd, The Development of the Quadrupole Mass Filter and Quadrupole Ion Trap, in: M.L. Gross, R.M. Caprioli (Eds.), *Encycl. Mass Spectrom.*, 2016: pp. 43–60.
- [216] E. de Hoffmann, V. Stroobant, *Mass spectrometry : principles and applications*, 3rd ed. ., Chichester : Wiley, Chichester, 2007.
- [217] Waters, SYNAPT G2 High Definition MS (HDMS) System Specifications, (2010) 1–4.  
file:///Users/Jasper/Documents/Papers2/Articles/2010/Waters/2010 Waters.pdf%5Cpapers2://publication/uuid/F16E743F-5D70-4C93-AB94-35D3E85758BA.
- [218] H.J. Räder, T.T.T. Nguyen, K. Müllen, MALDI-TOF mass spectrometry of polyphenylene dendrimers up to the megadalton range. elucidating structural integrity of macromolecules at unrivaled high molecular weights, *Macromolecules.* 47 (2014) 1240–1248.
- [219] J.M. Spraggins, D.G. Rizzo, J.L. Moore, M.J. Noto, E.P. Skaar, R.M. Caprioli, Next-generation technologies for spatial proteomics: Integrating ultra-high speed MALDI-TOF and high mass resolution MALDI FTICR imaging mass spectrometry for protein analysis, *Proteomics.* 16 (2016) 1678–1689.
- [220] I. V. Chernushevich, A. V. Loboda, B.A. Thomson, An introduction to quadrupole-time-of-flight mass spectrometry, *J. Mass Spectrom.* 36 (2001)

849–865.

- [221] N.J. Bright, R.P. Webb, S. Bleay, S. Hinder, N.I. Ward, J.F. Watts, K.J. Kirkby, M.J. Bailey, Determination of the deposition order of overlapping latent fingerprints and inks using secondary ion mass spectrometry, *Anal. Chem.* 84 (2012) 4083–4087.
- [222] B. Spengler, M. Hubert, R. Kaufmann, MALDI Ion Imaging and Biological Ion Imaging with a new Scanning UV-Laser Microprobe, in: *Proc. 42nd ASMS Conf. Mass Spectrom. Allied Top.*, 1994.
- [223] R.M. Caprioli, T.B. Farmer, J. Gile, Molecular Imaging of Biological Samples: Localization of Peptides and Proteins Using MALDI-TOF MS, *Anal. Chem.* 69 (1997) 4751–4760.
- [224] A.L. Dill, L.S. Eberlin, D.R. Ifa, R.G. Cooks, Perspectives in imaging using mass spectrometry, *Chem. Commun.* 47 (2011) 2741–2746.
- [225] A. Miki, M. Katagi, N. Shima, H. Kamata, M. Tatsuno, T. Nakanishi, H. Tsuchihashi, T. Takubo, K. Suzuki, Imaging of methamphetamine incorporated into hair by MALDI-TOF mass spectrometry, *Forensic Toxicol.* 29 (2011) 111–116.
- [226] T. Porta, C. Grivet, T. Kraemer, E. Varesio, G. Hopfgartner, Single hair cocaine consumption monitoring by mass spectrometric imaging, *Anal. Chem.* 83 (2011) 4266–4272.
- [227] G.S. Omenn, THE HUPO Human Plasma Proteome Project, *Proteomics - Clin. Appl.* 1 (2007) 769–779.
- [228] J.N. Adkins, S.M. Varnum, K.J. Auberry, R.J. Moore, N.H. Angell, R.D. Smith, D.L. Springer, J.G. Pounds, Toward a Human Blood Serum Proteome: Analysis By Multidimensional Separation Coupled With Mass Spectrometry, *Mol. Cell. Proteomics.* 1 (2002) 947–955.
- [229] G.L. Hortin, D. Sviridov, Diagnostic potential for urinary proteomics, *Pharmacogenomics.* 8 (2007) 237–255.
- [230] T.R. Shah, A. Misra, Proteomics, in: A. Misra (Ed.), *Challenges Deliv. Ther. Genomics Proteomics*, Elsevier, 2010: p. 686.
- [231] T. Seuberlich, M. Gsponer, C. Drögemüller, M.P. Polak, S. McCutcheon, D. Heim, A. Oevermann, A. Zurbrigge, Novel Prion Protein in BSE-affected

- Cattle, Switzerland, *Emerg. Infect. Dis.* 18 (2012) 3–4.
- [232] E. Illes-Toth, M.R. Ramos, R. Cappai, C. Dalton, D.P. Smith, Distinct higher-order alpha-synuclein oligomers induce intracellular aggregation Distinct higher-order  $\alpha$  -synuclein oligomers induce intracellular aggregation, *Biochem. J.* 468 (2015) 485–493.
- [233] C.N. Laatsch, B.P. Durbin-Johnson, D.M. Rocke, S. Mukwana, A.B. Newland, M.J. Flagler, M.G. Davis, R. a Eigenheer, B.S. Phinney, R.H. Rice, Human hair shaft proteomic profiling: individual differences, site specificity and cuticle analysis., *PeerJ.* 2 (2014) e506.
- [234] S. Dammeier, S. Nahnsen, J. Veit, F. Wehner, M. Ueffing, O. Kohlbacher, Mass-Spectrometry-Based Proteomics Reveals Organ-Specific Expression Patterns to Be Used as Forensic Evidence, *J. Proteome Res.* 15 (2016) 182–192.
- [235] J.A. Siepen, E.J. Keevil, D. Knight, S.J. Hubbard, Prediction of missed cleavage sites in tryptic peptides aids protein identification in proteomics, *J. Proteome Res.* 6 (2007) 399–408.
- [236] Y. Shen, J.M. Jacobs, D.G. Camp 2nd, R. Fang, R.J. Moore, R.D. Smith, W. Xiao, R.W. Davis, R.G. Tompkins, Ultra-high-efficiency strong cation exchange LC/RPLC/MS/MS for high dynamic range characterization of the human plasma proteome, *Anal Chem.* 76 (2004) 1134–44.
- [237] M.-C. Djidja, S. Francese, P.M. Loadman, C.W. Sutton, P. Scriven, E. Claude, M.F. Snel, J. Franck, M. Salzet, M.R. Clench, Detergent addition to tryptic digests and ion mobility separation prior to MS/MS improves peptide yield and protein identification for in situ proteomic investigation of frozen and formalin-fixed paraffin-embedded adenocarcinoma tissue sections., *Proteomics.* 9 (2009) 2750–63.
- [238] C. Zhang, H. Zhang, D.W. Litchfield, K.K.-C. Yeung, CHCA or DHB? Systematic Comparison of the Two Most Commonly Used Matrices for Peptide Mass Fingerprint Analysis with MALDI-MS, *Spectroscopy.* 25 (2010) 48–62.  
[http://lcproxy.shu.ac.uk/login?url=http://search.proquest.com/docview/212876919?accountid=13827%5Cnhttp://shulinks.shu.ac.uk/?ctx\\_ver=Z39.88-](http://lcproxy.shu.ac.uk/login?url=http://search.proquest.com/docview/212876919?accountid=13827%5Cnhttp://shulinks.shu.ac.uk/?ctx_ver=Z39.88-)

2004&ctx\_enc=info:ofi/enc:UTF-8&rft\_id=info:sid/ProQ:earthscijournals&rft\_val\_fmt=info:ofi/fmt:kev:mtx:journal&rft.g.

- [239] K. Heaton, C. Solazzo, M.J. Collins, J. Thomas-Oates, E.T. Bergström, Towards the application of desorption electrospray ionisation mass spectrometry (DESI-MS) to the analysis of ancient proteins from artefacts, *J. Archaeol. Sci.* 36 (2009) 2145–2154.
- [240] P.K. Sarkar, P.K. Prajapati, V.J. Shukla, B. Ravishankar, A.K. Choudhary, Toxicity and recovery studies of two ayurvedic preparations of iron, *Indian J. Exp. Biol.* 47 (2009) 987–992.
- [241] S. Beck, A. Michalski, O. Raether, M. Lubeck, S. Kaspar, N. Goedecke, C. Baessmann, D. Hornburg, F. Meier, I. Paron, N. a Kulak, J. Cox, M. Mann, The impact II, a very high resolution quadrupole time-of-flight instrument for deep shotgun proteomics, *Mol. Cell. Proteomics.* (2015) 2014–2029.
- [242] K.M. Legg, R. Powell, N. Reisdorph, R. Reisdorph, P.B. Danielson, Discovery of highly specific protein markers for the identification of biological stains, *Electrophoresis.* 35 (2014) 3069–3078.
- [243] K.P. Kirkbride, S. Kamanna, J. Henry, N. Voelcker, A. Linacre, “Bottom-up” *in situ* proteomic differentiation of human and non-human haemoglobins for forensic purposes by MALDI-ToF-MS/MS, *Rapid Commun. Mass Spectrom.* (2017).
- [244] S. Kamanna, J. Henry, N.H. Voelcker, A. Linacre, K. Paul Kirkbride, A mass spectrometry-based forensic toolbox for imaging and detecting biological fluid evidence in finger marks and fingernail scrapings, *Int. J. Legal Med.* (2017).
- [245] Y. Chen, L.K. Ju, Method for fast quantification of pitting using 3D surface parameters generated with infinite focus microscope, *Corrosion.* 71 (2015) 1184–1196.
- [246] W. Kaplonek, K. Nadolny, G.M. Królczyk, The use of focus-variation microscopy for the assessment of active surfaces of a new generation of coated abrasive tools, *Meas. Sci. Rev.* 16 (2016) 42–53.
- [247] S. Scherer, R. Danzl, Quality Assurance Throughout Optical 3D Surface

Measurement And True Color Visualization, (n.d.).

[http://family.alicon.com/index.php?id=19&no\\_cache=1&tx\\_msdownload\\_msdownloadfronted\[eleid\]=4617&tx\\_msdownload\\_msdownloadfronted\[action\]=download2&tx\\_msdownload\\_msdownloadfronted\[controller\]=File&cHash=dd466a1121d1604ee62794dfcef04001](http://family.alicon.com/index.php?id=19&no_cache=1&tx_msdownload_msdownloadfronted[eleid]=4617&tx_msdownload_msdownloadfronted[action]=download2&tx_msdownload_msdownloadfronted[controller]=File&cHash=dd466a1121d1604ee62794dfcef04001) (accessed January 13, 2016).

- [248] C. Macziewski, R. Spotts, S. Chumbley, Validation of Toolmark Comparisons Made At Different Vertical and Horizontal Angles, *J. Forensic Sci.* 62 (2017) 612–618.
- [249] T.N. Grieve, L.S. Chumbley, J. Kreiser, M. Morris, L. Ekstrand, S. Zhang, Objective Comparison of Toolmarks from the Cutting Surfaces of Slip-Joint Pliers, *AFTE J.* 46 (2014) 176–185.
- [250] D.A. Macdonald, The application of focus variation microscopy for lithic use-wear quantification, *J. Archaeol. Sci.* 48 (2014) 26–33.
- [251] S.M. Bello, I. De Groote, G. Delbarre, Application of 3-dimensional microscopy and micro-CT scanning to the analysis of Magdalenian portable art on bone and antler, *J. Archaeol. Sci.* 40 (2013) 2464–2476.
- [252] S.W. Hillson, S.A. Parfitt, S.M. Bello, M.B. Roberts, C.B. Stringer, Two hominin incisor teeth from the middle Pleistocene site of Boxgrove, Sussex, England, *J. Hum. Evol.* 59 (2010) 493–503.
- [253] S.M. Bello, S.A. Parfitt, C. Stringer, Quantitative micromorphological analyses of cut marks produced by ancient and modern handaxes, *J. Archaeol. Sci.* 36 (2009) 1869–1880.
- [254] S.M. Bello, *New Results from the Examination of Cut-Marks Using Three-Dimensional Imaging*, Elsevier Masson SAS, 2011.
- [255] S.M. Bello, C. Soligo, A new method for the quantitative analysis of cutmark micromorphology, *J. Archaeol. Sci.* 35 (2008) 1542–1552.
- [256] V.S. Williams, P.M. Barrett, M. a Purnell, Quantitative analysis of dental microwear in hadrosaurid dinosaurs, and the implications for hypotheses of jaw mechanics and feeding., *Proc. Natl. Acad. Sci. U. S. A.* 106 (2009) 11194–11199.
- [257] R. Abdalla, R.J. Mitchell, Y. fang Ren, Non-carious cervical lesions imaged by focus variation microscopy, *J. Dent.* 63 (2017) 14–20.

- [258] J.P.M. Lima, M.A.S. Melo, V.F. Passos, C.L.N. Braga, L.K.A. Rodrigues, S.L. Santiago, Dentin erosion by whitening mouthwash associated to toothbrushing abrasion: A focus variation 3D scanning microscopy study, *Microsc. Res. Tech.* 76 (2013) 904–908.
- [259] T. Winkler, E. Hoenig, R. Gildenhaar, G. Berger, D. Fritsch, R. Janssen, M.M. Morlock, A.F. Schilling, Volumetric analysis of osteoclastic bioresorption of calcium phosphate ceramics with different solubilities, *Acta Biomater.* 6 (2010) 4127–4135.
- [260] R. Danzl, F. Helmlí, S. Scherer, Focus Variation - A new Technology for High Resolution Optical 3D Surface Metrology, in: *Focus Var. - A New Technol. High Resolut. Opt. 3D Surf. Metrol.*, 2009: pp. 1–10.  
[http://www.alicon.at/home/fileadmin/alicon/pdf/FocusVariation\\_New\\_technology\\_for\\_optical\\_3D\\_surface\\_metrology\\_10th\\_InternatConfSlovSoc\\_2009\\_01.pdf](http://www.alicon.at/home/fileadmin/alicon/pdf/FocusVariation_New_technology_for_optical_3D_surface_metrology_10th_InternatConfSlovSoc_2009_01.pdf).
- [261] R. Danzl, F. Helmlí, S. Scherer, Focus variation - A robust technology for high resolution optical 3D surface metrology, *Stroj. Vestnik/Journal Mech. Eng.* 57 (2011) 245–256.

## Chapter 2

### **A proteomic approach for the rapid, multi-informative and reliable identification of blood**

## 2.1 Introduction

The detection of blood in stains or fingerprints at crime scenes can be an invaluable piece of evidence in the investigation of violent crimes. Crime scene investigators have several classes of enhancement techniques available to visualize the presence of blood, including optical, spectroscopic and chemical development methods [1]. In addition to limitations in common to all of the three classes of methods, chemical techniques are only presumptive methods, thus occasionally leading to false positives. These methods have been extensively reviewed by Sears [1] and all were reported to exhibit a lack of specificity; even haem-reactive compounds, the most specific class of blood reagents, may give false positives as horseradish, leather and extracts from plant material [2] show the same peroxidase activity exhibited by haem in human blood. For this reason, the author's director of studies has previously reported a rapid and specific MALDI-MS method to detect blood in stains and map this biofluid in bloodied fingerprints [3]. With this method, the  $m/z$  of both haem and intact haemoglobin was employed to reliably demonstrate the presence of blood. The method was applied to a real crime scene stain, proving successful in less than five minutes of preparation and acquisition time. Since blood provenance is also a forensic question of interest and the  $m/z$  of haem would not permit the determination of the blood source, the  $m/z$  of intact haemoglobin chains were exploited to distinguish between equine, human and bovine blood, based on the small differences in the protein amino acid sequence [3]. However, although the detection of blood at a molecular level provides much higher specificity and reliability, intact protein analysis by MALDI-mass spectrometry suffers from mass resolution and mass accuracy issues, which may become significant, especially if blood is mixed with other bio-fluids or protein sources.

The use of a bottom-up proteomic approach increases the reliability of protein identification because the mass of the smaller protein-derived peptides can be measured and separated more accurately (a few parts per million). This is due to the smaller number of amino acids in a peptide resulting in a lower mass difference to the theoretical, monoisotopic value caused by element mass fractions and isotopic abundances in comparison to a larger protein, where the higher number of amino

acids results in an overall higher mass difference. This approach would also enable the detection of additional blood-specific proteins, besides haemoglobin, allowing specificity and confidence in the determination of the blood presence to be further enhanced. The literature already contains many reports attempting to map the proteome of plasma and serum. Different authors concur on the extreme complexity of these matrices, with plasma being particularly challenging due to the wide range of concentrations of the proteins present (spanning 9 orders of magnitude) [4] and the huge heterogeneity due to the variety of protein glycoforms. In 2010, Liumbruno et al. extensively reviewed the literature covering the mapping of the blood proteome with all the techniques employed up to that date and the corresponding number of obtained protein identifications [5]. The majority of the methods employed separation techniques (gel electrophoresis-based or liquid chromatography) hyphenated with mass spectrometry, in both online and off-line approaches, employing ESI and MALDI, respectively, as mass spectrometry techniques.

Amongst the techniques used, the combination of 2D gel electrophoresis and mass spectrometry was reported to be able to identify 289 plasma proteins in 2002 [4]; cation exchange coupled to capillary gradient reversed phase liquid chromatography combined with mass spectrometry of digested peptides contributed to the identification of 490 blood serum proteins [6]. These numbers have further increased when depletion and sample enrichment methods were preliminarily employed. In a 2005 collaborative study coordinated by HUPO involving 35 laboratories, up to 3020 plasma/serum proteins were identified using a range of hyphenated techniques [7]; since the start of the HUPO project the number of identified proteins has rapidly increased to populate a database (<http://www.plasmaproteomedatabase.org/>) of 10546 proteins [8]. None of the approaches reported in the literature so far has involved the direct application of MALDI-MS on enzymatically digested blood. This is understandable, as in all of the previous reports the aim was to map the entirety of the blood proteome for medical and diagnostic purposes. However, in a forensic context, the detection of a handful of blood-specific proteins via the more reliable bottom-up proteomic approach using MALDI-MS would be more than appropriate. Furthermore, in forensic science, provided that reliability of the evidence is not

compromised, speed is paramount to investigations; the hyphenated methods reported can be labour-intensive and time-consuming, especially since some of them have employed preliminary purification to remove the most abundant proteins (e.g. albumin and haemoglobin).

Reported here is an optimised a method for the digestion of bloodstains followed by direct MALDI-MS analysis; the method couples high mass accuracy the peptide mass fingerprinting stage with further confirmatory analysis by tandem mass spectrometry. A classical in-solution digestion protocol was optimised for use on blood stains by investigating the optimal concentration of trypsin to employ as well as the optimal digestion time. The performance of this method was then critically compared to that of a second method employing Vmh2 hydrophobin to preliminarily coat the MALDI target plate. This protein belongs to the class I hydrophobins and it has been demonstrated to homogeneously self-assemble on hydrophilic or hydrophobic surfaces [9] and to subsequently strongly bind proteins, including enzymes in their active form such as trypsin [10]. The use of Vmh2 has been recently proposed in a lab-on-plate approach as a simple and effective desalting method, enabling decrease in the proteolysis time and increase of the peptides' signal-to-noise (S/N) for tryptic digestion [11]. It was found that both methods could be successfully used to: (i) reliably detect the presence of blood in stains, (ii) determine the blood provenance even when two different blood sources were mixed and (iii) to identify the presence of this biofluid in a 9-year-old sample that had been pre-treated with acid black 1 [12,13], a protein dye used for the nonspecific enhancement/visualisation of blood. As it is discussed in this chapter, the present data will no doubt impact on the effectiveness of forensic practice by providing much more reliable and informative evidence than currently used techniques, thus empowering both investigations (of cold cases too) and judicial debates.

## 2.2 Experimental

### 2.2.1 Materials

ALUGRAMSIL G/ UV<sub>254</sub> aluminium sheets, acetonitrile (ACN), ammonium bicarbonate (AmBic), trifluoroacetic acid (TFA), trypsin from bovine pancreas and alpha-cyano-4-hydroxycinnamic acid (CHCA) were obtained from Sigma-Aldrich (Dorset, UK). Trypsin gold was purchased from Promega, Southampton (UK) whereas Rapigest™ SF was purchased from Waters (Elstree, UK). Defibrinated horse blood was obtained from Fisher Scientific (USA). Unistik® 3 Neonatal & Laboratory single use lancets were obtained from Owen Mumford (Oxford, UK). Vmh2 ethanolic solution was prepared as previously described [10].

### 2.2.2 Instrumentation and data acquisition

Calibration over a  $m/z$  600–2800 range was performed prior to analysis using phosphorous red. MALDI-IMS/MS data were acquired in positive ion mode from  $m/z$  600 to 3000 at a mass resolution of 10,000 FWHM using a SYNAPT G2™ HDMS system (Waters Corporation, Manchester, UK) operating with a 1 kHz Nd:YAG laser. Full scan mass spectra were manually acquired over 45 seconds; all experiments were carried out in duplicate. The laser energy was set to 250 arbitrary units on the instrument; laser energy was increased to 270 arbitrary units for MALDI-IMS-MS/MS experiments. MS/MS analyses were conducted *in situ* on the most intense peaks. Fragmentation was carried out in the transfer region of the instrument, post ion mobility separation, therefore product ions retain the same drift time as the precursor ion. Collision energies ranging between 60–80 eV were used to obtain the best signal to noise ratio for product ions.

## 2.3 Methods

### 2.3.1 Initial method development and optimisation of digest protocol

Standard solutions of Hb and myoglobin were made up at 1 mg/mL in 70:30 Acetonitrile (ACN):0.2% TFA<sub>aq</sub>. All solutions were discarded after a maximum of 2 days of storage in the fridge (at 5-8°C).

Table xx outlines the conditions trialled on the above solutions, all employing 20 µg/mL trypsin gold and 37°C incubation temperature and combinations of one parameter of each set (i.e. only one detergent per sample). Using this approach, 1 µL of trypsin solution (with or without detergents) was added to 10 µL of Hb or myoglobin solution. Alternatively, 10 µL of sample were dried down with nitrogen and reconstituted in 40 µL 40 mM AmBic (NH<sub>4</sub>HCO<sub>3</sub>, pH 8) prior to addition of 10 µL of trypsin (with or without detergents).

<b>Digestion time</b>	<ul style="list-style-type: none"> <li>- 3h</li> <li>- 6h</li> <li>- overnight</li> </ul>
<b>Detergent addition</b>	<ul style="list-style-type: none"> <li>- 0.5% v/v β-Octylglucoside (10mM)</li> <li>- 2% v/v Mega-8 (0.1% w/v in 40mM AmBic)</li> <li>- 0.1% or 0.3% v/v Rapigest™ SF (1% w/v in ultrapure dH<sub>2</sub>O)</li> </ul>
<b>Pre-concentration</b>	<ul style="list-style-type: none"> <li>- None</li> <li>- Drying down with nitrogen, reconstituting in 40 µL 40 mM AmBic</li> </ul>
<b>Stopping of digestion</b>	<ul style="list-style-type: none"> <li>- Addition of 2 µL 5% TFA<sub>aq</sub></li> <li>- Placing in the -20°C freezer</li> </ul>

**Table 2.1** Digest conditions trialled on Hb and myoglobin solutions for method development.

Ten µL defibrinated horse blood were digested for 1, 3, 5 or 7 hours with 10 µL of 20 µg/mL trypsin with 0.1% Rapigest™ SF a.) directly, b.) after nitrogen-drying and reconstitution in 40 µL 40 mM AmBic or c.) after nitrogen-drying (reconstitution in trypsin).

All incubations were stopped by placing in the -20°C freezer (one sample) or the addition of 2µL 5%TFA<sub>aq</sub> (one sample).

A bichinchinonic acid (BCA) assay was carried to out to establish the protein concentration in whole, defibrinated horse blood. For this, standards of bovine serum albumin ranging from 25 µg/mL to 800 µg/mL were incubated with the BCA reagents according to the manufacturer's instructions, alongside two replicates of a dilution series of blood (initially undiluted and 1:1 to 1:50, then 1:200 to 1:1000 in a second experiment) for 30 minutes. The absorbance was measured at 562 nm and the

reading of the blank subtracted from all other readings. A standard calibration curve was then plotted to extrapolate the protein concentrations of the blood samples.

A 1:200 dilution of whole, defibrinated horse blood was prepared with dH<sub>2</sub>O. Ten  $\mu$ L of this were topped up with 40  $\mu$ L 40 mM AmBic or dried down with nitrogen and reconstituted in 40  $\mu$ L 40 mM AmBic prior to the addition of 9  $\mu$ L trypsin (20  $\mu$ g/mL with detergents 0.5%  $\beta$ -Octylglucoside, 2% Mega-8 or 0.1% Rapigest™ SF as above).

Samples were incubated for 1, 2, 3 or 4 hours at 37°C, 5%CO<sub>2</sub> and digestion stopped by the addition of 2  $\mu$ L 5% TFA<sub>aq</sub>.

All samples were spotted at 0.5  $\mu$ L and topped and pipette-mixed with 0.5  $\mu$ L CHCA 10 mg/mL CHCA (70:30 ACN:0.5% TFA<sub>aq</sub>) while wet.

### **2.3.2 Preparation and enzymatic digestion of blood samples**

Preliminary ageing experiments for in-solution digests were carried out as follows. For each ageing time point (5 hours, 1 day, 3 days and 7 days) and blood species under investigation (human, horse, cow from meat package, cow from a butcher's, pig from meat package, pig from a butcher's), 10  $\mu$ L of blood were pipetted onto a clean ceramic tile (previously cleaned with ACN) and thinly spread into squares of approximately 7 mm side length with a pipette tip, taking care not to let the different samples contaminate each other.

The tile was covered and placed into the environmental chamber at 25°C and 60% humidity.

Each separate sample was then extracted from the ceramic tile by pipetting 70  $\mu$ L of 50% ACN solution onto the dried blood regions after the corresponding ageing time had elapsed. The extracts were transferred to separate 1.5 mL plastic microcentrifuge tubes and 50:50 ACN:H<sub>2</sub>O was added up to 1 mL in volume; the tubes were subsequently placed in an ultrasonic bath for 10 min at 45 kHz frequency. Forty  $\mu$ L of 40mM AmBic was added to 10  $\mu$ L of each extract. Nine  $\mu$ L of 20  $\mu$ g/mL trypsin gold including 0.1% Rapigest™ SF were subsequently added and were allowed to digest for 1 hour at 37°C and 5% CO<sub>2</sub>. Proteolysis was stopped by the

addition of 2  $\mu\text{L}$  5% aqueous trifluoroacetic acid ( $\text{TFA}_{\text{aq}}$ ). 0.5  $\mu\text{L}$  of each in-solution digest were spotted onto a well plate with 0.5  $\mu\text{L}$  10 mg/mL CHCA (50:50 ACN:0.5%  $\text{TFA}_{\text{aq}}$  containing 4.8  $\mu\text{L}$  aniline) matrix solution spotted on top and pipette-mixed while wet.

For enzymatic digestions performed using the lab-on-plate approach, 10  $\mu\text{L}$  of defibrinated horse blood was spread across pre-cut 2  $\text{cm}^2$  ALUGRAMSIL G/UV<sub>254</sub> aluminium sheets pre-treated as previously described [14]. These were sealed in petri dishes with parafilm and placed in an environmental chamber for 5 hours at 25°C and 60% relative humidity. Under full ethical approval (HWB-BRERG23-13-14), human blood was obtained from the tip of the index finger using a Unistik® 3 Neonatal & Laboratory single use lancet and blood was then prepared as described for horse blood. The MALDI plates were preliminarily functionalised with Vmh2 hydrophobin and subsequently immobilised with trypsin from bovine pancreas as previously described [10]. The aluminium sheets with dried blood were carefully rolled into a glass vial, covered with 1 mL 50% ACN solution and ultra-sonicated for 10 min. One  $\mu\text{L}$  of sample solution was spotted on Vmh2-adsorbed enzyme wells (MALDI plate) containing immobilised trypsin. The on-plate digest reaction was carried out for 5 min at room temperature. The reaction was stopped by the addition of 0.5  $\mu\text{L}$  10 mg/mL CHCA matrix solution. After mass spectrometric analysis, the Vmh2 coating was removed by washing the MALDI plate with 10%  $\text{TFA}_{\text{aq}}$  (and gently polishing the surface), followed by washing with 100% acetonitrile, water and 100% acetone.

### **2.3.3 Blood provenance determination**

Ten  $\mu\text{L}$  of horse blood were mixed with 10  $\mu\text{L}$  of human blood. The mixture was digested using the in-solution and lab-on-plate protocols reported above. Samples were submitted to MALDI-MS analysis upon completion of the proteolysis.

### 2.3.4 Analysis of a 9-year-old bloodstain

Blood extracts were obtained from a ceramic tile exhibiting a 9-year-old bloody handprint, previously enhanced with acid black 1, by rubbing a swab previously wetted with 70:30 ACN:H<sub>2</sub>O over the sample region. The swab tip was cut and sonicated for 10min in 1mL 70:30 ACN:H<sub>2</sub>O to release the proteins. Twenty  $\mu$ L of the supernatant were dried under a stream of nitrogen and re-dissolved in 20  $\mu$ L of 50mM AmBic (pH 8) under sonication (10min). The blood extracts were subsequently digested in-solution or on the hydrophobin coated plate as previously described.

### 2.3.5 Data analysis

Mass spectra obtained from MassLynx™ (Waters Corporation, Manchester, UK) were either converted into txt files and imported into mMass [15,16], an open source multiplatform mass spectrometry software, or processed directly within MassLynx™ by means of peak smoothing, baseline correction and peak centroiding. Expasy (<http://www.expasy.org/>) was employed to generate *in silico* peptide lists of known proteins present in the blood species investigated.

Mass lists were generated by selecting “monoisotopic”, “MH+”, “trypsin higher specificity”, “2 missed cleavages” and “methionine oxidation”. Peptide lists were imported into mMass to create an “in-house” and local reference library. Mass lists including known matrix (or matrix cluster, adduct) and trypsin autolysis *m/zs* were used to preliminarily assign peaks and therefore exclude them from subsequent peptide assignment.

Peak assignments in mMass were performed automatically using the “compound search” tool and the in-house created library by setting the tolerance at 10 ppm with a “max charge” of 1 and ticking the box “monoisotopic”. Prior to peak assignment search, spectra were smoothed and de-isotoped. Peak assignment was not accepted if the S/N was lower than 3:1. Spectral processing consisted of smoothing, baseline correction and lock mass-based mass correction. Prior to performing an MS/MS Mascot (Matrix Science, London, UK) search, spectra were processed using

MassLynx™ with the MaxEnt 3 algorithm to deisotope and enhance the S/N [17]. Queries were searched against the “Swiss-Prot” database with parent and fragment ion tolerances set to 50 ppm and 0.1 Da, respectively. Two missed cleavages were also selected. Peptide mass fingerprint searches using mascot were generated with the peptide tolerance set to 5 ppm.

## **2.4 Results and discussion**

Although detection of blood at crime scenes or on evidential items is often a crucial piece of intelligence in the investigation of criminal offences, current forensic visualization methods do not offer the desired level of specificity [3]. This may result in incomplete or even in missing crucial information. In this paper the development of a rapid bottom-up proteomic method offering blood-specific signatures is reported. The developed methodology employs a recently proposed procedure involving immobilisation of trypsin on hydrophobin Vmh2 coated MALDI plates (“lab-on-plate” approach) [10], alongside a conventional in-solution digest

Although other methods for immobilising trypsin for enzymatic digestion have been reported the leader of this study found the use of Vmh2 to be very straightforward and had the reported protocols optimised for the detection and identification of blood. MALDI-MS profiles of blood were acquired from both in-solution digests and the lab-on-plate digests for comparative purposes.

### **2.4.1 Initial method development and optimisation of the in-solution digest approach**

Initially, method development and candidate familiarisation with the subject was attempted using 10 µL pure haemoglobin or myoglobin stock solutions and 20 µg/mL trypsin to produce a data set less complex than a digest of whole blood. Three incubation times (3 hours, 6 hours, overnight) were chosen to represent the range commonly reported in proteomic studies. Furthermore, the addition of detergents to the trypsin solution was trialled in order to improve tryptic digestion

as well as drying down of samples in view of removing potential interferences. Two methods of stopping the digestion were tested

Unfortunately, results were inconclusive and no trend toward one set of conditions was observed. For example, a 3-hour digest of Hb did not produce observable peptides, whereas under the same digestion conditions 3-5 myoglobin peptides were observed. However, when dried down and reconstituted in AmBic prior to a longer incubation period of 6 hours or overnight, Hb digests produced spectra with 15-20 putative peptide IDs, whereas myoglobin did not. Neither a 3-hour digest on a dried down Hb sample, nor a 6-hour digest on a myoglobin sample were successful. Similarly, no putative peptide signals were observed when digesting equine blood with either of the methods that had produced Hb or myoglobin signals.

Because successful Hb digestion evidently was no guarantee for the successful digestion of equine blood it was decided further tests would only be carried out employing equine blood. In addition to the above conditions, a sample set was dried down and reconstituted in trypsin directly, rather than in AmBic, in order to increase the protein concentration. Digestion times were chosen between one and seven hours in hopes of reducing the overall sample preparation time and because in previous experiments noise had been highest in overnight digests.

As in the previous set of experiments, results can best be described as mixed. For the samples that had not been pre-concentrated, the 7-hour digest with Rapigest™ produced the highest number (six) of putative peptide signals. In the sub-set of the dried down samples reconstituted directly in trypsin, the 1-hour digest with Rapigest™ yielded most putative peptide peaks (seven), whereas the 1-hour digests using the other pre-concentration approaches did not yield peptides at all. For the samples that had dried down and reconstituted in AmBic, the most successful sample was the 7-hour digest with Rapigest™, producing only one putative peptide signal. In general, more peptides had been expected to be present and no clear trend regarding the usefulness of pre-concentration or longer incubation times was observable, although it should be noted reconstitution in trypsin should be considered undesirable due to the low resulting overall volume of

the digest. Nonetheless, it became clear that the addition of TFA to stop digests produced resulted in better quality spectra in terms of noise, baseline and peptide signals. Due to the overall low number of peptides, no judgment was made on the best detergent at this point.

Instead, having become more familiar with the topic, the PhD candidate decided it would be useful to determine the protein concentration of the sample to be able to achieve a 50:1 substrate:trypsin ratio, rather than assume the sample requires concentration as had been suggested by the director of studies. For this reason, a BCA assay was carried out on whole, defibrinated horse blood.

The absorbance readings of the initial assay using blood:H<sub>2</sub>O dilutions of 1:1 to 1:50 exceeded the highest reading of the calibration curve and were disregarded, as extending the calibration curve would have introduced inaccurate measurements. Therefore, the assay was repeated using dilutions of 1:200 to 1:1000 blood:H<sub>2</sub>O. The mean readings of the two replicates of the bovine serum albumin standards were plotted into a calibration curve (not shown). The equation of the line of best fit ( $y = 0.0009x + 0.049$ ) was used to calculate the protein content of each sample of diluted equine blood based on its absorbance. These values were multiplied by the dilution factor of the sample to extrapolate the protein content of undiluted blood. The average protein content was determined to be 242.77 mg/mL by taking the mean of these values.

Based on this, it was established that a 50:1 substrate:trypsin ratio could be achieved by adding nine  $\mu\text{L}$  of 18.05  $\mu\text{g/mL}$  trypsin to a 10  $\mu\text{L}$  sample of a 1:200 dilution of blood. As a 20  $\mu\text{g/mL}$  trypsin solution was already present, this was employed from this point onward, also allowing for a degree of variation in protein content. Further experiments showed this concentration was also suitable for extracts of blood stains.

The number of possible peptide identifications (accepted with 0.1 Da mass tolerance) per detergent and incubation time can be found in Table 2.2. It can be seen that the longest incubation time of four hours is actually detrimental to the detection of a broad range of peptides, possibly due to increased trypsin autolysis,

and/or due to the generation of smaller peptides outside the target range of detection. Furthermore, it can be observed that the additional step of drying the blood down with nitrogen prior to the addition of AmBic does not seem to reproducibly produce superior results and its use may therefore not be beneficial.

In fact, the sample incubated for 1 hour with Rapigest™ SF without pre-drying produced the highest number of possible peptide matches (43), while the pre-dried 4-hour samples digested by Rapigest™ SF or Mega-8 resulted in the lowest number of possible matches (10). For this reason, the pre-drying step was discontinued and trypsin always supplemented with 0.1% Rapigest™ SF in a one hour digestion from this point onwards. Shorter incubation times were not trialled, but based on the observations during this experiment it is thinkable a further reduction of digestion time might suffice to yield similar or better results, thus increasing the rapidity of the method.

Peptide matches per x hours of incubation	1	2	3	4
Rapigest™ SF	43	17	39	23
Rapigest™ SF (N-dried)	27	20	36	10
β-Octylglucoside	35	35	30	11
β-Octylglucoside (N-dried)	39	32	34	19
Mega-8	28	23	28	20
Mega-8 (N-dried)	29	34	37	10

**Table 2.2** Number of putative peptide matches ( $\leq 0.1$  Da absolute error using MALDI-MS) of an in-solution digest of a 1:200 dilution of whole, defibrinated equine blood in relation to incubation time, sample preparation and detergent used.

It should also be noted that one of the most intense peaks consistently present in all equine blood spectra at  $m/z$   $1499.723 \pm 0.1$  Da was not attributable to any equine peptide under investigation nor trypsin autolysis or matrix peaks. For this reason, MS/MS was carried out on the signal in question and the resulting spectrum submitted to mascot server for identification. Interestingly, the signal was identified as a haemoglobin  $\alpha$  peptide originating from the rare Przewalski's horse (*Equus ferus przewalskii*). The supplier of the equine blood asserted that there are no Przewalski's horses in the donor herd, but was unable to provide breeding information to

investigate whether there may have been a single cross-bred horse in the herd. Because Przewalski's and domestic horses can produce fertile offspring [18] there may be the possibility of Przewalski's proteins unknowingly being passed on for several generations to a point where the incident of cross-breeding may have become forgotten and the animal is (mis-)classified as a domestic horse.

As no blood from a confirmed pure-bred horse was available for comparison, it could not be investigated further whether the presence of this protein may actually be more common amongst horses. Furthermore, no other protein sequences assigned to Przewalski's were available to cross-check against the acquired spectra. However, the sequence homology between Przewalski's and the domestic horse's Hb $\alpha$  is 99.3% (<http://www.uniprot.org/blast/uniprot/B201508012HN5US61EW>), i.e. only one amino acid difference in this case (tyrosine in horse and phenylalanine in Przewalski's at position 25), and could thus even be the result of a random single nucleotide polymorphism (codons for phenylalanine are UUC and UUU, tyrosine is encoded for by UAC and UAU).

Albeit small, this difference results in six peptide signals specific to either species (Table 2.3) when taking into account the post-translational modification of methionine oxidation, and even more when considering all post-translational modifications. While many of the Hb $\alpha$  signals can be attributed to both species due to the large sequence homology, two Przewalski's-specific peptides were found at *m/z* 1499.723 and 2043.004. In contrast, none of the equine-specific peptides were present and it can therefore be hypothesised that expression of the Przewalski's version of Hb $\alpha$  may be more common than expected amongst domestic horses. For this reason, it was also included as a peptide characteristic of equine blood in the following species-differentiation study.

Equine-specific m/z	Przewalski's- specific m/z
1515.718	1499.723
2058.999	2043.004
2501.253	2485.258
2554.239	2522.249
3097.519	3065.530
4369.113	4369.113

**Table 2.3** Hb $\alpha$  peptide signals specific to horse or Przewalski's horse (when taking into account methionine oxidation as a post-translational modification).

#### 2.4.2 In-solution and hydrophobic digests

In order to comparatively optimise both digestion methodologies, defibrinated horse blood was preliminarily employed. Both optimised methods yielded blood specific peptide signatures including those from myoglobin and the two chains of haemoglobin with a mass accuracy lower than 8 ppm (Table 2.4). In general, relevant peptide intensities are greater from the 1-hour in-solution digest; however the majority of peptides are still present employing the five minutes lab-on-plate digestion with generally a much better mass accuracy (Figure 2.1 A and B and Table 2.4). A mascot score of 46 was achieved for equine Hb $\beta$  with a total of 13 matches at a 5 ppm tolerance.

Horse blood protein	Peptide m/z	Sequence	In-solution relative error (ppm)	Lab-on-plate relative error (ppm)
<b>Myoglobin</b>	2232.087	<sup>120</sup> HPGDFGADAQGAMTKALELF R <sub>140</sub>	-	-2.330
<b>Haemoglobin <math>\beta</math></b>	2326.204	<sup>9</sup> AAVLALWDKVNEEEEVGGEALGR <sub>30</sub>	-5.717	-0.258
	1999.922	<sup>41</sup> FFDSFGDLSNPGAVMGNPK <sub>59</sub>	-6.000	6.300
	1930.029	<sup>66</sup> KVLHSFGEGVHHLNLK <sub>82</sub>	-5.440	-7.979
	1801.934	<sup>67</sup> VLHSFGEGVHHLNLK <sub>82</sub>	-7.547	-
	1449.796	<sup>133</sup> VVAGVANALAHKYH <sub>146</sub>	-7.380	-0.621
	1426.685	<sup>121</sup> DFTPELQASYQK <sub>132</sub>	-4.276	-
	1358.655	<sup>18</sup> VNEEEVGGEALGR <sub>30</sub>	-6.035	-1.693
	1274.726	<sup>31</sup> LLVVPWTQR <sub>40</sub>	-7.845	-1.020
	1265.830	<sup>105</sup> LLGNLVVVLAR <sub>116</sub>	-7.347	-
<b>Haemoglobin <math>\alpha</math></b>	2043.004	<sup>13</sup> AAWSKVGGHAGEFGAEALER <sub>32</sub>	-3.377	-0.098
	1499.724	<sup>18</sup> VGGHAGEFGAEALER <sub>32</sub>	-7.468	-1.134
	1833.892	<sup>42</sup> TYFPFDLSHGSAQVK <sub>57</sub>	-7.143	-0.055

**Table 2.4** Peptide mass fingerprinting of equine blood from in-solution and lab-on-plate digests.

Since high throughput is always one of the “desirables” for any new forensic protocol, the method employing Vmh2 is highly relevant since it has previously been observed that the proteolysis is most efficient if the sample is allowed to digest for no longer than five minutes. The optimised methodologies described in the methods section were subsequently applied to whole human blood. The digestion of whole human blood using the classic in-solution method resulted in a number of tentative protein identifications (Table 2.5). In addition to peptides resulting from haemoglobin  $\alpha$  (Hb $\alpha$ ) and  $\beta$  (Hb $\beta$ ), a number of other proteins were detected including complement C3, apolipoprotein A-1, alpha-1-antitrypsin, hemopexin, serotransferrin and alpha-2-macroglobulin. As seen in Table 2.5, the number of peptides originating from Hb $\alpha$  and Hb $\beta$  is marginally greater in the in-solution digest compared to the immobilised digest. However, it is apparent that there are peptides from proteins such as myoglobin, hemopexin and serotransferrin detected only via the lab-on-plate digest. Interestingly, using both methods, it was possible to tentatively assign multiple peptides to erythrocyte membrane protein band (EPB) 3 and 4.2. The significance of this is that some of the EPB 4.2 peptides detected are specific to human blood. A mascot score of 27 (with seven matches, using a 5 ppm tolerance) was achieved for human Hb $\beta$  alongside that of primates *Pan paniscus* and *Pan troglodytes*.

Human blood protein	Peptide <i>m/z</i>	Sequence	In-solution relative error (ppm)	Lab-on-plate relative error (ppm)
Haemoglobin $\beta$	767.489	<sup>61</sup> VKAHGKK <sub>67</sub>	-4.560	-10.814
	952.510	<sup>2</sup> VHLTPEEK <sub>9</sub>	-4.514	-5.564
	1274.726	<sup>32</sup> LLVVYPWTQR <sub>41</sub>	-1.883	-4.079
	1314.665	<sup>19</sup> VNVDEVGGEALGR <sub>31</sub>	-4.336	0.152
	1378.700	<sup>122</sup> EFTPPVQAAYQK <sub>133</sub>	2.829	-10.009
	1449.796	<sup>134</sup> VVAGVANALAHKYH <sub>147</sub>	-3.518	-3.173
	1669.891	<sup>68</sup> VLGAFSDGLAHLNLIK <sub>83</sub>	-5.090	-10.719
	1866.012	<sup>2</sup> VHLTPEEKSAVTALWGK <sub>18</sub>	-1.125	-
	2058.948	<sup>42</sup> FFESFGDLSTPDAVMGNPK <sub>60</sub>	-2.720	-2.331
	2228.167	<sup>10</sup> SAVTALWGKVVNVEVGGEAL GR <sub>31</sub>	-2.244	-2.468
	2529.219	<sup>84</sup> GTFATLSELHCDKLHVDPEN FR <sub>105</sub>	-0.079	-8.105
Haemoglobin $\alpha$	1071.554	<sup>33</sup> MFLSFPTTK <sub>41</sub>	-1.773	-1.680
	1087.626	<sup>92</sup> LRVDPVNFK <sub>100</sub>	-1.655	-0.552
	1171.668	<sup>2</sup> VLSPADKTNVK <sub>12</sub>	-6.913	-
	1529.734	<sup>18</sup> VGAHAGEYGAEALER <sub>32</sub>	-4.511	-3.792
	1833.892	<sup>42</sup> TYFPHFDLSHGSAQVK <sub>57</sub>	-2.345	-3.762
	2043.004	<sup>13</sup> AAWGKVGGAHAGEYGAEALER <sub>32</sub>	-5.923	-3.182
	2341.184	<sup>42</sup> TYFPHFDLSHGSAQVKGHGK <sub>62</sub>	-2.606	-2.520
	2582.271	<sup>18</sup> VGAHAGEYGAEALERMFLSFPTTK <sub>41</sub>	-1.123	-6.506
	2996.489	<sup>63</sup> VADALNAVAHVDDMPNALSALSDLHAHK <sub>91</sub>	-3.537	-3.137
Myoglobin	1685.868	<sup>135</sup> ALELFRKDMASNYK <sub>148</sub>	-	-5.101
Complement C3	887.458	<sup>842</sup> NEQVEIR <sub>848</sub>	-3.042	-3.268
	1334.710	<sup>672</sup> SVQLTEKRMVK <sub>682</sub>	8.167	-6.668
	1087.636	<sup>1592</sup> EALKLEEKK <sub>1600</sub>	-10.757	-9.654
Apolipoprotein A-1	1215.622	<sup>220</sup> ATEHLSTLSEK <sub>230</sub>	-4.113	-
	1230.709	<sup>240</sup> QGLLPVLESFK <sub>250</sub>	-0.975	-2.194
	1723.945	<sup>141</sup> QKVEPLRAELQEGAR <sub>155</sub>	-3.770	-4.002
	1815.851	<sup>48</sup> DSGRDYVSQFEQSALGK <sub>64</sub>	7.269	7.820
	1833.892	<sup>42</sup> TYFPHFDLSHGSAQVK <sub>57</sub>	-2.345	-3.762
	1908.985	<sup>158</sup> LHELQEKLSPGEMR <sub>173</sub>	-4.086	-
Alpha-1-antitrypsin	1318.676	<sup>248</sup> LGMFNIQHCKK <sub>258</sub>	-0.303	5.460
Hemopexin	965.443	<sup>403</sup> VDGALCMEK <sub>411</sub>	-5.904	9.426
	1060.579	<sup>84</sup> ELISERWK <sub>91</sub>	-	-1.886
	1070.574	<sup>214</sup> GEVPPRYPR <sub>222</sub>	-	2.615
Serotransferrin	1068.551	<sup>61</sup> KASYLDCIR <sub>69</sub>	-	9.733
	1855.868	<sup>531</sup> EGYYGYTGAFRCLVEK <sub>546</sub>	-0.162	-0.647
EPB 4.2	949.477	<sup>454</sup> EKMEREK <sub>460</sub>	5.055	8.320
	1048.546	<sup>451</sup> VEKEKMER <sub>458</sub>	-0.191	5.245
	1079.575	<sup>205</sup> WSQPVHVAR <sub>213</sub>	-9.448	-
	1113.488	<sup>428</sup> CEDITQNYK <sub>436</sub>	1.706	-
	1258.700	<sup>446</sup> EVLERVEKEK <sub>455</sub>	-2.383	1.986
EPB 3	949.477	<sup>284</sup> AAATLMSER <sub>292</sub>	5.055	8.320
	1328.699	<sup>731</sup> SVTHANALTVMGK <sub>743</sub>	-	-2.785
Alpha-2-macroglobulin	1334.722	<sup>350</sup> LSFVKVDSHFR <sub>360</sub>	-0.749	-

**Table 2.5** Peptide mass fingerprinting of whole human blood from in-solution and lab-on-plate digests.

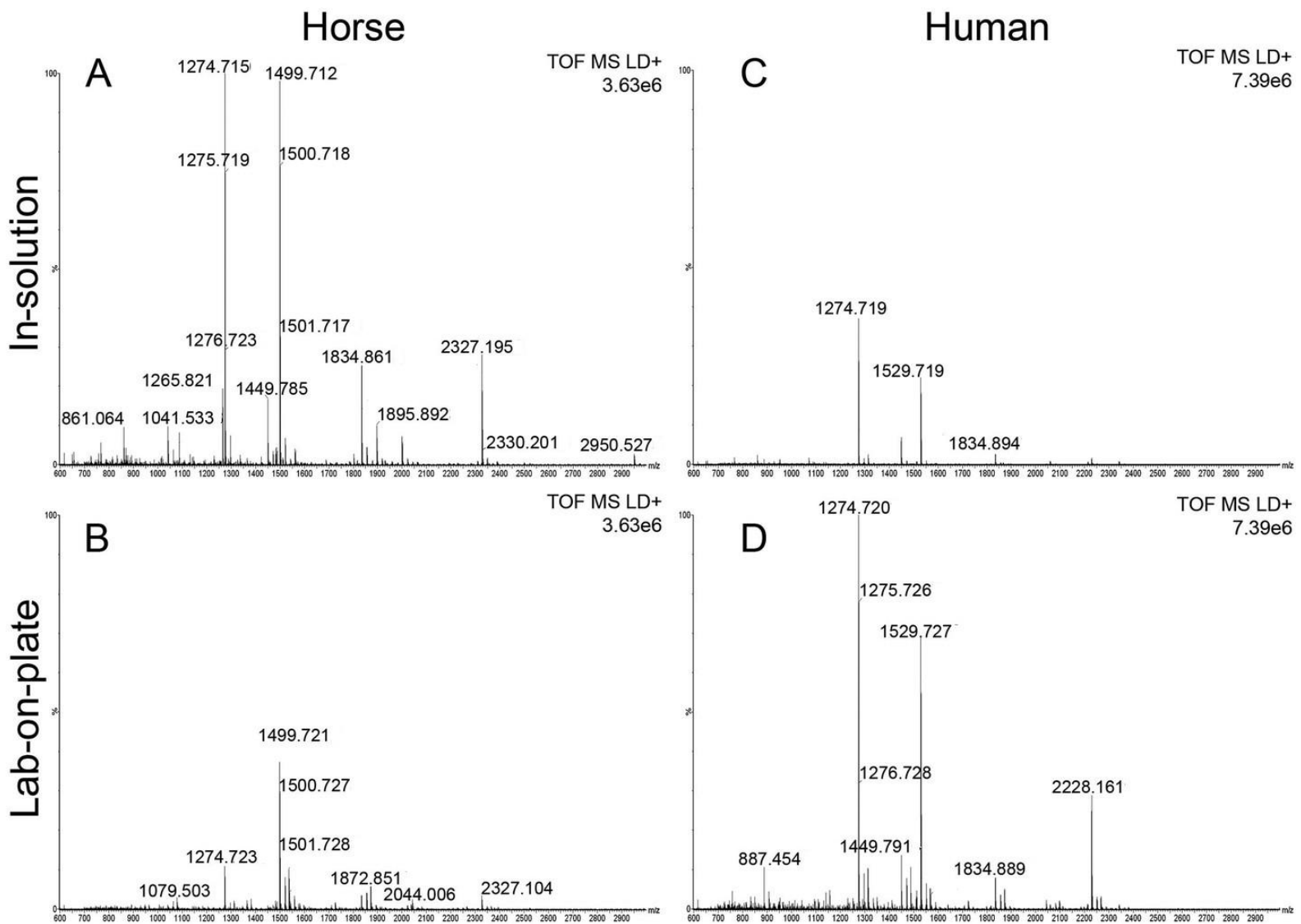


**Figure 2.1** MALDI-MS spectrum of digested blood. Panels A and B show the MALDI spectra of equine blood digested in-solution and via the lab-on-plate approach, respectively. Panels C and D show the MALDI spectra of whole human blood digested in-solution and via the lab-on-plate approach respectively.

In the case of whole human blood, the overall relevant peptide intensities were lower from the in-solution digest (Figure 2.1C) than the on-plate digest (Figure 2.1D); this is probably due to the analyses being performed on whole human blood as opposed to a defibrinated sample (less complex) as in the case of the equine blood.

A close evaluation of the data, in comparison with an optimised in-solution digestion of the duration of one hour (Figure 2.1 A and B), shows that the lab-on-plate protocol enabled the detection of the same number of blood proteins, but fewer blood protein-derived peptides (10/13 of the peptides from myoglobin, Hb $\alpha$  and Hb $\beta$  were observed in the in-solution digest).

As can be seen in Table 2.5, there are instances in which only one peptide could be putatively assigned to a protein (i.e. in the case of myoglobin, alpha-1-antitrypsin and alpha-2-macroglobulin). This is not standard practice in proteomics whereby, for increased identification reliability, at least two peptides should be assigned to a single protein. In the view of the author, this is not an issue to prevent claiming the presence of blood; based on the experiments carried out, the presence of two or more peptides from Hb $\alpha$  and Hb $\beta$  and another blood protein (e.g. myoglobin or serotransferrin) is suggested to be the proposed minimum for the confident identification of blood.

Encouraged by these data, the focus was moved onto investigating the opportunity to provide information of the provenance of blood. The author's research group has already reported preliminary data on blood provenance by MALDI-MS [3], an intact protein detection approach that was employed that, whilst successful in the instances investigated, may suffer from mass resolution and mass accuracy issues, thus reducing the level of reliability of the scientific evidence provided. At least one criminal case has been widely reported in the UK (Regina vs. Mrs Susan May) [19], in which determining with certainty the provenance of the blood detected would have resulted in a better informed or speedier outcome. The importance of determining blood provenance is further testified by a case from the USA reported in 1996. Here

the blood of the dog shot together with his owners aided the conviction of two men of murder; in this case it took a DNA test (in the first trial ever in the country to use animal DNA as evidence) to prove the presence of canine blood on the jacket of one of the murderers [20]. The comparison of the peptides obtained for equine and human blood (Figure 2.1 A,D and Table 2.4, Table 2.5) already demonstrate this as a feasible approach to determine blood provenance with a much higher specificity than previously shown [3].

To further demonstrate robustness of the method, both approaches were applied to a sample made from mixing both equine and human blood. Figure 2.2 shows the peptide mass spectral profiles obtained from in-solution (Figure 2.2A) and lab-on-plate (Figure 2.2B) digests of a mixture of human and equine blood. Although overall peptide signal intensity is higher for the in-solution digest spectrum, both digestion protocols enabled the detection of blood peptide markers specific to each species and putatively assigned peptides are shown in Table 2.6.

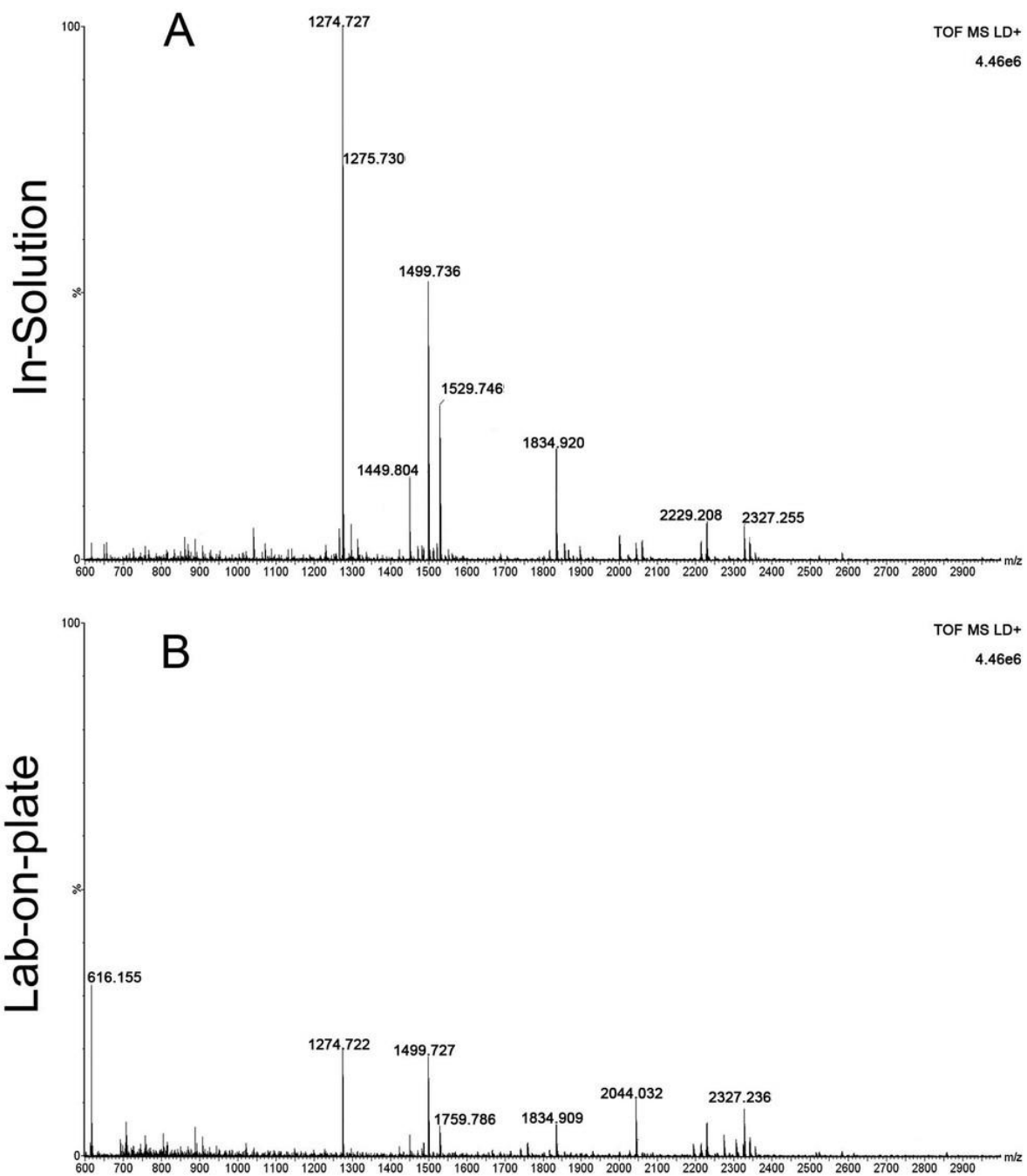


**Figure 2.2** MALDI-MS spectrum of mixed digested blood. Panels A and B show the mass spectral profile of whole human blood mixed with defibrinated horse blood using the in-solution and the lab-on-plate approach, respectively.

Blood protein	Peptide <i>m/z</i>	Sequence	In-solution Relative error (ppm)	Lab-on- plate Relative error (ppm)
Haemoglobin $\beta$ (human & equine)	1274.725	<sub>32</sub> LLVVYPWTQR <sub>41</sub>	1.412	-2.510
Serotransferrin (human)	1529.752	<sub>588</sub> KPVVEEYANCHLAR <sub>600</sub>	-3.464	-7.909
EPB4.2 (human)	1113.488	<sub>428</sub> CEDITQNYK <sub>436</sub>	-1.706	-5.029
	949.477	<sub>454</sub> EKMEREK <sub>460</sub>	-1.369	-2.527
Alpha-2- Macroglobulin (human)	1334.721	<sub>350</sub> LSFVKVDSHFR <sub>360</sub>	9.215	1.198
Haemoglobin $\alpha$ (equine)	1499.723	<sub>18</sub> VGGHAGEFGAEALER <sub>32</sub>	8.734	2.667
	1833.891	<sub>42</sub> TYFPHFDSLHGSAQVK <sub>57</sub>	-	9.160
Myoglobin (equine)	1815.902	<sub>2</sub> GLSDGEWQQVLNVWGK <sub>17</sub>	-0.660	1.872

**Table 2.6** Peptide mass fingerprinting of whole human blood mixed with defibrinated equine blood from in-solution and lab-on-plate digests. Table reports human and equine blood specific signatures.

However, due to the extensive sequence homology between the two species, it was not possible to solely use the *m/z* of these protein derived peptides or even the demonstrated presence of Hb $\beta$  tryptic peptide at *m/z* 1274.725 via MALDI-IMS-MS/MS analysis of the peptide ion (Figure 2.3A) as markers for species differentiation. However, subjected to MS/MS analysis, the tryptic peptide at *m/z* 1499.723 was identified as equine (*Equus ferus przewalskii*, to be precise) Hb $\alpha$  with mascot score of 99 (Figure 2.3B). Furthermore, the tryptic peptide *m/z* 1815.902 originating from myoglobin was also detected in the same spectrum. This peptide is specific to the equine protein sequence, thus more robustly demonstrating the presence of blood from equine provenance. Additionally, as expected from the *in silico* digestions, the detection of the human EPB 4.2 peptides, at *m/z* 949.477 and 1113.488 (present in the 1-hour in-solution digest spectrum and via the rapid lab-on-plate hydrolysis), as well as that of serotransferrin at *m/z* 1529.752, indicated the further presence of human blood, thus enabling the claim that the sample is of mixed

provenance, as well as indicating the individual species contributing to the blood sample under investigation. It is worth noting that, although there is a significant sequence homology between EPB 4.2 and  $\alpha$ -2-macroglobulin within humans and chimpanzees, the indication of EPB 4.2 to be specific to human within this discussion is only with respect to equine blood. Both the in-solution and the lab-on-plate approaches were successful in determining the double source of blood via manual interpretation. It should be noted that submission of the mixed-provenance spectrum to mascot with the same 5 ppm tolerance applied to the single-origin samples resulted in a single score of 21 with two matches for *Staphylococcus haemolyticus* antibacterial protein 1. Only when the matching tolerance was increased to 15 ppm a score of 36 with eight matches for Hb $\beta$  of *Gorilla gorilla gorilla*, *Homo sapiens*, *Pan paniscus* and *Pan troglodytes* was achieved. Equine proteins were not identified, presumably due to the complexity of the sample and the fact that mascot attempts to identify the single most probable protein rather than a mixture. This also highlights the requirement for searches to be performed with varying tolerances, as a higher tolerance search curiously does not include the matches of a lower tolerance search, further complicating the analysis.

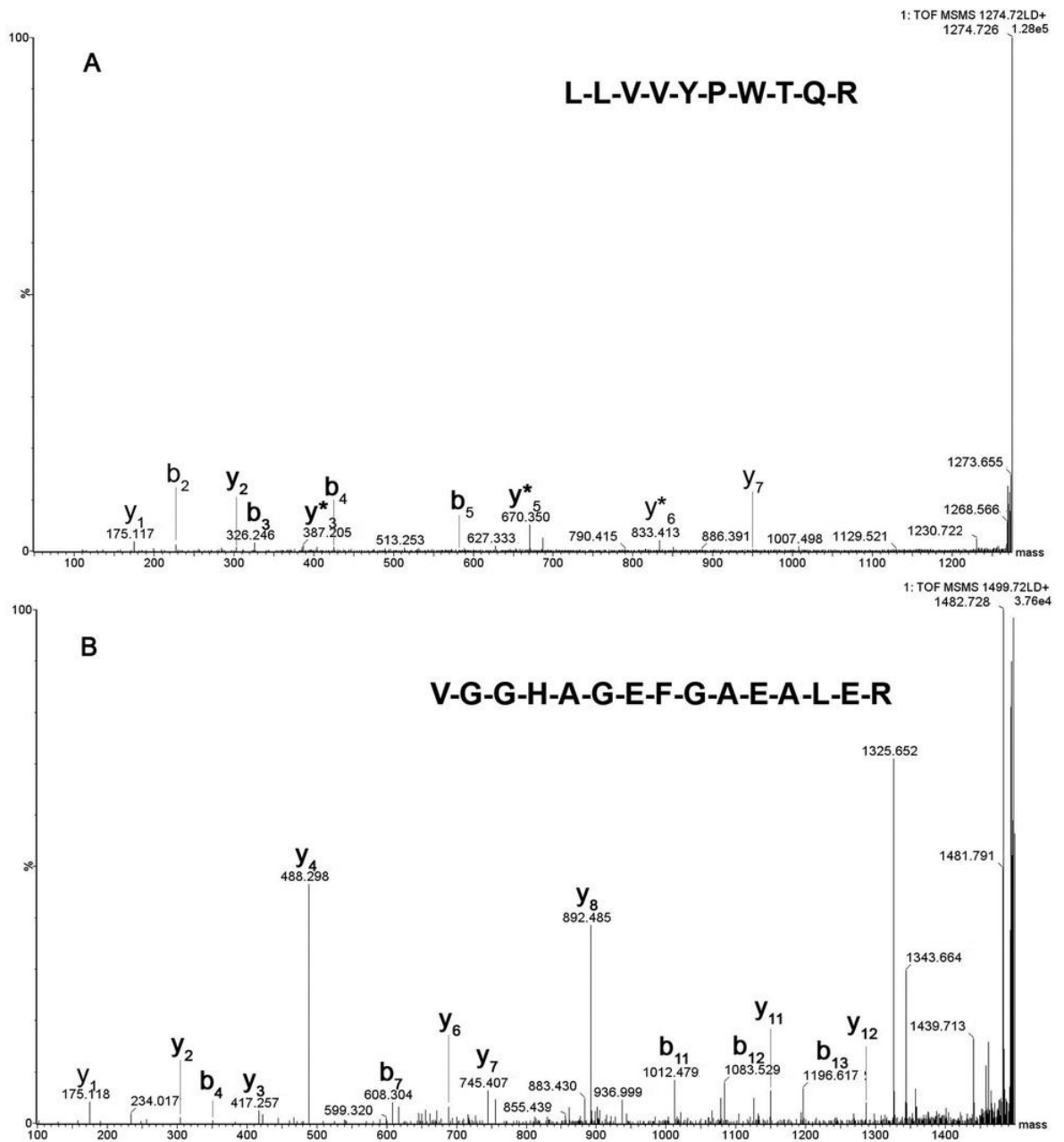


**Figure 2.3** MALDI-IMS-MS/MS of tryptic peptides  $m/z$  1274 (A, multi-species) and  $m/z$  1499.723 (B, Przewalski's), identified via mascot as Hb $\beta$  and Hb $\alpha$ , respectively. Both b and y ions are annotated with y\* representing the y-NH3 fragment ion.

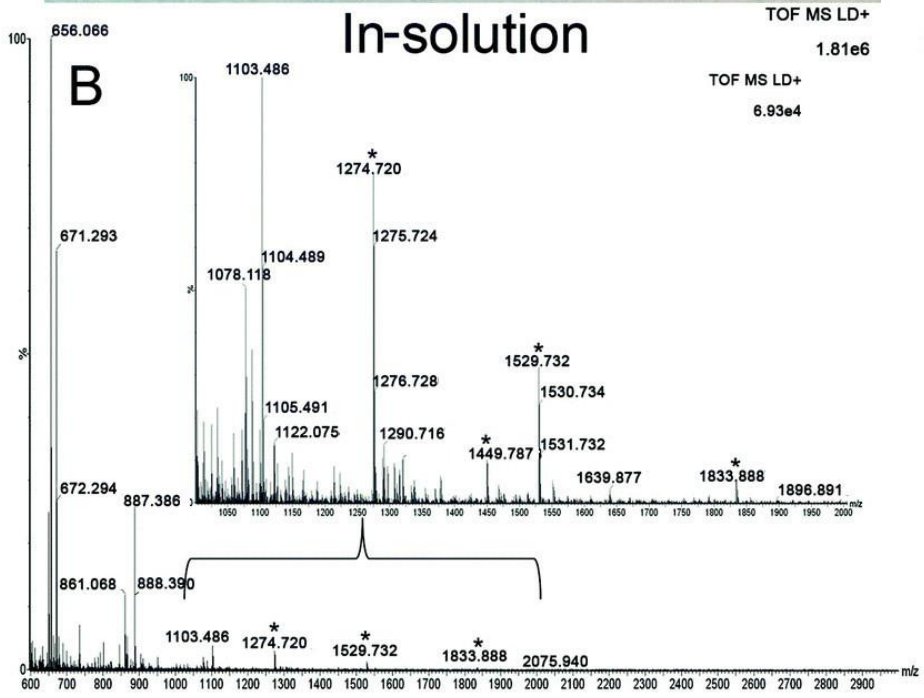


**Figure 2.4** Confirmation of the presence of blood from a 9-year-old forensically treated sample. Panel A shows the bloodied handprint from which the blood was swabbed (the blue-black colour is due to the treatment with the protein stain acid black 1). Panel B shows the mass spectral profile of the extract digested in-solution.

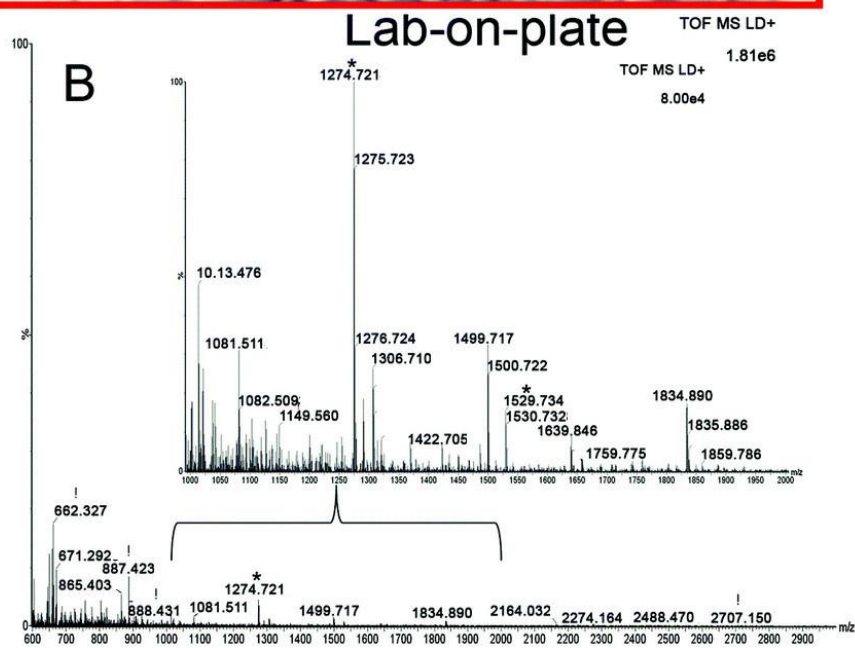
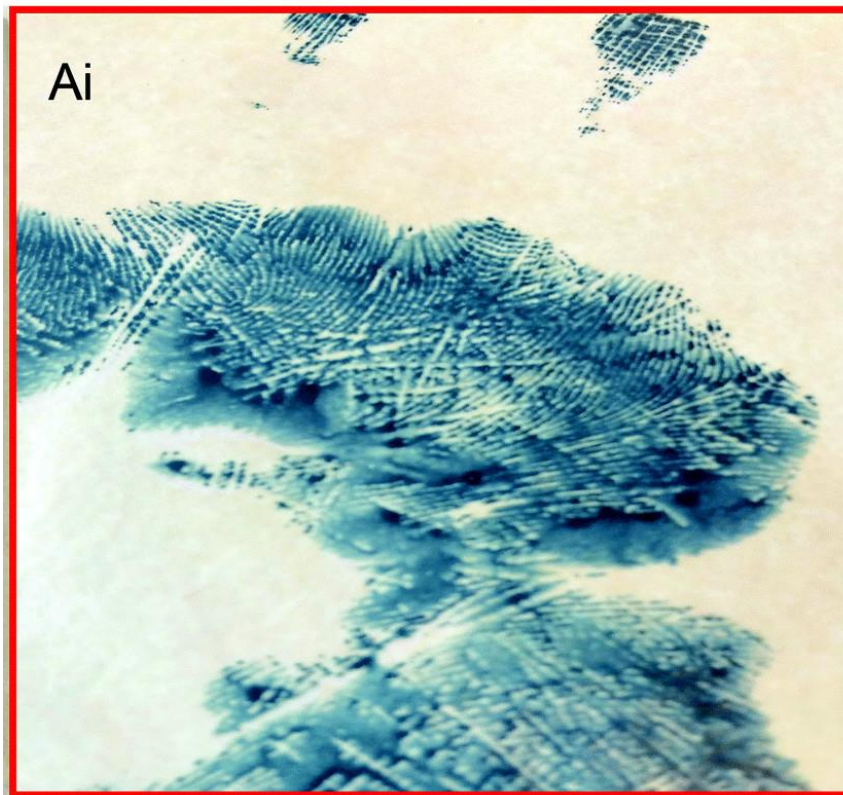


**Figure 2.5** Confirmation of the presence of blood from a 9-year-old forensically treated sample. Panel Ai shows the magnified region of the bloodied handprint (Figure 2.4) from which the blood was swabbed (the blue-black colour is due to the treatment with the protein stain acid black 1). Panel B shows the mass spectral profile of the extract digested via the lab-on-plate approach.

Finally, a method that is applicable not only to fresh bloodstains but also to much older ones would be highly desirable in the review of cold cases. Therefore, the Vmh2 lab-on-plate method was tested, in comparison with the classic optimised in-solution protocol, on a 9-year-old bloodied handprint which had been deposited on a ceramic tile and stored at room temperature (Figure 2.4A and Figure 2.5Ai). Spectra acquired from the analysis of the extract digested in-solution (Figure 2.4B) and via on-plate hydrolysis (Figure 2.5B) are shown, with corresponding expanded mass regions in the  $m/z$  range 1000–2000. A number of relevant tryptic peptides are present including Hb $\alpha$  peptides at  $m/z$  1087.625, 1529.734 and Hb $\beta$  peptides  $m/z$  1274.725 and 1449.796 to name a few (Table 2.7).

Blood protein	Peptide $m/z$	Sequence	In-solution Relative error (ppm)	Lab-on-plate Relative error (ppm)
<b>Haemoglobin <math>\alpha</math></b>	974.541	<sup>9</sup> TNVKAAWGK <sub>17</sub>	-	4.822
	1087.625	<sup>92</sup> LRVDPVNFK <sub>100</sub>	-5.424	-3.861
	1529.734	<sup>18</sup> VGAHAGEYGAEALER <sub>32</sub>	-1.503	0.326
	1833.891	<sup>42</sup> TYFPHFDLSHGSAQVK <sub>57</sub>	-2.508	-0.599
	2043.004	<sup>13</sup> AAWGKVGGAHAGEYGAEALER <sub>32</sub>	-	-1.517
<b>Haemoglobin <math>\beta</math></b>	1274.725	<sup>32</sup> LLVYPWTQR <sub>41</sub>	-1.725	-3.216
	1314.664	<sup>19</sup> VNVDEVGGEALGR <sub>31</sub>	-1.369	-
	1449.796	<sup>134</sup> VVAGVANALAHKYH <sub>147</sub>	-4.345	-3.586
	2058.947	<sup>42</sup> FFESFGDLSTPDAVMGNPK <sub>60</sub>	-	-1.019
<b>EPB 4.2</b>	1113.488	<sup>428</sup> CEDITQNYK <sub>436</sub>	-9.340	-
	949.477	<sup>454</sup> EKMEREK <sub>460</sub>	-	1.053
<b>Complement C3</b>	959.540	<sup>1592</sup> EALKLEEK <sub>1599</sub>	1.354	-

**Table 2.7** Blood peptide signatures detected from the 9-year old treated bloodied hand print.

Data obtained indicated that blood presence demonstration was possible with the in-solution approach, though both EBP 4.2 (indicating that the blood may be of human origin) and complement C3 were identified by one peptide only each. The lab-on-

plate approach did not allow the detection of the complement C3 protein (which is not highly specific to blood in any case) and also enabled the detection of only one EBP 4.2 peptide. However, for confirmatory purposes, as a tryptic digestion generates numerous peptides resulting in complex mixtures, often with overlapping signals, cross validation and identification using LC-MS/MS may be beneficial.

In addition to the ability to detect blood reliably and from such an old sample, it is very important to note that the bloodied handprint was preliminarily, 9 years prior, enhanced with acid black 1, a commonly used protein stain for blood enhancement. Successful blood identification in this instance demonstrates feasibility of the protocol to be integrated in the forensic workflow for blood enhancement/visualisation. The data obtained suggest that the acid black 1 does not interfere with the analyses, rather, that it may slow down degradation of the blood proteins over time.

Another aspect of the study that was not included in the publication was the preliminary ageing study. Although species differentiation has already been demonstrated above, this preliminary dataset was acquired in hopes of one day being able to provide complimentary information with regards to the time since bloodshed and gain insight on how the composition of a sample changes with time. The experiment included human and equine blood as well as “blood” of bovine and porcine origin obtained from meat packages and the butcher’s. (Technically, this is not pure blood but perhaps “meat juice” that *contains* blood and other solutions used in the slaughtering process. For ease of reading the word blood will be used throughout this thesis.) These samples were aged for 5 hours, 1 day, 3 days and 7 days, respectively, prior to extraction and digestion.

In fact, in-solution and lab-on-plate digests were both carried out on all of the samples, however the lab-on-plate digest did not produce characteristic peptide signals on the bovine and porcine samples (data not shown). The in-solution digest on the other hand produced spectra that easily allowed for numerous peptide identifications and species differentiation, showing its superiority over the lab-on-

plate approach. It was hypothesised this was due to the suspected sample impurities of “blood” samples coming from meat rather than pure blood samples.

Due to these samples highlighting the evident shortcomings of the approach, the principle investigators decided not to include them in the publication, against the concerns of the PhD candidate. Apparently, the aim of the collaboration with the developers of the lab-on-plate method had been to highlight its advantages and show its superiority, which would have been tainted by disclosure of the full data and therefore displeased the collaborator.

Furthermore, the candidate perceives the claim of a rapid 5-minute digestion to be deceiving, considering there are several preparation steps involved that add to the overall time. In fact, while the in-solution digest can be prepared for a multitude of samples in a few minutes and incubation time can be spent performing other duties outside the lab, the lab-on-plate digest requires a researcher to be present, performing different steps for each sample individually every few minutes. This led to the fact that the researchers performing the lab-on-plate digest spent the entire 1-hour digestion time of the in-solution approach (or more, depending on the number of samples) in the lab functionalising the plate and digesting samples. This can hardly be considered a time-saver, perhaps even more of a distraction of resources. Additionally, it was noted that an Erasmus student’s later attempts at following the publication’s method section to employ the lab-on-plate approach for the method validation study were not successful either. Although fresh hydrophobin had been obtained, no spectra characteristic of tryptic digests could be produced. Instead, large, unidentified but repeating interference peaks were observed in all spectra and results from previous experiments, e.g. using equine blood, could also not be reproduced. This, at best, suggests experienced researchers and clearer instructions are required to perform the lab-on-plate digestion, but certainly casts doubt on its reproducibility, reliability and usefulness.

Analysis of the aged samples digested with the in-solution approach, however, showed that some peptides can no longer be identified in the samples that had been aged for longer. When comparing the spectra of these different time points (Figure

2.6, using human as example), changing intensity ratios become apparent, perhaps reflecting protein and peptide degradation. Unfortunately, due to time constraints the spectra could not be thoroughly analysed from this point of view during the course of the candidate's PhD studentship, as additional replicates are necessary and the topic is so complex, providing room for numerous variables, it would perhaps warrant its own studentship. Technically, since only human blood could be obtained fresh from a bleeding fingertip, all other samples had already been aged for unknown periods anyway, further complicating the analysis. Furthermore, it is possible the defibrination of the equine blood could also have an effect on its behaviour when aged, regardless of the other storage conditions.

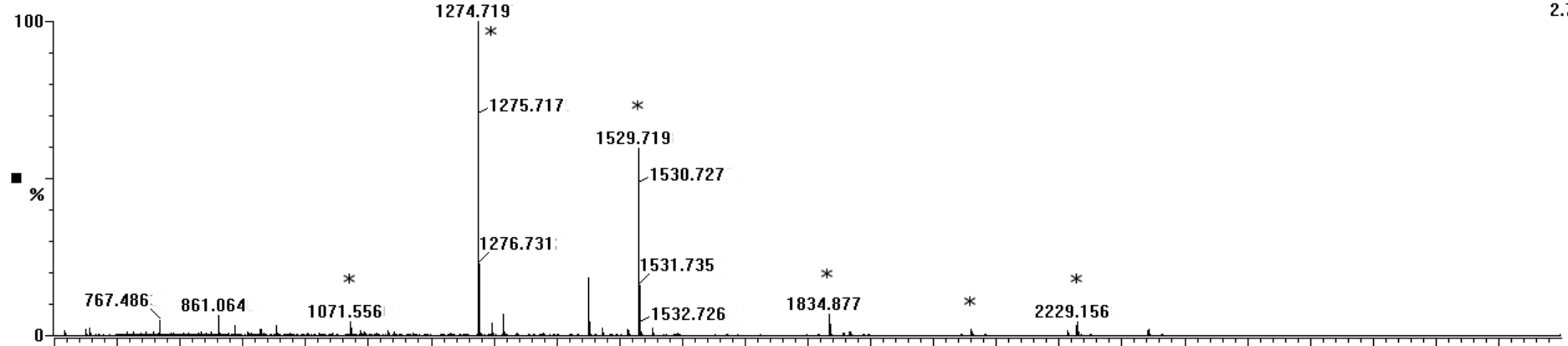
In addition to the ageing aspect another interesting forensic question concerned the differences between one specie's blood obtained from different sources, such as the meat package or the butcher's. When the preparation of a meal is used as a defence, like in the case of Susan May mentioned in chapter 1.1.2, this is where the blood can be expected to come from if indeed it is of animal origin. It is understandable that these spectra are busier compared to the pure human or equine spectra, due to the way the meat is treated and processed, making the sample more complex. Although, regrettably, no pure blood was available for comparison, it was interesting to note the differences between the two sources and their interfering signals (Figure 2.7, using bovine as example), suggesting different treatment methods.

Nonetheless, species-specific peptides could be tentatively identified in the residual blood from meat samples, supporting the method's suitability to discriminate between samples of human origin and those originating from handling meat.

Insolution 1hr digest with Rapigest

HUMAN\_5HR\_INSOLUTION\_RAPIGEST 42 [0.955] Cm [12:56]

TOF MS LD+  
2.75e6



HUMAN\_7DAY\_INSOLUTION\_RAPIGEST 20 [0.883] AM2 [Ar,10000.0,0.00,0.00]; ABS; Cm [16:57]

TOF MS LD+  
1.20e6

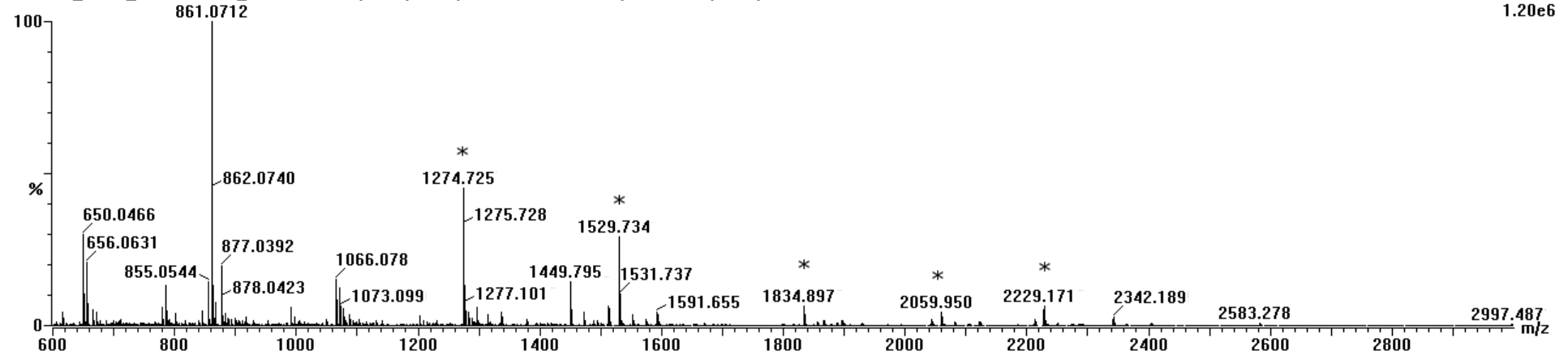


**Figure 2.6** MALDI-MS spectra of tryptic digests of extracts of human blood. A: aged for 5 hours, B: aged for 7 days. \* indicate putatively assigned blood peptides.

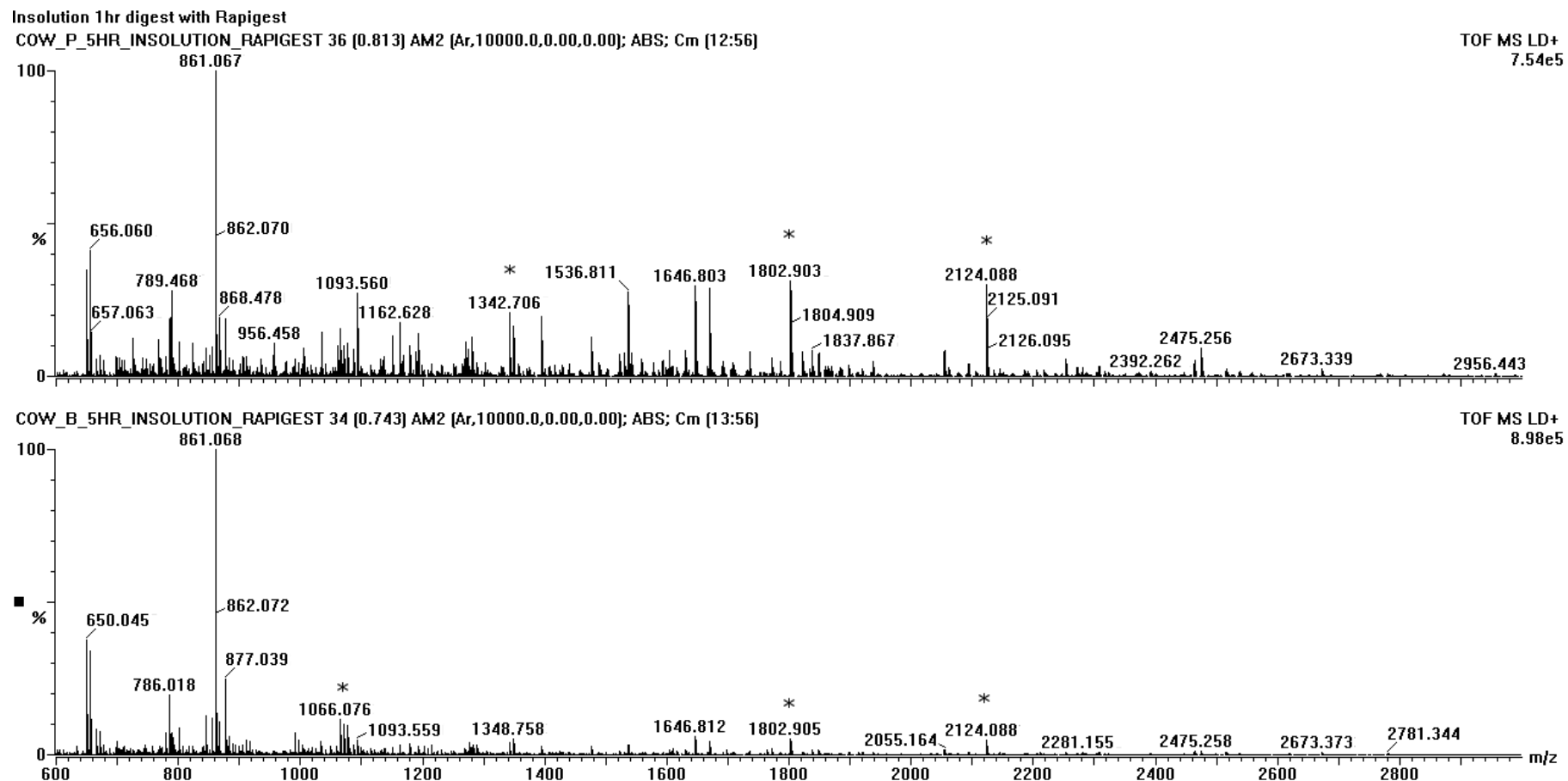


**Figure 2.7** MALDI-MS spectra of tryptic digests of extracts of bovine blood. A: blood obtained from a packet of meat, B: blood obtained from a butcher. \* indicate putatively assigned blood peptides.

## 2.5 Conclusions

The bottom-up method illustrated in this chapter will have a significant impact on forensic practice as well as on the overall criminal justice system by generating more robust and informative evidence. This is due to the high specificity of the method against current presumptive tests prone to generate false positives. Furthermore, the recovery of simultaneous information on blood provenance will both empower and speed up investigations as well as strengthening judicial debates. The study also crucially highlights compatibility with the necessary and prior application of blood enhancement techniques in combination with the analysis of very old blood samples, thus opening up new forensic opportunities for the review of cold cases. The lab-on-plate approach was shown to additionally offer rapid results (5 minutes of proteolysis time), which, in an operational forensic context, is a highly desirable feature, but lacks reproducibility and does not take into consideration the additional preparation time required to functionalise the plate for proteolysis. Following publication of these results, another group has also published proteomic data of blood digests. However, this was obtained using lengthy overnight digestion times, much lower trypsin concentrations and reporting only haemoglobin as the blood protein identified [21,22]. It can therefore be said that, especially in a forensic context, the approach presented in this thesis is advantageous due to its shorter digestion and analysis time, coupled with the higher degree of confidence resulting from the higher number of proteins and peptides identified.

These studies were also expanded in the groups' laboratories to include the reliable mapping of blood signatures on fingerprint ridges using MALDI-MS Imaging in order to link the suspect (through the biometric information) to the crime, as presented in the next chapter. Finally, validation has also been carried out (see chapter 4), whereby the requirement for the minimum number of blood peptide signatures for both blood detection and blood provenance determination was provided through a blind study in collaboration with the Minnesota Bureau of Criminal Apprehension/Elite Forensic Services LLC.

## 2.6 References

- [1] H.C. Lee, R.E. Gaensslen, *ADVANCES IN FINGERPRINT*, 3rd ed., CRC Press, London, 2013.
- [2] M. Stoilovic, Detection of semen and blood stains using polilight as a light source, *Forensic Sci. Int.* 51 (1991) 289–296.
- [3] R. Bradshaw, S. Bleay, M.R. Clench, S. Francese, Direct detection of blood in fingermarks by MALDI MS profiling and Imaging, *Sci. Justice.* 54 (2014) 110–117.
- [4] N.L. Anderson, N.G. Anderson, The human plasma proteome: history, character, and diagnostic prospects., *Mol. Cell. Proteomics.* 1 (2002) 845–867.
- [5] G. Liunbruno, A. D’Alessandro, G. Grazzini, L. Zolla, Blood-related proteomics, *J. Proteomics.* 73 (2010) 483–507.
- [6] J.N. Adkins, S.M. Varnum, K.J. Auberry, R.J. Moore, N.H. Angell, R.D. Smith, D.L. Springer, J.G. Pounds, Toward a Human Blood Serum Proteome: Analysis By Multidimensional Separation Coupled With Mass Spectrometry, *Mol. Cell. Proteomics.* 1 (2002) 947–955.
- [7] G.S. Omenn, THE HUPO Human Plasma Proteome Project, *Proteomics - Clin. Appl.* 1 (2007) 769–779.
- [8] V. Nanjappa, J.K. Thomas, A. Marimuthu, B. Muthusamy, A. Radhakrishnan, R. Sharma, A. Ahmad Khan, L. Balakrishnan, N.A. Sahasrabuddhe, S. Kumar, B.N. Jhaveri, K.V. Sheth, R. Kumar Khatana, P.G. Shaw, S.M. Srikanth, P.P. Mathur, S. Shankar, D. Nagaraja, R. Christopher, S. Mathivanan, R. Raju, R. Sirdeshmukh, A. Chatterjee, R.J. Simpson, H.C. Harsha, A. Pandey, T.S.K. Prasad, Plasma Proteome Database as a resource for proteomics research: 2014 update., *Nucleic Acids Res.* 42 (2014) D959-65.
- [9] L. De Stefano, I. Rea, E. De Tommasi, I. Rendina, L. Rotiroti, M. Giocondo, S. Longobardi, A. Armenante, P. Giardina, Bioactive modification of silicon surface using self-assembled hydrophobins from *Pleurotus ostreatus*, *Eur. Phys. J. E.* 30 (2009) 181–185.
- [10] S. Longobardi, A.M. Gravagnuolo, R. Funari, B. Della Ventura, F. Pane, E.

- Galano, A. Amoresano, G. Marino, P. Giardina, A simple MALDI plate functionalization by Vmh2 hydrophobin for serial multi-enzymatic protein digestions, *Anal. Bioanal. Chem.* 407 (2015) 487–496.
- [11] S. Longobardi, A.M. Gravagnuolo, I. Rea, L. De Stefano, G. Marino, P. Giardina, Hydrophobin-coated plates as matrix-assisted laser desorption/ionization sample support for peptide/protein analysis, *Anal. Biochem.* 449 (2014) 9–16.
- [12] V.G. Sears, T.M. Prizeman, Enhancement of Fingerprints in Blood - Part 1: The Optimisation of Amido Black, *J. Forensic Identif.* 50 (2000) 470–480.
- [13] V. Bowman, V. Sears, H. Bandey, S. Bleay, L. Fitzgerald, A. Gibson, S. Hardwick, A. Hart, D. Hewlett, T. Kent, S. Walker, *Manual of Fingerprint Development Techniques*, 2nd ed., Home Office Police Scientific Development Branch, Luton, 2004.
- [14] R. Wolstenholme, R. Bradshaw, M.R. Clench, S. Francese, Study of latent fingermarks by matrix-assisted laser desorption/ionisation mass spectrometry imaging of endogenous lipids, *Rapid Commun. Mass Spectrom.* 23 (2009) 3031–3039.
- [15] M. Strohm, M. Hassman, B. Kosata, M. Kodicek, N-Nitrosopiperazines form at high pH in post-combustion capture solutions containing piperazine: a low-energy collisional behaviour study., *Rapid Commun. Mass Spectrom.* 22 (2008) 905–908.
- [16] M. Strohm, D. Kavan, P. Novák, M. Volný, V. Havlíček, MMass 3: A cross-platform software environment for precise analysis of mass spectrometric data, *Anal. Chem.* 82 (2010) 4648–4651.
- [17] M.-C. Djidja, S. Francese, P.M. Loadman, C.W. Sutton, P. Scriven, E. Claude, M.F. Snel, J. Franck, M. Salzet, M.R. Clench, Detergent addition to tryptic digests and ion mobility separation prior to MS/MS improves peptide yield and protein identification for in situ proteomic investigation of frozen and formalin-fixed paraffin-embedded adenocarcinoma tissue sections., *Proteomics.* 9 (2009) 2750–63.
- [18] A.N. Lau, L. Peng, H. Goto, L. Chemnick, O. a. Ryder, K.D. Makova, Horse domestication and conservation genetics of Przewalski's horse inferred from

sex chromosomal and autosomal sequences, *Mol. Biol. Evol.* 26 (2009) 199–208.

- [19] K. Singh, D. Kyle, E. Weiss, Criminal Cases Review Commission, CCRC REPORT - STATEMENT OF REASONS for the case of Susan Hilda May, 1999. <http://susanmay.co.uk/ccrc.htm>.
- [20] Forensic Files - Historic cases, chief evidence., (n.d.). <https://www.youtube.com/watch?v=q8jL8S2yle8> (accessed July 24, 2015).
- [21] K.P. Kirkbride, S. Kamanna, J. Henry, N. Voelcker, A. Linacre, "Bottom-up" *in situ* proteomic differentiation of human and non-human haemoglobins for forensic purposes by MALDI-ToF-MS/MS, *Rapid Commun. Mass Spectrom.* (2017).
- [22] S. Kamanna, J. Henry, N.H. Voelcker, A. Linacre, K. Paul Kirkbride, A mass spectrometry-based forensic toolbox for imaging and detecting biological fluid evidence in finger marks and fingernail scrapings, *Int. J. Legal Med.* (2017).

## Chapter 3

### **Proteomics goes forensic: detection and mapping of blood signatures in fingermarks**

### **3.1 Introduction**

The Fingermark research group at Sheffield Hallam University has provided an extensive body of knowledge regarding the chemical analysis of latent fingermarks by MALDI-MS based methods [1–3]. These protocols enable the detection and mapping of a range of endogenous (substances naturally present in sweat), semi-exogenous (metabolite substances excreted in sweat) and exogenous species (contact substances) directly on the fingerprint ridges. This forensic opportunity provides investigators with a link between the biometric information (fingerprint molecular images) and specific intelligence on the lifestyle of the suspect and potentially circumstances of the crime. Amongst recoverable forensic intelligence, the reliable and robust detection of blood is highly desirable as this biofluid is frequently encountered at the scene of violent crimes or when criminals break in, as they may cut themselves, and may aid with the reconstruction of the chain of events taking place during the crime. As is also the case for latent fingermarks, the presence of blood may not be obvious to the naked eye; the blood might have been concealed (e.g. by attempts of the perpetrator to clean the crime scene) or could be present in invisible amounts; even "red stains" on their own or in association with fingermarks need to be confirmed as blood as opposed to other matrices. For this reason, blood enhancement techniques are primarily applied by investigators in compliance with the protocols described by the fingermark visualisation manual [4] produced by the Home Office UK.

#### **3.1.1 Blood enhancement techniques currently employed**

While several techniques are available for the enhancement and detection of blood at a crime scene and have been reviewed [5–8], they are only presumptive, meaning that they may lead to false positives [9–15]. For example acid dyes, used for blood enhancement, target proteins and, as such, they would stain positive for blood, semen and saliva, because in all of these biofluids proteins are found in high abundance. The most commonly used blood enhancement techniques, which rely on the catalytic peroxidase activity of the ferrous ion in the haem group, are also presumptive and they are prone to both false positives (given that substances other than blood are capable of peroxidase activity) and false negatives (due to the

presence of substances that inhibit the reaction with haem). Both false positives and negatives generate incorrect information potentially misleading the investigations and court cases. The majority of the blood enhancement techniques are also destructive of the ridge pattern. For example Luminol, a fluorescent haem-reactive chemical frequently used to visualise blood traces at a crime scene, is likely to cause ridge diffusion due to the lack of a fixative step [4]. Immunogenic tests also belong to this category of techniques as they require swabbing or cutting prior to blood extraction [16]; as such, these methods cannot be employed for blood marks.

### **3.1.2 Blood visualisation analytical techniques**

For the aforementioned reasons, the analytical community has invested significant efforts into developing alternative methods enabling the reliable visualisation and identification of blood using molecular or "analytical" markers. Recent approaches employ spectroscopic techniques such as Raman spectroscopy [17–23], Fourier-transform-infrared spectroscopy (ATR FT-IR) [24], or Hyperspectral Imaging (HSI) [25,26].

Raman spectroscopy yields scattering peaks characteristic for blood by exciting the sample at a wavelength of 752 nm [27] or 785 nm [28]. These peaks correspond to: (i) (oxy)haemoglobin (1000, 1368, 1542 and 1620  $\text{cm}^{-1}$ ) and probably fibrin (967, 1248, 1342 and 1575  $\text{cm}^{-1}$ ) [27] for excitation at 752 nm. It has been reported that oxyhaemoglobin and haemoglobin denaturation products (419, 570, 677, 754, 1128, 1311, 1374, 1398, 1549, 1582, 1638  $\text{cm}^{-1}$ ) are also detected at 785 nm excitation and at low laser power (1.9 mW). These peaks are, however, subject to shifts as a function of higher laser power and age before and after drying [28]. HSI records the reflectance spectrum of a sample in the visible light region, where blood exhibits characteristic absorption bands: a strong, narrow absorption band centred at 415 nm (Soret band) and two weaker, broader bands between 500 and 600 nm ( $\beta$  and  $\alpha$  bands) [26]. The technique is not only capable of identifying substances based on their reflectance spectra, but also of generating images mapping their distribution. This was investigated by Edelman *et al.* for application to various forensic traces [29] and was trialled on mock crime scenes for the detection and identification of blood [30]. However, limitations are the unsuitability of red and dark substrates and the

requirement for a reference spectrum which, in a crime scene scenario, cannot be guaranteed to be free of blood [26]. Furthermore, in theory, a non-blood substance with a sharp absorption band at 415 nm would give rise to a false positive result, though to date such a substance has not been reported. Finally, the Soret band shifts to shorter wavelengths by an appreciable amount as blood ages – it is this hypsochromic shift that researchers are using to date blood. This would give rise to false negatives if one is only looking for this peak in addition to the fact that the  $\alpha$  and  $\beta$  bands disappear within some months.

ATR FT-IR peaks correspond to the vibrational stretching of structural bonds and functional groups. In the analysis of blood, peaks are produced by amides A ( $3292\text{ cm}^{-1}$ ), I ( $1651\text{ cm}^{-1}$ ), II ( $1540\text{ cm}^{-1}$ ) and III ( $1350\text{--}1220\text{ cm}^{-1}$ ), methyl stretches of plasma lipids ( $2956\text{ cm}^{-1}$ ), methyl bending of amino acid sidechains, lipids and proteins ( $1456\text{ cm}^{-1}$ ), fibrinogen/methyl bending of amino acid side chains, lipids and proteins ( $1359\text{ cm}^{-1}$ ) and carbohydrates ( $1250\text{--}925\text{ cm}^{-1}$ ). ATR FT-IR can also be used in imaging mode to generate maps of distribution of analytes in various general biological systems [31] including breast cancer tissue [32], as well as in forensic applications investigating illicit substances in lifted [33] and unlifted fingerprints [34] and questioned documents [35], and has potential to be used to map blood distribution as well. However, the aforementioned species are not exclusive to blood, thus introducing potential for false positives, with the added complication that confident analyte identification can be difficult in complex samples.

Similarly, Raman spectroscopy can be used to produce images as described and reviewed by Steward *et al.* [36] and has been employed in determining the sequence of ink crossings [37] as well as in conjunction with HSI [38]. However, it should be noted that while Raman is a non-destructive technique capable of producing images, the detection of blood is solely dependent on haemoglobin and its denaturation products [28], making the identification approach less reliable and robust.

Reports on blood detection using mass spectrometry and in particular MALDI-MS profiling have been present in the literature since 2004 [39–41]. This work based the

confirmatory test on the presence of blood by detecting either a number of distinct blood proteins and peptides [39], haemoglobin ( $\alpha$ - and  $\beta$ -chain) [40] or its bioinorganic prosthetic group haem [41]. This provides a more specific means to claim the presence of blood, although the analysis of intact haemoglobin could pose a problem in aged and contaminated samples; it has been shown that the use of luminol prevents the detection of the haemoglobin  $\alpha$ - and  $\beta$ -chains with the usually employed MALDI matrices (such as  $\alpha$ -cyano-4-hydroxycinnamic acid), although identification was possible with the use of a different matrix, 2,6-dihydroxyacetophenone (DHAP) with di-ammonium hydrogen citrate (DHAC) [40].

### **3.1.3 Application of MALDI-MS based techniques for the reliable visualisation and identification of blood**

Inspired by the work published using MALDI-MS, method development was undertaken at the research group's laboratory to adapt and apply these methods for the direct profiling and imaging of blood in fingermarks [42]. In this work, Bradshaw *et al.* demonstrated the opportunity to map both haem and haemoglobin directly on the fingerprint ridges, keeping their integrity and thus enabling, in a real forensic scenario, the preservation of the link between the biometric information and the event(s) of bloodshed. Such an approach was possible for both fresh and aged (7 days) fingerprints, enabling further mass spectrometric confirmatory tests for the presence of haem. This approach also enabled the detection of additional blood-specific proteins besides haemoglobin, increasing confidence in the determination of the presence of blood. Though a clear advancement in terms of both reliable confirmation of blood and the preservation of the integrity of the fingerprint evidence, an even higher level of specificity of the analytical method would be desirable in order to robustly inform both investigations and court cases.

Top down proteomics could be an alternative approach given that the blood profile is very specific. Constant instrument developments may also offer the opportunity of post-source fragmentation enabling partial protein identification. However, instrumental capability for this type of analysis is not widespread; furthermore the sheer numbers of proteins present in blood, the differential protein concentration

spanning several orders of magnitude and the presence of lipids affecting protein ionisation could render the application of this technique problematic.

The use of bottom up proteomics is much more established and would indeed increase the reliability of protein identification as it is well known that the mass accuracy that can be achieved on the protein-derived peptides is much higher (in the order of parts per million) than that achievable for intact proteins. The literature already contains many reports attempting to map the proteome of plasma and serum, though none of the approaches had involved the direct application of MALDI-MS on enzymatically digested blood [43–47]. This is understandable, as in all of the previous reports the aim was to map the entirety of the blood proteome for medical and diagnostic purposes. However, in a forensic context, the detection of a handful of blood-specific proteins via a bottom up proteomic approach using MALDI-MS would be more than appropriate. This research hypothesis was developed in this group's laboratories into a study demonstrating the opportunity to recover multiple blood protein signatures in as little as 5 minutes of sample digestion [48], targeting not only haemoglobin, but also a range of other blood-specific proteins to strengthen the evidential value of the analysis. This work also showed that molecular signatures enable provenance discrimination and that they can also be retrieved from very old samples which were pre-treated with blood enhancement techniques, thus opening a new investigative avenue for cold cases.

#### **3.1.4 Scope and results of the study presented**

The work outlined in this paper is complementary to the work of both Bradshaw *et al.* [42] and Patel *et al.* [48], bridging the gap between the two; in particular a proof of concept has been achieved through the step-wise development of an *in situ* proteolysis method in order to detect and map blood-specific proteins in fresh blood marks and analysis via MALDI-MSI directly on the ridge pattern. In this work, blood marks were digested *in situ* using trypsin and incubated for 3 hours, prior to MALDI-MSI and ion mobility-MS/MS (IMS-MS/MS) analyses. Although any alteration, even minute, to the chemical and physical state of a fingermark is to be considered destructive (even optical methods though they have the lowest degree of

destructivity), the application of this *in situ* proteomic protocol enables the ridges to keep their integrity and original pattern including second level details (*minutiae*), thus also allowing the biometric information to be conveyed. Furthermore, compared with spectroscopic techniques, the application of MALDI-MS based methods can generate additional and more specific information as it relies on "molecular signatures" rather than "analytical signatures", which can also be verified by MS/MS methods as shown in this work. In particular, the use of ion mobility has been particularly crucial for the reliable identification and confirmation of blood signatures, thus adding the required level of confidence in judicial debates.

## **3.2 Materials and methods**

### **3.2.1 *In situ* tryptic digestion of blood fingerprints for MALDI-MS Imaging (MALDI-MSI)**

For trypsin spotting experiments, blood fingerprints were prepared by pricking a clean finger with a Unistik® 3 Neonatal & Laboratory single use lancet (Owen Mumford, Oxford, UK) under full ethical approval (HWB-BRERG23-13-14). A droplet of blood was forced out the bleeding fingertip which was rubbed against another clean fingertip. This second finger was then used to deposit blood marks onto ALUGRAMSIL G/ UV254 aluminium sheets (Sigma-Aldrich, Dorset, UK) pre-treated as previously described [49].

For trypsin spraying experiments, a clean finger was pricked using Accu-Chek Multiclix kit (Boots, Sheffield UK) according to the method for distributing material across the fingertips previously described [42]. Trypsin was employed to enzymatically digest blood directly on a blood mark using different methods. Initially trypsin was spotted at concentrations of 125 µg/mL, 250 µg/mL, 500 µg/mL, 1 mg/mL, 2 mg/mL and 3 mg/mL in 50 mM ammonium bicarbonate (AmBic), at pH 8, containing 0.1% RapiGest™ SF, by depositing 0.5 µL onto the blood mark.

In another experiment, quarter split blood marks underwent acoustic spotting of trypsin using the automatic spotter Portrait® 630 (Labcyte Inc., Sunnyvale, USA) at

trypsin concentrations of either 100 µg/mL, 150 µg/mL, 200 µg/mL or 250 µg/mL in 50 mM AmBic at pH 8 containing 0.1% RapiGest™ SF. In the work reported here, 50 cycles were performed, with one droplet per position deposited onto the split blood marks during each cycle. A total of approximately 8.5 nL of trypsin solution was therefore acoustically printed onto the mark, per spot. Additional blood mark quarters underwent differential trypsin spray coating, as reported for the acoustic ejection, using a SunCollect autosprayer (KR Analytical, Sandbach, UK); here 9 layers of trypsin were delivered at a flow rate 2 µL/min and a nitrogen pressure of 3 bar. All trypsinised samples were placed on polystyrene floats in a Coplin jar half-filled with 50:50 methanol:H<sub>2</sub>O, sealed with parafilm and incubated for 3 hours at 37°C. The jar's lid was wrapped in paper tissue to prevent condensation forming on the glass and dropping onto the sample.

### **3.2.2 Matrix deposition**

After incubation, all the digested blood fingerprint samples were sprayed using the SunCollect (KR Analytical, Sandbach, UK) with 5 layers of 5 mg/mL CHCA in 70:30 ACN:0.5%TFA<sub>aq</sub>, containing equimolar amounts of aniline to CHCA (i.e., 1 mL of 5 mg/mL CHCA solution contained 2.4 µL aniline) at a flow rate 2 µL/min and a nitrogen pressure of 3 bar.

### **3.2.3 Instrumentation and data acquisition**

Mass spectrometric images of blood marks using manually spotted trypsin were obtained in the *m/z* range 650-3000 using a modified Applied Biosystems API “Q-Star” Pulsar *i* hybrid quadrupole time-of-flight (QTOF) instrument (Concord, Ontario, Canada). The orthogonal MALDI source of the Q-Star instrument has been modified to incorporate a SPOT 10 kHz Nd:YVO<sub>4</sub> solid-state laser [50] (Elforlight Ltd., Daventry, UK) with a wavelength of 355 nm, a pulse duration of 1.5 ns and producing an elliptical spot size of 100 × 150 µm. Images were acquired at a spatial resolution of 150 × 150 µm in raster mode, using ‘oMALDI Server 5.1’ software supplied by MDS Sciex (Concord, Ontario, Canada) and data processed using BioMap 3.7.5 software (Novartis, Basel, Switzerland) with a bin size of two. MALDI-MS images of

blood marks either sprayed with trypsin (SunCollect, KR Analytical, Sandbach, UK) or robotically spotted with this enzyme (Portrait 630<sup>®</sup>, Labcyte Inc., Sunnyvale, USA) were acquired in positive ion mode in the  $m/z$  range 600 - 3000 using a SYNAPT<sup>™</sup> G2 HDMS system (Waters Corporation, Manchester, UK) operating with a 1 kHz Nd:YAG laser, at a mass resolution of 10,000 FWHM (sensitivity mode) and at a spatial resolution of 150  $\mu\text{m}$ . Calibration over a 600-2800 Da mass range was performed prior to analysis using phosphorous red. The laser energy was set to 250 arbitrary units in MS mode and increased to 270 arbitrary units for MALDI-ion mobility-MS/MS experiments. In particular, MS/MS analyses were conducted *in situ* on the peaks exhibiting a S/N of at least 14. Fragmentation was carried out in the transfer region of the instrument, post ion mobility separation, therefore product ions retain the same drift time as the precursor ion. Collision energies ranging between 60-80 eV were used to obtain the best signal to noise ratio for product ions.

### 3.2.4 Data analysis

Mass spectra opened using MassLynx<sup>™</sup> (Waters Corporation, Manchester, UK) were either converted into txt files and imported into mMass, an open source multiplatform mass spectrometry software [51], or processed directly performing peak smoothing, baseline correction and peak centroiding. UniprotKB (<http://www.uniprot.org/>, UniProt release 2015\_11) was employed to generate *in silico* peptide lists of known proteins present in blood. Mass lists were generated by selecting “*monoisotopic*”, “*MH<sup>+</sup>*”, “*trypsin*”, “*2 missed cleavages*”, “*methionine oxidation*” and *taxonomy "human"*. Peptide lists were imported into mMass to create an “in house” and local reference library. Data analysis of mass images was performed using BioMap 3.7.5 software (Novartis, Basel, Switzerland) or the HDI software (Waters Corp. Manchester, UK). Prior to peak assignment search, spectra were smoothed and de-isotoped. Peak assignment was not accepted if the S/N was lower than 3:1. Spectral processing consisted of smoothing, baseline correction and lock mass-based mass correction. Prior to performing an MS/MS Mascot (Matrix Science, London, UK) search, spectra were processed using MassLynx<sup>™</sup> with the MaxEnt 3 algorithm to deisotope and enhance the S/N. Queries were searched against the "Swiss-Prot" database

(*release 2015\_11*) with parent and fragment ion tolerances set to 50 ppm and 0.1 Da respectively. Two missed cleavages were also selected.

### 3.3 Results and discussion

The ability of MALDI-MSI to spatially map the distribution of proteins and peptides in fingerprints opens up the potential to establish the link between the event of bloodshed and the biometric information, thus linking a suspect to a crime. For this reason, this study aimed to optimise the *in situ* proteolytic digestion of blood marks for analysis via MALDI-MSI.

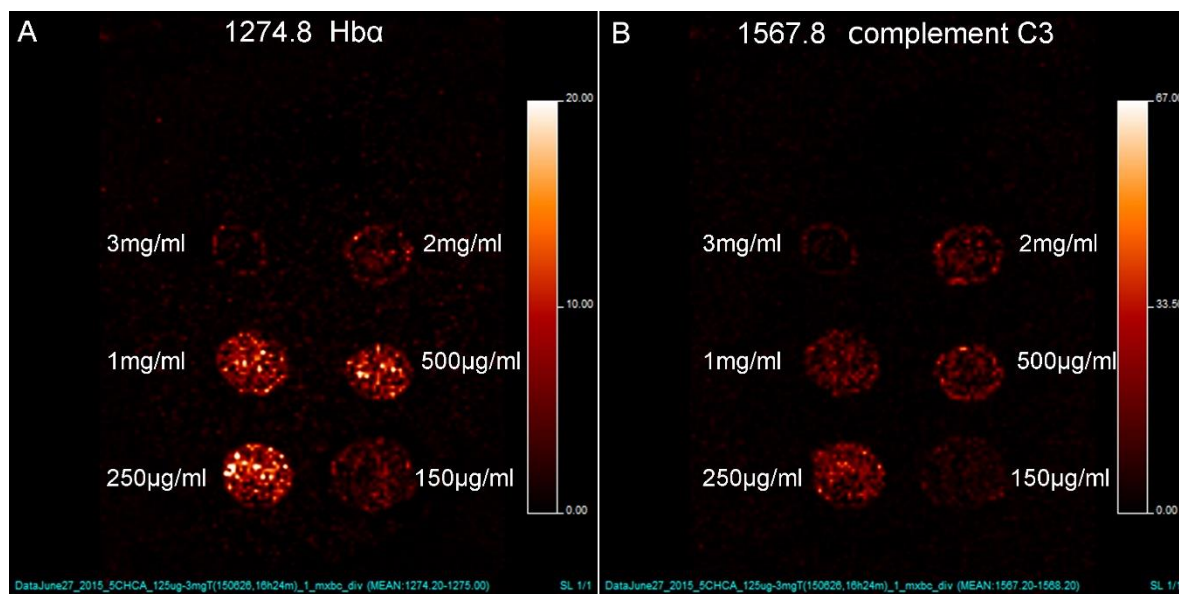


**Figure 3.1** MALDI-MS Imaging of *in situ* proteolysis of a blood fingerprint. Figure shows the molecular images of blood-specific peptides localised to the digest areas. *In situ* digests were performed by spotting of the blood mark with trypsin in 6 different concentrations and incubating at 37°C for 3 hours. Trypsin appeared to be most efficient when used in concentration of 250 µg/mL.

#### 3.3.1 Optimisation of trypsin concentration: MALDI-MSI of enzymatic digestion spots deposited on blood marks

Due to the high protein concentration of blood [43], it was necessary to adapt the amount and concentration of trypsin used for blood proteolysis, as the 20 µg/mL trypsin frequently reported in the literature for on tissue and fingerprint digests

[2,50,52] did not yield any peptides when applied to blood fingerprints (data not shown). In the initial experiments aimed to determine the optimal trypsin concentration, a human blood mark was spotted with concentrations of 125 µg/mL, 250 µg/mL, 500 µg/mL, 1 mg/mL, 2 mg/mL and 3 mg/mL trypsin and digested at 37°C for 3 hours before matrix application and the acquisition of MALDI-MSI data. Analysis of these binned data revealed multiple blood peptide peaks localised only in the spotted digest regions such as apolipoprotein A1 at  $m/z$  1529.8 (theoretical monoisotopic  $m/z$  1529.78), complement C3 at  $m/z$  1337.8 and 1567.8 (theoretical monoisotopic  $m/z$  1334.71 and 1567.88 respectively), haemoglobin  $\alpha$  at  $m/z$  1274.8 and 1529.8 (theoretical monoisotopic  $m/z$  1274.72 and 1529.73), serotransferrin at  $m/z$  1529.8 (theoretical monoisotopic  $m/z$  1529.75) and  $\alpha$ -2-macroglobulin at  $m/z$  1334.8 and 1394.6 (theoretical monoisotopic  $m/z$  1334.72 and 1394.68 respectively); Figure 3.1 reports peptide images at  $m/z$  1274.8, putatively identified as a haemoglobin  $\alpha$  and at  $m/z$  1567.8, putatively identified as a complement C3 peptide (theoretical  $m/z$  1567.9) as an example. The blood fingerprint area digested with 250 µg/mL trypsin showed the highest intensity peaks for those peptides, indicating that this would be the most promising concentration to bring forward into subsequent imaging experiments. The use of high trypsin concentrations of 500 µg/mL and above was discontinued, as a significantly lower intensity and/or absence of blood peptide signatures was attributed to an unsuitable trypsin:protein ratio, whereas trypsin concentrations between 100 and 250 µg/mL were chosen for further investigation on quarters of a blood mark split into four. In terms of the performance of the different trypsin concentrations tested, these results were reproducible through different repeats, though peptide intensities varied according to the different amounts of blood present within each repeat affecting the ratio trypsin:protein. It is in fact important to remember that despite the optimisation of the reproducibility in the deposition of blood marks (see Materials and Methods section), slightly different amounts of blood could have been deposited within each repeat. The amount of blood in the droplet could only have been measured and kept consistent if an exact amount of blood was pipetted off the finger after squeezing and pipetted back onto an uncontaminated finger. This method was trialled by the donor, however it was not possible to deposit prints with clear ridge detail due to the blood beginning

to coagulate and dry in the pipette tip. The first blood fingerprint generated by contact with the relevant surface was employed for the study each time (primary marks).

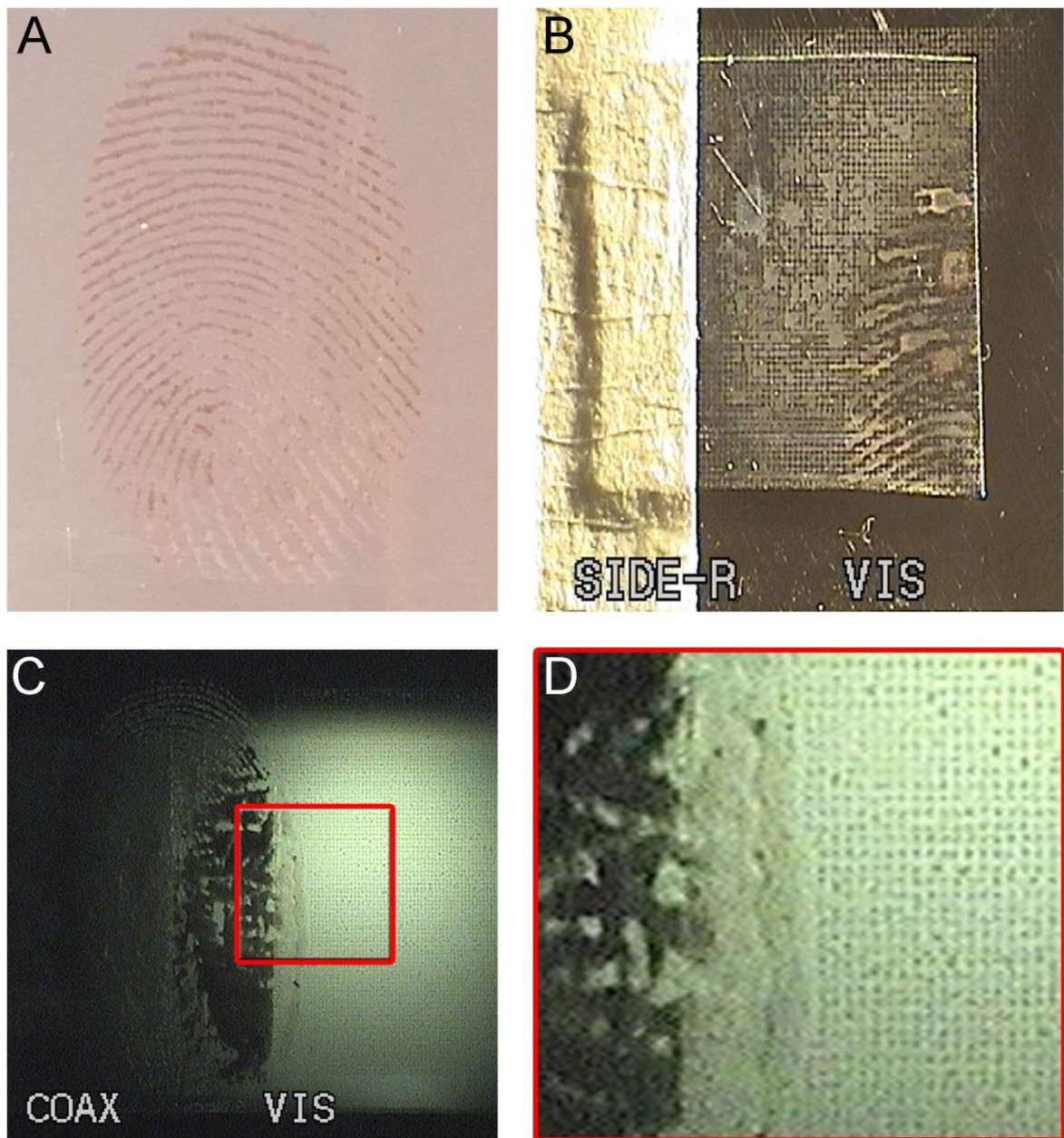


**Figure 3.2** Acoustic spotting of trypsin on blood marks. Figure shows the visual image of the blood mark prior to splitting into quarters (A). Trypsin spots within the mark and surrounding the mark are visibly merged and distorted in certain areas of the aluminium slide (B). A distorted, ridge-merged blood mark was also visible on a polylysine glass slide after trypsin deposition (C) with an expanded region showing an unaffected area (no spot merging) where blood was not present (D).

### **3.3.2 Optimisation of trypsin deposition for mapping blood signatures on the ridges of blood marks**

In order to spatially map blood peptides on the fingerprint ridges, subsequent experiments made use of the acoustic reagent multispotter (Portrait 630®) to deposit discrete trypsin nano-droplets at a spot-to-spot spatial resolution of 200 µm.

However, when a blood mark quarter deposited on an aluminium slide was spotted with 100 µg/mL trypsin at a resolution of 200 µm, it was observed that spots were spreading into each other (Figure 3.2B); trypsin spots surrounding the mark are also visibly merged and distorted in certain areas of the aluminium slide (Figure 3.2B). Lower volumes of trypsin were trialled (as low as 1.7 nL per spot) in combination with different concentrations, though none of the combinations avoided the merging issue. In order to test the hypothesis that it was the particular surface of deposition that caused this issue, a polylysine-coated glass slide was used as a sample support (Figure 3.2C). Again, the trypsin nano-droplets were observed to merge across the blood mark resulting in a pool of protease. Conversely, the Portrait® deposited the trypsin solution in a precise manner where blood was not present (Figure 3.2D); other deposition surfaces, such as lifting tape and a stainless steel MALDI target plate were investigated and all exhibited the same issue suggesting the combination of surface of deposition and, majorly the viscosity of blood to be the problem causing spot merging due to insufficient drying of trypsin during the various spotting cycles. The spot merging issue eventually led to the choice to discontinue the use of the Portrait as a possible trypsin depositor for this particular application.

The next best option was therefore the use of an automatic sprayer for the deposition of trypsin (and subsequently matrix) and the SunCollect automated pneumatic sprayer was employed with the intention to deposit trypsin concentrations at 100 µg/mL, 150 µg/mL, 200 µg/mL and 250 µg/mL on four different quarters of a blood mark. It was observed, however, that with increasing trypsin concentrations, the spray was less and less uniform leading to capillary blockage and syringe breakage, most likely due to increased viscosity and back pressure build-up, respectively. For this reason, only three quarters of the blood mark could be sprayed with a maximum

usable trypsin concentration of 200 µg/mL to evaluate which concentration would be most suitable for future spraying of entire marks (Figure 3.3). In order to increase the trypsin concentration further when using the pneumatic depositor, additional method development work including minor instrumental modifications was carried out later to counteract the potential increase in viscosity with higher protease concentrations. (Due to time constraints this could only be done after the submission deadline for the publication presented in this chapter.)

Examination of the imaging data obtained (Figure 3.3) revealed blood peptide signatures on the blood fingerprint ridges for all the three trypsin concentrations investigated. Figure 3.3 shows example images for five peptide species (*m/z* 767.407, 886.507, 953.549, 974.529, 1068.581) putatively assigned to complement C3 (2 peptides), hemopexin, Hbα and serotransferrin, respectively. These species have been reported in Table 3.1.

possible peptide identity	theoretical <i>m/z</i>	observed <i>m/z</i>	relative error (ppm)
<b>Complement C3</b>	767.393	767.407	18.895
<b>Complement C3</b>	886.510	886.507	-3.722
<b>Hemopexin</b>	953.546	953.549	3.251
<b>Haemoglobin alpha</b>	974.541	974.529	-12.723
<b>Serotransferrin</b>	1068.598	1068.581	-15.721

**Table 3.1** Putatively identified blood peptide signatures within MALDI-MSI of blood marks

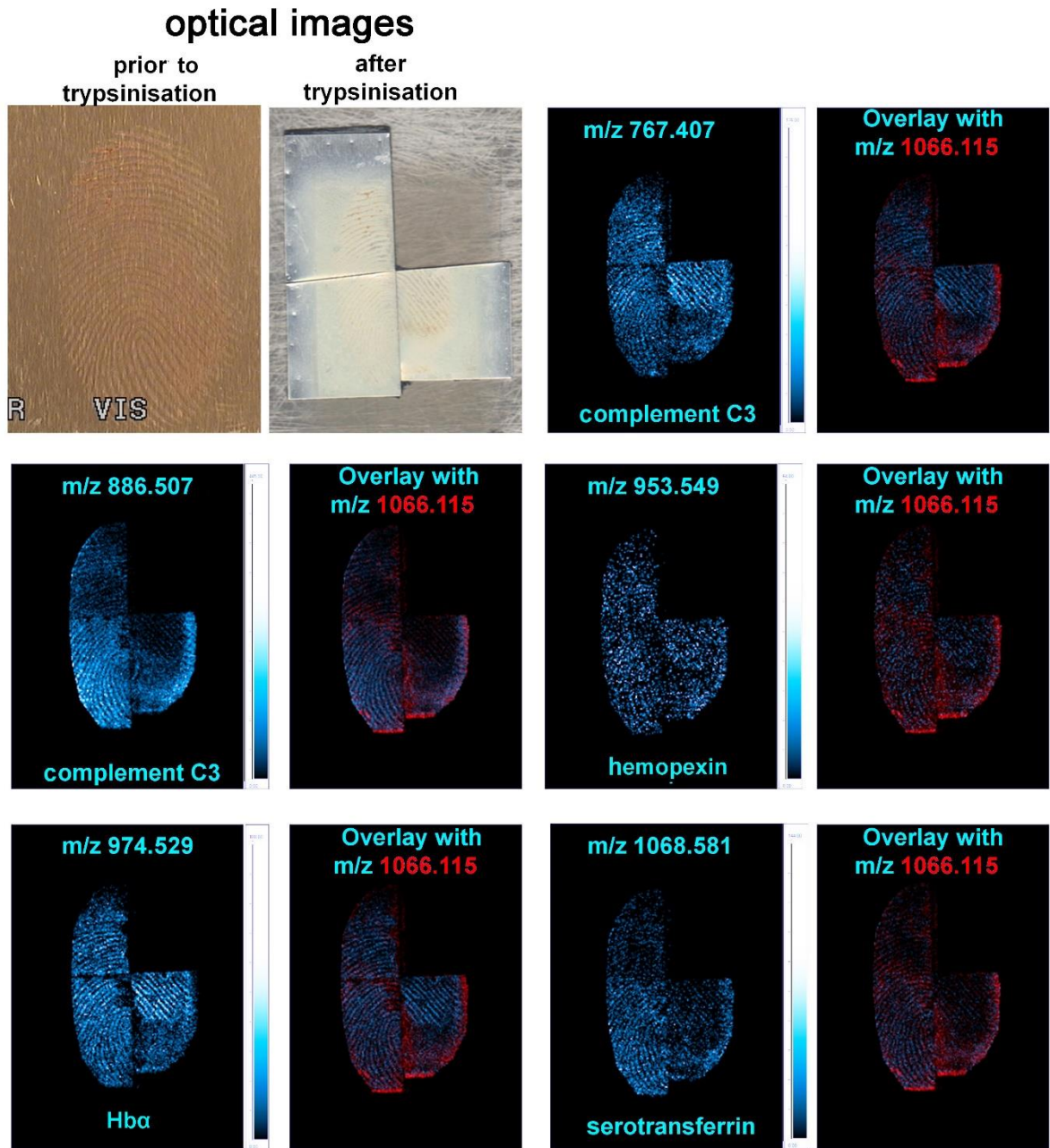


**Figure 3.3** MALDI-MS Image of *in situ* proteolysis of a blood fingerprint. Figure shows molecular images of blood-specific peptides generated by spraying trypsin at one of four different concentrations (anti-clockwise, starting top left: 100, 150, 200 and 250  $\mu\text{g}/\text{mL}$ ) on the blood mark using the SunCollect. The trypsin concentration of 250  $\mu\text{g}/\text{mL}$  could not be delivered to due limitations in the sprayer capabilities. Each peptide image has also been overlaid with the matrix signal at  $m/z$  1066.115. The figure suggests that the best ridge reconstruction performance could be achieved using a trypsin concentration of or between 150 and 200  $\mu\text{g}/\text{mL}$ .

To prove that these are genuine blood signatures a control experiment was performed by spraying trypsin at a concentration of 100 µg/mL on a latent fingerprint ("control", not blood contaminated) from the same donor and subsequently subjected to MALDI-MSI.

Spectra of the control latent mark extracted from the MALDI-MS images generated are reported in Figure 3.4 as a comparison with the spectra extracted from the MALDI-MS images generated from the same blood mark shown in Figure 3.3. Results reported in Figure 3.4 show that the aforementioned blood signatures (highlighted in red in the spectra in Figure 3.4, shown in blue in the image of the blood mark in Figure 3.3) are absent in the latent mark and therefore not endogenous but exclusively present when blood is present. With respect to Figure 3.3 and Figure 3.4, the spectrum showing the ion signal at  $m/z$  1274.737 assigned to Hb $\alpha$  was additionally reported as present in the blood mark and absent in the latent mark. This peptide generated a speckled image, which is why it was not previously reported in Figure 3.3. This control experiment demonstrates not only specificity but selectivity of the method.

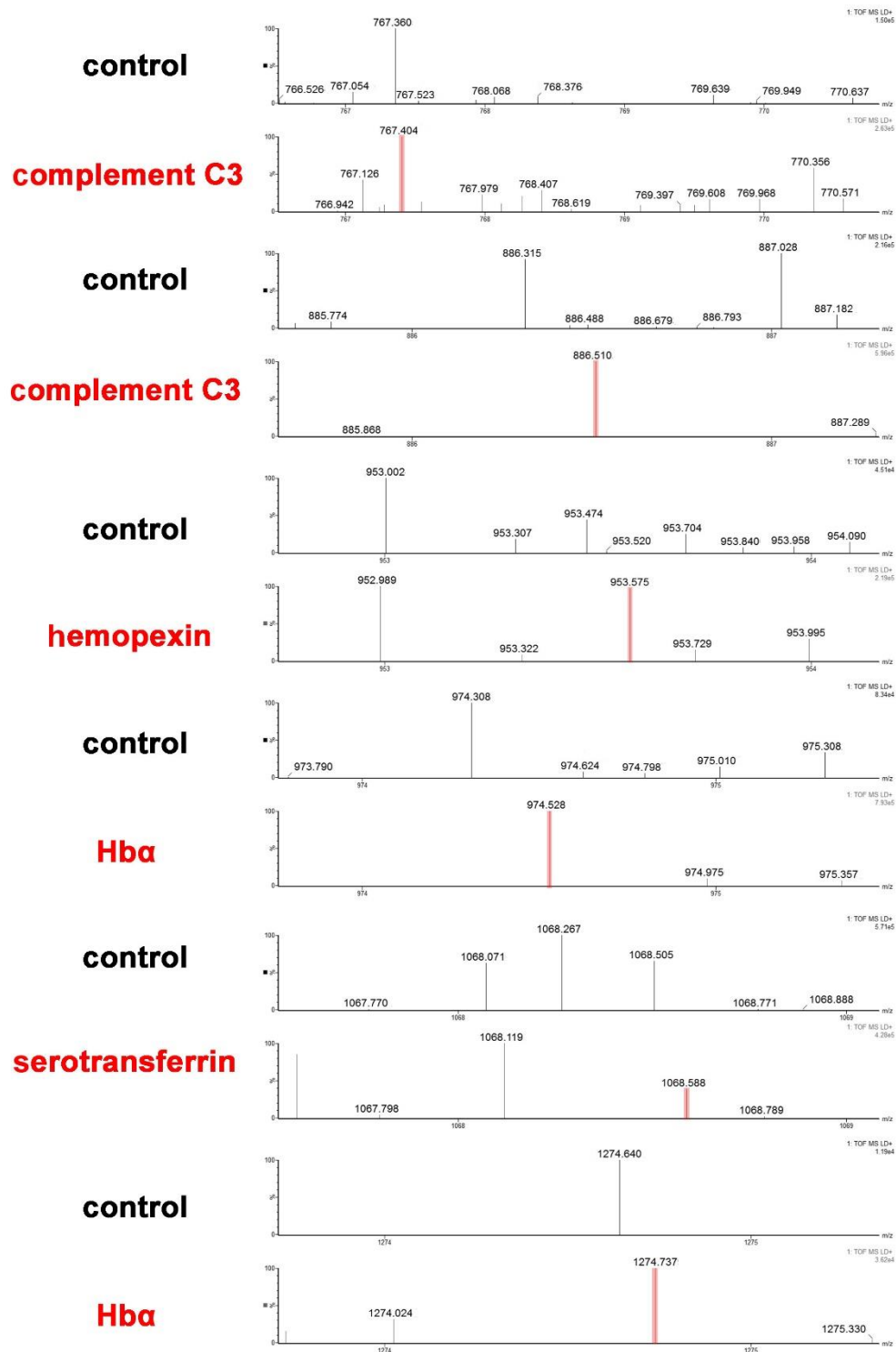


**Figure 3.4** Comparison of spectra extracted from MALDI-MS images of a latent mark (control) versus a blood mark. In a latent fingermark (not contaminated by blood) enzymatically digested using 100 µg/mL of trypsin, the blood peptide signatures (red) previously mapped and reported in Figure 3.3 are absent.

Finally, to prove that the putatively identified peptide sequences could not belong to other proteins (other than the reported blood proteins) with which they might demonstrate sequence homology, a BLAST search was performed for each of the peptides in question. The search has revealed 100% sequence homology exclusively with the putatively reported blood peptide (data not shown). To further prove the exclusive presence of blood peptides on the mark's ridges, an overlay of each peptide image with a matrix peak image at  $m/z$  1066.115 is also reported in Figure 3.3.

Of the peptides identified, two produced the most abundant signal when digested with 200  $\mu\text{g}/\text{mL}$  trypsin solution, whereas two were most abundant when digested with 150  $\mu\text{g}/\text{mL}$  trypsin and one appeared to be equally abundant with both trypsin concentrations. While this may complicate the determination of the most suitable trypsin concentration, it is a result to be expected given the differential abundance of the proteins in blood; while some proteins are present in blood in high concentrations, such as albumin (30-50  $\text{mg}/\text{mL}$  in healthy individuals), others have been reported with concentrations as little as 0-5  $\text{pg}/\text{mL}$  for Interleukin 6 [43]. This circumstance gives rise to sub-optimal substrate:enzyme ratio for some proteins. In fact, though some peptide peaks are still present, the overall TIC is much reduced with higher trypsin concentrations (above 250  $\mu\text{g}/\text{mL}$ ). This result is reproducible within the same conditions, which here refer to the blood amount being used. Blood amounts were controlled as much as possible by using the same lancet depth each time on the Accu-Chek Multiclix device (see section 3.2.1). Differential abundance may also negatively impact on the uniformity of distribution across the blood mark and eventually on the ridge pattern molecular image reconstruction. This may result in seemingly inferior results in one area, where in fact this area may have not contained "optimal" amount of the target species to begin with, thus resulting in non-uniform distribution both within the same and between the different quarters. The spraying method was found to be reproducible through all repeats performed to date with regards to the proteolytic efficiency of trypsin used in the different concentrations trialled.

### 3.3.3 Key findings

Data presented here suggest that both 150 µg/mL and 200 µg/mL trypsin are suitable for the *in situ* digestion of blood marks, however taking into consideration the results of the manually spotted image it would be beneficial to also evaluate 250 µg/mL, although this will require some modification of existing instrumentation. In the data obtained to date, additional ion signal *m/z*s could be observed and matched to blood peptides, but showed a speckled distribution rather than a continuous fingerprint ridge pattern when imaged. Despite the known difficulties in successfully performing *in situ* MS/MS experiments, these were optimised and Figure 3.5 shows an example confirming the presence of the  $\alpha$  and  $\beta$  chains of haemoglobin by selecting the precursor ions at *m/z* 1274.725 and 1529.734, respectively.

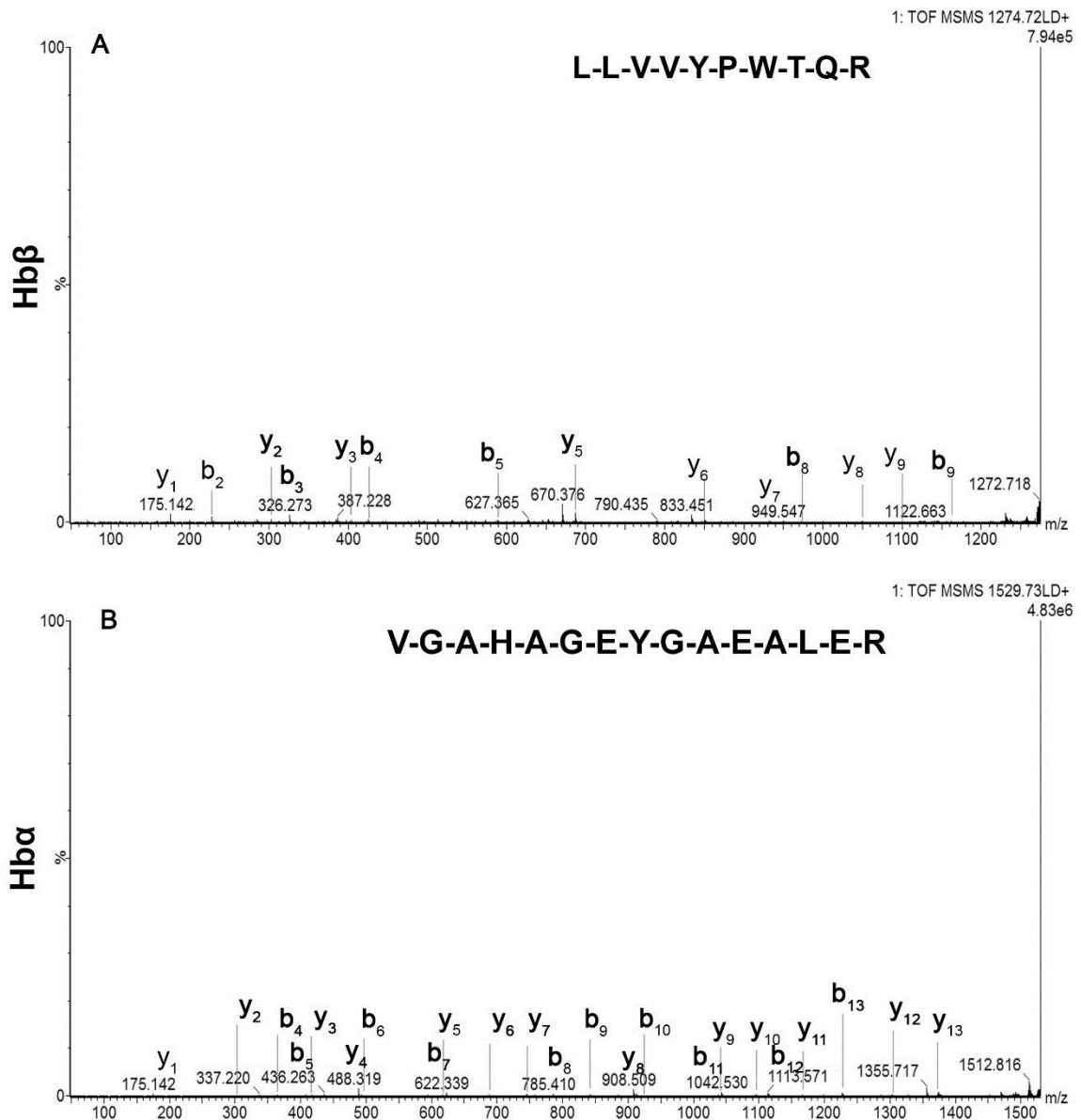


**Figure 3.5** MALDI-IMS-MS/MS of tryptic peptides at  $m/z$  1274.725 (A, multi-species) and  $m/z$  1529.734 (B, human), identified via mascot as Hb $\beta$  and Hb $\alpha$ , respectively, with both b and y ions annotated.

### 3.4 Concluding remarks

Mapping of blood signatures onto the ridge pattern of a fingerprint can provide crucial information in a forensic investigation, linking the suspect to the events of bloodshed. Here a sample preparation method has been developed to undertake trypsin proteolysis *in situ*, thus enabling blood peptides to be mapped in a fingerprint and hence facilitating reconstruction of "molecular blood images of the ridge pattern".

Results also indicate that the use of the acoustic ejector is unsuitable as the high viscosity of blood causes trypsin spot merging, thus preventing mapping of blood signatures onto fingerprint ridges. In contrast, the automatic sprayer employed here allowed successful imaging of the fingerprint ridges. Further instrumental developmental work is planned to enable the deposition of higher concentrations of trypsin with the intention to improve the quality of molecular images and the blood peptide signal intensity. A separate and in-depth study is required here, trialling the method and adjustments to it (trypsin concentration) needed for different amounts of blood tested in order to determine the blood amount range for which a certain trypsin concentration still yields the desired blood peptide signatures. This is also important as the amount of blood found in crime scene marks may differ from that employed here as a reference model, thus requiring different concentrations of trypsin to fulfil the optimal substrate:enzyme ratio. Once this study has been carried out it will be necessary to combine its findings with an estimation of the amount of blood present in a given piece of evidence in order to select an appropriate trypsin concentration. While the author has already demonstrated in MALDI profiling bottom-up proteomic experiments that it is possible to retrieve blood signatures from blood evidence as old as 9 years, future work will include testing the optimised sample preparation/imaging methods on blood fingerprints of different age to prove analytical robustness.

The work illustrated here also opens up new avenues of investigation; similarly to the concept previously demonstrated by the author's group with regards to establishing the order of deposition of fingerprints and condom lubricants using MALDI-MSI [53], it may be possible to determine whether blood peptides are present exclusively on the ridges, which would suggest that a mark was left by a bloodied finger, or on the entire sample surface including ridges and valleys, which would suggest a mark having been deposited onto a bloodied surface (or contaminated with blood after deposition). Differentiating between these scenarios would then enable investigators to reach a more confident conclusion and establish a stronger link between the fingerprint donor and the event of bloodshed.

### 3.5 References

- [1] S. Francese, R. Bradshaw, L.S. Ferguson, R. Wolstenholme, M.R. Clench, S. Bleay, Beyond the ridge pattern: multi-informative analysis of latent fingerprints by MALDI mass spectrometry., *Analyst*. 138 (2013) 4215–28.
- [2] E. Patel, M.R. Clench, A. West, P.S. Marshall, N. Marshall, S. Francese, Alternative Surfactants for Improved Efficiency of In Situ Tryptic Proteolysis of Fingerprints, *J. Am. Soc. Mass Spectrom.* 26 (2015) 862–872.
- [3] G. Groeneveld, M. de Puit, S. Bleay, R. Bradshaw, S. Francese, Detection and mapping of illicit drugs and their metabolites in fingerprints by MALDI MS and compatibility with forensic techniques, *Sci. Rep.* 5 (2015).
- [4] H.L. Bandey, S.M. Bleay, V.J. Bowman, R.P. Downham, V.G. Sears, *Fingerprint Visualisation Manual*, 1st ed., Centre for Applied Science and Technology (St. Albans), 2014.
- [5] L.C.A.M. Bossers, C. Roux, M. Bell, A.M. McDonagh, Methods for the enhancement of fingerprints in blood, *Forensic Sci. Int.* 210 (2011) 1–11.
- [6] S.S. Tobe, N. Watson, N.N. Daéid, Evaluation of six presumptive tests for blood, their specificity, sensitivity, and effect on high molecular-weight DNA, *J. Forensic Sci.* 52 (2007) 102–109.
- [7] M. Cox, A study of the sensitivity and specificity of four presumptive tests for blood., *J. Forensic Sci.* 36 (1991) 1503–1511.
- [8] B. Marchant, C. Tague, Developing Fingerprints in Blood : A Comparison of Several Chemical Techniques, *J. Forensic Identif.* 57 (2007) 76–93.
- [9] T.I. Quickenden, J.I. Creamer, A study of common interferences with the forensic luminol test for blood., *Luminescence.* 16 (2001) 295–8.
- [10] J.H. An, K.J. Shin, W.I. Yang, H.Y. Lee, Body fluid identification in forensics, *BMB Rep.* 45 (2012) 545–553.
- [11] S.L. Morgan, M.L. Myrick, *Rapid Visualization of Biological Fluids at Crime Scenes using Optical Spectroscopy (Grant Report)*, 2011.
- [12] F. Barni, S.W. Lewis, A. Berti, G.M. Miskelly, G. Lago, Forensic application of the luminol reaction as a presumptive test for latent blood detection, *Talanta.* 72 (2007) 896–913.
- [13] A. Castelló, M. Alvarez, F. Verdú, Accuracy, reliability, and safety of luminol

- in bloodstain investigation, *J. Can. Soc. Forensic Sci.* 35 (2002) 113–121.
- [14] S.M. Bleay, V.G. Sears, H.L. Bandey, A.P. Gibson, V.J. Bowman, R. Downham, L. Fitzgerald, T. Ciuksza, J. Ramadani, C. Selway, Chapter 5 : Alternative finger mark development techniques, in: *Fingerpr. Source B.*, 2012.
- [15] T.I. Quickenden, P.D. Cooper, Increasing the specificity of the forensic luminol test for blood., *Luminescence.* 16 (2001) 251–253.
- [16] B.A. Schweers, J. Old, P.W. Boonlayangoor, K.A. Reich, Developmental validation of a novel lateral flow strip test for rapid identification of human blood (Rapid Stain Identification™-Blood), *Forensic Sci. Int. Genet.* 2 (2008) 243–247.
- [17] W.R. Premasiri, J.C. Lee, L.D. Ziegler, Surface-Enhanced Raman Scattering of Whole Human Blood, Blood Plasma, and Red Blood Cells: Cellular Processes and Bioanalytical Sensing, *J. Phys. Chem.* 116 (2012) 9376–9386.
- [18] S. Boyd, M.F. Bertino, D. Ye, L.S. White, S.J. Seashols, Highly Sensitive Detection of Blood by Surface Enhanced Raman Scattering, *J. Forensic Sci.* 58 (2013) 753–756.
- [19] V. Sikirzhytski, A. Sikirzhytskaya, I.K. Lednev, Multidimensional Raman spectroscopic signatures as a tool for forensic identification of body fluid traces: A review, *Appl. Spectrosc.* 65 (2011) 1223–1232.
- [20] V. Sikirzhytski, A. Sikirzhytskaya, I.K. Lednev, Advanced statistical analysis of Raman spectroscopic data for the identification of body fluid traces: Semen and blood mixtures, *Forensic Sci. Int.* 222 (2012) 259–265.
- [21] K. Virkler, I.K. Lednev, Raman spectroscopy offers great potential for the nondestructive confirmatory identification of body fluids, *Forensic Sci. Int.* 181 (2008) 1–5.
- [22] V. Sikirzhytski, K. Virkler, I.K. Lednev, Discriminant analysis of Raman spectra for body fluid identification for forensic purposes, *Sensors.* 10 (2010) 2869–2884.
- [23] K. Virkler, I.K. Lednev, Raman spectroscopic signature of blood and its potential application to forensic body fluid identification, *Anal. Bioanal. Chem.*

396 (2010) 525–534.

- [24] K. De Wael, L. Lepot, F. Gason, B. Gilbert, In search of blood - Detection of minute particles using spectroscopic methods, *Forensic Sci. Int.* 180 (2008) 37–42.
- [25] ChemImage, *Hyperspectral Imaging Provides Detection and High Contrast Imaging of Biological Stains (White Paper)*, (2015).  
[www.chemimage.com/docs/white-papers/biological-stains-white-paper.pdf](http://www.chemimage.com/docs/white-papers/biological-stains-white-paper.pdf) (accessed July 19, 2015).
- [26] B. Li, P. Beveridge, W.T. O'Hare, M. Islam, The application of visible wavelength reflectance hyperspectral imaging for the detection and identification of blood stains, *Sci. Justice.* 54 (2014) 432–8.
- [27] S. Boyd, M.F. Bertino, S.J. Seashols, Raman spectroscopy of blood samples for forensic applications, *Forensic Sci. Int.* 208 (2011) 124–128.
- [28] P. Lemler, W.R. Premasiri, A. DeIMonaco, L.D. Ziegler, NIR Raman spectra of whole human blood: Effects of laser-induced and in vitro hemoglobin denaturation, *Anal. Bioanal. Chem.* 406 (2014) 193–200.
- [29] G.J. Edelman, E. Gaston, T.G. van Leeuwen, P.J. Cullen, M.C.G. Aalders, Hyperspectral imaging for non-contact analysis of forensic traces, *Forensic Sci. Int.* 223 (2012) 28–39.
- [30] G.J. Edelman, T.G. van Leeuwen, M.C.G. Aalders, Hyperspectral imaging of the crime scene for detection and identification of blood stains, in: *Proc. SPIE - Int. Soc. Opt. Eng.*, 2013: p. 87430A.
- [31] S.G. Kazarian, K.L.A. Chan, ATR-FTIR spectroscopic imaging: recent advances and applications to biological systems, *Analyst.* 138 (2013) 1940.
- [32] J. Anastassopoulou, E. Boukaki, C. Conti, P. Ferraris, E. Giorgini, C. Rubini, S. Sabbatini, T. Theophanides, G. Tosi, Microimaging FT-IR spectroscopy on pathological breast tissues, *Vib. Spectrosc.* 51 (2009) 270–275.
- [33] C. Ricci, S.G. Kazarian, S. Bleay, Spectroscopic Imaging of Latent Fingermarks Collected with the Aid of Gelatin Tape, *Anal. Chem.* 79 (2007) 5771–5776.
- [34] P.H.R. Ng, S. Walker, M. Tahtouh, B. Reedy, Detection of illicit substances in fingerprints by infrared spectral imaging, *Anal. Bioanal. Chem.* 394 (2009)

2039–2048.

- [35] W. Dirwono, J.S. Park, M.R. Agustin-Camacho, J. Kim, H.M. Park, Y. Lee, K.B. Lee, Application of micro-attenuated total reflectance FTIR spectroscopy in the forensic study of questioned documents involving red seal inks, *Forensic Sci. Int.* 199 (2010) 6–8.
- [36] S. Stewart, R.J. Priore, M.P. Nelson, P.J. Treado, Raman Imaging, *Handb. Raman Spectrosc.* 5 (2001) 337–360.
- [37] A. Braz, M. López-López, C. García-Ruiz, Raman imaging for determining the sequence of blue pen ink crossings, *Forensic Sci. Int.* 249 (2015) 92–100.
- [38] B.M. Davis, A.J. Hemphill, D.C. Maltaş, M.A. Zipper, P. Wang, D. Ben-Amotz, Multivariate hyperspectral Raman imaging using compressive detection., *Anal. Chem.* 83 (2011) 5086–92.
- [39] H. Yang, B. Zhou, H. Deng, M. Prinz, D. Siegel, Body fluid identification by mass spectrometry, *Int. J. Legal Med.* 127 (2013) 1065–1077.
- [40] R. Seraglia, a. Teatino, P. Traldi, MALDI mass spectrometry in the solution of some forensic problems, *Forensic Sci. Int.* 146 (2004) 83–85.
- [41] H.-S. Youn, R.S. Burkhalter, R. Timkovich, Identification of hemes and related cyclic tetrapyrroles by matrix-assisted laser desorption/ionization and liquid secondary ion mass spectrometry., *Rapid Commun. Mass Spectrom.* 16 (2002) 1147–52.
- [42] R. Bradshaw, S. Bleay, M.R. Clench, S. Francese, Direct detection of blood in fingerprints by MALDI MS profiling and Imaging, *Sci. Justice.* 54 (2014) 110–117.
- [43] N.L. Anderson, N.G. Anderson, The human plasma proteome: history, character, and diagnostic prospects., *Mol. Cell. Proteomics.* 1 (2002) 845–867.
- [44] G. Liunbruno, A. D'Alessandro, G. Grazzini, L. Zolla, Blood-related proteomics, *J. Proteomics.* 73 (2010) 483–507.
- [45] J.N. Adkins, S.M. Varnum, K.J. Auberry, R.J. Moore, N.H. Angell, R.D. Smith, D.L. Springer, J.G. Pounds, Toward a Human Blood Serum Proteome: Analysis By Multidimensional Separation Coupled With Mass

- Spectrometry, *Mol. Cell. Proteomics*. 1 (2002) 947–955.
- [46] G.S. Omenn, THE HUPO Human Plasma Proteome Project, *Proteomics - Clin. Appl.* 1 (2007) 769–779.
- [47] V. Nanjappa, J.K. Thomas, A. Marimuthu, B. Muthusamy, A. Radhakrishnan, R. Sharma, A. Ahmad Khan, L. Balakrishnan, N.A. Sahasrabudhe, S. Kumar, B.N. Jhaveri, K.V. Sheth, R. Kumar Khatana, P.G. Shaw, S.M. Srikanth, P.P. Mathur, S. Shankar, D. Nagaraja, R. Christopher, S. Mathivanan, R. Raju, R. Sirdeshmukh, A. Chatterjee, R.J. Simpson, H.C. Harsha, A. Pandey, T.S.K. Prasad, Plasma Proteome Database as a resource for proteomics research: 2014 update., *Nucleic Acids Res.* 42 (2014) D959-65.
- [48] E. Patel, P. Cicatiello, L. Deininger, M.R.R. Clench, G. Marino, P. Giardina, G. Langenburg, A. West, P. Marshall, V. Sears, S. Francese, A proteomic approach for the rapid, multi-informative and reliable identification of blood, *Analyst*. 141 (2016) 191–198.
- [49] R. Wolstenholme, R. Bradshaw, M.R. Clench, S. Francese, Study of latent fingermarks by matrix-assisted laser desorption/ionisation mass spectrometry imaging of endogenous lipids, *Rapid Commun. Mass Spectrom.* 23 (2009) 3031–3039.
- [50] P.J. Trim, M.-C. Djidja, S.J. Atkinson, K. Oakes, L.M. Cole, D.M.G. Anderson, P.J. Hart, S. Francese, M.R. Clench, Introduction of a 20 kHz Nd:YVO<sub>4</sub> laser into a hybrid quadrupole time-of-flight mass spectrometer for MALDI-MS imaging, *Anal. Bioanal. Chem.* 397 (2010) 3409–3419.
- [51] M. Strohal, D. Kavan, P. Novák, M. Volný, V. Havlíček, MMass 3: A cross-platform software environment for precise analysis of mass spectrometric data, *Anal. Chem.* 82 (2010) 4648–4651.
- [52] L.M. Cole, M.-C. Djidja, J. Bluff, E. Claude, V. a Carolan, M. Paley, G.M. Tozer, M.R. Clench, Investigation of protein induction in tumour vascular targeted strategies by MALDI MSI., *Methods*. 54 (2011) 442–53.
- [53] R. Bradshaw, R. Wolstenholme, R.D. Blackledge, M.R. Clench, L.S. Ferguson, S. Francese, A novel matrix-assisted laser desorption/ionisation mass spectrometry imaging based methodology for the identification of

sexual assault suspects., *Rapid Commun. Mass Spectrom.* 25 (2011) 415–22.

## Chapter 4

### **Blind study and other applications – a tale of forensic method validation**

## 4.1 Introduction

In criminal cases it can be very important to determine if a substance collected as evidence is blood or contains blood. While DNA analysis is undoubtedly useful for determining the individual human source of the trace, it is not commonly used for simultaneous body fluid identification. Protocols have been reported for co-extraction of DNA and RNA, and this has been investigated for body fluid identification, however this results in lower sensitivity for DNA analysis [1,2]. The mRNA markers used for the identification of blood are in fact not unique to blood but can be found in other tissues and cell types in varying expression levels [3].

If it is a requirement to determine the species of origin of the blood further issues with the use of DNA/RNA are encountered. Although amplification systems for animal DNA exist, a different set of primers is required for each species and multiplex systems have been found to be unreliable [4]. This means that presumptive knowledge of the species origin of a presumed blood trace is required, or alternatively a range of primers must be trialled in an attempt to determine the species source.

Another consideration that needs to be made is the fact that several BETs result in reduced sensitivity of DNA recovery and analysis [5]. This is especially important when looking at long-term effects. This can have considerable impact on cold case investigations, as it is recommended to perform DNA analysis within 30 days of enhancement [5]. Furthermore, the swabbing required for DNA or RNA extraction makes it unsuitable for analysis of suspected blood fingerprints, where it is desirable to maintain ridge detail.

In the previous chapters the development of a proteomic approach using MALDI-MS to allow confident detection and species determination of blood in stains was reported [6]. This methodology is based on the detection of blood-specific tryptic peptides and their species-specific differences in the amino acid sequences. The protocol has been further developed to allow the visualisation of the distribution of blood peptides in fingerprints via MALDI-MSI [7], thus establishing a link between

the biometric information and the event of bloodshed. Additionally, the problems previously encountered relating to the delivery of trypsin concentrations higher than 200 µg/mL with the SunCollect autosprayer [7], as reported in chapter 3, were overcome. By using a larger internal diameter capillary (ID 100 µm), additional experiments were able to establish 250 µg/mL as the most suitable concentration for the controlled samples used so far. It was therefore agreed to proceed using this concentration.

However, the samples used for the development of these methods were ideal samples of known provenance on substrates suitable for MALDI-MS. Therefore, the work reported in this chapter aimed to validate previous results and test the method's suitability for unknown, forensically relevant samples.

In order to allow for removal of fingerprint samples from the crime scene and their mass spectrometric analysis, a lifting step is required. While this is common practice for latent fingerprints and a variety of lifting tapes are available, the chemistry of latent prints differs from that of blood marks. As this can be expected to have an effect on a tape's ability to lift blood residue, a range of tapes was trialled in this work to identify a product suitable for lifting and MALDI-MSI analysis.

Furthermore, suspected blood marks are often subjected to BETs at the crime scene to visualise them, improve contrast or presumptively test for blood. A non-enhanced mark would be unlikely to be submitted for further testing. Although previous work had been performed on non-enhanced marks and those that had been treated with acid black 1 (AB1), many other BETs are available. Previous work carried out at SHU has studied MALDI-MSI of latent fingerprints and the enhancement techniques they can be subjected to [8]. It seemed appropriate and necessary to investigate potential interferences of various BETs with the proposed MALDI-MS workflow for blood analysis and to add into this study an examination of species specificity. The rationale for the species study was that all but one sample analysed in the SHU group's previous publications had been of known provenance. Although species differences appeared prominent and identifications were made with confidence, the

species subset was small and identification bias cannot be excluded due to previous knowledge.

To address these issues and provide suitable validation, a blind study was devised. Samples were prepared externally by Dr. Glenn Langenburg (CEO of Elite Forensic Services, LLC, Minnesota, USA) without disclosing their origins to SHU investigators and included human blood, animal blood from five different species, human biofluids and non-biofluid samples. Additionally, some of the samples were enhanced with common BETs, but it was not disclosed which particular BET was used or which samples were enhanced. Because samples were prepared on silver-coloured aluminium slides, this meant that in some instances it was difficult to determine if a sample had been enhanced. This was due to the fact that for example, whilst light coloured enhancement techniques like acid yellow 7 are meant to improve contrast on dark substrates, they remain poorly visible on lighter backgrounds like that employed in this study. In some instances, enhancement could therefore only be inferred from a sample's appearance under certain light conditions such as UV light.

The study successfully demonstrated that MALDI-MS allows the confident detection of human blood in unknown, enhanced and non-enhanced stains with a 100% success rate. Refinement of the data analysis approach was necessary to facilitate identification and species determination of animal blood, especially concerning some of the employed enhancement techniques. Whilst no extensive in-house database had been created for the identification of non-blood biofluids, they were readily distinguishable from blood samples and the presence of a few characteristic peptides allowed their preliminary identification. Future work can be envisioned involving the more extensive characterisation of those biofluid proteomes for more confident identification. Non-biofluid samples were successfully classed as such, although no further identifications were attempted.

One fingerprint sample was successfully identified as a human blood mark and another as a non-biofluid mark, both maintaining ridge detail.

## 4.2 Methods and materials

### 4.2.1 Lifting of non-enhanced and AB1-enhanced bloodied marks

A white ceramic tile was cleaned with Mr. Muscle window and glass cleaning detergent (S.C. Johnson & Son, Racine, USA) and subsequently wiped with Distel high level laboratory disinfectant (Tristel Solutions Ltd., Snailwell, UK) prior to sample deposition. Bloodied fingermarks were prepared by pricking a clean finger with a lancet and rubbing it against another clean fingertip to achieve an even distribution. This second finger was then used to deposit bloodied marks onto the tile. Optical images of bloodied marks before and after AB1-enhancement and lifting were obtained on a Foster+Freeman VSC 4CX (Evesham, UK).

The following strategies were applied independently from each other, each on a fresh set of marks so lifting was not attempted on the same mark twice. Originally, CSI pre-cut lifting tape 96113 was peeled off straight away after smoothing out across the mark. Next, pressure was applied to the tape on top of the mark for 30 s, 1 min, 1 min 30 s, 2 min, 2 min 30 s and 3 min before lifting. Lastly, the tile was placed in a humidity chamber at 25°C and 70%, 80% or 90% humidity for 5, 10 or 15 minutes before application of the tape, followed by 30 s pressure and lifting.

Bloodied marks were enhanced using the ethanol/water-based formulation of acid black 1 (AB1) as described in the Home Office fingermark visualisation manual [9]. The fixing solution (23 g/L 5-sulphosalicylic acid in dH<sub>2</sub>O) was applied to the tile with a dropper pipette, ensuring the mark was covered and kept wetted for 5 minutes. Subsequently, the substrate (a white ceramic tile) was tilted to allow the solution to drain onto a paper towel, and briefly air dried. The staining solution (1 g AB1 in 1L 5:25:70 acetic acid:ethanol:dH<sub>2</sub>O) was applied, left to stain for 4 minutes and removed in the same manner. Lastly, the washing solution (5:25:70 acetic acid:ethanol:dH<sub>2</sub>O) was applied for 3 minutes and the substrate gently agitated. After draining, the process was repeated once more.

<b>Tape</b>	<b>Supplier</b>
CSI pre-cut lifting tape - fingerprint (#96113)	CSI Equipment Ltd (Woburn Sands, UK)
Permacel J-Lar® Clear to the Core lifting tape 25mm (#96105)	
CSI Flexi tape (3M Polytape 1-1410; #96104)	
CSI specialist tape - fingerprint (#96160)	
Cellulose Clear Tape ref. 3M 607 (3M Pressure Sensitive tape; #C32810)	WA Products (Burnham on Crouch, UK)
Sirchie fingerprint lifting clear tape (#S144L)	
Sirchie Search Polythene Lifting Tape Transparent (#S169PPA)	
Serilux Style lifter (#B20653-100)	
3M Magic Tape	local stationery shop
Clear, black and white gelatine lifters	BDA via WA Products Ltd (Burnham on Crouch, UK)
ZarPro™ fluorescent blood lifting strips	Tri-Tech Forensics

**Table 4.1** Lifting tapes and gelatine lifters trialled including suppliers.

Preliminary tests were performed on enhanced marks, exerting 30 s of pressure using a variety of different tapes (Table 4.1). ZarPro™ blood lifting strips were used as per the manufacturer's instructions. J-Lar® tape was also used to lift immediately after smoothing onto the mark, without pressure application.

#### **4.2.2 Preparation of blind samples**

ALUGRAMSIL G/UV254 aluminium slides (Sigma-Aldrich, Dorset, UK) were prepared as previously described [10] and used as deposition surfaces for the blind samples. Blind samples were prepared by Dr. Glenn Langenburg, CEO of Elite Forensic Services LLC (Saint Paul, Minnesota, USA). The sample set included blood from a human donor as well as pig, cow, chicken, deer and wild boar blood, human biofluids and non-biofluid samples, which were deposited as stains and fingermarks.

Each slide contained 2 separate stains or fingerprints. Some of the samples were enhanced with BETs, the exact nature of which was not disclosed.

#### **4.2.2.1 Tryptic digestion and MALDI-MS**

Stain samples were extracted into 1 mL 70:30 ACN:H<sub>2</sub>O by pipetting some of the solution onto the stain, pipetting-mixing and scratching off the dried residue to reconstitute in the extraction solution. This extract was transferred back into the 1 mL solution, which was then sonicated at 45 kHz for 10 minutes.

In-solution digests were prepared following the previously devised protocol [6] and spotted with 0.5 µL of 5 mg/mL CHCA in 70:30 ACN:0.5%TFA<sub>aq</sub> containing equimolar amounts of aniline (2.4 µL per mL matrix).

*In situ* digests were prepared as previously described [7], employing a trypsin concentration of 250 µg/mL incl. 0.1% Rapigest™ SF and a 100 µm internal diameter capillary on the SunCollect autosprayer (KR Analytical, Sandbach, UK).

MALDI-MS data were acquired in positive ion mode in the *m/z* range 650 - 3600 using a SYNAPT™ G2 HDMS system (Waters Corporation, Manchester, UK) operating with a 1 kHz Nd:YAG laser, at a mass resolution of 10,000 FWHM (sensitivity mode). Images were acquired at a spatial resolution of 150 µm. Calibration over a 650 - 3600 *m/z* range was performed prior to analysis using phosphorous red. The laser energy was set to 250 arbitrary units.

Mass spectra opened using MassLynx™ (Waters Corporation, Manchester, UK) were either converted into txt files and imported into mMass, an open source multiplatform mass spectrometry software [11], or processed directly performing peak smoothing, baseline correction and peak centroiding. UniprotKB (<http://www.uniprot.org/>, UniProt release 2015\_11) was employed to generate *in silico* peptide lists of known proteins present in blood. Mass lists were generated by selecting “*monoisotopic*”, “*MH<sup>+</sup>*”, “*trypsin*”, “*2 missed cleavages*”, “*methionine oxidation*”. Peptide lists were imported into Microsoft Excel and mMass to create an

“in house” and local reference library. A FASTA database containing the relevant blood peptides was generated for use in Waters Protein Lynx Global Server software. Data analysis of mass images was performed within the HDI 1.4 software (Waters Corp. Manchester, UK). Prior to peak assignment search, spectra were smoothed and de-isotoped. Peak assignment was not accepted if the S/N was lower than 3:1. Spectral processing consisted of smoothing, baseline correction and lock mass-based mass correction.

## **4.3 Results and Discussion**

### **4.3.1 Lifting of bloodied fingermarks**

Since blood marks are currently not routinely recovered from crime scenes, due to the absence of further analysis techniques, prior to the work described here identification of a suitable lifting tape was not required. The use of MALDI-MSI of blood marks, however, changes this and has brought about a need to identify a tape suitable for lifting blood marks to facilitate their intact removal from a crime scene or evidential object.

Initially, the lifting tape previously used by the author’s group for the study of latent marks [12] (CSI pre-cut lifting tape 96113) was used to attempt to lift blood marks. Despite exerting pressure for various lengths of time and subjecting the samples to 70-90% humidity prior to lifting attempts, the blood did not stick to the lifting tape and marks could not be lifted. Due to the different chemical composition of blood marks versus latent marks it is entirely plausible that a tape used for the lifting of latent marks is unsuitable for blood marks.

For this reason, a variety of other tapes (stationery tapes and tapes intended for fingerprint lifting) of different compositions were trialled under the assumption they would present different characteristics including potentially stronger adhesive properties. Regrettably, detailed information about the constituents were not publicly available, therefore only claimed performance characteristics could be employed in choosing different tapes.

During preliminary trials of lifting non-enhanced bloodied marks with the aid of manually applying pressure for 30 s to the various different tapes, a faint residue not dissimilar to non-blood marks was observed on some tapes. However, by the time the last mark out of a series of nine was lifted the residue had already become invisible, presumably due to evaporation. Therefore, the capture of optical images was not possible. Also, contrast was poor, making it hard to determine if lifting had been successful. Hence it was decided to continue the trials on enhanced marks with improved contrast.

#### **4.3.2 Lifting of AB1-enhanced marks**

AB1-enhancement was performed in accordance with the Home Office protocol described in the Fingerprint Visualisation Manual [9].

When attempting to lift the enhanced marks of the substrate with the exertion of 30 s of manual pressure, J-Lar® clear to the core tape and Sirchie 144L tape showed the most promising results in the preliminary trials, lifting at least near-complete marks (Figure 4.1 and Figure 4.2), whereas other tapes only lifted small areas with poor ridge detail (data not shown). ZarPro™ lifts were also promising, however due to the vastly different structure and chemistry of the lifts, a lot of method optimisation will be required to allow for their MALDI-MSI analysis. (Their surface coating absorbed trypsin and matrix and did not allow for the generation of ions with the previously established method. Due to time constraints, the method was not optimised further for this particular lift.)

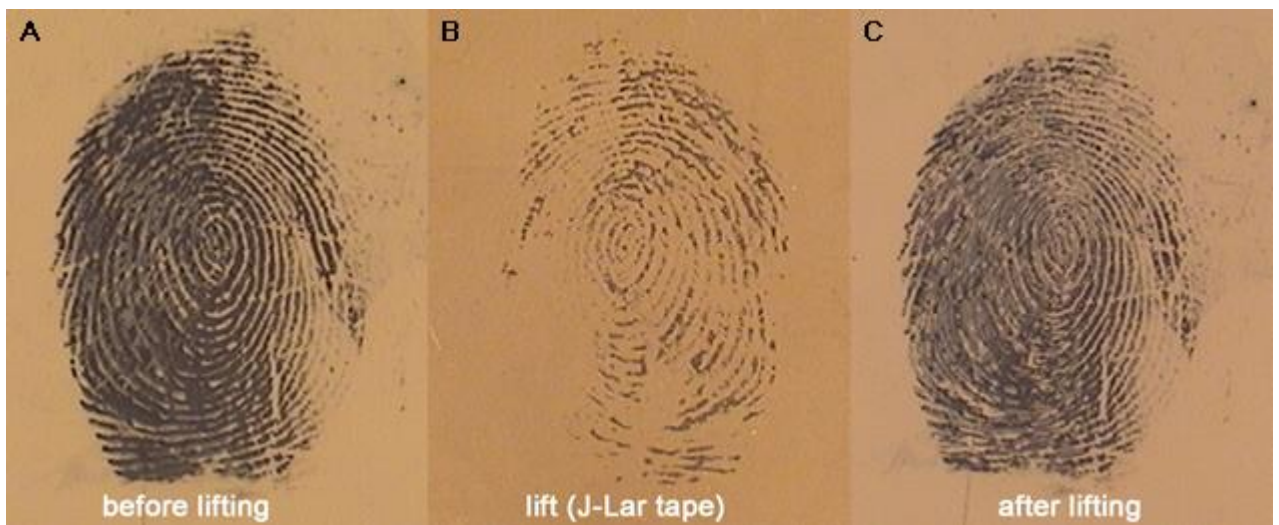


**Figure 4.1** A: AB1-enhanced blood mark on a ceramic tile, B: lift of A with J-Lar® tape, C: mark A after lifting

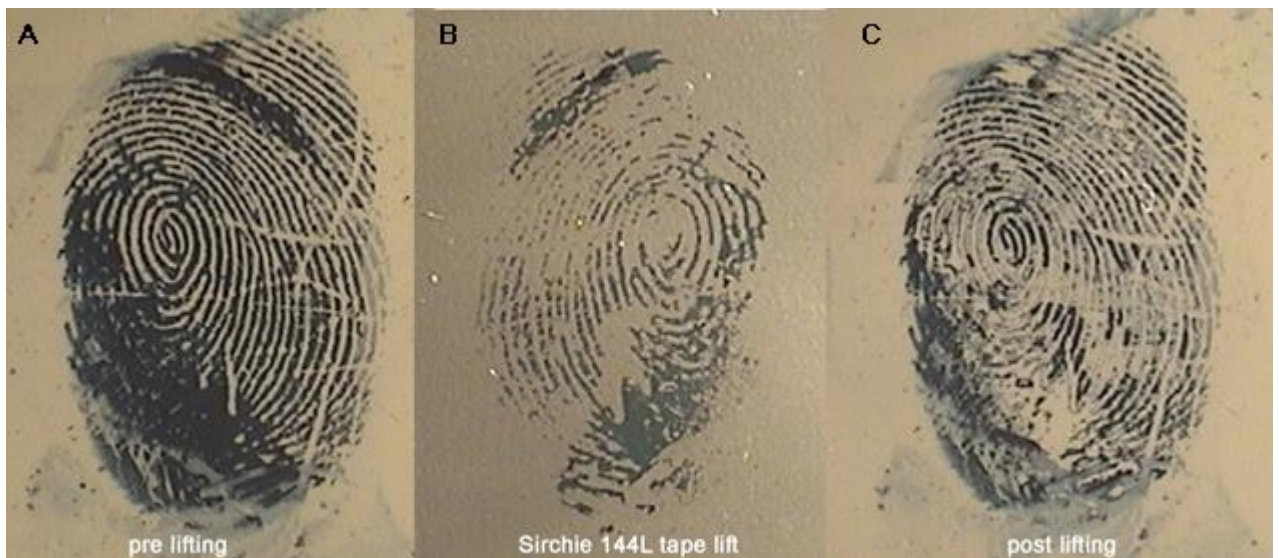


**Figure 4.2** A: AB1-enhanced blood mark on a ceramic tile, B: lift of A with Sirchie 144L tape, C: mark A after lifting

Furthermore, it was found out by accident that lifting the tape straight after deposition onto a mark produces a visibly better lift than exerting 30 s of pressure (Figure 4.3). This was verified by comparing 5 repeats of both practices and hence, the no-pressure approach is recommended and has been used for subsequent MALDI-MSI.

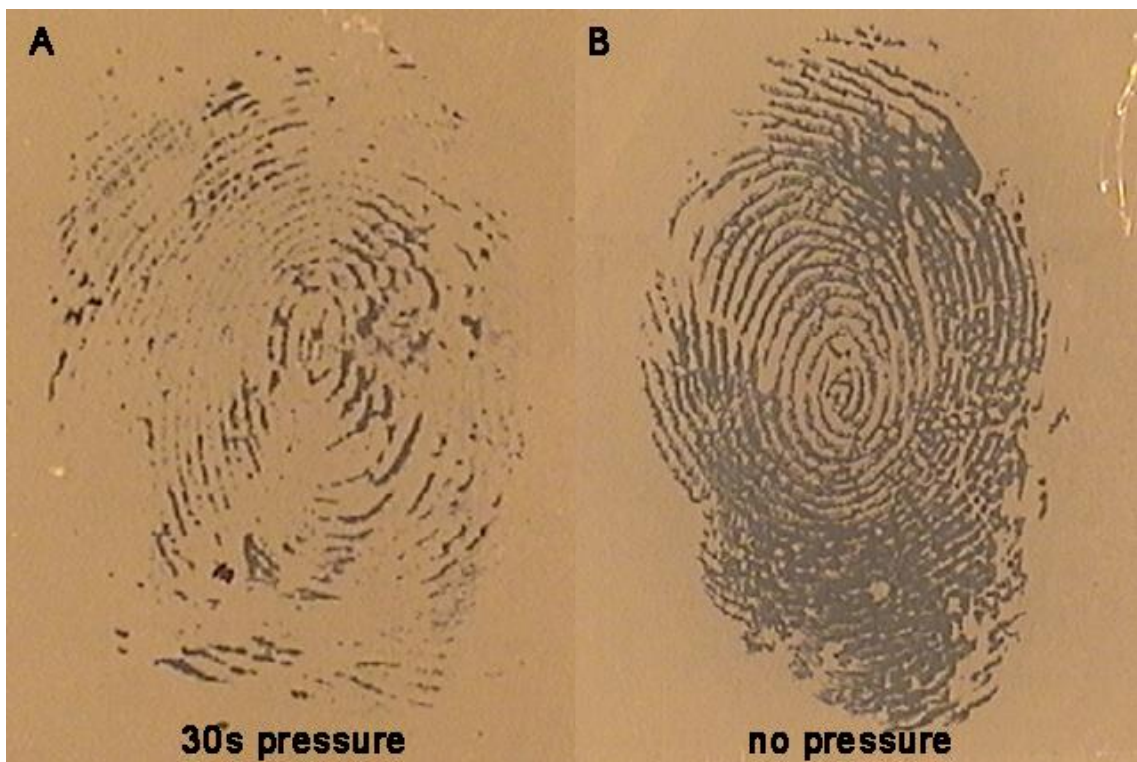


**Figure 4.3** AB1-enhanced blood marks lifted with J-Lar® tape with (A) the application of 30 s of pressure and (B) lifted immediately, without pressure application.

It was, however, noted that occasionally there were marks that could not be lifted successfully by any tape or method, even though prepared, enhanced and "lifted" at the same time as the other marks in that sample set, which were successfully lifted. This was the case even for the more successful J-Lar® and Sirchie 144L tapes, which lifted marks in the same sample set but failed to lift the "problematic marks". The marks in question did not visually differ from each other and it remains unclear why they could not be lifted when treated and stored exactly as the other marks, calling for further investigation of this matter.

In order to further evaluate the operational suitability of the J-Lar® and Sirchie tapes, *in situ* digests followed by MALDI-MSI were performed on lifts obtained with both tapes. Figure 4.4 shows the distribution of two ions putatively identified as the  $[M+H]^+$  ions of peptides originating from ceruloplasmin of various species origin (including human, porcine or bovine) and human haemoglobin  $\beta$  (Hb $\beta$ ) in a lift obtained with J-Lar® tape. Although in this instance the blood was known to be of human origin, the

detection of the peptide at  $m/z$  932.480 (theoretical  $m/z$  932.520; k.SAVTALWGK.v) confirms the species provenance within the sub-set of species considered in the study. It should be noted, however, that the two exemplary peptides presented here are not proteotypic and can be found in other species that could not be included in this study, such as primates or sea mammals.

The data obtained show that neither AB1-enhancement nor the tapes' chemistry hindered MALDI-MSI analysis and detection of blood peptides in the lifted blood mark. Although imaged peptides could not be identified with the same mass accuracy as in profiling experiments ( $\pm 10$  ppm) [6], the experiment provided valuable proof that the technique is suited to potential real world forensic applications with the use of the lifting tapes identified here.

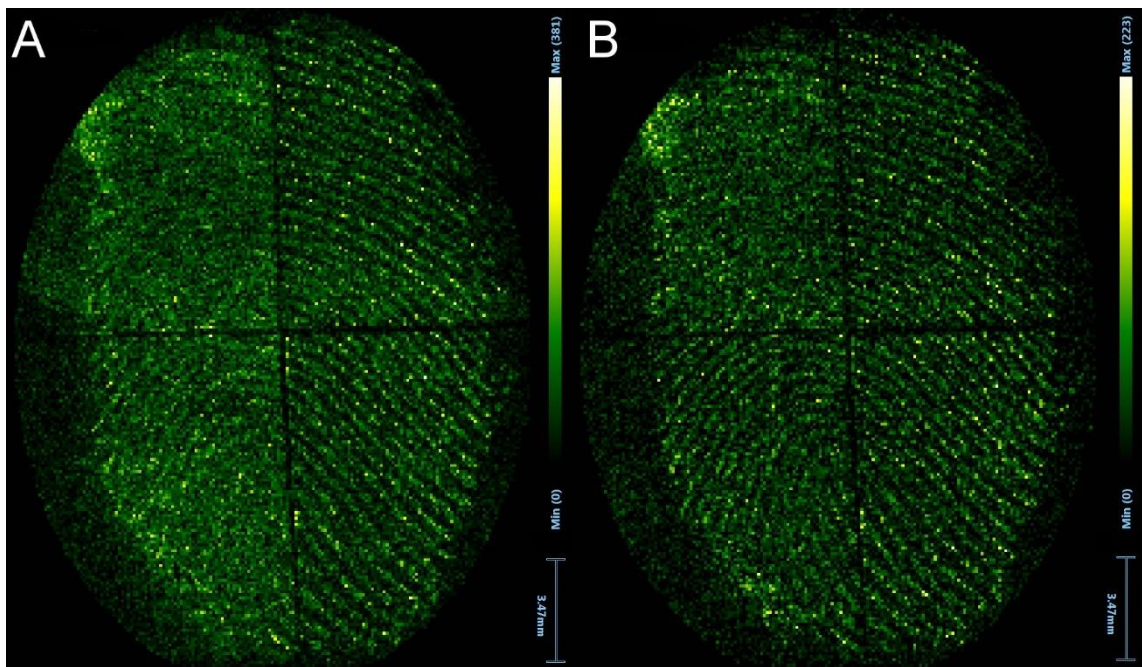


**Figure 4.4** MALDI-MSI data of a tryptically digested, AB1-enhanced blood mark lifted with J-Lar® tape. Image shows distribution of A:  $m/z$  752.399 (theoretical  $m/z$  752.430 – multi-species ceruloplasmin; r.IGGSYKK.l) and B:  $m/z$  932.480 (theoretical  $m/z$  932.520 – human or chimpanzee Hb $\beta$ ; k.SAVTALWGK.v).

### 4.3.3 Analysis of blind samples with MALDI-MS profiling

Blind sample stains were extracted, digested and analysed following the previously developed protocol (see chapter 2). This included exporting data acquired using Waters MassLynx software into .txt-files, importing the .txt files in the free mMass software package and performing smoothing and peak-picking in this package. In mMass, peaks below a S:N of 3:1 were not accepted. Peptide identifications were achieved by employing the software's *in silico* digestion and matching function.

In an initial round of analysis, data from 11 samples were compared to the in-house peptide database of human, bovine (cow), porcine (pig, wild boar), cervine (deer) and phasianine (chicken). All human blood samples (n=2) were correctly identified as such via identification of commonly observed human blood peptides, including proteotypic peptides such as the  $m/z$  2808.340 (theoretical  $m/z$  2808.344; k.DYELLCLDGTRKPVVEEYANCHLAR.a) putatively identified as from human serotransferrin. Additionally, all non-blood samples (n=3) were correctly classed as such based on the absence of commonly observed blood peptides. However, the six animal blood samples in the preliminary cohort were initially misclassified as non-blood because they did not present like typical blood spectra but appeared rather noisy. Furthermore, between the noise commonly observed or expected signals, such as the Hb $\beta$  peptide at  $m/z$  1274.725 (r.LLVVYPWTQR.f), appeared to be absent or only present in very low abundance that was easily masked by the noise. (Note:  $m/z$  1274.725 had previously been observed in abundance in all blood samples and was therefore initially seen as a marker for the presence of blood.) Figure 4.5 shows a comparison between one of the correctly identified human blood samples (bottom panel) and a bovine blood sample (top panel) that was initially misclassified. It can be seen that in the bovine sample,  $m/z$  1274.725 is only present in low abundance and somewhat masked by noise. Other blood peptides expected to be present in bovine blood are completely hidden by noise, such  $m/z$  1529.734 (Hb $\alpha$  human, bovine; k.VGAHAGEYGAEALER.m), or absent entirely, like  $m/z$  1833.891 (Hb $\alpha$  human, bovine; k.TYFPHFDLSHGSAQVK.g). This observation combined with the lack of reference spectra had led to the misclassification.

It should, however, be noted that there might have been differences in the sample composition of the animal blood samples compared to human blood due to the way they were collected. Human samples, in this instance, were pure blood drawn by a phlebotomist, whereas animal blood was not obtainable this way. Animal samples are likely to originate from roadkill or meat packages and can thus have been exposed to several contaminants as well as being diluted. This can also be hypothesised from visual comparison of the two stains as seen in the inserts in Figure 4.5, where the bovine stain appears more faint and dilute than the human blood stain. Although visual appearance can of course be misleading and cannot serve for sample identification, it might be viewed as an indicator of potentially reduced protein content here.

Despite the initial lack of identification, upon closer inspection chicken and bovine blood presented some signals that were not present in any of the other spectra and could therefore potentially serve as species markers. In bovine blood, this was  $m/z$  1669.835, which can putatively be identified as myoglobin of bovine or cervine origin (k.ALELFRNDMAAQYK.v) or chicken apolipoprotein A1 (theoretical  $m/z$  1669.836; k.LREDMAPYYKEVR.e). The peptide had also been observed in a previous study by this group in the analysis of bovine samples obtained from the residual blood and juices found in meat packages (Appendix 4, S 4.1). In chicken blood,  $m/z$  1749.793 was prominently observed in all spectra, although no putative identification could be made. This could, however, be due to the fact that chicken protein sequences could only be found for eight of the 17 blood proteins selected for this study. Additionally, Espinoza *et al.* [13] previously reported that they found a minimum of 2-5 haemoglobin variants in each species and in some instances none of them matched the previously reported variants. It is hence possible that the signals observed could not be identified because they originate from a protein or protein variant not currently in the database. This is especially true for the identification of deer, where only four, and wild boar, where no protein sequences were available in the database. Regrettably, although Espinoza *et al.* [13] reported to have found at least five

different haemoglobin variants for elk/red deer-sub species and 16 for white-tailed deer, they appear to not have entered them into UniProtKB.

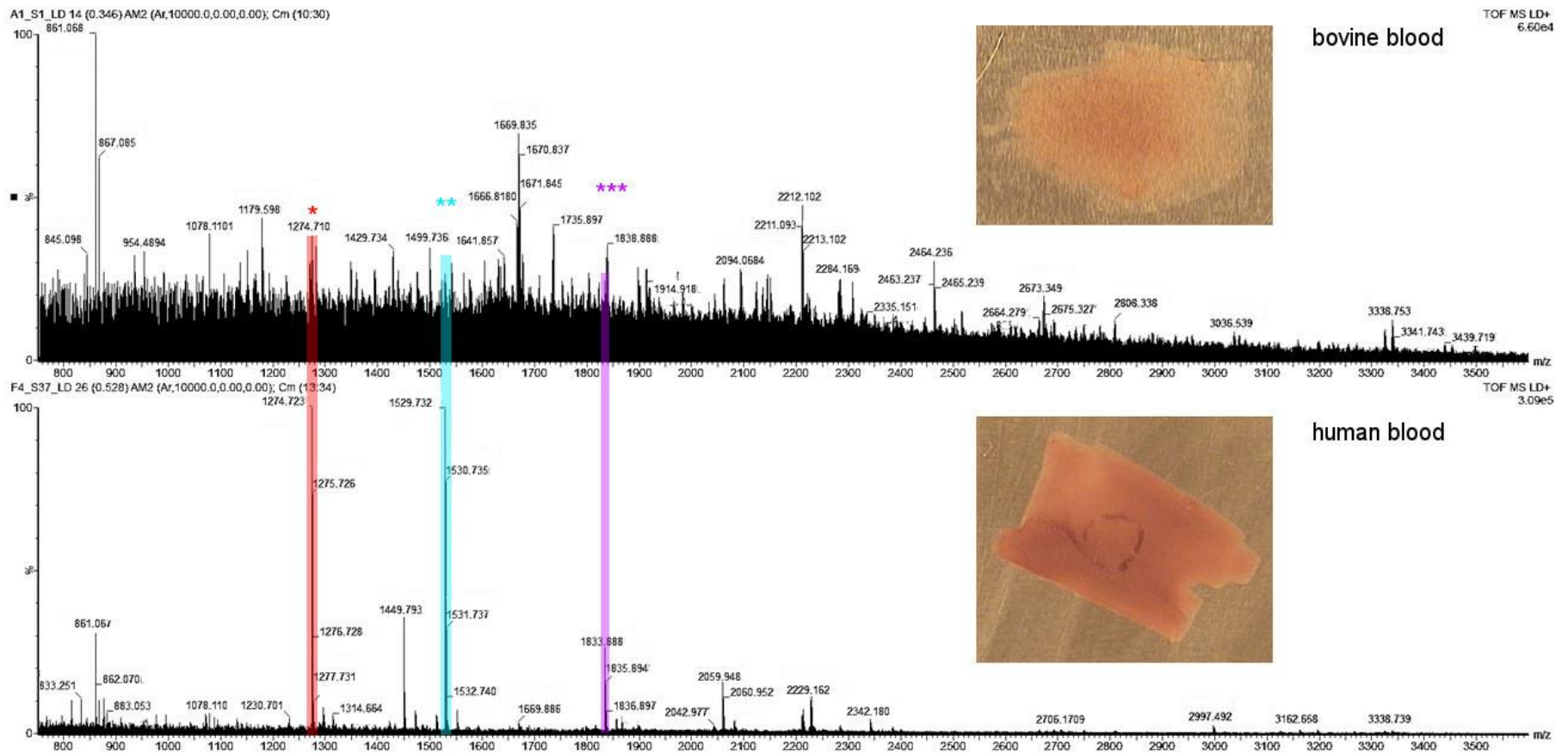


**Figure 4.5** MALDI-MS spectra of blind samples. Top panel shows bovine blood sample that was originally misclassified as a non-blood sample. Bottom panel shows human blood sample. Coloured boxes inserted for ease of comparison of some peptides expected in the bovine sample. \* denotes  $m/z$  1274.725 (Hb $\beta$  human, bovine, porcine, cervine; r.LLVVYPWTQR.f), \*\* denotes  $m/z$  1529.734 (Hb $\alpha$  human, bovine; k.VGAHAGEYGAEALER.m), \*\*\* denotes  $m/z$  1833.891 (Hb $\alpha$  human, bovine; k.TYFPHFDLSHGSAQVK.g), all referring to theoretical  $m/z$ . Inserts show the visual appearance of the stains before extraction.

Another problem that became evident when reanalysing the misidentified samples was that the two porcine samples in this initial cohort produced entirely different mass spectra. This was true both comparing the two different samples, but also comparing different spots of the same sample, which suggests considerable differences in ionisation efficiency. This understandably made the observation of characteristic signals very difficult. Even signals putatively identified as porcine serotransferrin, the signals with theoretical  $m/z$ s 1205.594 (r.DDTQCLARVGK.t) and 1803.945 (r.ENMSKAVKNGPLVSCVK.k), were only present in low abundance and easily masked in some spectra.

In contrast, another porcine sample that hadn't been included in the initial round of identifications was easily identified as such based on the abundant presence of  $m/z$  1274.711 (r.LLVVYPWTQR.f) and  $m/z$  1422.703 (k.VGGQAGAHGAEALER.m), identified as human, bovine, porcine or cervine Hb $\beta$  and porcine Hb $\alpha$ , respectively. Both of these signals had also been observed in previous studies of porcine blood obtained from a butcher (Appendix 4, S 4.2). (Note: Curiously, the bovine peptide observed in this blind study had only been detected in the sample from a meat packet, but not the one from a butcher. This further underlines the vast differences in the treatment of the two and therefore the possible variety of samples encountered.) Upon inspection of the optical images obtained prior to extraction, it was noted that the two misclassified samples exhibited fluorescent properties under UV light at 365 nm, whereas the correctly identified porcine sample did not, but perhaps appeared a little more red. This suggested that those samples had been subjected to an enhancement technique that was perhaps aimed at improving contrast on dark surfaces or under UV light, as it was not observable on the light sample background in visible light. (However, at the time of submission of this thesis the details of any enhancement used were not available). Due to the considerable differences observed between these data and those obtained from the correctly identified porcine sample, it can be hypothesised that this particular enhancement technique results in some sort of interference with the proposed MALDI-MS workflow, perhaps resulting in inefficient tryptic digestions or analyte ionisation. For

this reason, consideration should be given to the recommendation of the use of a specified sub-set of enhancement techniques when MALDI-MS analysis is desired.

While the human blood samples had been identified correctly, the misclassification of animal blood samples posed an unexpected problem to the analysis strategy. For most samples, putative peptide identifications could be made for peptides originating from multiple species, although with little confidence due to the low signal intensities with some being identified in such noisy areas that their validity had to be doubted or refuted. Although characteristic signals could be identified for some, not all species included in the study had been encountered yet, resulting in a lack of known characteristic signals for deer and wild boar blood. Due to the differences in spectra obtained from porcine samples, identification of characteristic signals was difficult. Furthermore, basing an identification on one or two potential peptides or other unidentified signals is less than ideal, especially when no confident determination can be made as to where these signals originate from.

For this reason, the data analysis strategy was altered in hopes of achieving more reliable identifications and reducing analysis time by automating the process. The Waters software protein lynx global server (PLGS) was used in conjunction with an in-house FASTA database of the blood proteins selected for this study. Mass spectra were loaded into PLGS and a database search performed to match signals present in the spectra to blood peptides. However, rather than matching and identifying individual peptides, the software appeared to attempt to find a single protein identification. As such, it for example reported probabilities of 99.7% for human Hb $\beta$  and 0.3% for human Hb $\alpha$  in a human blood sample, although peptides originating from both, and additional proteins, were present. Consequently, other proteins and their peptides were given probability scores of 0%. Additionally, in a chicken blood spectrum human and other species proteins were still identified with higher probabilities than the chicken proteins. Human  $\alpha$ -2-macroglobulin was for example given a 71.68% probability rating, whereas chicken albumin and Hb $\beta$  were only assigned 0.08% probability as the most probable chicken proteins identified. A definitive and correct species identification was not achieved using this strategy.

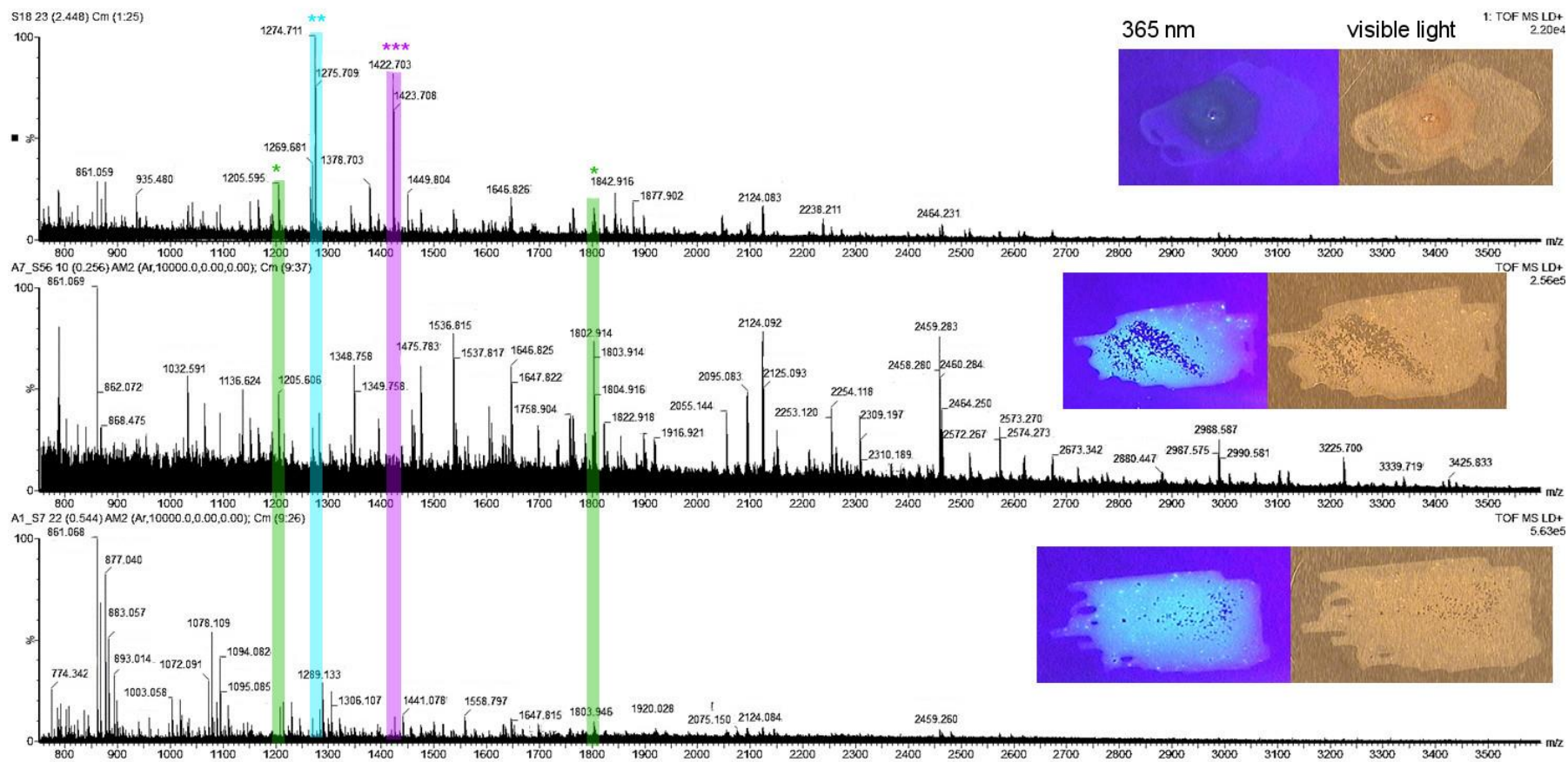


**Figure 4.6** MALDI-MS spectra of blind samples. Top panel shows porcine blood sample that was correctly identified, middle and bottom panel show porcine samples originally misclassified as non-blood samples. \* denotes possible porcine-specific signals, \*\* denotes  $m/z$  1274.725 (Hb $\beta$  human, bovine, porcine, cervine; r.LLVVYPWTQR.f), \*\*\* denotes  $m/z$  1422.708 (Hb $\alpha$  porcine; k.VGGQAGAHGAEALER.m), all referring to theoretical  $m/z$ . Inserts show the visual appearance of the stains before extraction under visible light (right) and UV light at 365 nm (left).

In order to achieve confident identifications and reduce the number of matches made to signals hidden in noise, the baseline and signal-to-noise threshold were increased. However, the problem remained that a higher number of human or other species proteins and peptides were putatively identified than of the true species origin. This is likely due to a combination of two facts: 1) the exclusion of putative identifications due to their lower S:N-ratio, and more importantly 2) the different number of proteins included in the database per species. As previously mentioned, 17 protein sequences are included for human, whereas only 8 were available for chicken and 4 for deer. For this reason, the number of putatively identified human peptides can be much larger than that of other species peptides, even in animal samples, and sequence variations are not taken into account.

Unfortunately, this means that at the moment, whilst the automated system can quickly identify blood samples based on the presence of several species' blood peptides, it cannot confidently identify which animal species they originated from. The ability to determine which putative peptide identifications were valid and which were made to noise did not appear to be increased in comparison to mMass analysis. However, mMass allows questioned regions of the spectra to be expanded and for matches to be removed if found invalid, although checking for such invalid identifications can be quite a lengthy process and PLGS is certainly the faster option. The presentation of results in or generated through mMass was preferred over that of PLGS, though, and a table listing all identifications can be found in Appedix 4, S4.4.

For further analysis, it was decided to perform preliminary screening of spectra for the presence of haemoglobin peptides using mMass. This is based on the hypothesis that a blood sample from a healthy donor will always contain Hb peptides, as it is the most abundant protein considered in the study. Conversely, samples without identifiable Hb peptides can be considered to be highly unlikely to contain blood. This is, of course, under the assumption that none of the sample collection or BETs employed prior to analysis negatively affected the protocol's ability to generate

peptide ions, and that all donors were healthy and do not express blood protein variants.

Following this approach, Hb peptides were putatively identified in 43 out of 86 samples, of which 30 presented abundant signals previously observed in human blood samples. Further analysis confirmed that proteotypic human blood peptides could be identified in all of those 30 samples, including one that contained EDTA, an anticoagulant commonly employed in containers used for blood draws. It should be noted that putative Hb identifications were also made in a small number of additional spectra, but these were discarded as being invalid due to the identified signals not representing valid peaks despite having been assigned a S:N above 3, but generally below 10, by the software. However, the 43 spectra with valid Hb identifications also included four samples that were identified as non-blood samples, although it should be noted that in all instances only one putative low abundance Hb peptide was identified and the spectra did not otherwise have the overall appearance of blood spectra.

Perhaps more worryingly, the 43 spectra for which Hb peptide assignments could not be made for, thus indicating non-blood samples, also included five animal blood samples. These consisted of the two previously misclassified porcine samples, two chicken samples, of which one had been previously misclassified, and one bovine sample. These could only be putatively identified through the presence of the aforementioned characteristic signals observed in the initial round of analysis of only a few samples, after which the analysis approach was adjusted, or not at all in the case of porcine blood. Again, it should be noted the approach of basing identifications on seemingly characteristic, but unidentified signals is not desirable, as these signals could originate from other sources or contaminants specific to the sample collection procedure. This approach should, at this stage, merely be seen as an indication of the possible blood species provenance. Despite best efforts, no Hb peptide identifications could be made for these samples and it can only be hypothesised that pre-treatment interfered with the technique or extraction, digestion

or ionisation failed for another unknown reason such as the Hb variants present in these samples not being in the UniProt database.

In total, the study putatively identified three chicken, six bovine and three porcine blood samples, including the five mentioned above, which were only identified through the presence of characteristic, but unidentified signals. Interestingly, the 3<sup>rd</sup> porcine spectrum did not only contain abundant Hb signals, but was easily identifiable as porcine blood based on the presence of an abundant signal from the proteotypic porcine Hb $\alpha$  peptide at  $m/z$  1422.703 (theoretical  $m/z$  1422.708), as seen in Figure 4.6.

Of the 43 samples for which Hb peptide identifications could not be made, six exhibited characteristic peaks observed in the semen or saliva spectra identified in the first round of analysis. This allowed putative identification of five semen samples and one saliva sample. The generation of in-house bio-fluid peptide libraries is envisioned as future work in order to support these preliminary identifications.

Consequently, the study identified 38 samples as non-biofluid samples. An overview of sample numbers, identification and pre-treatment can be found in Table 4.2. below.

<b>sample number</b>	<b>ID summary</b>	<b>1. ID level (Is it blood?)</b>	<b>2. ID level (Is it human blood?)</b>	<b>3. ID level (If not human blood, which animal species?)</b>	<b>4. ID level (If not blood, is it a biofluid and which?)</b>
<b>1</b>	bovine	yes	no	bovine	-
<b>2</b>	human	yes	yes	-	-
<b>3</b>	human	yes	yes	-	-
<b>4</b>	chicken	yes	no	chicken	-
<b>5</b>	bovine	yes	no	bovine	-
<b>6</b>	human	yes	yes	-	-
<b>7</b>	porcine	yes	no	porcine	-
<b>8</b>	human	yes	yes	-	-
<b>9</b>	human	yes	yes	-	-

sample number	ID summary	1. ID level (Is it blood?)	2. ID level (Is it human blood?)	3. ID level (If not human blood, which animal species?)	4. ID level (If not blood, is it a biofluid and which?)
10	non-biofluid	no	-	-	no
11	human	yes	yes	-	-
12	non-biofluid	no	-	-	no
13	non-biofluid	no	-	-	no
14	human	yes	yes	-	-
15	human	yes	yes	-	-
16	human	yes	yes	-	-
17	human	yes	yes	-	-
18	porcine	yes	no	porcine	-
19	human	yes	-	-	-
20	bovine	yes	no	bovine	-
21	non-biofluid	no	-	-	no
22	human	yes	yes	-	-
23	non-biofluid	no	-	-	no
24	non-biofluid	no	-	-	no
25	non-biofluid	no	-	-	no
26	non-biofluid	no	-	-	no
27	semen	no	-	-	semen
28	bovine	yes	no	bovine	-
29	non-biofluid	no	-	-	no
30	non-biofluid	no	-	-	no
31	human	yes	yes	-	-
32	semen	no	-	-	semen
33	human	yes	yes	-	-
34	human	yes	yes	-	-
35	chicken	yes	no	chicken	-
36	non-biofluid	no	-	-	no
37	human	yes	yes	-	-
38	bovine? (low 1669)	yes?	no	bovine	-
39	human	yes	yes	-	-
40	non-biofluid	no	-	-	no
41	non-biofluid	no	-	-	no
42	human	yes	yes	-	-
43	human	yes	yes	-	-
44	non-biofluid	no	-	-	no
45	non-biofluid	no	-	-	no
46	non-biofluid	no	-	-	no

sample number	ID summary	1. ID level (Is it blood?)	2. ID level (Is it human blood?)	3. ID level (If not human blood, which animal species?)	4. ID level (If not blood, is it a biofluid and which?)
47	semen	no	-	-	semen
48	human	yes	yes	-	-
49	saliva	no	-	-	saliva
50	human	yes	yes	-	-
51	non-biofluid	no	-	-	no
52	non-biofluid	no	-	-	no
53	human	yes	yes	-	-
54	bovine	yes	no	bovine	-
55	non-biofluid	no	-	-	no
56	porcine	yes	no	porcine	-
57	non-biofluid	no	-	-	no
58	semen	no	-	-	semen
59	human	yes	yes	-	-
60	non-biofluid	no	-	-	no
61	human	yes	yes	-	-
62	human	yes	yes	-	-
63	chicken	yes	no	chicken	-
64	human	yes	yes	-	-
66	non-biofluid	no	-	-	no
67	non-biofluid	no	-	-	no
68	non-biofluid	no	-	-	no
69	non-biofluid	no	-	-	no
70	human	yes	yes	-	-
71	human (odd spectrum, low abundance - enhancement inference?)	yes	yes	-	-
72	non-biofluid	no	-	-	no
73	non-biofluid	no	yes	-	no
74	non-biofluid	no	-	-	no
75	sweat? (several intense peaks, but none identified)	no	-	-	no/sweat?
76	semen	no	-	-	semen
77	human	yes	yes	-	-

sample number	ID summary	1. ID level (Is it blood?)	2. ID level (Is it human blood?)	3. ID level (If not human blood, which animal species?)	4. ID level (If not blood, is it a biofluid and which?)
78	non-biofluid	no	-	-	no
79	non-biofluid	no	-	-	no
113	non-biofluid	no	-	-	no
132	non-biofluid	no	-	-	no
141	non-biofluid	no	-	-	no
158	non-biofluid	no	-	-	no
160	non-biofluid	no	-	-	no
162	human	yes	yes	-	-
171	non-biofluid	no	-	-	no
175	non-biofluid	no	-	-	no

**Table 4.2** Table of putative identifications of in-solution samples in the blind study.

The 1000 most abundant peaks of each spectrum were also submitted to a mascot search against the SwissProt database with a tolerance of 5 ppm. Results of the top hits have been compiled in Table 4.3 alongside the identifications made in Table 4.2. As observed in chapter 2, this low tolerance was required for correct species identification in some samples, but detrimental in others. The same problem was observed in this dataset; several of the previously clearly identified human blood samples did not return human protein scores unless matched with a tolerance of 10 or 15 ppm, if at all. This was observed despite the abundant presence of the Hb $\beta$  peptide at theoretical  $m/z$  1274.725, which curiously, in some cases, was even matched to other species' Hb $\beta$  with homologous peptide sequence but to human Hb $\beta$ . In sample 19, for example,  $m/z$ s 1274.715 and 1274.731 were matched to Hb $\beta$  of *Helarctos malayanus* and several other animal species with -7.67 ppm and 4.78 ppm, respectively, for the peptide with the sequence r.LLVVYPWTQR.f – the same sequence as the human Hb $\beta$  peptide at  $m/z$  1274.725, which does not appear in the list of mascot scores for this sample. With a 5 ppm tolerance, the only score returned for this sample is for human tumor suppressor ARF. It is understandable that in some cases the mass accuracy of the data might not be sufficient to allow correct mascot identification with a tolerance of 5 or 10 ppm, however the fact that 5 ppm matches are not included in a search with a 10 ppm tolerance further complicates analysis,

as each sample would be required to be matched with varying tolerances to obtain all scores. Furthermore, selection of the score perceived to be “most appropriate” appears to be subjective and perhaps biased by previous sample identification. It should also be noted that mascot scores were all below 70, the significance threshold ( $p < 0.05$ ) reported by the software, meaning that the matches could be random events. Looking at the identifications returned by mascot it can be concluded that its use does not appear to aid the correct identification of challenging samples. On the contrary, the software misclassified samples whose IDs were unequivocally established, perhaps due to issues with mass accuracy or sample complexity. As this was the case with pure human blood samples, it is not surprising that the software provided no benefit in the analysis of complex animal blood samples that were potentially contaminated or diluted through their collection procedures.

sample number	ID summary	top mascot score
1	bovine	57 for Beta-enolase <i>Oryctolagus cuniculus</i>
2	human	33 for Hb $\beta$ <i>Hylobates lar</i> , <i>Gorilla gorilla gorilla</i> , <i>Homo sapiens</i> , <i>Pan paniscus</i> , <i>Pan troglodytes</i>
3	human	27 for Hb $\beta$ <i>Hylobates lar</i> , <i>Gorilla gorilla gorilla</i> , <i>Homo sapiens</i> , <i>Pan paniscus</i> , <i>Pan troglodytes</i>
4	chicken	24 for Isocitrate lyase (Fragment) <i>Acinetobacter calcoaceticus</i>
5	bovine	20 for Small, acid-soluble spore protein N <i>Bacillus cytotoxicus</i>
6	human	37 for Hb $\beta$ <i>Gorilla gorilla gorilla</i> , <i>Homo sapiens</i> , <i>Pan paniscus</i> , <i>Pan troglodytes</i>
7	porcine	21 for 60S acidic ribosomal protein P2 <i>Rhodotorula glutinis</i>
8	human	37 for Hb $\beta$ <i>Hylobates lar</i> , <i>Gorilla gorilla gorilla</i> , <i>Homo sapiens</i> , <i>Pan paniscus</i> , <i>Pan troglodytes</i>
9	human	24 for Hb $\beta$ <i>Gorilla gorilla gorilla</i> , <i>Homo sapiens</i> , <i>Pan paniscus</i> , <i>Pan troglodytes</i>
10	non-biofluid	18 for 50S ribosomal protein L14 <i>Hamiltonella defensa</i> subsp. <i>Acyrtosiphon pisum</i>
11	human	56 for Hb $\beta$ <i>Gorilla gorilla gorilla</i> , <i>Homo sapiens</i> , <i>Pan paniscus</i> , <i>Pan troglodytes</i>
12	non-biofluid	18 for 30S ribosomal protein S20 <i>Mycobacterium abscessus</i>
13	non-biofluid	20 for 50S ribosomal protein L13, chloroplastic <i>Gracilaria tenuistipitata</i> var. <i>liui</i>

<b>14</b>	human	15 for Cytochrome c oxidase subunit 8A, mitochondrial <i>Eulemur fulvus fulvus</i>
<b>15</b>	human	53 for Hb $\beta$ <i>Hylobates lar</i>
<b>16</b>	human	57 for Hb $\beta$ <i>Hylobates lar</i> , <i>Gorilla gorilla gorilla</i>
<b>17</b>	human	33 for Hb $\beta$ <i>Hylobates lar</i> (32 for Hb $\beta$ <i>Homo sapiens</i> )
<b>18</b>	porcine	23 for Photosystem I reaction center subunit IV (Fragment) <i>Thermosynechococcus vulcanus</i>
<b>19</b>	human	20 for Tumor suppressor ARF <i>Homo sapiens</i>
<b>20</b>	bovine	17 for 50S ribosomal protein L34 <i>Sulfurimonas denitrificans</i>
<b>21</b>	non-biofluid	20 for 50S ribosomal protein L15 <i>Methanococcus aeolicus</i>
<b>22</b>	human	36 for Hb $\beta$ <i>Gorilla gorilla gorilla</i> , <i>Homo sapiens</i> , <i>Pan paniscus</i> , <i>Pan troglodytes</i>
<b>23</b>	non-biofluid	20 for ATP synthase subunit epsilon-like protein, mitochondrial <i>Homo sapiens</i>
<b>24</b>	non-biofluid	20 for H/ACA ribonucleoprotein complex subunit 1 <i>Debaryomyces hansenii</i>
<b>25</b>	non-biofluid	17 for Brevinin-1AVb <i>Rana arvalis</i>
<b>26</b>	non-biofluid	18 for 50S ribosomal protein L14 <i>Clostridium acetobutylicum</i>
<b>27</b>	semen	19 for 30S ribosomal protein S2, chloroplastic <i>Piper cenocladum</i>
<b>28</b>	bovine	19 for 30S ribosomal protein S7 <i>Corynebacterium urealyticum</i>
<b>29</b>	non-biofluid	16 for 50S ribosomal protein L36, chloroplastic <i>Acorus calamus</i> , <i>Aethionema cordifolium</i> and 45 other species
<b>30</b>	non-biofluid	18 for 30S ribosomal protein S20 <i>Verminephrobacter eiseniae</i>
<b>31</b>	human	18 for 50S ribosomal protein L34 <i>Buchnera aphidicola</i> subsp. <i>Cinara cedri</i>
<b>32</b>	semen	21 for Hydrophobin-like protein MPG1 <i>Magnaporthe oryzae</i>
<b>33</b>	human	62 for Hb $\beta$ <i>Gorilla gorilla gorilla</i> , <i>Homo sapiens</i> , <i>Pan paniscus</i> , <i>Pan troglodytes</i>
<b>34</b>	human	17 for Ribosome maturation factor RimP <i>Prochlorococcus marinus</i>
<b>35</b>	chicken	20 for Taicatoxin, alpha-neurotoxin-like component (Fragment) <i>Oxyuranus scutellatus scutellatus</i>
<b>36</b>	non-biofluid	19 for 30S ribosomal protein S14 <i>Methylococcus capsulatus</i>
<b>37</b>	human	46 for Hb $\beta$ <i>Hylobates lar</i> , <i>Gorilla gorilla gorilla</i> , <i>Homo sapiens</i> , <i>Pan paniscus</i> , <i>Pan troglodytes</i>
<b>38</b>	bovine	15 for Sperm protamine P1 <i>Saimiri sciureus</i>
<b>39</b>	human	16 for 50S ribosomal protein L20 <i>Bradyrhizobium</i> sp.

<b>40</b>	non-biofluid	17 for 50S ribosomal protein L36 1 <i>Clavibacter michiganensis subsp. michiganensis</i> and <i>subsp. sepedonicus</i> , <i>Leifsonia xyli subsp. xyli</i>
<b>41</b>	non-biofluid	18 for Hbβ <i>Tamias merriami</i>
<b>42</b>	human	39 for <i>Homo sapiens</i> , <i>Pan paniscus</i> , <i>Pan troglodytes</i>
<b>43</b>	human	20 for Fallaxidin-3.1.1 <i>Litoria fallax</i> , Fallaxidin-3.2.1 <i>Litoria fallax</i>
<b>44</b>	non-biofluid	20 for 50S ribosomal protein L34 <i>Deinococcus deserti</i>
<b>45</b>	non-biofluid	20 for 50S ribosomal protein L36 <i>Leptothrix cholodnii</i>
<b>46</b>	non-biofluid	14 for 50S ribosomal protein L33 <i>Chlamydia muridarum</i> and 4 other <i>Chlamydia</i> strains
<b>47</b>	semen	20 for 50S ribosomal protein L31 type B <i>Rhodococcus erythropolis</i>
<b>48</b>	human	19 for 50S ribosomal protein L34 <i>Sulfurimonas denitrificans</i>
<b>49</b>	saliva	20 for 50S ribosomal protein L34e <i>Pyrococcus furiosus</i>
<b>50</b>	human	27 for Hbβ <i>Hylobates lar</i>
<b>51</b>	non-biofluid	17 30S ribosomal protein S27ae <i>Methanothermobacter thermautotrophicus</i>
<b>52</b>	non-biofluid	15 for Peptide PGLa-B2 <i>Xenopus borealis</i>
<b>53</b>	human	46 for Hbβ <i>Gorilla gorilla gorilla</i> , <i>Homo sapiens</i> , <i>Pan paniscus</i> , <i>Pan troglodytes</i>
<b>54</b>	bovine	22 for UPF0218 protein MTH_266 <i>Methanothermobacter thermautotrophicus</i>
<b>55</b>	non-biofluid	20 for Histone H4 (Fragment) <i>Medicago sativa</i>
<b>56</b>	porcine	45 for Beta-enolase <i>Sus scrofa</i>
<b>57</b>	non-biofluid	19 for 30S ribosomal protein S20 <i>Buchnera aphidicola subsp. Baizongia pistaciae</i>
<b>58</b>	semen	19 for Ribonuclease PH <i>Sphingomonas wittichii</i>
<b>59</b>	human	27 for Hbβ <i>Hylobates lar</i>
<b>60</b>	non-biofluid	16 for 30S ribosomal protein S16 <i>Prochlorococcus marinus</i>
<b>61</b>	human	17 for 60S ribosomal protein L31 <i>Drosophila melanogaster</i>
<b>62</b>	human	27 for Hbβ <i>Hylobates lar</i>
<b>63</b>	chicken	22 for Translation initiation factor IF-1 <i>Chlorobaculum tepidum</i>
<b>64</b>	human	18 for 50S ribosomal protein L24 <i>Anaeromyxobacter dehalogenans</i> , <i>Anaeromyxobacter sp.</i> and <i>Anaeromyxobacter dehalogenans</i>

<b>66</b>	non-biofluid	18 for Putative uncharacterized protein ycf15 <i>Cucumis sativus</i>
<b>67</b>	non-biofluid	16 for 50S ribosomal protein L36 <i>Amoebophilus asiaticus</i>
<b>68</b>	non-biofluid	19 for Histone H1.C2 <i>Trypanosoma cruzi</i>
<b>69</b>	non-biofluid	10 for 50S ribosomal protein L23 <i>Synechococcus sp.</i>
<b>70</b>	human	19 for 50S ribosomal protein L33 <i>Clostridium kluyveri</i>
<b>71</b>	human	19 for 50S ribosomal protein L34, chloroplastic <i>Phaeodactylum tricorutum</i>
<b>72</b>	non-biofluid	15 for 50S ribosomal protein L34 <i>Borrelia hermsii</i>
<b>73</b>	non-biofluid	20 for 50S ribosomal protein L18 <i>Leptospira borgpetersenii serovar Hardjo-bovis</i>
<b>74</b>	non-biofluid	12 for Cono-RFamide CNF-Tx1.3 <i>Conus textile</i>
<b>75</b>	sweat	23 for Ascaphin-8 <i>Ascaphus truei</i>
<b>76</b>	semen	16 for 50S ribosomal protein L36 <i>Coxiella burnetii</i>
<b>77</b>	human	23 for Hb $\beta$ <i>Hylobates lar</i>
<b>78</b>	non-biofluid	18 for Spermatid nuclear transition protein 1 <i>Mus musculus, Rattus norvegicus</i>
<b>79</b>	non-biofluid	18 for 50S ribosomal protein L23 <i>Aeromonas hydrophila subsp. hydrophila</i>
<b>113</b>	non-biofluid	17 for Trypsin inhibitor 2b <i>Sechium edule</i>
<b>132</b>	non-biofluid	16 for Ceratotoxin-B <i>Ceratitidis capitata</i>
<b>141</b>	non-biofluid	12 for F420-non-reducing hydrogenase vhu subunit U <i>Methanococcus voltae</i>
<b>158</b>	non-biofluid	16 for 30S ribosomal protein S21 <i>Lactobacillus acidophilus, Lactobacillus delbrueckii subsp. Bulgaricus, Lactobacillus helveticus, Lactobacillus johnsonii</i>
<b>160</b>	non-biofluid	16 for Virescein <i>Heliothis virescens</i>
<b>162</b>	human	54 for Hb $\beta$ <i>Hylobates lar</i> (53 for Hb $\beta$ <i>Gorilla gorilla gorilla, Homo sapiens, Pan paniscus, Pan troglodytes</i> )
<b>171</b>	non-biofluid	17 for 50S ribosomal protein L32-1 <i>Listeria innocua serovar 6a, Listeria welshimeri serovar 6b</i>
<b>175</b>	non-biofluid	19 for Ceratotoxin-B <i>Ceratitidis capitata</i>

**Table 4.3** Table of putative identifications of in-solution samples in the blind study and their respective top mascot scores achieved with a 5 ppm tolerance.

#### 4.3.4 Analysis of blind sample fingermarks with MALDI-MSI

In order to validate the previously presented method for MALDI-MSI of blood fingermarks (see chapter 3), blind sample marks were digested and analysed as described in section 3.2.1, employing the SunCollect autosprayer to deliver nine layers of trypsin at a concentration of 250 µg/mL. This, again, included marks contaminated with human or animal blood as well as other biofluids or non-biofluid substances. For time reasons, only partial images were generated, and the sample cohort was much smaller than that of the blind stains. Additionally, a number of samples did not produce images with visible ridge detail or identifiable peptides. It was hypothesised that this was due to humidity being too high during digestion, although the experimental set up was not altered. This hypothesis stemmed from the observation that samples were visibly wet when removed from the incubator, although the tissue wrapped around the lid of the Coplin jar was still dry, thus ruling out condensate dropping onto the samples. It was envisioned to reduce the humidity by not sealing the Coplin jar with parafilm or perhaps even leaving the lid ajar. However, because no additional samples were available and due to time constraints, this altered set up could not be tested to date. For this reason, only few images with ridge detail could be obtained and analysed.

Nonetheless the putative identification of several proteotypic human blood peptides was possible in one sample, alongside their mapping onto ridge detail, as seen in Figure 4.7. This allowed confident detection of human blood in this fingermark, which had been pre-enhanced with acid yellow 7. It should be noted, however, that the mass accuracy of the identifications made in imaging is much lower than in MALDI-MS profiling, but comparable ppm error values have been achieved in imaging of known samples (e.g. 18 ppm for  $m/z$  1000.498 in the known sample compared to 14 ppm in the blind sample or -45 ppm for  $m/z$  1274.725 in the known compared to -61 ppm in the blind sample). Additionally, the digest efficiency and therefore number of peptides can be expected to be reduced *in situ* compared to in solution digests. This is due to the fact that cells and proteins cannot be lysed or sterically accessed for tryptic digestion as efficiently and trypsin requires a moist environment to be effective, which in turn can disrupt ridge detail.

An additional mark was correctly identified as a non-biofluid mark. Considering the unexpected problems in detecting animal blood or identifying species origin in in solution digests, it is perhaps not surprising that this was even more problematic in the analysis of MALDI-MSI data. Due to the reduced digestion efficiency and therefore reduced number of peptide signals in images as well as lower mass accuracy, it was not possible to confidently identify animal blood in the blind fingerprints provided in the small sample set analysed in this study. It can be hypothesised that this will be possible with more concentrated animal blood samples and following the generation of a more robust library of reference samples. Nonetheless, it can be considered a great achievement that human samples were identified correctly in all instances.

#### **4.3.5 MALDI-MS analysis of a 34-year old ninhydrin-enhanced sample**

To evaluate the method's suitability for cold case samples and extend the work previously reported in this area [6], a 34-year old ninhydrin-enhanced sample was analysed. Although the overall signal intensity was understandably lower than that observed in fresh samples and the spectrum obtained (see Figure 4.8) contained abundant unidentified masses such as  $m/z$  881.258 (which does not correlate to matrix or trypsin peaks and could represent a degradation product), relevant blood peptide peaks could still readily be identified and have been listed in Table 4.4. More so, detection of  $m/z$  2058.950 confirms that the sample is of human origin, as the Hb $\beta$  peptide it was matched to is proteotypic.

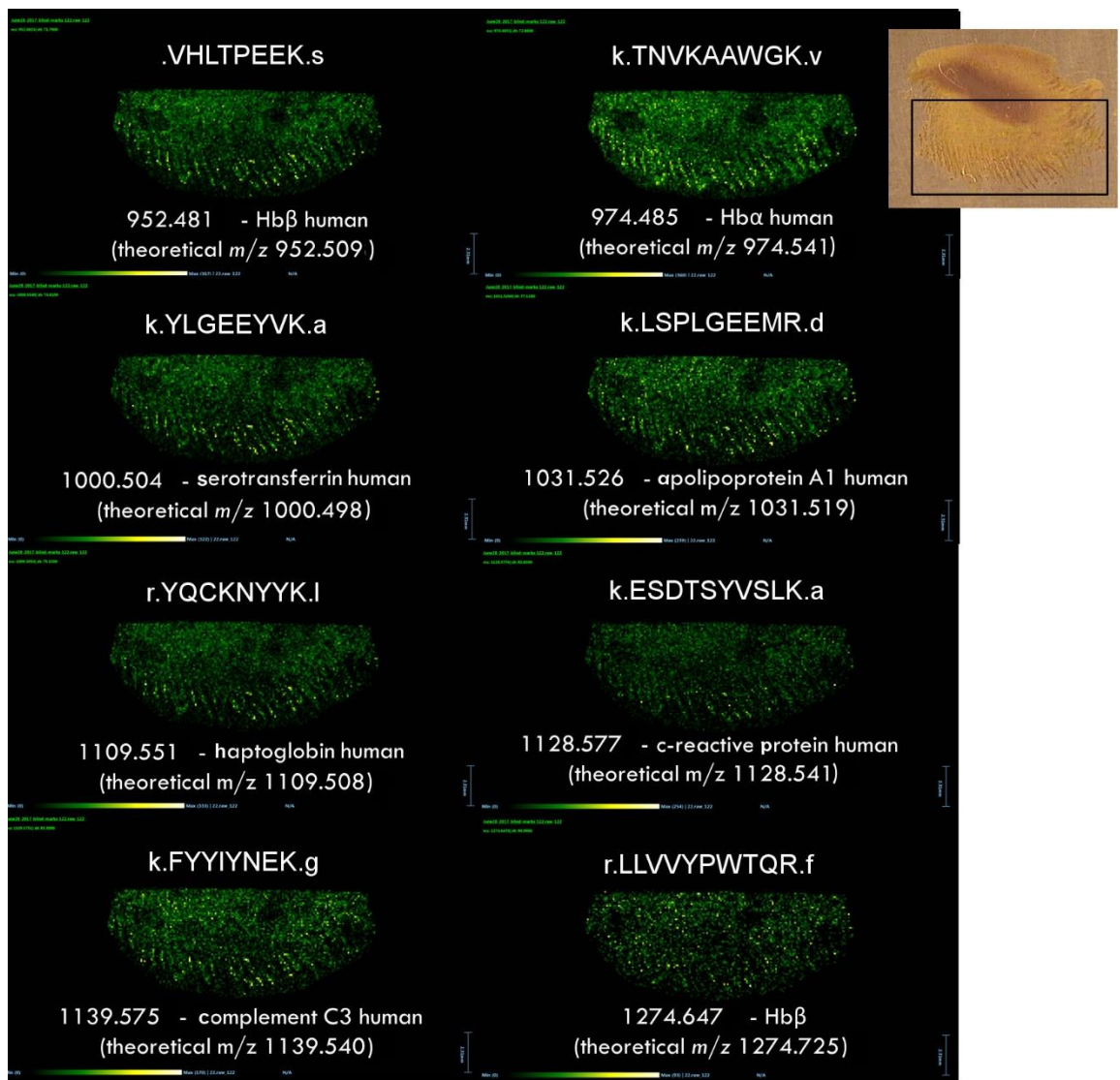


**Figure 4.7** MALDI-MSI data of a blind sample with putatively identified human blood peptides and their sequences. Black rectangle of the insert shows the area of the mark that was treated and imaged.

37YO SAMPLE RB 13 (0.341) AM2 (Ar,10000.0,0.00,0.00); ABS; Cm (9.39)

TOF MS LD+  
1.72e4

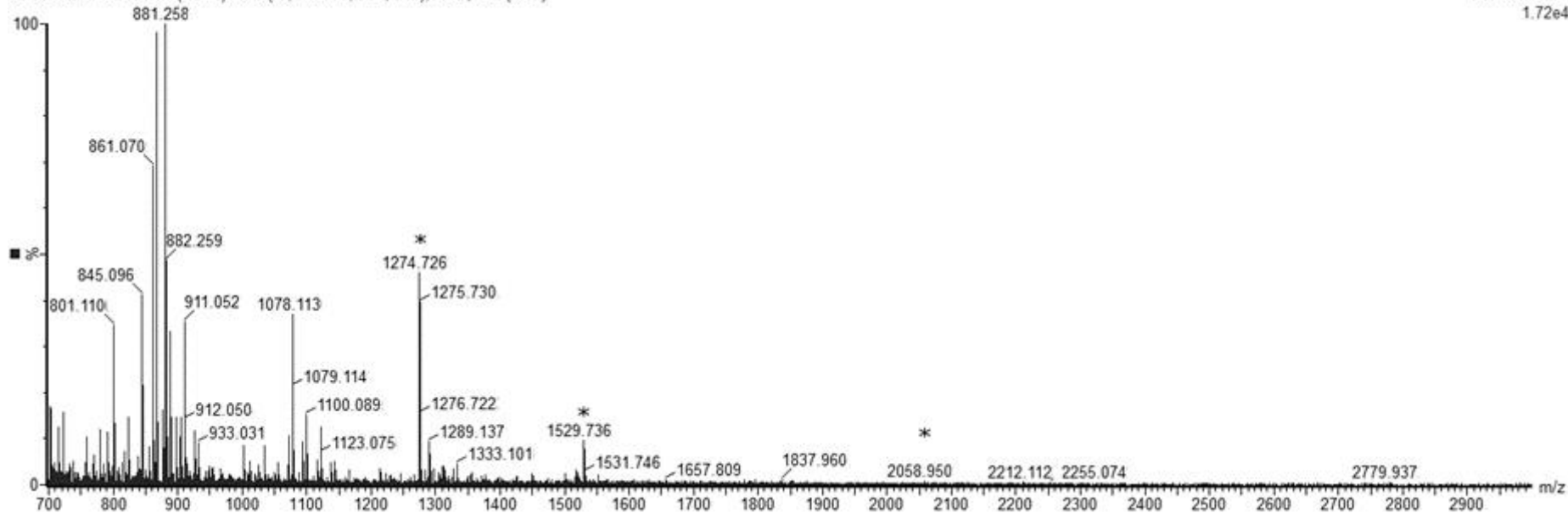


**Figure 4.8** MALDI-MS spectrum of a 34-year old ninhydrin-enhanced tryptically digested blood sample. \* denote identified haemoglobin  $\alpha$  and  $\beta$  peptides.

Possible peptide identity	Theoretical <i>m/z</i>	Observed <i>m/z</i>	Relative error (ppm)	Peptide sequence
Albumin	1296.705	1296.695	7.018	r.LAKTYETTLEK.c
EPB4.2	708.335	708.341	-9.176	k.MEREK.d or k.EKMER.e (both 1 Oxidation)
Haemoglobin $\alpha$	1529.734	1529.736	-1.307	k.VGAHAGEYGAEALE R.m
Haemoglobin $\alpha$	1071.554	1071.556	-1.773	r.MFLSFPTTK.t
Haemoglobin $\beta$	1274.726	1274.727	-1.098	r.LLVVYPWTQR.f
Haemoglobin $\beta$	952.510	952.506	3.990	.VHLTPEEK.s
Haemoglobin $\beta$	1314.665	1314.659	4.488	k.VNVDEVGGEALGR.I
Haemoglobin $\beta$	1449.796	1449.788	5.587	k.VVAGVANALAHKYH .
Haemoglobin $\beta$	1378.700	1378.687	9.429	k.EFTPPVQAAYQK.v
Haemoglobin $\beta$	2058.948	2058.950	-1.214	r.FFESFGDLSTPDAV MGNPK.v
Haptoglobin	1290.730	1290.730	0.310	k.DIAPTLTLYVGK.k
Haptoglobin	1378.694	1378.687	4.497	r.YQCKNYYKLR.t or r.YQCKNYYKLR.t
Serotransferrin	1529.753	1529.736	10.917	r.KPVEEYANCHLAR.a
Serotransferrin	1379.700	1379.693	5.436	w.WCALSHHERLK.c

**Table 4.4** Putative blood peptide identifications obtained from a digest of a 34-year old ninhydrin-enhanced sample.

#### 4.4 Conclusion

The method presented in this chapter allowed confident detection and identification of human blood in 100% of the blind samples investigated. This includes samples containing EDTA, pre-enhanced samples and those of up to 34 years in age, thus confirming wide applicability of the technique and highlighting its potential for cold cases. Additionally, human blood peptides could be identified and mapped to ridge detail of a fingerprint, thus confirming the method's suitability for the analysis of blood fingerprints. In conjunction with the lifting tapes identified as suitable for lifting

blood marks and MALDI-MSI analysis, this can provide valuable intelligence for a variety of criminal investigations.

Due to the more complex sample composition and lack of reference spectra, identification and species differentiation of non-human blood samples was not always possible. In some instances, characteristic signals were observed that allowed the tentative identification of an animal species; however it was not possible to give firm assignments to them. It is possible, however, that they originate from protein variations not listed in the database. In addition to this, basing identification on just one or two signals is far from desirable, especially when the origin of the signals is not known. Further optimisation of the processing and analysis workflow, e.g. through the use of more advanced software that can filter out noise more efficiently and label peptide peaks with more confidence, as well as the generation of a reference library is required in order to improve confidence. Other biofluids have exhibited characteristic, identifying signals and the generation of additional in-house libraries will allow their confident identification including peptide assignment. Nonetheless, being able to distinguish human blood from any other samples is undoubtedly the most important criterion in common crime scene investigations and has been achieved satisfactorily.

Aside from its speed, another benefit of the method is the fact that if the further development of the reference libraries is achieved, presumptive knowledge of the sample chemistry in order to confirm the presence of a biofluid or particular species blood will not be required. This will allow one rapid analysis to deliver multi-informative and specific intelligence to an investigation, where previously multiple separate tests would have been required and not necessarily been able to deliver confirmatory evidence.

## 4.5 References

- [1] T. Conti, E. Buel, Forensic stain identification by RT-PCR analysis (Report), 2009.
- [2] M. Bauer, D. Patzelt, A method for simultaneous RNA and DNA isolation from dried blood and semen stains, *Forensic Sci. Int.* 136 (2003) 76–78.
- [3] A.D. Roeder, C. Haas, mRNA profiling using a minimum of five mRNA markers per body fluid and a novel scoring method for body fluid identification, *Int. J. Legal Med.* 127 (2013) 707–721.
- [4] C. Haas, E. Hanson, A. Kratzer, W. Bär, J. Ballantyne, Selection of highly specific and sensitive mRNA biomarkers for the identification of blood, *Forensic Sci. Int. Genet.* 5 (2011) 449–458.
- [5] C.J. Frégeau, O. Germain, R.M. Fourney, Fingerprint enhancement revisited and the effects of blood enhancement chemicals on subsequent profiler Plus fluorescent short tandem repeat DNA analysis of fresh and aged bloody fingerprints., *J. Forensic Sci.* 45 (2000) 354–380.
- [6] E. Patel, P. Cicatiello, L. Deininger, M.R.R. Clench, G. Marino, P. Giardina, G. Langenburg, A. West, P. Marshall, V. Sears, S. Francese, A proteomic approach for the rapid, multi-informative and reliable identification of blood, *Analyst.* 141 (2016) 191–198.
- [7] L. Deininger, E. Patel, M.R. Clench, V. Sears, C. Sammon, S. Francese, Proteomics goes forensic: detection and mapping of blood signatures in fingermarks, *Proteomics.* 16 (2016) 1707–1717.
- [8] R. Bradshaw, S. Bleay, R. Wolstenholme, M.R. Clench, S. Francese, Towards the integration of matrix assisted laser desorption ionisation mass spectrometry imaging into the current fingermark examination workflow., *Forensic Sci. Int.* 232 (2013) 111–24.
- [9] H.L. Bandey, S.M. Bleay, V.J. Bowman, R.P. Downham, V.G. Sears, *Fingermark Visualisation Manual*, 1st ed., Centre for Applied Science and Technology (St. Albans), 2014.
- [10] R. Wolstenholme, R. Bradshaw, M.R. Clench, S. Francese, Study of latent fingermarks by matrix-assisted laser desorption/ionisation mass spectrometry imaging of endogenous lipids, *Rapid Commun. Mass*

Spectrom. 23 (2009) 3031–3039.

- [11] M. Strohalm, D. Kavan, P. Novák, M. Volný, V. Havlíček, MMass 3: A cross-platform software environment for precise analysis of mass spectrometric data, *Anal. Chem.* 82 (2010) 4648–4651.
- [12] R. Bradshaw, W. Rao, R. Wolstenholme, M.R. Clench, S. Bleay, S. Francese, Separation of overlapping fingerprints by Matrix Assisted Laser Desorption Ionisation Mass Spectrometry Imaging, *Forensic Sci. Int.* 222 (2012) 318–326.
- [13] E.O. Espinoza, N.C. Lindley, K.M. Gordon, J.A. Ekhoﬀ, M.A. Kirms, Electrospray Ionization Mass Spectrometric Analysis of Blood for Differentiation of Species, *Anal. Biochem.* 268 (1999) 252–261.

## Chapter 5

# **Investigation of infinite focus microscopy for the determination of the association of blood with fingermarks**

## 5.1 Introduction

Blood fingermarks are a type of evidence frequently encountered at the scene of violent crimes and confirmation of the presence of blood in association with a fingermark can greatly inform investigations and judicial debates by corroborating or disproving a suspect's/defendant's statement.

The first challenge is the false positive- and false negative-free detection and confirmation of the blood presence. Various presumptive techniques for the enhancement and detection of blood have been developed and are currently employed [1–4]. However, these methods are prone to false positives as they lack specificity. This group has previously developed a multi-informative, confirmatory approach for detecting blood and establishing its provenance in stains [5] as well as fingermarks [6,7] employing matrix-assisted laser desorption/ionisation-mass spectrometry (MALDI-MS). Additionally, MALDI-MS has allowed the detection of multiple blood signatures in stains [5] and their visualisation on fingermark ridges [6,7]. The specificity of the method is thought to greatly reduce false positives/negatives due to its detection of multiple blood-specific peptides. In comparison, presumptive techniques are based on a reaction with for example proteins, haem or haemoglobin as the only substance indicative of the presence of blood. These reactions can be facilitated by a large variety of other compounds, making the techniques prone to false positives.

The second challenge is to determine the type of association between a fingermark and blood. There are three different types of blood-fingermark association: type A - blood marks, which originate from a bloodied fingertip, where blood would in principle be only expected on the ridges; type B - marks in blood, which originate from a clean fingertip contacting a blood-containing surface, where blood would in principle be expected on ridges and in the valleys of the mark; type C - coincidental association, which originates from a clean fingertip contacting a clean surface and subsequent contamination with blood for example as a result of blood spatter (also called faux blood marks). In this case blood might also be expected on ridges and in valleys of the mark.

These three types of association are indicative of three distinct forensic scenarios and three different crime scene dynamics, the distinction of which could greatly contribute to the reconstruction of the events around the bloodshed. MALDI-MSI could have theoretically enabled the differentiation between type A association and the remaining two scenarios. A first insight into this capability was provided in previous work with regards to the order of deposition of fingermarks associated with condom lubricants [8], where it was possible to distinguish a mark left by a contaminated finger (type A) from a mark left by a clean finger on a contaminated surface (type B). However, due to the nature of association types B and C, a two-dimensional MALDI-MS image does not allow their differentiation, as the contaminant is expected to be present throughout the entire image in both cases. However, this may be a too simplistic approach to the problem.

Conventionally, the type of association is determined by experts including blood spatter analysts, who examine the evidence by eye and base their opinion on their expertise and experience with this type of evidence. However, this method of identification is highly subjective and can lead to incorrect decisions, as some marks visually present the same characteristics but may indeed stem from different types of association, therefore potentially leading to incorrect conclusions as to the dynamics of the bloodshed. Praska and Langenburg [9] reported that type C latent fingermarks subsequently exposed to blood and treated with blood enhancement techniques could appear as genuine type A blood marks, the differentiation between which ranges from difficult to impossible. They also reported that the interaction between latent mark and blood or blood dilution can differ and produce both faux blood marks and tonal reversals depending on the age of the mark, angle and duration of contact with blood as well as possible dilution factors of blood. In general, the production of faux blood marks and tonal reversals was unpredictable [9]. Furthermore, it has been reported that the appearance and clarity or tonal reversal of ridge detail is affected by conditions of deposition such as angle, blood volume, drying time and pressure, as well as environmental factors including humidity, air flow and temperature of blood, body and air [10]. Additionally, the observation has been reported that, contrary to popular belief, tonal reversal is not produced by

excessive pressure of deposition, but rather by longer drying time of blood on the finger prior to deposition and, as this has been achieved with marks left by a bloodied finger, cannot be seen as indicative of marks in blood, where the hypothesis might be that the ridges push blood away or, upon removal of the finger, lift it out of the blood. A diagram has been produced to show the proposed mechanism of the generation of tonally reversed blood marks [10]. All of these observations indicate an extremely challenging scenario for both visual inspection from experts and for MALDI-MSI capabilities and a different approach that is analytical and objective must be identified.

The use of various different microscopy techniques in forensic analysis has been extensively reviewed [11], outlining their applications in the identification of toolmarks, fracture patterns, fibres and ballistic evidence as well as biological specimens such as hair, pollen and insects, to name a few. Despite the array of techniques and set ups, most microscopes only generate two-dimensional data and have to be focused on one feature of the sample, thereby not allowing height or topology features to be measured without rotating or re-locating the sample, which often is impossible or impractical.

In recent years, with the advent of focus variation, newer techniques such as confocal microscopy and infinite focus microscopy (IFM, also referred to as focus variation microscopy or FVM) have been developed, allowing for the computational generation of a 3D image of the topology of a sample via acquisition of images on multiple focal planes. While confocal microscopy is based on transmitted light and routinely used for biological samples, the same cannot be said about IFM, which is based on reflected light. Background information about its development and principle of operation is reported in the literature [12,13]; in brief, the software generates an optical image with a large depth of field by stacking images of each focal plane and producing an in-focus image based on the coordinate points that are best focussed. This then allows the representation of the topology of a sample. Therefore, IFM allows the combination of rapid, non-contact microscopic images with 3D topology data of complex geometric samples presenting an angle of up to 85°, highly reflective

surfaces and high surface roughness. This can be achieved with a vertical and lateral resolution of down to 10 nm and 400 nm, respectively. Additionally, several analytical tools are available within the software, allowing various measurements to be performed on the sample, ranging from profiles, heights and volumes to statistical surface parameters.

As the sample stage is considerably larger than a usual microscope stage and can hold items weighing up to 20 kg [12], IFM is frequently used in quality control and analysis of wear in material engineering and production processes, e.g. measuring metal parts and corrosion [12,14]. In addition, it has been applied to characterise biological samples that are not amenable to confocal microscopy due to their opacity, such as teeth and bones, in a medical context [13,15,16], as well as the analysis of archaeological and anthropological samples [17–22] and even the comparison of toolmarks in a forensic context [23,24].

Following this promising trend, it was decided to combine the biological and forensic aspects and apply IFM to blood fingermarks. Given the topographical capabilities of IFM, it was hypothesised that the application of this technique would allow the distinction of the three scenarios A, B and C previously described above. In particular, this group hypothesised that employing IFM, it might be possible to determine if there are significant differences in ridge and valley height between the different scenarios by obtaining 3D measurements of representative samples. For example, it can be theorised that in scenario C, blood covering a latent mark would fill the valleys and cover the ridges, presenting a relatively flat surface with ridge heights becoming undetectable. As opposed to scenario C, in scenario B, a mark deposited in blood might present significantly detectable ridge heights in comparison with the valleys. Furthermore, ridge heights observed in scenario A marks are expected to be different from B and C marks as there is no blood present in the valleys. If the "ridge height determination concept" was proven, this would allow for more facile and quantifiable differentiation of blood marks and reduce the likelihood of erroneous or conflicting conclusions due to subjective analysis, especially of particularly challenging samples.

This chapter describes a range of measurements to test the overall hypothesis that IFM can distinguish between the three different types of blood-fingerprint association. In order to establish the validity of subsequent measurements on marks associated with blood, the error of measurement was determined by measuring the same feature on a stable, non-biological sample, a penny coin, five times a day for five days. Following this, a range of surfaces and lifting tapes were investigated with regards to their suitability as surfaces of deposition allowing the generation of IFM images and subsequent ridge height measurements. Of particular interest was the surface roughness which could have interfered with height measurements.

Once lifting tape had been identified as a suitable substrate, a time course experiment was performed obtaining measurements on blood fingerprints over the course of 33 days in order to observe changes in ridge heights, as the composition of fingerprints is known to start changing immediately after deposition, which might affect the ability to differentiate between scenarios. Additionally, a range of samples encompassing the three types of association was analysed in an attempt to distinguish between associations A, B and C. However, height measurements obtained differed drastically from the previous sample sets obtained on lifted type A marks and largely fell within the standard error of measurement. It was determined that this was likely due to the surface properties of the substrate, such as the wettability, which affects the spreading of blood and therefore the ridge height of a sample. Considering the variability of this type of evidence in real forensic cases with regards to the different surfaces of deposition, the range of forensically viable samples amenable to this analytical approach appears to be small. Taking into account the large effect that the various surfaces of deposition may have on the ability of IFM to quantifiably differentiate between deposition scenarios, despite a promising hypothesis, the technique was deemed to be unsuitable for the purpose intended by this study.

## **5.2 Methods**

### **5.2.1 Determination of error of measurement**

In order to establish the robustness of IFM measurements, a method was devised to determine the standard error of the instrument. In particular, a sample was selected with discernible features that the researchers were confident would not change during the duration of the measurement. To this end, a prominent feature, in this instance the profile of the Queen's nose, was measured on a one pence coin five times a day for five consecutive days and at different orientations of the coin. Unique features within the sample, such as dents or grooves, were used to reproducibly position the measurement line, in this case across the Queen's nose from one dent on the coin to another.

### **5.2.2 Sample preparation**

Initially, blood marks were deposited directly on aluminium slides (prepared as previously described [25] and used in chapters 2 and 3), glass slides and various lifting tapes and gel lifters (Table 5.1) in order to establish their suitability for the acquisition of IFM images.

Blood fingermarks were prepared as described in section 3.2.1. Depletion series were produced by loading the fingertip with blood only once before depositing 5 consecutive fingermarks in order to deplete the amount of blood present on each mark.

For subsequent experiments, a white ceramic tile was cleaned with a window cleaning detergent (Mr. Muscle) and subsequently wiped with laboratory disinfectant prior to use as a sample deposition surface. Samples deposited onto the tile were then enhanced using acid black 1 (AB1) as described in the Home Office edited fingermark visualisation manual [26].

J-Lar® clear to the core tape was used to lift AB1-enhanced primary deposition blood marks by carefully adhering the tape over the mark, using

sufficient force to ensure good contact, minimising air bubbles but making sure the mark was not modified or smeared by the pressure applied by the finger. For storage and analysis, samples were taped into Petri dishes with the adhesive side facing up and kept at ambient temperature.

<b>Tape</b>	<b>Supplier</b>
<b>CSI pre-cut lifting tape - fingerprint (#96113)</b>	CSI Equipment Ltd (Woburn Sands, UK)
<b>Permacel J-Lar® Clear to the Core lifting tape 25mm (#96105)</b>	
<b>CSI Flexi tape (3M Polytape 1-1410; #96104)</b>	
<b>CSI specialist tape - fingerprint (#96160)</b>	
<b>Cellulose Clear Tape ref. 3M 607 (3M Pressure Sensitive tape; #C32810)</b>	WAProducts (Burnham on Crouch, UK)
<b>Sirchie fingerprint lifting clear tape (#S144L)</b>	
<b>Sirchie Search Polythene Lifting Tape Transparent (#S169PPA)</b>	
<b>Serilux Style lifter (#B20653-100)</b>	
<b>3M Magic Tape</b>	local stationary shop
<b>Clear, black and white gelatine lifters</b>	BDA via WA Products Ltd (Burnham on Crouch, UK)

**Table 5.1** Lifting tapes and gels trialled including supplier.

Samples consisting of non-enhanced blood marks, marks in blood and marks with blood in coincidental association were prepared directly onto plasticised PVC cards. The chemical nature of the PVC card was confirmed through FTIR-ATR analysis. Blood marks were prepared as depletion series using either 5 µL (2 consecutive depositions) or 20 µL (4 consecutive depositions) of blood. For the preparation of marks in blood, different volumes between 5-30 µL were spread out into ovals of 2-3 cm length, which were left to dry 1-2 minutes, depending on blood volume, before the deposition of a clean fingermark in the blood. Faux blood marks were created by depositing a latent mark on the substrate, air drying for 72 hours and then dropping 15-20 µL of whole blood or diluted blood (50:50 H<sub>2</sub>O: blood) on top of it. After 3

minutes of exposure to blood, the slide was tilted to drain the bio-fluid in order to allow ridge detail to become visible, as it would otherwise be obscured by a near-opaque blood stain.

### **5.2.3 Data acquisition**

All images were obtained on an Alicona IFM (Alicona Imaging GmbH, Grambach, Austria) at a lens magnification of 5x. Brightness, contrast and image resolution were adjusted as necessary to ensure high quality images. Ridge height was analysed via profile form measurements of the acquired data using the instrument's software InfiniteFocus® (IFM Version 3.5.1.5).

For time course experiments, unique features within the sample were used to align them against the field of vision and for placement of the measurement line in order to ensure the same area of the sample was measured each time.

### **5.2.4 Statistical analysis**

Excel (version 14.0.7188.5002) and Prism (version 7.03) were used for calculation of the standard error and Dixon's Q outlier test ( $Q = \frac{|\text{suspect-nearest}|}{[\text{largest-smallest}]}$ ), plotting of trend lines and generation of graphs of time course data.

### **5.2.5 Contact angle measurements**

Contact angle measurements were performed using a Data Physics SCA202 contact angle instrument. Data Physics OCA20 software was used to measure contact angle from the captured images. The collection parameters are given in Table 5.2. Contact angle measurements were made in duplicate, at randomly selected regions on each substrate.

Contact Angle Method	Sessile Drop
Dosing Liquid	18M $\Omega$ water
Dosing volume	0.1 $\mu$ L
Dosing rate	0.5 $\mu$ L /s
Syringe Type/Volume	Hamilton 100 $\mu$ L
Computation Method	Ellipse Fitting
Software	OCA20

**Table 5.2** Contact angle collection parameters.

### 5.3 Results and discussion

A sample stable over time with discernible features, in the form of a one pence coin, was used to establish the reproducibility of IFM measurements (establishing standard deviation) and evaluate variation between measurements. Using this sample, it was anticipated that differences in measured step height could be attributed solely to measurement variation. The findings were then used to inform the analysis of biological samples with regards to whether changes observed could be attributed to measurement variation or truly represented a change in the sample.

Five IFM images of the Queen's nose on the same one pence coin were acquired per day on five consecutive days, using the same instrument settings (resolution, z range, contrast, brightness), but different orientations of the coin (see example in Figure 5.1). Characteristic features surrounding the nose were identified and used as markers to set the measurement line (step height profile), which was placed as reproducibly as possible using the distance between characteristic dents for each measurement. Five measurements were obtained in order to determine if minor differences in the placement of the measurement line had an effect on the step height profile observed.

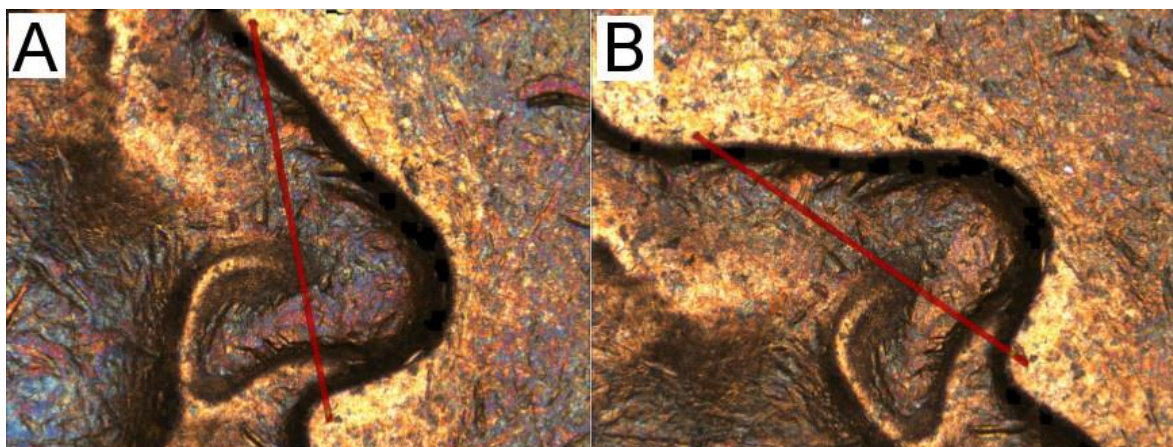


**Figure 5.1** IFM images of the same coin in different orientations (A and B) with the measurement line placed in the same position, aligned to two dents in the coin.

Some variations in the step height measurements obtained from five replicates grouped by acquisition day can be observed between multiple measurements of the same image (Figure 5.2). However, the majority of sample measurements appear to cluster well, indicating that minor differences in the placement of the measurement line do not have a drastic effect on the step height determination. This is also evidenced by 16 out of 25 sample images exhibiting a relative standard deviation (RSD) <1% across all five measurements, six with an RSD <2% and only three images showing an RSD between 2% and 2.8%, two of which can be corrected to <1% when performing the Dixon's Q outlier test and rejecting one measurement each accordingly.

The overall mean of the 123 measurements (25 acquisitions with 5 measurements each, two measurements rejected) obtained was calculated to be 103.7  $\mu\text{m}$  with a minimum of 87.4  $\mu\text{m}$ , a maximum of 111.6  $\mu\text{m}$  and a standard deviation ( $\sigma$ ) of 4.6. Based on this, the coefficient of variation was calculated to be 4.6% ( $\sigma/\text{mean} \times 100$ ), meaning that there can be  $\pm 4.6\%$  error of measurement in each measurement obtained.

As a range of sample surfaces can be expected to be present in crime scene scenarios, some consideration had to be given to the selection of such surfaces for this study as no standard protocols are available for the selection of representative

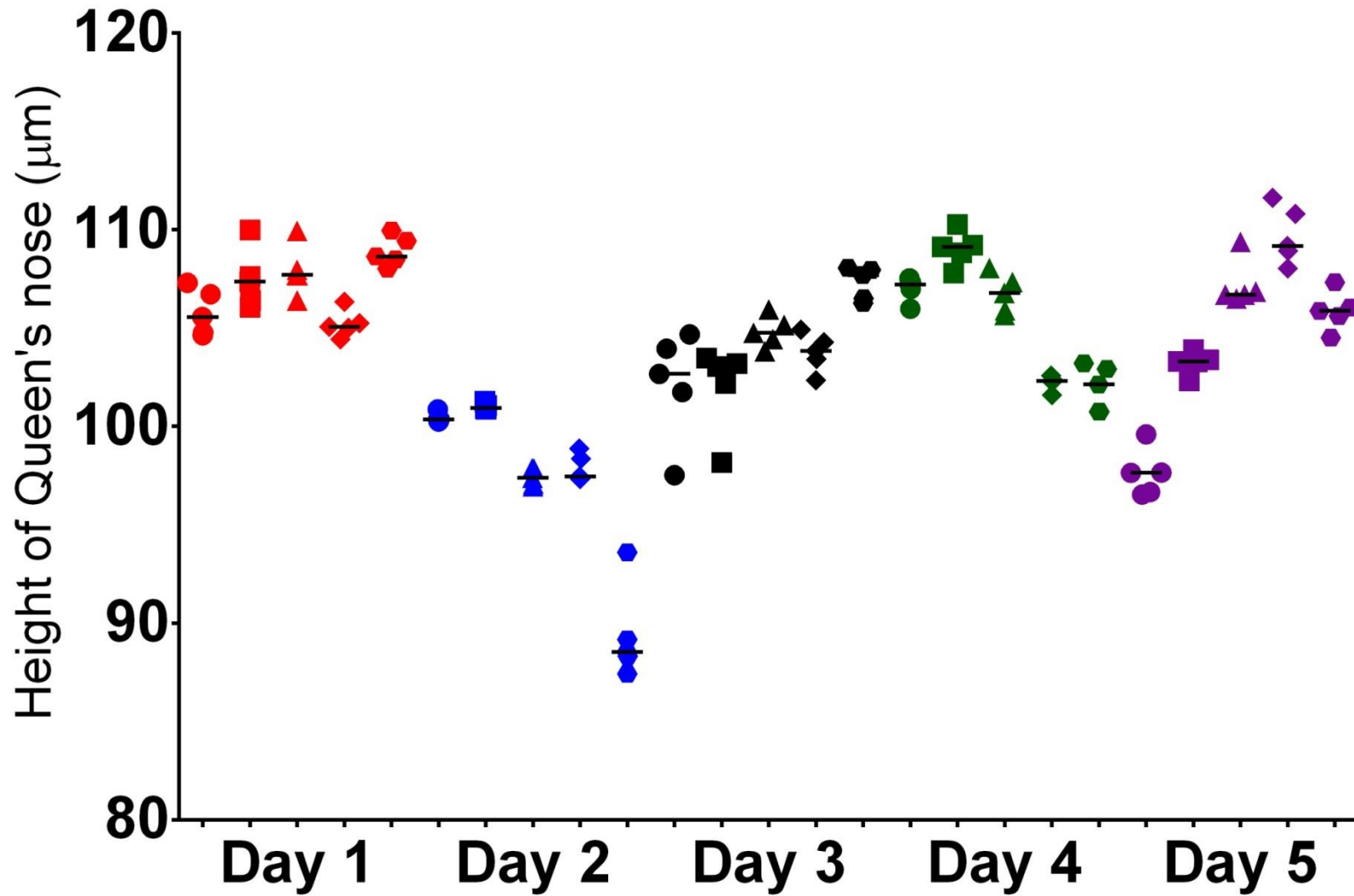


**Figure 5.2** Step height IFM measurements replicates of five image acquisitions (each shown by a different shape) per day (colour coded) of the same penny coin in different orientations and their median.

sample surfaces. In general, enhancement techniques for fingermarks and blood are applied as suitable for porous, semi-porous or non-porous surfaces. It can be hypothesised that these surface properties also affect fingermark ridge heights, e.g. by absorbing some of the deposit or the deposit heights due to an uneven surface. Similarly, it can be expected that some substrates, such as smooth, non-porous surfaces, will be more suitable for this study than others; Uneven or porous surfaces can be expected to affect and distort ridge heights to a degree where the background surface roughness interferes with the target measurements. In contrast, it can be hypothesised that wet blood or fingermark residue would spread further on smooth surfaces before it dries than it would on uneven or porous surfaces, resulting in smaller observable ridge heights. In addition to these considerations, forensically relevant surfaces had to be chosen with regards to the possibility to remove them from the crime scene for analysis, or to the possibility to lift the fingermark, taking into account the IFM's stage size and operating mechanism as well as techniques likely to be carried out at the crime scene prior to IFM analysis of a sample.

For these reasons, the suitability of a selection of different analysis surfaces was established in preliminary studies. Aluminium slides are an historically suitable surface of deposition for this research group investigating fingermarks by MALDI-MS based methods [27] and it was chosen as a reference representation of non-porous but not completely smooth surfaces. Glass slides were also selected as representing smooth and non-porous surfaces. Additionally, various lifting tapes and gel lifters were selected to account for the fact that the majority of samples would require to be lifted to allow transportation from the crime scene. The selected surfaces were investigated with regards to their surface roughness, interactions with blood and the ability to yield good quality IFM images without considerable loss of data.

IFM image acquisition is based on the reflectance of light; consequently glass slides and gel lifters were found to be unsuitable because, although fingermark ridges were visible, no data could be acquired from the

surrounding surface. This resulted in black regions in the images acquired that represent loss of data. This made evaluation of the surface roughness impossible, as the clean surface could not be measured.

While aluminium slides yielded suitable images, it was found that when larger volumes of blood, such as droplets or pools, were used to create marks in blood or coincidentally associated marks, the residue would not adhere to the surface once dried and would start to flake off. Consequently, they had to be disregarded as a suitable substrate. Example images of each surface can be seen in Figure 5.3.

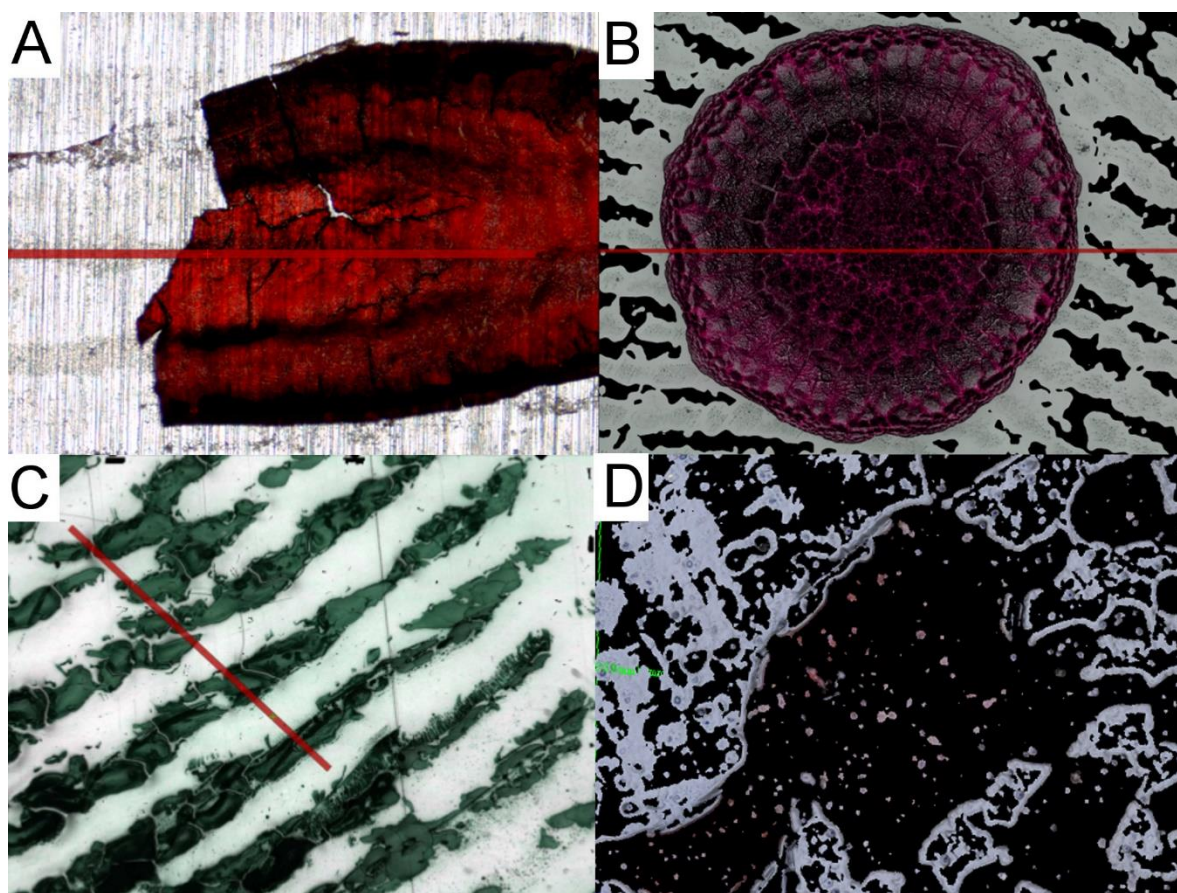


**Figure 5.3** Example images obtained from A: a blood drop on a latent mark on aluminium; B: a blood drop on a latent mark on glass; C: an AB1-enhanced bloodied mark lifted with J-Lar® tape; D: a blood drop on a latent mark on a clear gelatine lifter.

However, lifting tape was identified as a viable analysis surface for IFM measurements and several tapes were trialled for the lifting of bloodied fingermarks. Due to different compositions of the tape backing as well as the adhesives used,

details of which were not disclosed in the product information for most tapes, not all lifting tapes provided equal results in lifting blood marks. In fact, a larger number of fingerprint lifting tapes did not visibly lift any blood mark residue and due to the faint nature of some blood marks and more so their lifts, contrast was poor. For this reason and because crime scene marks would most likely be enhanced prior to collection, acid black 1 (AB1)-enhancement was performed on the blood marks to increase contrast and allow easier visual inspection of whether lifting was successful. Various tapes were trialled and Sirchie 144L and J-Lar® Clear to the Core tapes in combination with AB1-enhancement of the blood mark produced the highest quality lifts with regards to the largest portions or the entirety of the mark being lifted. Other tapes either did not lift at all or only lifted small partial and incomplete areas of the mark and were therefore found unsuitable. Comparing the success rate and mark portion lifted between Sirchie 144L and J-Lar® Clear to the Core, the J-Lar® product was shown to be the most promising tape amongst those tested and hence used in a time course study to evaluate potential changes in ridge heights of the blood marks over time. The investigation of lifted marks could also be beneficial in those cases where photography of enhanced blood marks is not sufficient and lifting is required in order to facilitate removal of the mark for laboratory analysis. Therefore, standards treated using this approach would have a larger applicability to real life scenarios.

Ten primary deposition type A blood fingerprints (hereafter M1-M10) were enhanced with AB1 and lifted with J-Lar® tape. Additionally, two depletion series of five marks each (M11-M20) were enhanced and lifted in the same manner. IFM measurements were acquired from the same area of a mark on the day of deposition (day 0), 5 days later and then at 7-day intervals up to 33 days in order to determine if potential changes in ridge height over time might affect discrimination between different deposition scenarios. It was noted that some marks did not produce images of sufficient quality on some days (and therefore those images had to be excluded from the dataset) and not all deposited impressions could be lifted successfully. Characteristic features in each mark, such as ending ridges or islands, were then used as reference points to place a measurement line in the image, which was used to determine the ridge height of the sample post acquisition. Using the

protocol described in the Methods section, five measurements were obtained per image.

At each time point, an image of the same region of the mark was collected (aligned to the field of view using characteristic features in each mark) and the same reference points used for placement of the measurement line. Figure 5.4-Figure 5.6 show time course plots for each fingerprint including the five repeat measurements for each acquisition. As was observed previously in the coin sample, multiple measurements on the same image exhibit low amounts of scattering, and for the majority of samples measurements appear consistent. It was however observed that the measurements fluctuated between days without a clear trend amongst all samples, therefore the Dixon's Q test ( $Q = \frac{|\text{suspect-nearest}|}{[\text{largest-smallest}]}$ ) for outliers was performed on the mean ridge height ( $n=5$ ) of the most suspect samples (M1, 2, 3, 5 and 7), assuming normal distribution of the data. From this analysis, day 33 of mark 3 represented an outlier that was rejected ( $Q = 0.711$  for a sample size of the 6 time points obtained, with  $Q \geq 0.621$  critical for  $P=0.05$ ).

In an attempt to detect potential trends in the data, lines of best fit were calculated and plotted for the time course data. Comparing Figure 5.4, Figure 5.5 and Figure 5.6, however, it was evident that different trends for different marks could be observed. Marks 1, 7, 8, 9, 10 and 12 appear to exhibit a decrease in ridge height, possibly suggesting evaporation of water, marks 3, 4 and 5 demonstrate a trend towards increased ridge height, potentially indicating collection of dust/debris, and marks 2, 6 and 13 show little change in ridge height. The decrease in ridge height for marks 7, 8 and 12 fits better to an exponential function as they decrease (Figure 5.7), which would support the hypothesis of exponential loss of water over time due to evaporation. It should be noted, however, that all marks had been stored together in the same way and such a scatter of results was therefore unexpected.

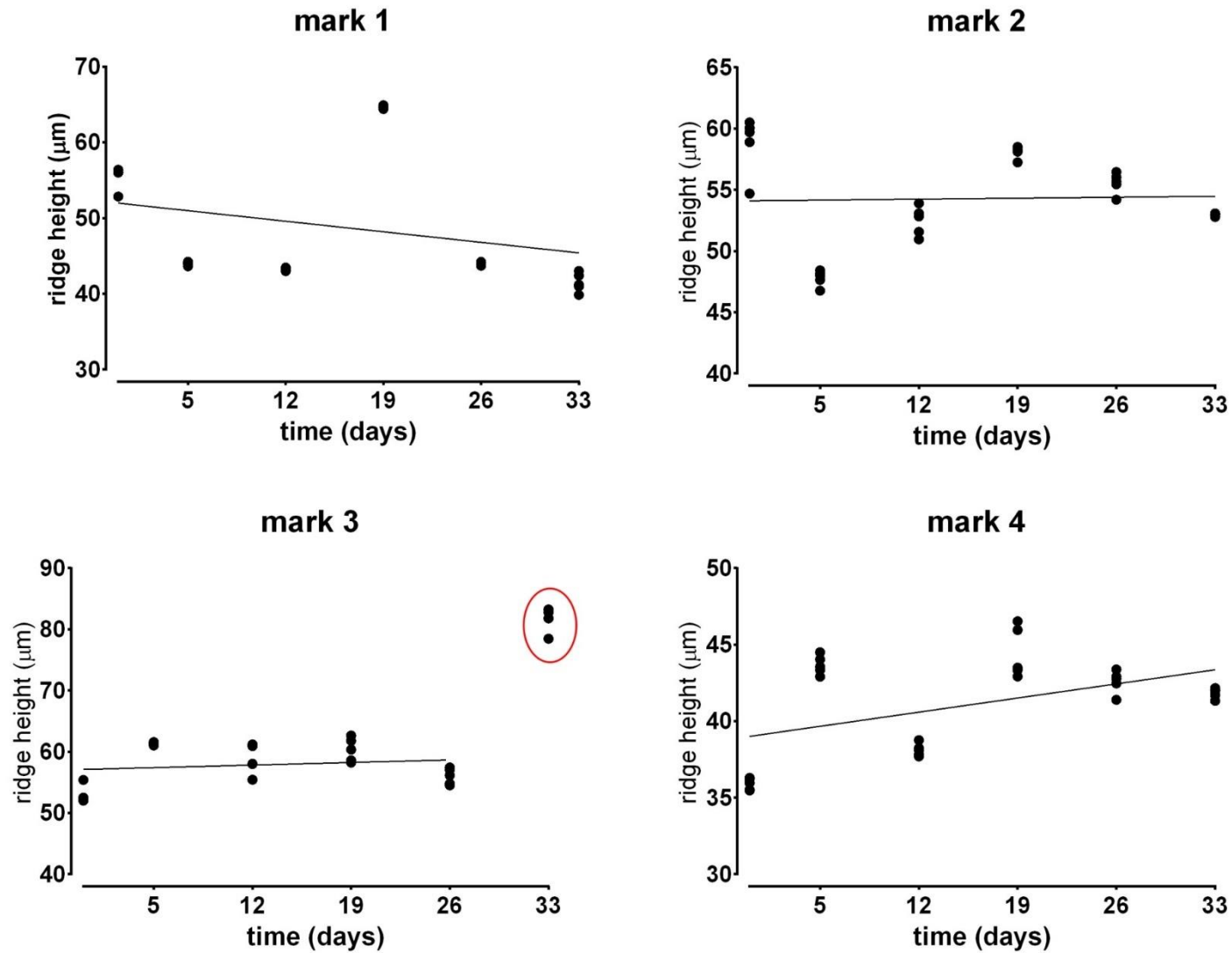


**Figure 5.4** IFM time course with linear regression of AB1-enhanced bloodied fingermarks 1-4 lifted with J-Lar® tape. (Note: Mark 3, day 33, highlighted in red, is likely an outlier as calculated by Dixon's Q and has therefore been rejected.)

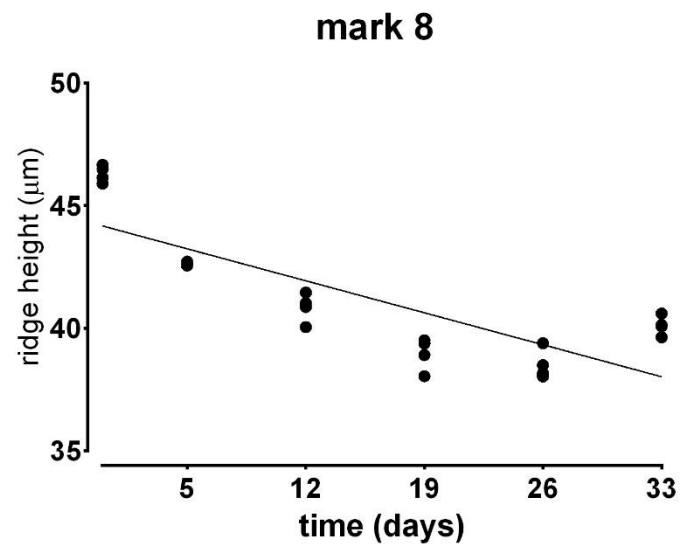
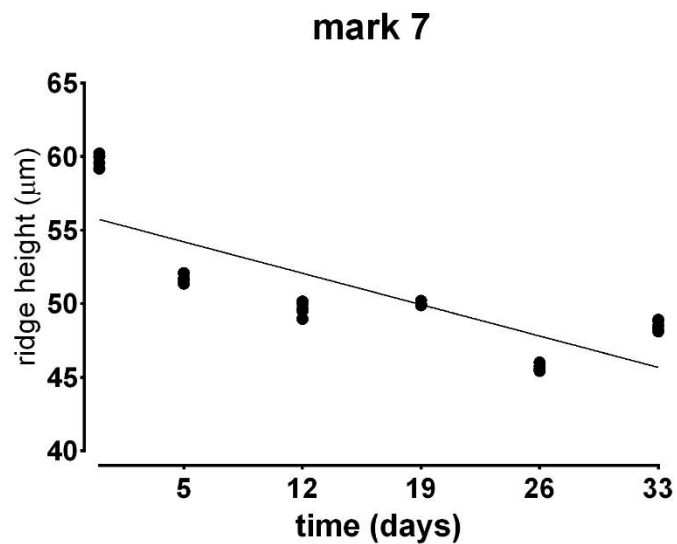
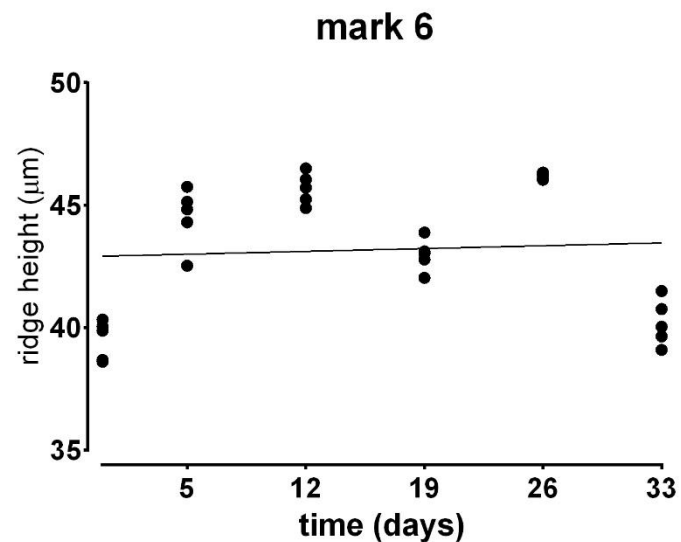
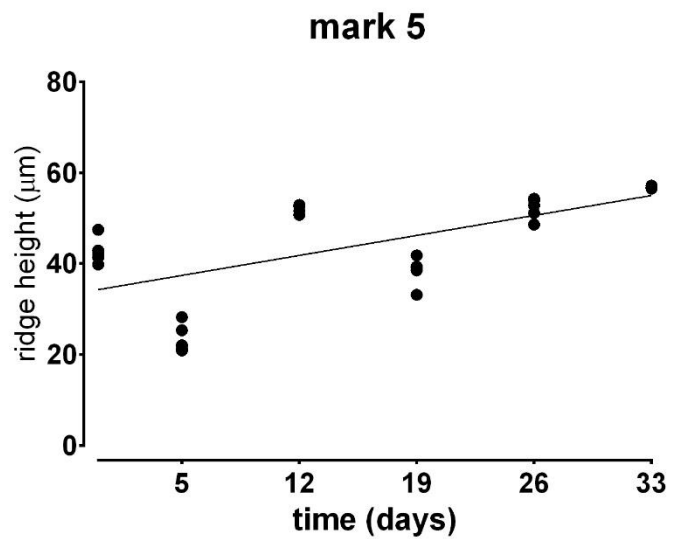


**Figure 5.5** IFM time course with linear regression of AB1-enhanced bloodied fingermarks 5-8 lifted with J-Lar® tape.

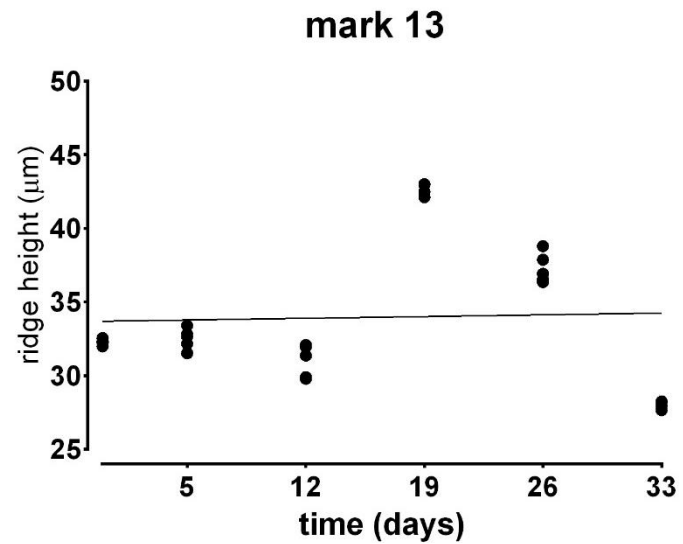
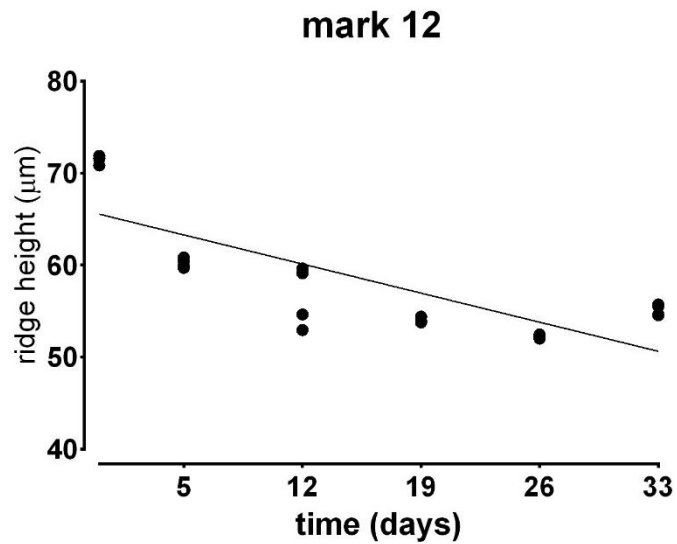
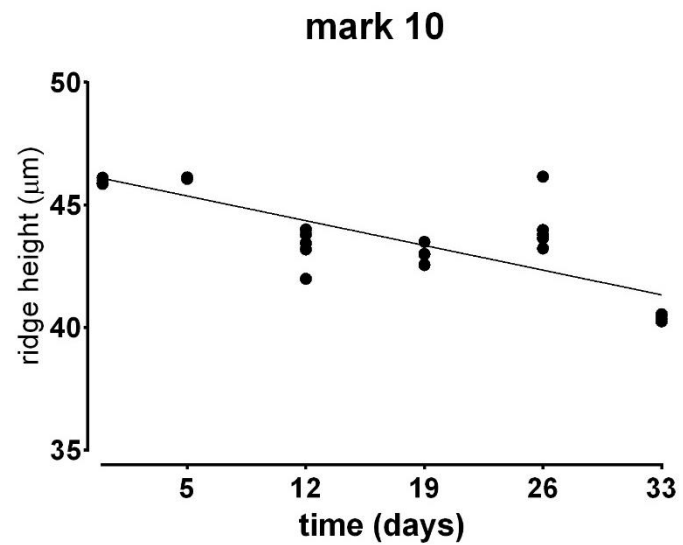
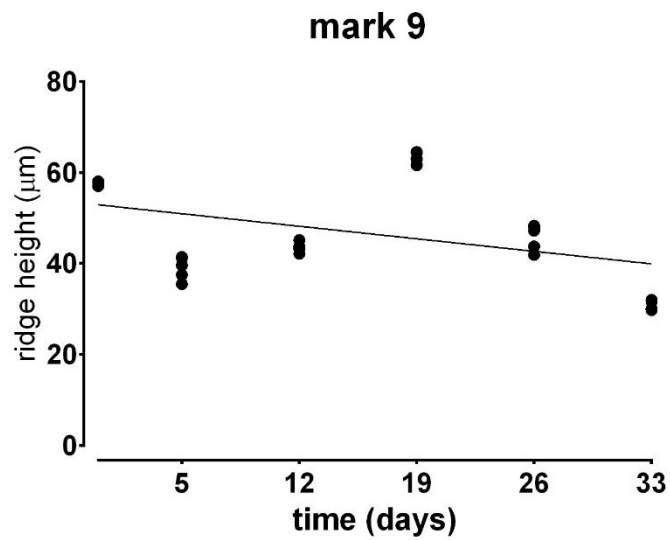


**Figure 5.6** IFM time course with linear regression of AB1-enhanced bloodied fingermarks 9,10, 12 and 13 lifted with J-Lar® tape.

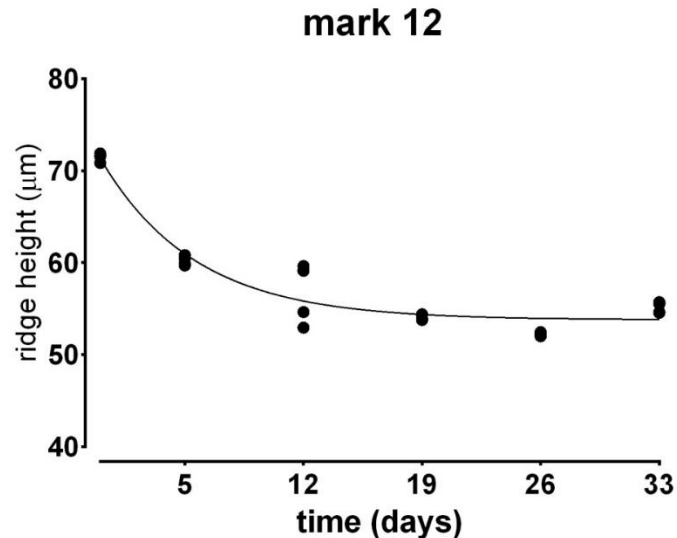
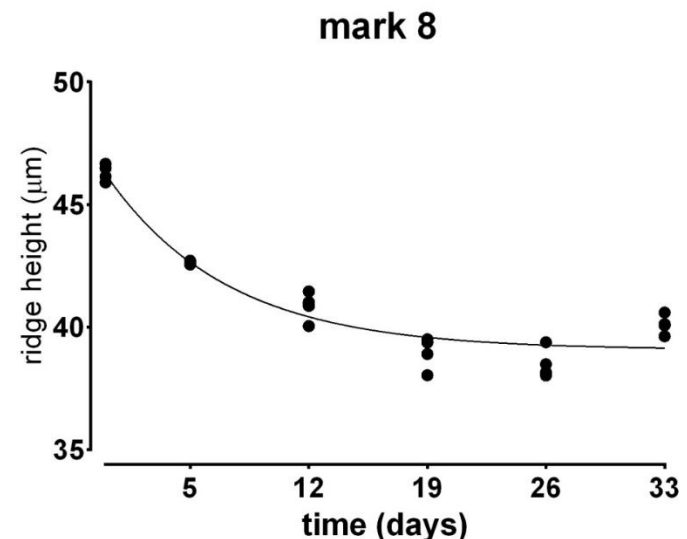
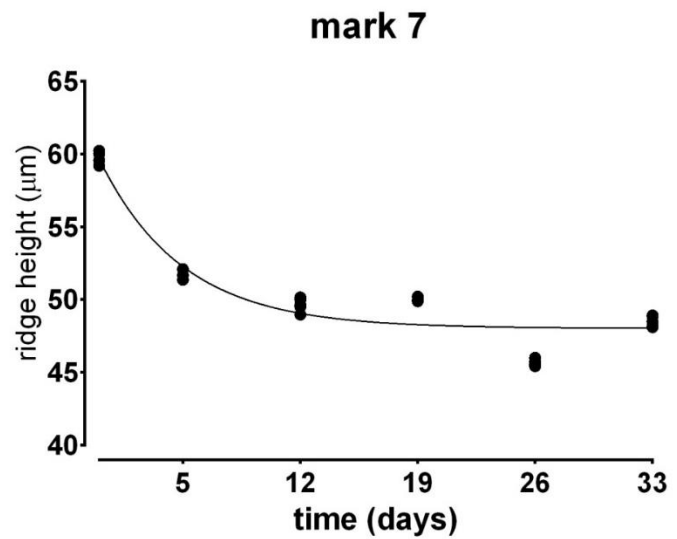


**Figure 5.7** IFM time course of AB1-enhanced bloodied fingermarks 7, 8 and 12 lifted with J-Lar® tape, fitted with exponential regression for marks where this appeared to fit best.

Comparison of these data with the previously established standard error of measurement (4.6%) shows that the minimum and maximum ridge height values for each mark across all time points show a much greater variation than 4.6%. This is therefore likely to show change in the sample over time rather than an error in measurement, although a consistent trend with regards to increasing or decreasing ridge height was not observed.

Since it was unclear if the scatter of results was due to the samples or the measurement strategy, experiments were conducted using samples from different types of blood-fingerprint association, as it was hypothesised that measurements of bloodied ridges outside the fluctuating 25  $\mu\text{m}$  and 84  $\mu\text{m}$  range might be observed for other scenarios, therefore still permitting their differentiation within the 4.6% RSD measurement error.

Samples of all three deposition scenarios were deposited on PVC plastic cards and step heights measured using the strategies outlined previously. On this substrate across the different deposition types, volumes and drying times, periodically, but unusually, samples exhibited ridge heights of a maximum of 12.4  $\mu\text{m}$ , with the majority ranging around 2-3  $\mu\text{m}$  (see Figure 5.8-Figure 5.13 as example) and a few being as low as 400 nm (remaining data not shown).

Although the absolute ridge height values are not of primary importance, the fact they did not separate into clear groups according to the different deposition scenarios is. Not only did the measurements mostly fall within the range of the instrument's error of measurement of 4.6% ( $\sigma$ ), but they also failed to exhibit any obvious differences between deposition scenarios, making their differentiation impossible in this case. It should be noted that for dark samples it was difficult to obtain measurements due to the lack of contrast and reflectivity, and even where acquisition was possible, ridges were not measurable within the blood. The results were further investigated as to why the ridge heights, even of the same deposition scenario, were so much lower on PVC (Figure 5.8-Figure 5.13) than those analysed in previous experiments (Figure 5.12) and ridge height measurements often did not match up with the observed position of the ridge, i.e. the valley was measured to be higher than the ridge (Figure 5.13). Figure 5.8-Figure 5.13 show a dark red line on the optical image obtained, which is the

measurement line. The graph below the optical image corresponds to this measurement line, i.e. shows the profile height from one end of the dark red line to the other. The red and green marks on the image correspond to the marks of the same colour on the graph and show the profile height at those specific points in the image and graph, respectively. In Figure 5.13 it therefore becomes evident that the red mark in the valley of the fingerprint was measured to be  $6.4199\ \mu\text{m}$  higher than the green point on the fingerprint ridge, the opposite of what could be expected.

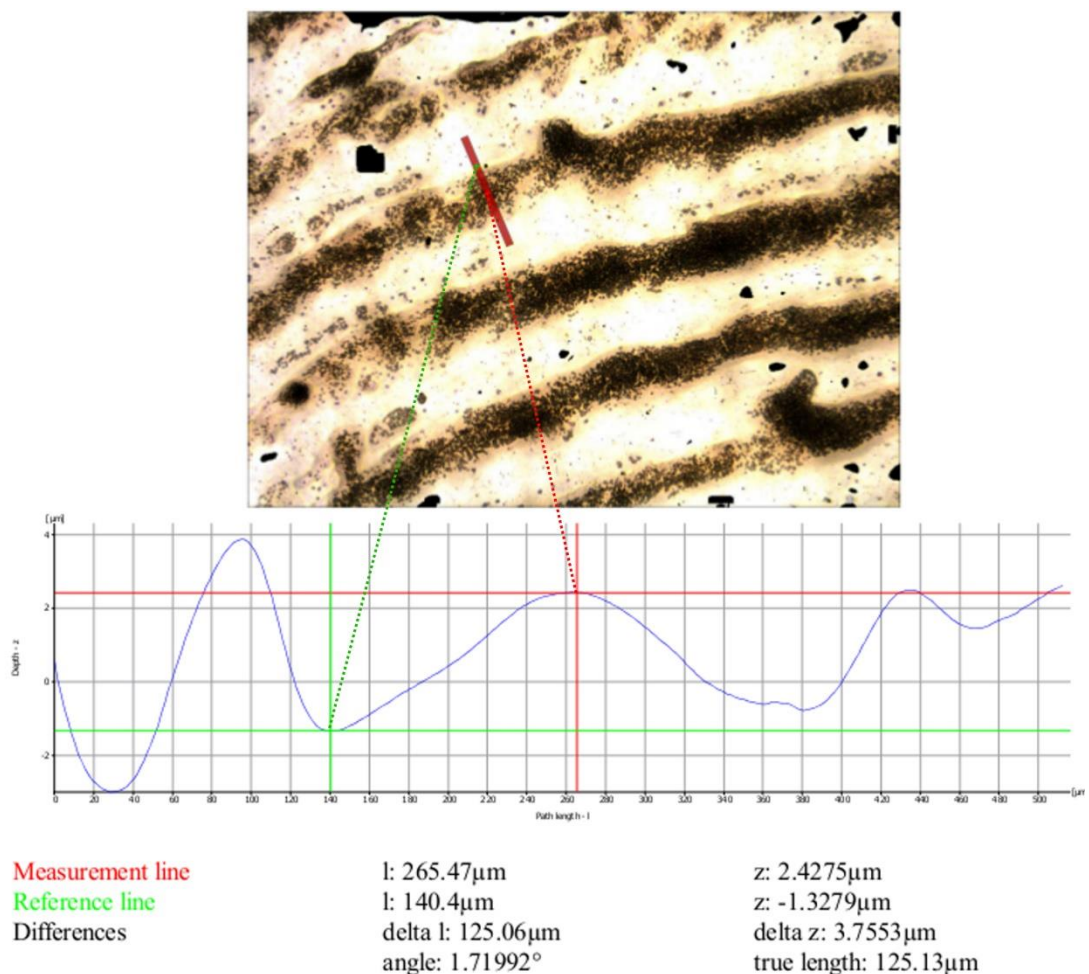


**Figure 5.8** IFM image and profile measurement graph obtained on a bloodied mark (3rd depletion in 20  $\mu\text{L}$  depletion series). Note the dark red line on the image shows the measurement line to which the graph corresponds, whereas the dotted lines connect specific measurement points (+ signs on the image) with the corresponding measurements on the graph. Delta z describes the height difference between the two measurement points.

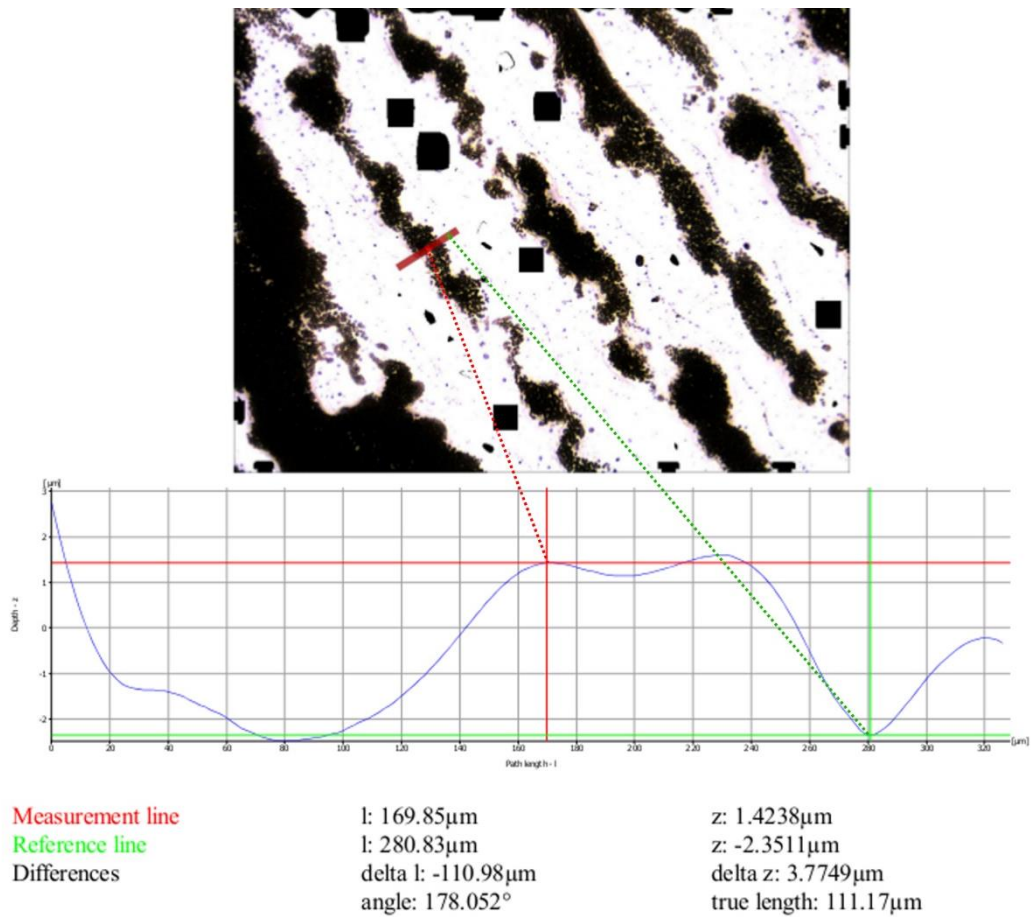


**Figure 5.9** IFM image and profile measurement graph obtained on a mark in 10 µL blood. Note the dark red line on the image shows the measurement line to which the graph corresponds, whereas the dotted lines connect specific measurement points (+ signs on the image) with the corresponding measurements on the graph. Delta z describes the height difference between the two measurement points.

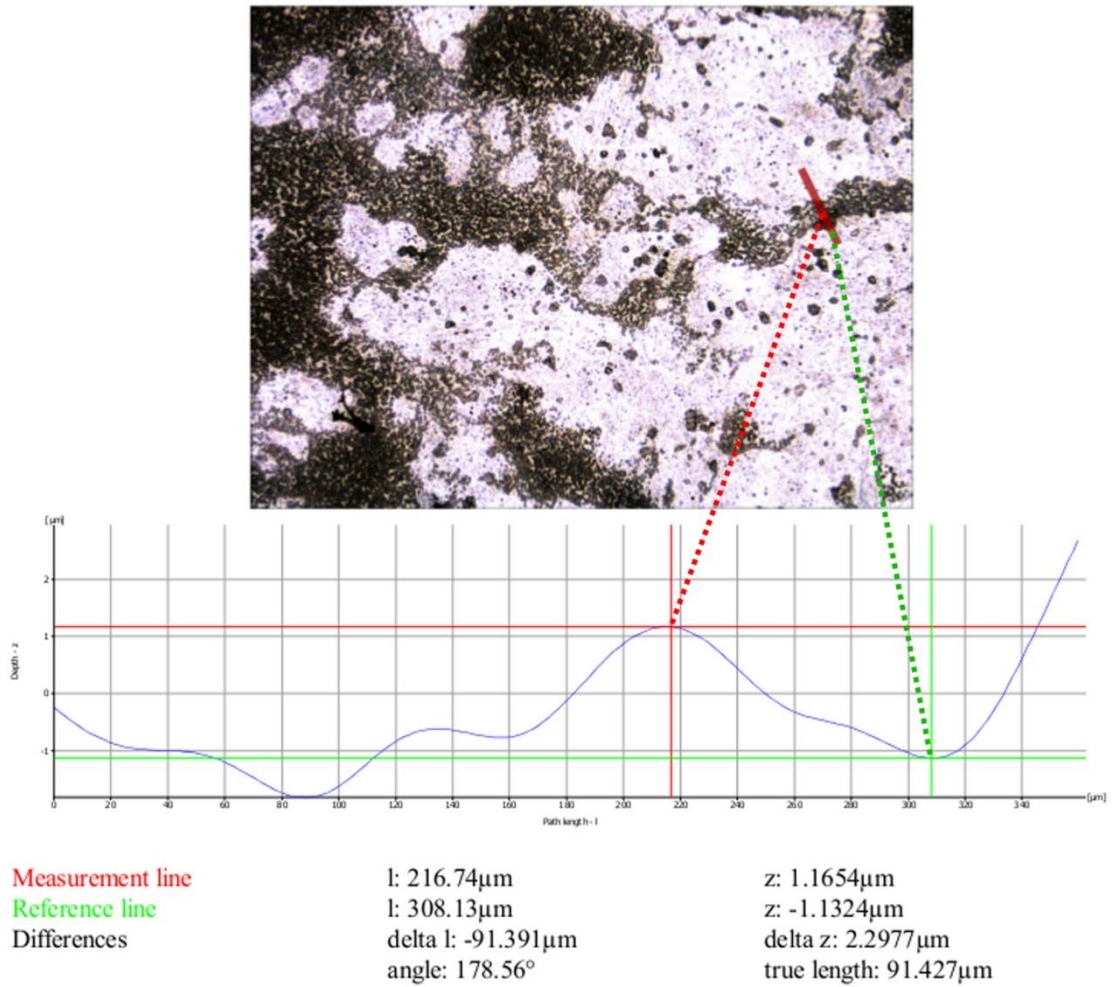


**Figure 5.10** IFM image and profile measurement graph obtained on a faux blood mark (15-20  $\mu\text{L}$  blood). Note the dark red line on the image shows the measurement line to which the graph corresponds, whereas the dotted lines connect specific measurement points (+ signs on the image) with the corresponding measurements on the graph. Delta z describes the height difference between the two measurement points.

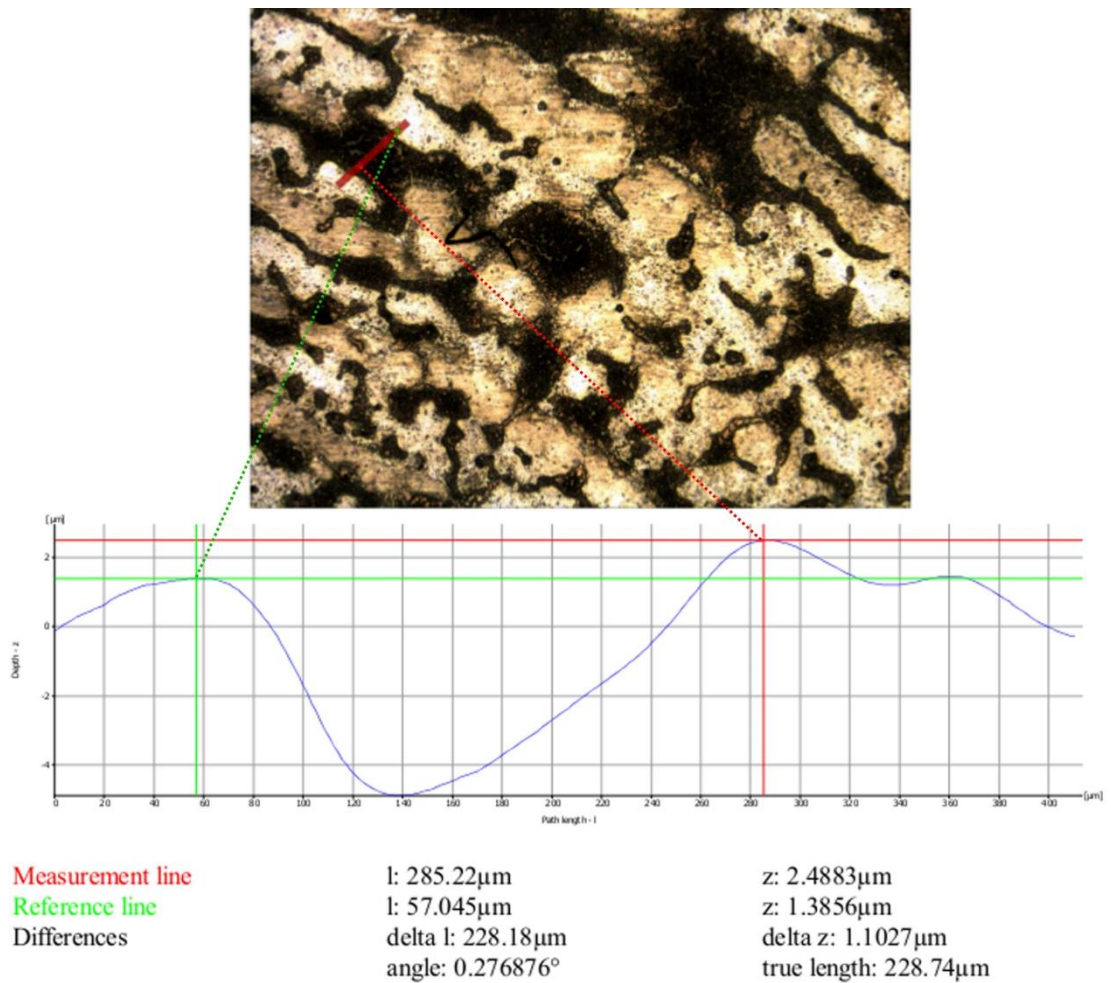


**Figure 5.11** IFM image and profile measurement graph obtained on a faux blood mark (50:50 dilution). Note the dark red line on the image shows the measurement line to which the graph corresponds, whereas the dotted lines connect specific measurement points (+ signs on the image) with the corresponding measurements on the graph. Delta z describes the height difference between the two measurement points.

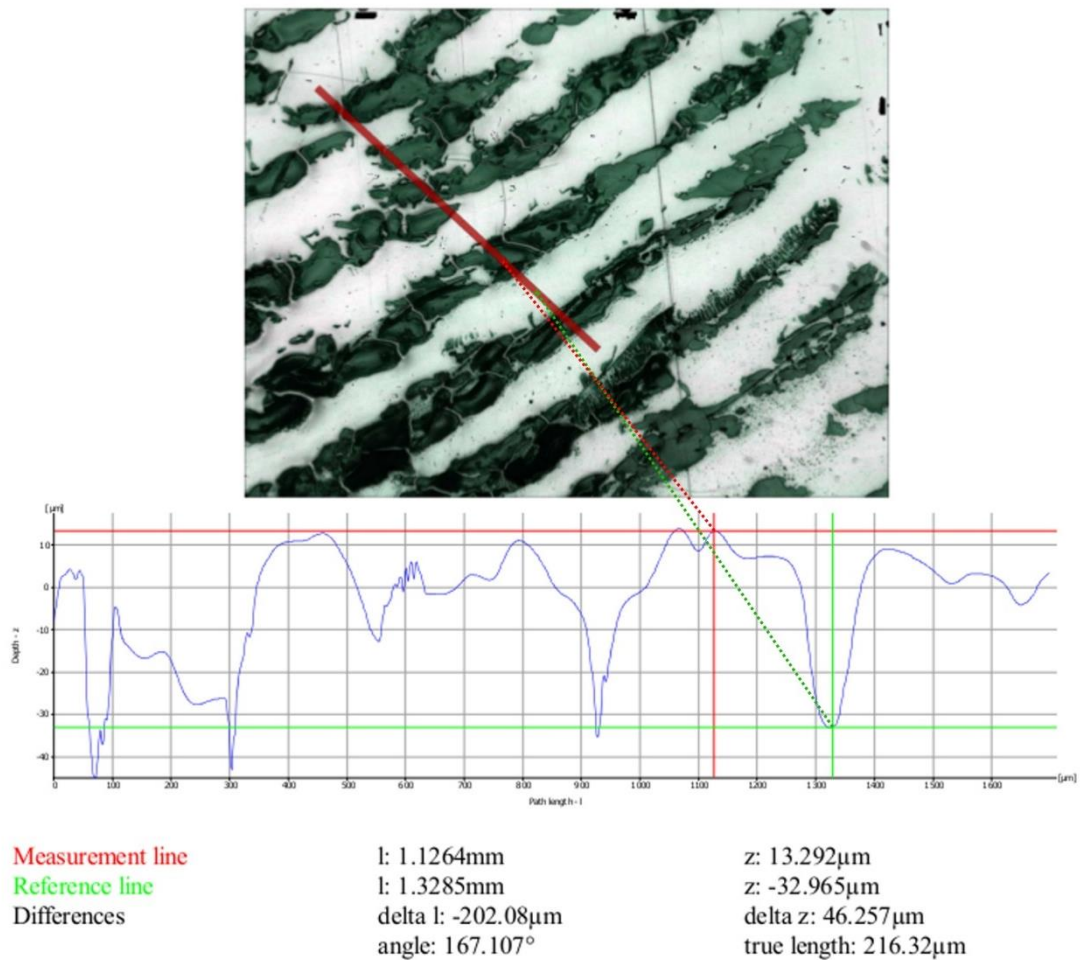


**Figure 5.12** IFM image and profile measurement graph obtained on an AB1-enhanced bloodied mark lifted with J-Lar® tape. Note the dark red line on the image shows the measurement line to which the graph corresponds, whereas the dotted lines connect specific measurement points (+ signs on the image) with the corresponding measurements on the graph. Delta z describes the height difference between the two measurement points.

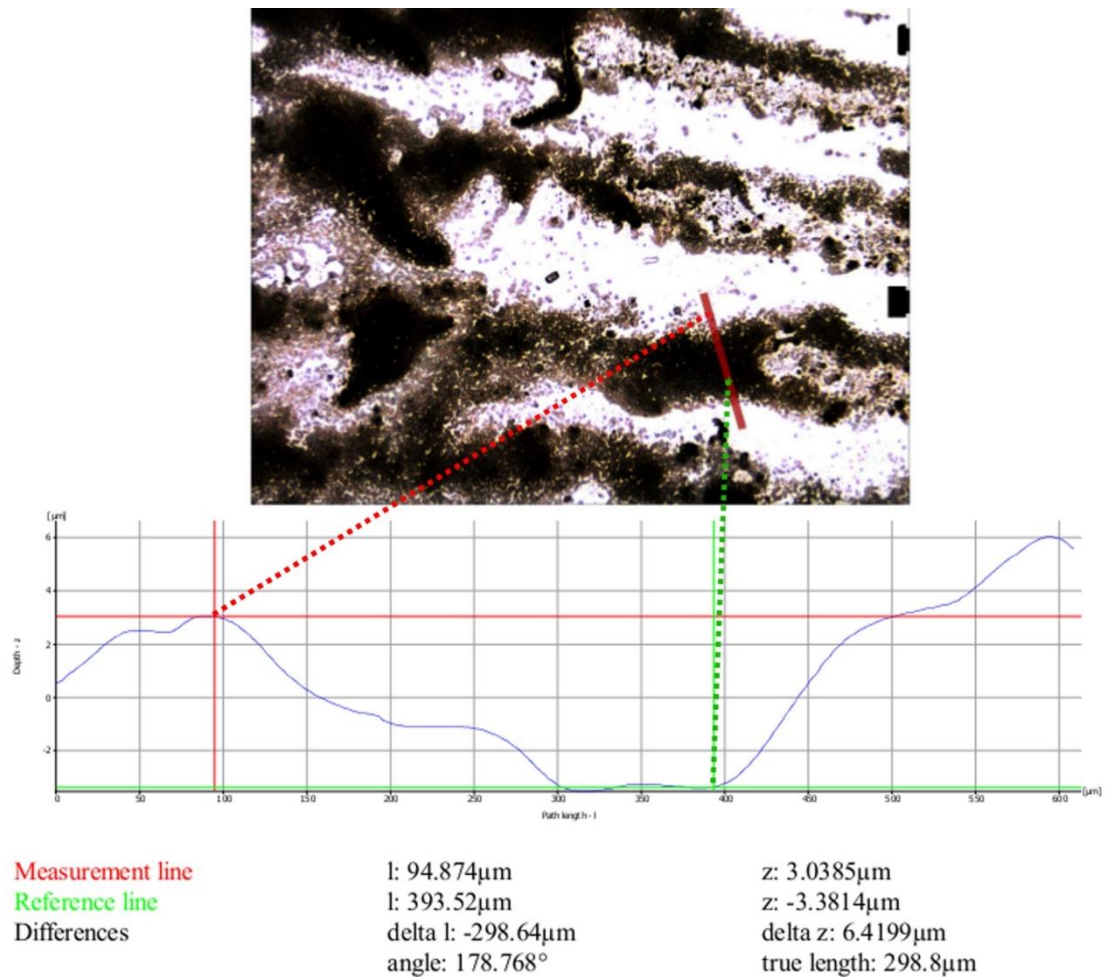


**Figure 5.13** IFM image and profile measurement graph obtained a mark in blood, showing an example for the measurement mismatch observed in some images: It can be seen the green measurement point on the ridge is lower than the red point in the valley. Note the dark red line on the image shows the measurement line to which the graph corresponds, whereas the dotted lines connect specific measurement points (+ signs on the image) with the corresponding measurements on the graph. Delta z describes the height difference between the two measurement points.

Clearly, understanding the different substrate chemistries and surface topographies should facilitate the elucidation of the nature of these differences. In order to investigate why ridge heights differed so drastically between the different substrates, contact angle measurements were undertaken. Although blood marks were initially deposited and left to dry on a ceramic tile before lifting, the determination of the contact angle indicated a much larger contact angle (128-128.2 $^\circ$ ) for the lifting tape than the PVC plastic (64-64.4 $^\circ$ ), meaning that any liquids or deposits exhibit reduced spreading across the surface in the case of the lifting tape, due to the nature of the adhesive coating. Any substance, in this

case blood marks, deposited on PVC on the other hand could spread out much more before drying, thereby reducing the final ridge height. This finding implies that measurements of any deposition scenario will be highly dependent on the original substrate, which cannot be controlled in a forensic case scenario, therefore greatly limiting the forensic applicability and feasibility of the method despite the ability to analyse lifted samples. For this reason, it would appear that the scope and applicability of IFM for the determination of the order of deposition of blood marks is somewhat limited. It may be feasible to outline idealised scenarios where the methodology is applicable, but it does not have the desired wide appeal for inclusion into a standardised set of protocols within a routine crime scene work-flow.

## **5.4 Conclusions**

This study aimed to determine the feasibility of using IFM for the differentiation of different types of blood association with fingermarks based on ridge height measurement. This knowledge would inform investigations and provide more objective conclusions than those currently relying on the expert observation by naked eye. The scenarios in question include marks left by a bloodied finger, marks left in blood and clean, latent marks subsequently contaminated with blood (coincidental association), e.g. blood spatter or during attempted clean-up of a crime scene, which can be virtually impossible to differentiate from one another due to the large visual similarity.

The IFM instrument's relative standard error of measurement was established to be 4.6% based on measurements of a stable sample coin. The changes in ridge height of a time course experiment conducted on lifted, pre-enhanced marks left by a bloodied finger were observed to have an RSD larger than 4.6%, but findings regarding trends (or lack thereof) observed in ridge heights over time were inconclusive. Some marks showed increased ridge heights while others exhibited a decrease or reasonably stable ridge heights over time, despite all marks being stored under the same conditions.

The range of ridge height values determined on marks with blood pertaining to each of the three different deposition scenarios were found to be highly dependent on the deposition surface, pre-enhancement or lack thereof and chemistry of the lifting tape, as for example, ridge heights on PVC were much smaller than on the previously investigated lifting tape and did not allow differentiation between the scenarios. As a range of different surfaces can be expected to be encountered at crime scenes and it is impossible to provide appropriate control measurements for each such surface, it was determined that the forensic applicability of the method would be very limited. Despite a promising hypothesis and the potential of success for some selected surfaces, IFM was therefore deemed unsuitable for the reliable, quantifiable differentiation of the three types of blood-fingerprint association as per initial research hypothesis based on the capabilities of the technique.

## 5.5 References

- [1] L.C.A.M. Bossers, C. Roux, M. Bell, A.M. McDonagh, Methods for the enhancement of fingerprints in blood, *Forensic Sci. Int.* 210 (2011) 1–11.
- [2] S.S. Tobe, N. Watson, N.N. Daéid, Evaluation of six presumptive tests for blood, their specificity, sensitivity, and effect on high molecular-weight DNA, *J. Forensic Sci.* 52 (2007) 102–109.
- [3] M. Cox, A study of the sensitivity and specificity of four presumptive tests for blood., *J. Forensic Sci.* 36 (1991) 1503–1511.
- [4] B. Marchant, C. Tague, Developing Fingerprints in Blood : A Comparison of Several Chemical Techniques, *J. Forensic Identif.* 57 (2007) 76–93.
- [5] E. Patel, P. Cicatiello, L. Deininger, M.R.R. Clench, G. Marino, P. Giardina, G. Langenburg, A. West, P. Marshall, V. Sears, S. Francese, A proteomic approach for the rapid, multi-informative and reliable identification of blood, *Analyst.* 141 (2016) 191–198.
- [6] R. Bradshaw, S. Bleay, M.R. Clench, S. Francese, Direct detection of blood in fingerprints by MALDI MS profiling and Imaging, *Sci. Justice.* 54 (2014) 110–117.
- [7] L. Deininger, E. Patel, M.R. Clench, V. Sears, C. Sammon, S. Francese, Proteomics goes forensic: detection and mapping of blood signatures in

- fingermarks, *Proteomics*. 16 (2016) 1707–1717.
- [8] R. Bradshaw, R. Wolstenholme, L.S. Ferguson, C. Sammon, K. Mader, E. Claude, R.D. Blackledge, M.R. Clench, S. Francese, Spectroscopic imaging based approach for condom identification in condom contaminated fingermarks., *Analyst*. 138 (2013) 2546–57.
- [9] N. Praska, G. Langenburg, Reactions of latent prints exposed to blood., *Forensic Sci. Int.* 224 (2013) 51–8.
- [10] G. Langenburg, Deposition of bloody friction ridge impressions, *J. Forensic Identif.* 58 (2008) 355–389. [http://mail.latent-prints.com/images/Langenburg\\_Bloody\\_Fingerprints\\_2008.pdf](http://mail.latent-prints.com/images/Langenburg_Bloody_Fingerprints_2008.pdf) (accessed November 13, 2014).
- [11] B.P. Wheeler, L.J. Wilson, *Practical Forensic Microscopy: A Laboratory Manual*, 1st ed., John Wiley & Sons Ltd, Chichester, 2008.
- [12] W. Kaplonek, K. Nadolny, G.M. Królczyk, The use of focus-variation microscopy for the assessment of active surfaces of a new generation of coated abrasive tools, *Meas. Sci. Rev.* 16 (2016) 42–53.
- [13] R. Abdalla, R.J. Mitchell, Y. fang Ren, Non-carious cervical lesions imaged by focus variation microscopy, *J. Dent.* 63 (2017) 14–20.
- [14] Y. Chen, L.K. Ju, Method for fast quantification of pitting using 3D surface parameters generated with infinite focus microscope, *Corrosion*. 71 (2015) 1184–1196.
- [15] J.P.M. Lima, M.A.S. Melo, V.F. Passos, C.L.N. Braga, L.K.A. Rodrigues, S.L. Santiago, Dentin erosion by whitening mouthwash associated to toothbrushing abrasion: A focus variation 3D scanning microscopy study, *Microsc. Res. Tech.* 76 (2013) 904–908.
- [16] T. Winkler, E. Hoenig, R. Gildenhaar, G. Berger, D. Fritsch, R. Janssen, M.M. Morlock, A.F. Schilling, Volumetric analysis of osteoclastic bioresorption of calcium phosphate ceramics with different solubilities, *Acta Biomater.* 6 (2010) 4127–4135.
- [17] D.A. Macdonald, The application of focus variation microscopy for lithic use-wear quantification, *J. Archaeol. Sci.* 48 (2014) 26–33.
- [18] S.M. Bello, I. De Groote, G. Delbarre, Application of 3-dimensional microscopy and micro-CT scanning to the analysis of Magdalenian portable art on bone and antler, *J. Archaeol. Sci.* 40 (2013) 2464–2476.

- [19] S.W. Hillson, S.A. Parfitt, S.M. Bello, M.B. Roberts, C.B. Stringer, Two hominin incisor teeth from the middle Pleistocene site of Boxgrove, Sussex, England, *J. Hum. Evol.* 59 (2010) 493–503.
- [20] S.M. Bello, S.A. Parfitt, C. Stringer, Quantitative micromorphological analyses of cut marks produced by ancient and modern handaxes, *J. Archaeol. Sci.* 36 (2009) 1869–1880.
- [21] S.M. Bello, *New Results from the Examination of Cut-Marks Using Three-Dimensional Imaging*, Elsevier Masson SAS, 2011.
- [22] S.M. Bello, C. Soligo, A new method for the quantitative analysis of cutmark micromorphology, *J. Archaeol. Sci.* 35 (2008) 1542–1552.
- [23] C. Macziewski, R. Spotts, S. Chumbley, Validation of Toolmark Comparisons Made At Different Vertical and Horizontal Angles, *J. Forensic Sci.* 62 (2017) 612–618.
- [24] T.N. Grieve, L.S. Chumbley, J. Kreiser, M. Morris, L. Ekstrand, S. Zhang, Objective Comparison of Toolmarks from the Cutting Surfaces of Slip-Joint Pliers, *AFTE J.* 46 (2014) 176–185.
- [25] R. Wolstenholme, R. Bradshaw, M.R. Clench, S. Francese, Study of latent fingermarks by matrix-assisted laser desorption/ionisation mass spectrometry imaging of endogenous lipids, *Rapid Commun. Mass Spectrom.* 23 (2009) 3031–3039.
- [26] H.L. Bandey, S.M. Bleay, V.J. Bowman, R.P. Downham, V.G. Sears, *Fingermark Visualisation Manual*, 1st ed., Centre for Applied Science and Technology (St. Albans), 2014.
- [27] S. Francese, R. Bradshaw, N. Denison, An update on MALDI mass spectrometry based technology for the analysis of fingermarks – stepping into operational deployment, *Analyst.* 142 (2017) 2518–2546.

## Chapter 6

### **Conclusions and future work**

Currently used tests and enhancement techniques for the detection of blood are not confirmatory because they target generic compounds of blood, such as proteins or amino acids. Even the supposedly haem-reactive tests are actually based on a redox-reaction that can be facilitated by a multitude of other compounds. For this reason, a range of false positives is encountered frequently. However, the confident detection of blood can be of great importance in a criminal investigation, as well as establishing species provenance.

To solve this problem, the author selected 17 blood-specific proteins as suitable targets for the confident detection of blood. The work presented in this thesis centred on the development and optimisation of a bottom-up proteomic approach in conjunction with MALDI-MS analysis. Based on the knowledge of the theoretical protein sequences and their species-specific differences, it was hypothesised that this would allow the confident detection of blood and its provenance determination.

Following the determination of the total protein content of blood, the digestion protocol was optimised with regards to the use of a suitable trypsin concentration. It was found that in order to be able to use the commonly employed 20 µg/mL trypsin solution, blood samples needed to be either diluted 1:200 for known volumes, or diluted by extracting the blood stain from the surface of deposition. In preliminary tests, the protocol and resulting peptide yield were optimised by trialling the addition of various detergents and the use of different digestion times. Comparing signal intensities and the number of peptide identifications, the digestion time for in-solution digests was optimised to 1 hour with the help of the detergent Rapigest™ SF.

This protocol was then applied to human and equine blood samples and binary mixtures thereof to demonstrate the principle. MALDI-MS analysis allowed the detection of blood-specific peptides in all of those samples as well as provenance determination through the presence of proteotypic peptides. This was possible even in the mixed sample, thus confidently establishing the presence of both species' blood in the sample.

To validate these results obtained on samples of known provenance, a range of blind samples was analysed. These included blood samples of human and four different animal species origin, biofluid samples and non-biofluid samples. Additionally, some samples were pre-enhanced with unknown BETs, thus theoretically indicating the presence of blood to crime scene personnel.

In this blind study, human blood was confidently detected and identified as such in all instances, including pre-enhanced samples, samples of up to 34 years in age and one containing the anticoagulant EDTA. This was possible through the identification of proteotypic human blood peptides. Unfortunately, not all animal blood samples were recognised as such due to the absence of abundant peptide signals commonly expected, such as haemoglobin peptides. Overall, animal blood spectra did not present abundant signals, making it easy to mistake them for non-biofluid spectra. It is thought that this is due to differences in the sample collection, as animal samples are likely to have been obtained through transfer from roadkill or from meat packages. This means they may be more dilute and perhaps have been exposed to various contaminants. Additionally, it is possible that some of the BETs used to enhance the samples resulted in interference with proteolysis or ionisation.

Nonetheless, characteristic signals were observed in chicken and bovine blood samples that allowed those species to be putatively identified in other samples. It should be noted, however, that to date these signals could not be identified and species determination based on them should therefore not be considered definitive or confident. The signals considered to be characteristic for bovine blood had also been observed in bovine samples in a previous study; however no additional reference spectra were available. It is possible that these characteristic signals originate from sequence variations in the commonly observed proteins, but were not identifiable as such due to lack of available sequence information on these variations. Considering 2-5 haemoglobin variants are reportedly found in each species, the absence of commonly observed Hb peptides would not be surprising if another Hb variant was present, perhaps resulting in the more abundant signals detected.

In addition to the animal blood samples, several other biofluid samples were correctly identified as such based on the presence of characteristic signals. The generation of a robust in-house database of biofluid peptides is envisioned for the future to increase confidence in those identifications and facilitate peptide matching. Additional samples were confidently classed as non-biofluid samples based on the absence of blood peptides and other characteristic signals.

The study thus allowed the correct classification of human biofluid and blood samples. Whilst the analysis approach currently employed struggles with the detection and provenance determination of animal blood, human blood was confidently detected and identified in all instances. The analysis of additional reference samples for the generation of a more robust peptide library is envisioned for animal samples.

Nonetheless, the ability to confidently differentiate human blood from all other samples with a robust analytical workflow is a big step forward for forensic sciences and criminal investigations. The confident identification of human blood in a sample even 34 years after deposition and enhancement further undermines the technique's forensic applicability and shows great potential for the analysis of cold case samples.

In addition to the aforementioned shortcomings of currently used BETs, most techniques require swabbing or scraping of the sample, thus destroying spatial information contained for example in blood fingermarks. This intelligence can be of great importance in criminal investigations, linking a fingerprint to an event of bloodshed and therefore a suspect to a crime.

In order to apply the proteomic methodology mentioned above to suspected blood fingermarks, a protocol for *in situ* digestion was optimised for blood. This included trialling trypsin concentrations between 100 µg/mL and 3 mg/mL to account for the higher protein concentration in localised, undiluted samples and the lower efficiency of *in situ* digestion. Several instruments and instrumental settings were investigated for the application of the protease to blood marks. The high trypsin concentrations employed in this study led to capillary blockages in the SunCollect

autosprayer, which was routinely employed for controlled deposition of lower trypsin concentrations and matrix onto imaging samples. This problem was thought to be due to increased viscosity of the solution and was overcome by fitting the autosprayer with a larger internal diameter capillary.

The optimised protocol employs nine layers of 250 µg/mL trypsin including 0.1% Rapigest™ SF and a 3-hour incubation period. This approach allowed for mapping of the spatial distribution of blood peptides onto fingerprint ridge detail, thus establishing that the fingerprint donor had blood on their fingers and linking them to the crime.

Again, the protocol was trialled on blind samples and confidently identified one fingerprint each to be contaminated with human blood and a non-biofluid, respectively. Due to the problems encountered in provenance determination in stain samples, species determination of animal blood was not possible in fingerprints. However, this might be partly due to the small sample set and the fact that several samples did not exhibit ridge detail when imaged. This was due to the humidity being too high and trypsin pooling on the sample, resulting in peptide dislocation from the ridges, although the digestion set up was not changed. This problem should be resolvable by reducing the humidity.

Furthermore, the overall mass spectra and peptide yield observed in *in situ* digestions vastly differed from in-solution digests, as very few signals were observed in the higher mass range. It is thus possible that some animal-specific blood peptides were not observed due to their higher mass. Additionally, the mass accuracy obtainable in MALDI-MS imaging was lower than in profiling, thereby further complicating the analysis.

Nonetheless, detection and identification of human blood in fingerprints was possible, as well as the mapping of peptides onto ridge detail in marks deposited on ideal surfaces or lifted using a suitable lifting tape. Several tapes were trialled and J-Lar® clear to the core tape was identified as most suitable for lifting, tryptic digestion and MALDI-MSI of blood marks following AB1-enhancement.

When blood marks are concerned, several scenarios of deposition can be encountered at a scene. A) bloodied mark, left by bloodied fingertip, B) mark in blood or C) coincidental association (or faux blood mark), where a clean, latent mark is subsequently contaminated with blood. Scenario C can for example occur during attempted clean-up of a crime scene when blood is wiped across the perpetrator's mark, but also when unrelated marks are covered in blood spatter during a crime. As this can indicate a vastly different sequence of events than a type B mark in blood, it is of paramount importance to be able to distinguish the scenarios from one another. MALDI-MSI theoretically allows the differentiation of scenario A, where blood peptides are only expected on the ridges, from B and C, where blood peptides are expected on the entire surface. However, MALDI-MSI does not allow the order of deposition to be established, as it currently cannot determine if the fingermark is underneath or on top of the blood. To date, determining the order of deposition is purely based on an examiner's expertise and no numerical approach appears to be available. As differentiating between scenarios is complicated and different scenario marks often visually appear to exhibit the same characteristics, this is far from ideal.

For this reason, the hypothesis was postulated that type A, B and C marks would present different heights of ridges and valleys that could allow their differentiation based on numerical data. In order to measure those ridge heights, infinite focus microscopy was employed. Pre-enhanced bloodied marks were lifted with J-Lar® lifting tape and IFM measurements obtained over the course of 33 days in order to evaluate possible changes over time. Whilst ridge heights did vary over time, no clear trend could be established, as some marks exhibited a decrease and other an increase in ridge heights. Despite this information, it was still possible that differences in ridge heights between the deposition scenarios would be so drastic that their differentiation would be easily achieved, even with fluctuating heights. Hence, samples of all deposition types were deposited on PVC plastic cards and ridge heights measured. Unfortunately, the heights observed in this set of experiments were consistent between different scenarios, and also differed vastly from the previous set of samples analysed on lifting tape. It was thus determined that the chemistry and surface properties of the deposition surface, such as surface tension and contact angle, had a significant effect on the results.

As such, the ability of IFM to differentiate between different scenarios of deposition greatly depends on the deposition surface. However, this cannot be controlled in real life forensic scenarios and a great variety of surfaces can be expected. Therefore, in conclusion IFM was deemed unsuitable for the purpose of delivering quantifiable, numeric data to allow for establishing the order of deposition of blood fingermarks.

However, recent advances in mass spectrometry appear to show potential to solve the problem at hand. Prof. Spengler has presented his group's development of an autofocus laser suitable for 3D surface profiling using atmospheric pressure LDI or MALDI-MSI [1]. Instead of employing a laser with a fixed focus point that becomes defocused with changes in the sample height and doesn't deliver data on those areas, Spengler's technique allowed the detection and mapping of analytes in 3D. It stands to reason that this instrumentation should be able to determine whether blood is present on top or underneath a fingermark by not only detecting and re-focussing on minute changes in the height of the sample, but also chemically mapping its topology. Analysing a mark in blood, the sample topology is expected to consist of blood on the surface of deposition and in the fingermark valleys. The fingermark ridges on top of the blood, however, are expected to allow the detection of the usual components of latent, non-blood fingermarks, provided the currently reported vertical resolution of 1.5  $\mu\text{m}$  is sufficient to distinguish between the layers of the sample. A fingermark covered in blood, on the other hand, is expected to consist of blood peptides on the entire top layer, regardless of different heights of covered ridges and blood-filled valleys. Additionally, unless tryptic digestion re-distributes blood, this could even allow for the combination of proteomic analysis with determination of the order of deposition into one single analysis, making the developed protocols truly multi-informative.

- [1] M. Kompauer, S. Heiles, B. Spengler, Chemical and topographical 3D surface profiling using atmospheric pressure LDI and MALDI MS imaging, (2017). <http://dx.doi.org/10.1038/protex.2017.103>.

**Word count: 42,700** (without citations, including abstract)

# Publications and dissemination

## Publications

L. Deininger, E. Patel, M.R. Clench, V. Sears, C. Sammon, S. Francese, Proteomics goes forensic: detection and mapping of blood signatures in fingermarks, *Proteomics*. 16 (2016) 1707–1717.

Patel, E., Cicatiello, P., Deininger, L., Clench, M. R., Marino, G., Giardina, P., et al. (2016). A Proteomic Approach for the Rapid, Multi-Informative and Reliable Identification of Blood. *The Analyst*, 141(1), 191–198.

## Poster presentations

- British Mass Spectrometry Society (BMSS) 2015 Annual Meeting (Birmingham, UK)
- BMSS 3rd Mass Spectrometry Imaging Symposium 2016 (Sheffield, UK)
- American Society for Mass Spectrometry (ASMS) 2016 Annual Meeting (San Antonio, Texas, USA)
- 15th East Midlands Proteomics Workshop 2016 (Nottingham, UK)
- Forensic Futures 2016 (Manchester, UK)
- BMSS 4th Mass Spectrometry Imaging Symposium 2017 (Sheffield, UK)
- International Association of Forensic Sciences (IAFS) 2017 triennial meeting (Toronto, Canada)

## Oral presentations

- International Congress on Analytical Proteomics (ICAP) 2015 (Costa de Caparica, Portugal), with a 5-minute shotgun presentation
- BMSS 2016 Annual Meeting (Eastbourne, UK)

## Prizes

- Barber prize for best early career oral presentation at BMSS 2016
- Prize for best poster at East Midlands Proteomics Workshop 2016

## Appendix 1

Protein	detected concentration [ $\mu\text{g/mL}$ ]	Reference
Haemoglobin	126500 - 155100	[1]
Albumin	35000 - 50000	[2]
	43100 $\pm$ 8500	[3]
Haptoglobin	3800 - 7800	[2]
	1790 $\pm$ 1260	[3]
Fibrinogen	2610 $\pm$ 840	[3]
	2000 - 4500	[2]
Transferrin	2000 -4000	[2]
	1870 $\pm$ 490	[3]
$\alpha$ -1-antitrypsin	2000 -4000	[2]
	1690 $\pm$ 370	[3]
$\alpha$ -2-macroglobulin	1600 - 3800	[2]
	1709 $\pm$ 590	[3]
IgG1	7160 $\pm$ 5190	[3]
IgA	3410 $\pm$ 1950	[3]
IgG2	2910 $\pm$ 2310	[3]
IgM	2730 $\pm$ 3100	[3]
IgG4	2400 $\pm$ 2300	[3]
$\alpha$ 1-acid glycoprotein	1480 $\pm$ 480	[3]
Apo-A1	1170 $\pm$ 490	[3]
IgG3	1070 $\pm$ 600	[3]
Apo-B	900 $\pm$ 440	[3]
Apo-C3	160 $\pm$ 100	[3]
IgD	670 $\pm$ 370	[3]
Inter- $\alpha$ -trypsin inhibitor	200 - 700	[2]
$\alpha$ -1-anti-chymotrypsin	300 - 600	[2]
Fibronectin	300	[2]
Complement C5	40 - 150	[2]
Complement C8	70 - 90	[2]
Transcortin	60 - 80	[2]

<b>Protein</b>	<b>detected concentration [<math>\mu\text{g/mL}</math>]</b>	<b>Reference</b>
<b>Complement C1r</b>	50	[2]
<b>Complement C1r subcomponent-like protein</b>	39	[4]
<b>Insulin-like growth factor-binding protein 3</b>	20	[4]
<b>Complement C2</b>	10 - 30	[2]
<b>Coagulation factor XIII</b>	10 - 20	[2]
<b>Protein Z-dependent protease inhibitor</b>	9.8	[4]
<b>Coagulation factor XI</b>	8.3	[4]
<b>Vasorin</b>	7.5	[4]
<b>C-reactive protein</b>	7.1	[4]
<b>Sulfhydryl oxidase 1</b>	6.6	[4]
<b>Pigment epithelial-derived factor (PEDF)</b>	5	[2]
<b>Lysozyme C</b>	5	[4]
<b>Biotinidase</b>	3.2	[4]
<b>Mannose-binding protein C</b>	3	[4]
<b>IgGFc-binding protein</b>	1.9	[4]
<b>Vinculin</b>	1.7	[4]
<b>Adiponectin</b>	1.1	[4]
<b>Basement membrane-specific heparan sulfate proteoglycan core protein</b>	0.78	[4]
<b>Cofilin-1</b>	0.65	[4]
<b>Thrombospondin-4</b>	0.54	[4]
<b>Talin-1</b>	0.47	[4]
<b>Pleckstrin</b>	0.39	[4]
<b>Peptidase inhibitor 16</b>	0.24	[4]

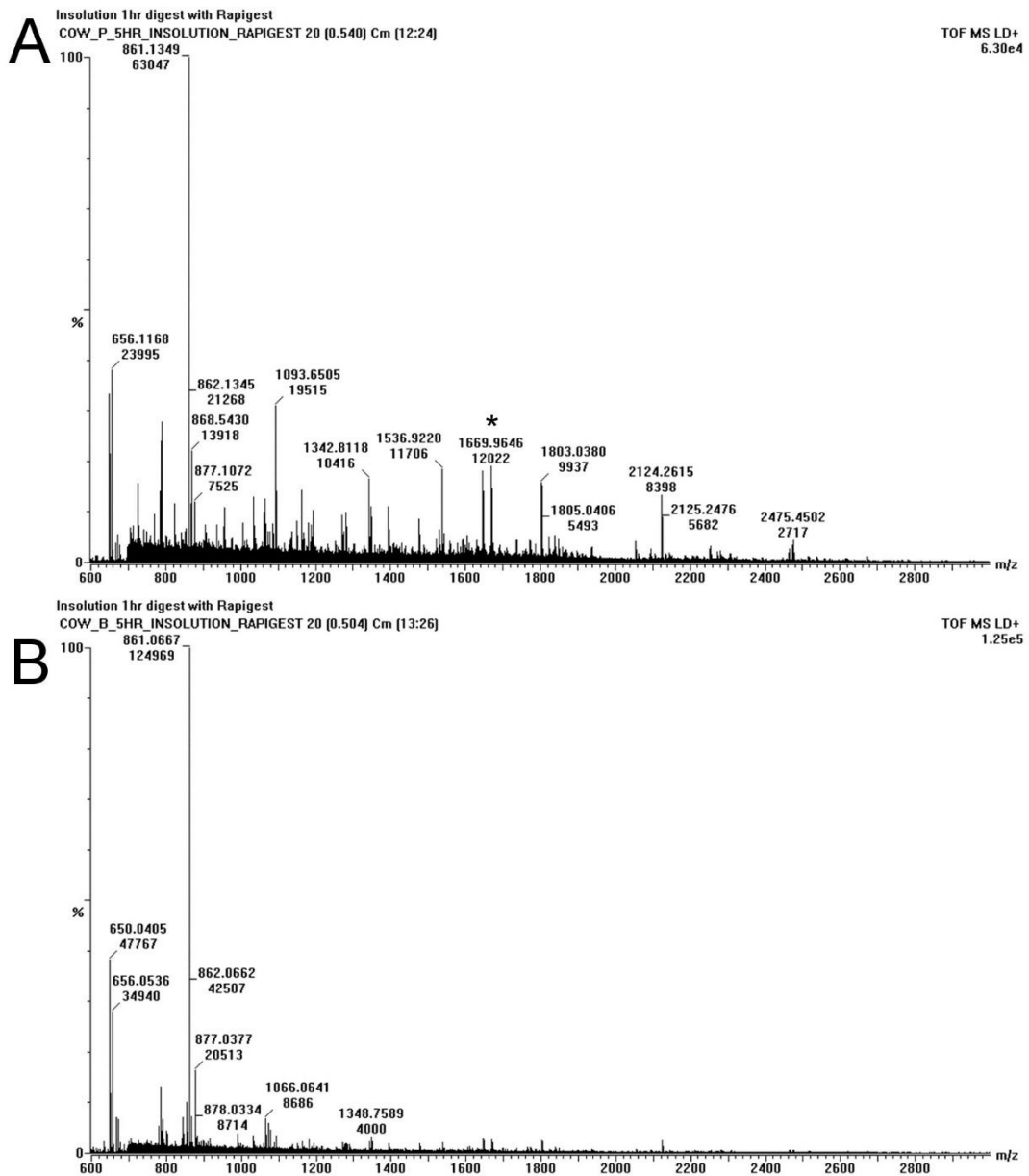
<b>Protein</b>	<b>detected concentration [<math>\mu\text{g/mL}</math>]</b>	<b>Reference</b>
<b>Matrix metalloproteinase-2 (MMP-2)</b>	~ 0.2	[2]
<b>Multimerin-1</b>	0.12	[4]
<b>Hepatocyte growth factor activator (HGFA)</b>	~ 0.08	[2]
<b>Zyxin</b>	0.054	[4]
<b>Filamin-A</b>	0.05	[4]
<b>T-lymphocyte activation antigen (CD80)</b>	0.04 -0.1	[2]
<b>PDZ and LIM domain protein 1</b>	0.033	[4]
<b>Latent-transforming growth factor beta-binding protein 1</b>	0.024	[4]
<b>Integrin alpha-IIb</b>	0.021	[4]
<b>Tubulin alpha-4A chain</b>	0.02	[4]
<b>Ras suppressor protein 1</b>	0.015	[4]
<b>Vasodilator-stimulated phosphoprotein</b>	0.012	[4]
<b>Alpha-actinin-1</b>	0.012	[4]
<b>Tubulin beta-1 chain</b>	0.0011	[4]
<b>A disintegrin and metalloproteinase with thrombospondin motifs 13</b>	0.011	[4]
<b>macrophage stimulatory protein (MSP)</b>	0.01 - 0.03	[2]
<b>Myosin regulatory light chain 12B</b>	0.003	[4]
<b>Integrin beta-3</b>	0.0029	[4]
<b>Human megakaryote stimulating factor (MSF)</b>	~ 0.001	[2]

Protein	detected concentration [ $\mu\text{g/mL}$ ]	Reference
Interleukin-1 receptor (IL-1 R)	~ 0.001	[2]
LIM and senescent cell antigen-like-containing domain protein 1	0.0005	[4]
Erythrocyte band 7 integral membrane protein	0.0003	[4]
Beta-parvin	0.0001	[4]
Band 3 anion transport protein	0.0001	[4]
Interleukin-12 $\beta$ chain (IL-12 p40)	0.000077	[2]
Fibroblast growth factor-12 (FGF-12)	~ 0.00001 - 0.00003	[2]

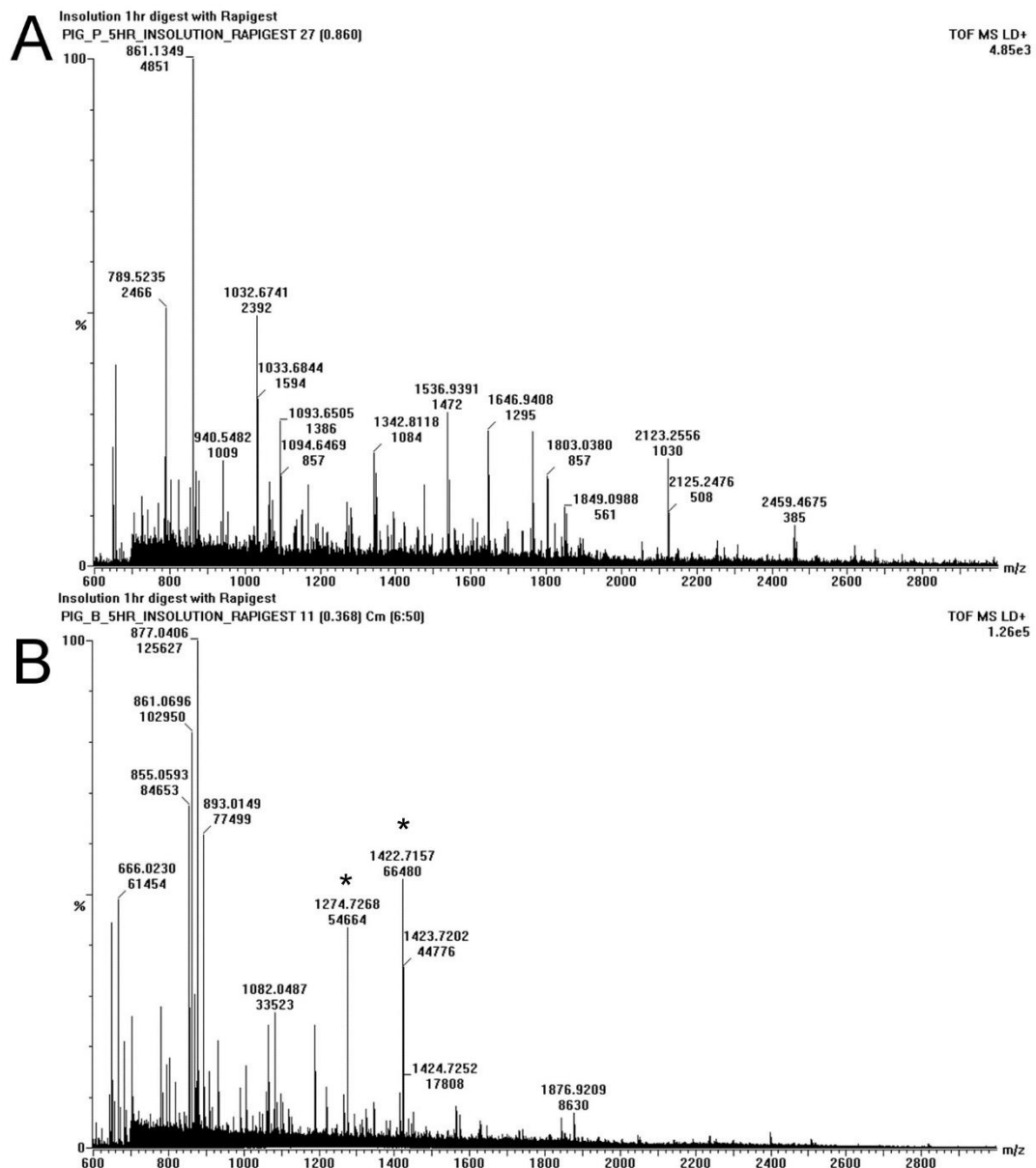
**S 1.1** Non-comprehensible table of a variety of (blood) proteins and their normal concentration ranges in blood, in decreasing order. (Compiled by Erasmus student Judith Schramm)

- [1] E. Beutler, J. Waalen, The definition of anemia : what is the lower limit of normal of the blood hemoglobin concentration ? The definition of anemia : what is the lower limit of normal of the blood hemoglobin concentration ?, *Blood*. 107 (2006) 1747–1750. doi:10.1182/blood-2005-07-3046.
- [2] Y. Shen, J.M. Jacobs, D.G. Camp 2nd, R. Fang, R.J. Moore, R.D. Smith, W. Xiao, R.W. Davis, R.G. Tompkins, Ultra-high-efficiency strong cation exchange LC/RPLC/MS/MS for high dynamic range characterization of the human plasma proteome, *Anal Chem*. 76 (2004) 1134–44. doi:10.1021/ac034869m.
- [3] C. Petibois, G. Cazorla, A. Cassaigne, G. Dél  ris, Plasma protein contents determined by Fourier-transform infrared spectrometry., *Clin. Chem*. 47 (2001) 730–8. <http://www.ncbi.nlm.nih.gov/pubmed/11274025>.
- [4] R.C. Bollineni, I.J. Guldvik, H. Gr  nberg, F. Wiklund, I.G. Mills, B. Thiede, A differential protein solubility approach for the depletion of highly abundant proteins in plasma using ammonium sulfate, *Analyst*. 140 (2015) 8109–8117. doi:10.1039/C5AN01560J.

# Appendix 4



**S 4.1** MALDI-MS spectra of tryptically digested bovine “blood” samples obtained from A: residual juices in meat packet, B: a butcher. \* denotes theoretical  $m/z$  1669.8353 putatively identified as bovine Myoglobin, which was observed as a characteristic signal in the study. Note its absence in the sample obtained from the butcher.



**S 4.2** MALDI-MS spectra of tryptically digested porcine “blood” samples obtained from A: residual juices in meat packet, B: a butcher. \* denotes theoretical  $m/z$  1274.7114 (r.LLVVYPWTQR.f) and  $m/z$  1422.7036 (k.VGGQAGAHGAEALER.m) putatively identified as as human, bovine, porcine or cervine Hb $\beta$  and porcine Hb $\alpha$ , respectively. Both were observed in one porcine sample in the blind study, but not detected in two others. Note their absence in the sample obtained from the meat package.